

**Modelling Alzheimer's Disease: Transgenic Expression
of Amyloid beta Peptides in the Nematode
Caenorhabditis elegans Neurons**

Submitted by

Neha Sirwani

BSc (Biotechnology), MSc (Biotechnology and Bioinformatics)

A thesis submitted in total fulfilment

of the requirements for the degree of

Doctor of Philosophy

School of Life Sciences

College of Science, Health and Engineering

La Trobe University

Victoria, Australia

August 2020

Table of Contents

Table of Contents	i
List of Figures	vii
List of Tables	x
Abbreviations	xi
Abstract	xiii
Statement of Authorship	xiv
Acknowledgements	xv
Chapter One	1
General introduction	1
1.1 Alzheimer’s disease pathology	1
1.1.1 Amyloid precursor protein processing	3
1.1.2 A β peptide as a driver of neurotoxicity.....	5
1.1.3 Amyloid cascade hypothesis.....	8
1.2 Animal models of AD	10
1.3 <i>Caenorhabditis elegans</i> as a model to study age-related neurodegeneration	15
1.4 <i>C. elegans</i> behaviours to study age-related neurodegeneration.....	19
1.5 <i>C. elegans</i> models for AD research	24
1.5.1 Analysis of <i>C. elegans</i> orthologs of human AD genes	24
1.5.2 Transgenic <i>C. elegans</i> models of A β and tau toxicity	28
1.6 Aims and scope of the thesis.....	37
Chapter Two	39
Molecular and behavioural characterisation of a transgenic <i>C. elegans</i> strain expressing the human amyloid-beta protein in neurons.....	39
2.1 Introduction.....	39
2.2 Materials and Methods.....	41

2.2.1 Materials	41
2.2.2 Maintenance of <i>C. elegans</i> strains	41
2.2.3 Preparation of <i>C. elegans</i> transgenic strains	42
2.2.4 Construction of expression plasmids	45
2.2.5 Generating standard curves from plasmid and genomic DNA for copy number PCR assay	47
2.2.6 Single worm lysis for PCR	48
2.2.7 Copy number PCR assay	48
2.2.8 Total RNA isolation and cDNA synthesis	48
2.2.9 RT-qPCR.....	49
2.2.10 Lifespan analysis.....	49
2.2.11 Brood size assay.....	50
2.2.12 Egg retention assay	51
2.2.13 Rate of egg production assay	51
2.2.14 Chemotaxis assay.....	51
2.2.15 Associative learning assay	52
2.2.16 Memory loss assay	53
2.2.17 Motility assays	54
2.2.18 Basal and enhanced slowing response assays	54
2.2.19 Statistical analysis	55
2.3 Results.....	56
2.3.1 Construction of a pan-neuronal A β containing transgenic strain.....	56
2.3.2 Pan-neuronal strain WG643 shows multiple copies of the A β transgene.....	56
2.3.3 Subtle decrease in growth rate of the A β -expressing transgenic strain WG643	58
2.3.4 Pan-neuronal A β strain shows reduction in lifespan.....	60
2.3.5 Pan-neuronal A β -expressing strain shows age-related deficits in locomotion	62
2.3.6 Pan-neuronal A β -expressing strain shows changes in chemotactic response towards volatile odorants	66
2.3.7 Pan-neuronal A β -expressing strain shows decrease in fecundity	68
2.3.8 Pan-neuronal A β -expressing strain showed deficits in dopaminergic signalling.....	70

2.3.9 Pan-neuronal A β -expressing strain showed deficits in associative learning and short-term memory	73
2.4 Discussion	76
2.4.1 Successful integration and expression of A β in the transgenic <i>C. elegans</i> strain WG643	76
2.4.2 Reduced lifespan and healthspan in the A β -expressing strain.....	79
2.4.3 A β expression impacts locomotion in transgenic strain WG643	79
2.4.4 A β -expressing transgenic <i>C. elegans</i> strain WG643 has disease relevant phenotypes	81
2.5 Conclusion	83
Chapter Three	84
Behavioural phenotyping of strains expressing varying levels of amyloid β transgene driven by three different pan-neuronal promoters	84
3.1 Introduction.....	84
3.2 Methods.....	87
3.2.1 Construction of expression plasmids and generation of transgenic <i>C. elegans</i> expressing pan-neuronal transgenes by microinjection	87
3.2.2 Microscope details for pan-neuronal GFP-expressing strain WG625	88
3.2.3 Strains used in this chapter.....	88
3.2.4 Statistical analysis	89
3.3 Results.....	90
3.3.1 Pan neuronal A β 1-42 expressing strains show variation in copy number and expression	90
3.3.2 Pan-neuronal A β 1-42-expressing transgenic <i>C. elegans</i> strains show significant reduction in lifespan.....	92
3.3.3 The strains <i>Prgef-1::Aβ</i> and <i>Punc-119::Aβ</i> show reduction in length on day 12.....	94
3.3.4 Pan-neuronal A β 1-42-expressing strains show defects in egg-laying behaviour.....	96
3.3.5 Pan-neuronal A β 1-42-expressing strains show subtle changes in chemotactic abilities	98
3.3.6 The transgenic A β 1-42 expressing strains show a significant reduction in motility parameters	100

3.3.7 Pan-neuronal A β -expressing strains <i>Psnb-1::Aβ</i> and <i>Prgef-1::Aβ</i> show diminished basal slowing response mediated by dopamine.....	104
3.4 Discussion	107
3.4.1 Transgenic A β 1-42 expressing <i>C. elegans</i> strains show variation in A β expression	107
3.4.2 Pan-neuronal A β 1-42-expressing strain show premature death and reduction in fecundity	109
3.4.3 Pan-neuronal A β 1-42-expressing strains <i>Psnb-1::Aβ</i> and <i>Prgef-1::Aβ</i> show a severe decline in motility	110
3.4.4 Defects in chemotaxis observed in all A β 1-42-expressing strains	111
3.4.5 Pan-neuronal A β 1-42-expressing strains show deficits in dopaminergic signalling.....	111
3.5 Conclusion	113
Chapter Four	114
Comparison of transgenic strains expressing different versions of the A β transgene in the <i>C. elegans</i> nervous system	114
4.1 Introduction.....	114
4.2 Methods.....	121
4.2.1 Construction of transgenic <i>C. elegans</i> expressing A β variants in the neurons	121
4.2.2 Strains used in this chapter.....	122
4.2.3 Statistical analysis	122
4.3 Results.....	123
4.3.1 Copy-number PCR assay shows a range of A β copies in the transgenic strains	123
4.3.2 Transgenic <i>C. elegans</i> strains containing the A β variant transgenes show low levels of A β transgene expression in comparison to the human A β 1-42 expressing strains.	123
4.3.3 Pan-neuronal mouse A β -expressing strain WG724 is longer lived than the human A β -expressing strain.	125
4.3.4 Measurement of growth rate of variant A β -expressing transgenic strains ..	129
4.3.5 A β variant expressing strains show differences in egg-laying behaviour compared to the human A β 1-42 expressing strains	131
4.3.6 A β variant expressing strains WG709 and WG664 show subtle differences in crawling compared to the A β 1-42 expressing strain WG663	133

4.3.7 A β variant expressing strains WG724 and WG666 show subtle differences in swimming compared to the A β 1-42 expressing strain WG643	137
4.3.8 A β variant expressing strains show distinct age-related changes in chemotactic ability towards volatile odorants.....	141
4.3.9 Double transgenic A β -expressing strains WG664 and WG666 show deficits in dopaminergic signalling starting at Day 4.	143
4.4 Discussion	147
4.4.1 <i>C. elegans</i> expressing A β 4-42 show deficits in egg-laying behaviour but improved movement and chemotaxis relative to A β 1-42	147
4.4.2 Mouse A β -expressing strain does not show noteworthy behavioural deficits	149
4.4.3 Simultaneous expression of A β 1-42 and A β 1-42G37L in <i>C. elegans</i> neurons does not causes reduction in <i>in vivo</i> A β toxicity.....	150
4.5 Conclusion	153
Chapter Five	154
Phenotypic consequences of amyloid β expression in a <i>ptl-1</i> null genetic background	154
5.1 Introduction.....	154
5.2 Methods.....	158
5.2.1 Competitive PCR strategy.....	158
5.2.2 Strains used in this chapter.....	158
5.2.3 Statistical analysis	158
5.3 Results.....	159
5.3.1 Generation of a transgenic <i>C. elegans</i> strain WG673 expressing pan-neuronal A β in a <i>ptl-1</i> null background	159
5.3.2 Transgenic A β ; <i>ptl-1</i> strain WG673 shows changes in growth rate	161
5.3.3 Expression of A β in a <i>ptl-1</i> mutant background shows reduction in longevity	161
5.3.4 Transgenic <i>C. elegans</i> strain expressing A β in a <i>ptl-1</i> null background shows impaired egg-laying	163
5.3.5 Transgenic <i>C. elegans</i> strain expressing A β in a <i>ptl-1</i> null background shows improvement in olfactory response towards volatile odorants	165
5.3.6 Expression of A β peptide in a <i>ptl-1</i> mutant genetic background results in impaired locomotory behaviour	167

5.3.7 Transgenic <i>C. elegans</i> strain expressing A β in a <i>ptl-1</i> null background shows deficits in dopaminergic signalling	173
5.4 Discussion	176
5.4.1 A β expression in tau null background results in behavioural changes in specific neuronal subsets.....	177
5.4.2 Some behavioural deficits are a result of neuronal A β expression irrespective of the genetic background	178
5.5 Conclusion	179
Chapter Six	181
General discussion	181
6.1 Neuronal A β 1-42 expression results in age-associated behavioural deficits.....	182
6.2 Behavioural deficit dependent on A β concentration.....	185
6.3 Different variants of A β result in specific behavioural deficits.	188
6.4 Phenotypic impact of A β expression in different genetic background.	190
6.5 Conclusions and future prospects	191
Supplementary Information	194
Supplementary tables	194
Supplementary information for Chapter 2	198
Supplementary information for Chapter 3	212
Supplementary information for Chapter 4	218
Supplementary information for Chapter 5	224
Bibliography	230

List of Figures

Figure 1.1: Comparison of APP processing in normal and AD brain by α -, β - and γ -secretases.....	4
Figure 1.2: The amyloid (or A β) cascade hypothesis.....	6
Figure 1.3: Life cycle of the nematode <i>Caenorhabditis elegans</i>	16
Figure 1.4: Overview of the <i>C. elegans</i> nervous system.....	18
Figure 2.1: Cloning of <i>snb-1</i> fragment.	46
Figure 2.2: Transgenic stable integrated strain WG643 showing presence and expression of A β minigene.....	57
Figure 2.3: <i>C. elegans</i> growth estimated by body size measurements of early (day 4), middle-aged (day 8) and old (day 12) worms.	59
Figure 2.4: Pan neuronal A β -expressing strain shows reduced longevity.....	61
Figure 2.5: Age-related changes in worm motility parameters in solid media.	63
Figure 2.6: Age-related changes in worm swimming parameters.....	65
Figure 2.7: A β -expressing strain WG643 shows a change in chemotactic response..	67
Figure 2.2.8: Pan-neuronal A β expression results in impaired egg-laying.....	69
Figure 2.9: Pan-neuronal A β -expressing strain shows deficits in dopaminergic signalling.	71
Figure 2.10: Pan-neuronal A β -expressing strain shows deficits in learning and memory.	74
Figure 3.1: Comparison of A β expression levels in the pan-neuronal A β strains.....	91
Figure 3.2: Transgenic <i>C. elegans</i> strains expressing A β peptide in the neurons show reduction in life span.	93
Figure 3.3: <i>C. elegans</i> growth and aging estimated by body size measurements of early (day 4), middle-aged (day 8), and old (day 12) worms.....	95
Figure 3.4: Comparison of egg-laying assays in transgenic A β -expressing <i>C. elegans</i> strains.	97

Figure 3.5: Variation in chemotactic response of A β -expressing transgenic <i>C. elegans</i> strains towards volatile odorants on Day 4 and Day 8	99
Figure 3.6: P an-neuronal A β -expressing strains show age-dependent reduction in motility on solid media.....	101
Figure 3.7: Pan-neuronal A β -expressing strains show age-dependent reduction in motility on liquid media.....	103
Figure 3.8: Pan-neuronal A β -expressing strains show diminished basal slowing response mediated by dopamine.....	105
Figure 3.9: Dose response curves explaining the correlation between the levels of A β expression and the severity of disease.	112
Figure 4.1: N-terminally truncated A β peptides.	116
Figure 4.2: Schematic model of hypothetical glycine zipper-mediated interaction between A β α -helical regions.....	118
Figure 4.3: Comparison of A β expression levels in the pan neuronal A β strains. ...	124
Figure 4.4: Transgenic <i>C. elegans</i> strains expressing A β variants in the neurons show reduction in the lifespan.	126
Figure 4.5: Double transgenic <i>C. elegans</i> strain WG666 expressing A β and A β shows slow growth as estimated by body size measurements of early (day 4), middle-aged (day 8) and old (day 12) adults.....	130
Figure 4.6: Transgenic <i>C. elegans</i> strains expressing different versions of the A β peptide show egg-laying defects.	132
Figure 4.7: Age-related changes in motility of transgenic A β -expressing strains on solid media.	134
Figure 4.8: Age-related changes in motility of transgenic <i>C. elegans</i> strains in liquid media.	138
Figure 4.9: Chemotaxis of transgenic <i>C. elegans</i> strains towards A) Diacetyl B) Benzaldehyde.....	142
Figure 4.10: Transgenic <i>C. elegans</i> strains expressing A β peptides show diminished basal slowing response.....	144

Figure 5.1: Reduction in Aβ transcript level when expressed in a <i>ptl-1</i> null genetic background.....	160
Figure 5.2: <i>C. elegans</i> growth estimated by body size measurements of early (day 4), middle-aged (day 8) and old (day 12) adults.	162
Figure 5.3: Shortened lifespan of WG673 strain expressing Aβ peptide in a <i>ptl-1</i> genetic background.....	164
Figure 5.4: Transgenic <i>C. elegans</i> strain Aβ;<i>ptl-1</i> shows deficits in egg-laying behaviour.	166
Figure 5.5: Transgenic <i>C. elegans</i> strain expressing Aβ peptide in a <i>ptl-1</i> genetic background causes increase in chemotactic responses towards volatile odorants. .	168
Figure 5.6: Transgenic <i>C. elegans</i> strain expressing Aβ in a <i>ptl-1</i> genetic background showed age-related locomotory defects on solid media.....	170
Figure 5.7: Transgenic <i>C. elegans</i> strain expressing Aβ in a <i>ptl-1</i> genetic background enhances the severity of the motility defects on liquid media.....	172
Figure 5.8: Transgenic <i>C. elegans</i> strain expressing Aβ peptide in a <i>ptl-1</i> genetic background show deficits in dopaminergic signalling.....	174
Figure 6.1: Measurable outputs of neuronal health.	184
Figure 6.2: Schematic representing the <i>C. elegans</i> locomotory circuit.....	186

List of Tables

Table 1.1: Suitability and limitations of commonly utilized model organisms to study AD. Adapted and modified from (Gotz et al., 2004)	13
Table 1.2: Knockouts of <i>C. elegans</i> orthologues of human AD genes. Adapted from (Ewald and Li, 2010)	26
Table 1.3: <i>C. elegans</i> toxicity models of human proteins implicated in AD (adapted and modified from (Ewald and Li, 2010))	29
Table 2.1: Values for G and A obtained by using the Gompertz equation.....	62
Table 3.1: Values for G and A obtained by using the Gompertz equation.....	94
Table 4.1: Median and maximum life span values (Mean \pm SEM)	128
Table 4.2: G and A estimates derived from Gompertz equation.....	128
Table 4.3: Comparison of crawling parameters between transgenic Aβ-expressing strains	136
Table 4.4: Comparison of swimming parameters between transgenic Aβ-expressing strains	139
Table 4.5: Summary of the basal slowing response assays.....	145
Table 4.6: Summary of the enhanced slowing response assays	146
Table 6.1: Correlation between expression levels and severity of disease phenotype	188

Abbreviations

°C	Degree celsius
μl	Micro litre
μM	Micro molar
AD	Alzheimer's disease
ADDLs	Aβ-derived diffusible ligands
APL-1	Amyloid like protein
APOE	Apolipoprotein E
APLP	Amyloid precursor like proteins
APP	Amyloid precursor protein
Aβ	Amyloid beta
BACE	β-secretase enzyme
bp	Base pair(s)
cDNA	Complementary DNA
CGC	<i>Caenorhabditis</i> Genetics Centre
CI	Chemotaxis index
CNS	Central nervous system
CRISPR	Clustered regularly interspaced short palindromic repeat
CSF	Cerebrospinal fluid
DMSO	Dimethyl sulphoxide
dNTPs	Deoxynucleotide 5'-triphosphates
DTT	Dithiothreitol
EDTA	Ethylene diamine tetra acetic acid disodium salt
F1	First filial generation
F2	Second filial generation
F3	Third filial generation
FPKM	Fragments per kilobase of transcript per million mapped reads
FUdR	Fluorodeoxyuridine
GFP	Green fluorescent protein
gm	Gram(s)
h	Hour
Kb	Kilobase pairs
L1	First larval stage
L2	Second larval stage
L3	Third larval stage
L4	Fourth larval stage
M	Molar
MAP	Microtubule-associated protein
MCI	Mild cognitive impairment
MCS	Multiple cloning site
ml	Milli litre

MRDT	Mortality rate doubling time
MS	Mass Spectrometry
NCBI	National Centre for Biotechnology Information
NFT	Neurofibrillary tangles
NGM	Nematode growth medium
NTC	No template control
P0	Parental generation
PBS	Phosphate buffered saline
PCR	Polymerase chain reaction
PHF	Paired helical filaments
qPCR	Quantitative PCR
rpm	Revolutions per minute
RT-qPCR	Quantitative reverse transcription PCR
s	Second(s)
SD	Standard deviation
SEM	Standard error of mean
STAM	Short term associative memory
UTR	Untranslated region
WIR	Wave initiation rate

Abstract

Alzheimer's disease (AD), the most common form of dementia, is a complex age-related neurodegenerative disorder, leading to cognitive impairment and loss of associative learning. The pathological hallmarks of AD are the presence of neurofibrillary tangles composed of aggregates of hyperphosphorylated protein tau and senile plaques composed of aggregates of fibrillar amyloid β ($A\beta$) peptides, with $A\beta_{1-42}$ peptide being the most abundant. These $A\beta$ peptides have been proposed to contribute to the pathophysiology of the disease; however, there are few tools available to test this hypothesis. This project utilised the model organism, *Caenorhabditis elegans*, as an *in vivo* system to study the toxicity associated with these $A\beta$ species. To do this, a panel of transgenic *C. elegans* strains expressing the human $A\beta$ peptides targeted to the neurons using the pan-neuronal promoters, *snb-1* and *rgef-1*, was generated and the *in vivo* $A\beta$ toxicity was studied using well-established behavioural assays. Molecular characterisation of the new transgenic strains was carried out at the genomic and transcript level, demonstrating variation in the $A\beta$ transgene copy number and transcript abundance between strains. Behavioural phenotyping of the transgenic *C. elegans* strain expressing the full length $A\beta_{1-42}$ species, driven by the pan-neuronal promoter *snb-1*, showed that $A\beta$ expression affects neuronal function. Phenotypic data showed strong age-related defects in motility, changes in chemotactic abilities, reduced longevity, deficits in learning behaviour and changes in healthspan indicators such as maximum speed and fecundity. Subsequent work focused on investigating differences in the timing and level of $A\beta$ expression between strains differing in copy number and promoter, and possible correlations between expression level or timing and the severity of the disease phenotype. No previous reports have established a dose-response relationship between $A\beta$ peptide expression level and disease. Furthermore, the *in vivo* toxicity associated with the different $A\beta$ species, namely the N-truncated $A\beta_{4-42}$, mouse $A\beta_{1-42}$ and the $A\beta_{1-42G37L}$ was compared to the full-length human $A\beta_{1-42}$ species. Lastly, the causal mechanisms of $A\beta$ pathogenesis in a different genetic background were explored by manipulating AD-associated downstream genes such as tau. This work provides a new toolkit to investigate the *in vivo* toxicity of neuronal $A\beta$ expression and the molecular and cellular mechanisms underlying AD progression, in addition to permitting, for the first time, a direct test of the dose-response relationship between $A\beta$ peptide expression and disease. These strains may be used in subsequent screens to develop novel therapeutics to treat Alzheimer's disease.

Statement of Authorship

Except where references are made in the text, this thesis contains no material published elsewhere or extracted in whole or in part from a thesis submitted for the award of any other degree or diploma.

No other person's work has been used without due acknowledgement in the main text of the thesis.

This thesis has not been submitted for the award of any degree or diploma in any other tertiary institution.

This work was supported by an Australian Government Research Training Program Scholarship and La Trobe University Postgraduate Research Scholarship.



Neha Sirwani

21/07/2020

Acknowledgements

I would like to acknowledge all the wonderful people whose help and support has made this thesis possible.

First and foremost, I would like to express my deepest gratitude and sincere appreciation towards my principal supervisor Associate Professor Warwick Grant for his conscientious guidance, unwavering support, endless patience, for believing in me, and for all the opportunities. His expertise in worm biology and his commitment towards the project was a significant influence in shaping many of the concepts presented in this thesis. His guidance has made me a far better student than I could have hoped to be, and I could not have imagined having a better advisor and mentor for my PhD. I would also like to thank my co-supervisor Dr Gawain McColl for his constructive feedback at various stages of the project. I am profoundly grateful to my mentor Dr Stephen Doyle whose meticulous suggestions and precious guidance have not only been monumental in driving this project but have also inspired me to become an independent researcher. I would also like to express my sincere gratitude to Dr Shannon Hedtke for her valuable suggestions, support, enthusiasm, encouragement, and organising the required resources for all the experiments. Heartfelt thanks to Kirsten Grant for performing all the microinjections and for generating the transgenic strains. My research would have been impossible without her support and painstaking efforts. Special thanks to Dr Mark Jois for allowing me access to the WormLab software. I would also like to thank my RPP chair Dr Jacqueline Orian for her time and suggestions at various stages of my candidature.

This work was supported by STE Bridging Postgraduate Scholarship, Understanding disease RFA PhD Scholarship, and La Trobe University Full Fee Research Scholarship.

I would also like to extend my heartfelt gratitude to all the *C. elegans* worms that were sacrificed to generate the data required for this project.

My sincere thanks to all the past and present Grant lab members for creating a cordial working environment. I would like to thank Himal Shrestha for his assistance with statistical analysis in R and Dr Spencer Gang for sharing his knowledge and expertise in chemotaxis assays. Heartfelt thanks to the academic staff at the department of Animal, Plant and Soil Sciences, department of Physiology, Anatomy and Microbiology,

department of Biochemistry and Genetics, and Centre for AgriBioscience for their support and encouragement.

Special thanks to my dear friends, Dr Shilpa Kapoor, Dr Rahul Srivastava, Dr Ritushree Jain, Dr Serpil Kucuktepe, Fahad Rasheed, Devinder Kaur, Sharanya Rajesh and Ajay Yadav for their invaluable friendship, support, encouragement and at times scientific input through all these years.

I am forever indebted to my parents for their unconditional love, care, infinite patience and for providing me with all the opportunities and experiences that have made me the person I am today, and whose career pursuits continue to inspire my own. Special thanks to my adorable siblings, Roma and Pankaj for being my pillars of strength, for their love and encouragement in all my endeavours and their fun-filled conversations. I would also like to pay special regards to my paternal grandmother Chandrabai Sirwani who always enforced the importance of education since my childhood. I am blessed to have you all in my life.

This acknowledgement is incomplete without expressing my deepest gratitude to my beloved husband Arpit whose presence has had a profound impact on my life. Special thanks to him for being my best friend, for putting up with my odd hours, for always taking care of me and for sharing this exceptional life changing journey with me. Needless to say, all omissions and errors are mine.

I would like to dedicate this thesis to the loving memory of my maternal grandmother Parvati Sundrani, who continues to inspire me every single day!

Chapter One

General introduction

1.1 Alzheimer's disease pathology

Dementia is a clinical term used to define the progressive impairment of brain function, affecting memory, cognition, and personality. It imposes a significant challenge to the health and aged care sectors and affects almost 1 in 3 people over the age of 65 (O'Brien and Wong, 2011). According to the Australian Bureau of Statistics (2018), dementia is the second leading cause of death in Australia. Based on the Dementia Prevalence Data 2018-2058, the estimated number of people living with dementia in 2020 is 459,000 and this is expected to increase to 590,000 by 2028 and 1076,000 by 2058. The most common form of dementia is Alzheimer's disease (AD) accounting for up to 50-75% of all dementia cases. The histopathological characteristics of AD were described over 100 years ago in 1906 by a German psychiatrist, Dr. Alois Alzheimer, who published a report describing the pathological changes in the cerebral cortex of a 55-year-old woman named Auguste with progressive dementia, displaying behavioural and psychiatric symptoms including paranoia, delusions, hallucinations, and impaired memory, which got progressively worse over 5 years until she died of another illness in 1906 (Verdile G., 2009).

AD is a complex, progressive, and multifactorial neurodegenerative disorder. The exact cause is unclear; however, disease presentation and progression are influenced by one or more genetic, epigenetic, and environmental factors (Huang and Mucke, 2012). Since it is the most common form of dementia, it has emerged as a major public health issue with the rise of an aging population (Barage and Sonawane, 2015; Ewald and Li, 2010; Stelzma et al., 1995). Globally, AD is mainly prevalent in 10% of the population over the age of 65, showing dramatic increase with age, with approximately 50% of people at the age of 85 at the risk of developing the disease (Huang and Mucke, 2012). Behavioural symptoms include progressive declines in short-term memory, spatial attention, reasoning

and languages, leading to difficulties in performing daily functional activities and withdrawal from social life (Zhao et al., 2014).

In the human AD brain, there is an overall loss of brain volume as a result of neuronal death and shrinkage in specific regions of the brain resulting in neurotransmitter deficits and inflammation (Gomez-Isla et al., 1997; Huang and Mucke, 2012; Mucke, 2009). In addition, the disease causes loss of specific neuronal subsets and synaptic dysfunction (Huang and Mucke, 2012). Some neuronal subsets are more vulnerable to damage than others, such as neuronal circuits in the neocortex, hippocampus and basal forebrain cholinergic system (Price and Sisodia, 1998; Price et al., 1998a; Price et al., 1998b). The two important pathological hallmarks of the disease are the intracellular neurofibrillary tangles (NFTs) formed by the aggregates of hyperphosphorylated tau protein accumulating in the form of paired helical filaments and the extracellular senile plaques composed of aggregates of amyloid beta (A β) peptides (Kosik et al., 1986). There are two major forms of AD: (i) late onset sporadic AD and (ii) early onset familial AD, which differ depending on etiological, pathological, genetic and biochemical factors (Sadigh-Eteghad et al., 2015).

The late onset sporadic form of AD accounts for 90% of the cases and occurs after the age of 65 (Campion et al., 1999; Chartier-Harlin et al., 1991; Miklossy et al., 2003; Murrell et al., 1991). The presence of the apolipoprotein E (ApoE) ϵ 4 allele is shown to be a risk factor for late onset AD (Meyer et al., 1998; Sadigh-Eteghad et al., 2012). ApoE is a cholesterol and lipid carrier in the brain critical for A β catabolism. In addition, ApoE receptors are responsible for the clearance of A β across the blood brain barrier in AD (Mawuenyega et al., 2010; Wildsmith et al., 2013). On the other hand, the early-onset familial AD is genetically determined and has been reported in patients as young as 25, accounting for 5-10% of the AD cases. A number of mutations have been associated with early onset AD, including those in genes that encode the amyloid precursor protein (APP), presenilin 1 (PS1) and, presenilin 2 (PS2) (Bertram et al., 2010). APP (described in more detail below) has been associated with AD in a number of ways; for example, individuals with Down syndrome carry an extra copy of the APP gene due to trisomy of chromosome 21, which has been proposed to cause high incidence of early onset AD (Millan Sanchez et al., 2012; Rovelet-Lecrux et al., 2006). Therefore, increase in APP

expression may also be a risk factor for late-onset AD (Brouwers et al., 2006). Presenilins are a part of the γ -secretase complex active site and are involved in APP cleavage and production of A β (De Strooper, 2003). Mutations in the presenilin protein can change the activity of the γ -secretase complex resulting in an increase in the ratio of A β _{42/40} species which readily aggregate to form senile plaques (Ridge et al., 2013). However, it is difficult to determine the temporal sequence of events leading to the disease pathology due to the inaccessibility of the human brain (Link, 2005).

1.1.1 Amyloid precursor protein processing

APP has been identified as a key molecule involved in the pathogenesis of AD and belongs to a family of amyloid precursor like proteins (APLP). The APP family of proteins consist of APLP1, APLP2 and APP. Although APLP1 and APLP2 share a high degree of similarity to APP within the intracellular and extracellular domain, these proteins lack the A β domain (Slunt et al., 1994; Sprecher et al., 1993; Wasco et al., 1992; Wasco et al., 1993a; Wasco et al., 1993b). All of them are single-pass membrane proteins with large extracellular domains, however, only APP generates amyloidogenic fragments due to the presence of an internal A β site (O'Brien and Wong, 2011). APP is an integral transmembrane glycoprotein that consists of the following domains: an N-terminal signal peptide, a large ectodomain with sites for N-glycosylation, an amyloid region (A β), an alternatively spliced kunitz-type serine protease inhibitor (KPI) domain, a single membrane spanning helix, and a short cytoplasmic tail (Price et al., 1998a). The alternate splicing of the APP transcript generates 8 isoforms, 3 being the most common. The isoform predominantly expressed in the central nervous system is 695 amino acids in length, whereas the other two 751 and 770 amino acid isoforms are ubiquitously expressed (Bayer et al., 1999). Although the precise function of APP is unclear, several studies have indicated that it plays an important role in the neurite outgrowth modulation (Hoe et al., 2009), copper homeostasis regulation (Bellingham et al., 2004), synaptic transmission and formation, and synaptic function and activity (Herard et al., 2006; Priller et al., 2006). As shown in Figure 1.1, APP is processed by three secretase enzymes,

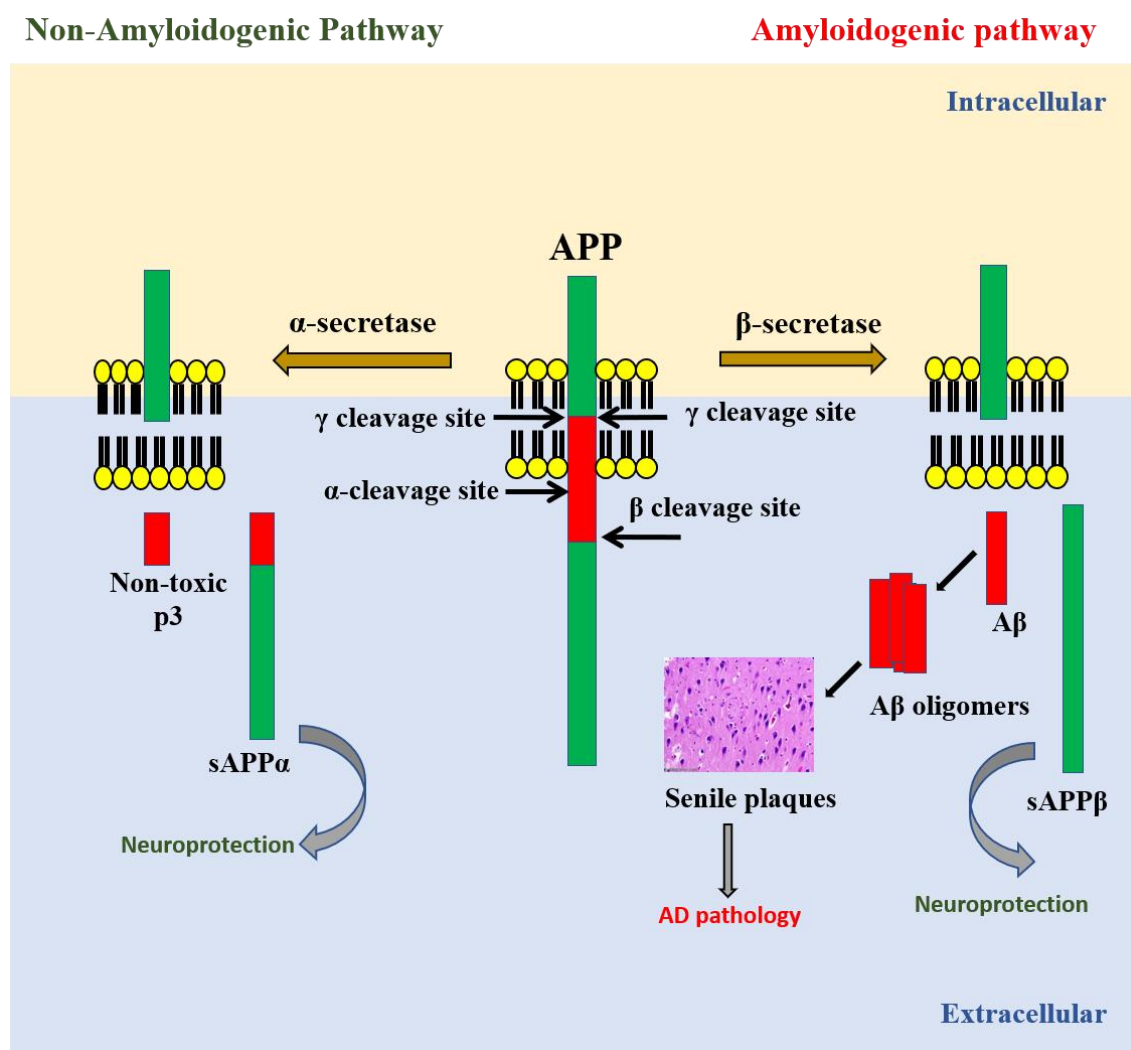


Figure 1.1: Comparison of APP processing in normal and AD brain by α -, β - and γ -secretases.

In the normal human brain, APP is processed via non-amyloidogenic pathway, where it is cleaved by α - and γ - secretases within the A β domain to yield soluble sAPP α and non-toxic p3 fragments. In the AD human brain, APP is processed via amyloidogenic pathway, being first cleaved by β -secretase to give soluble sAPP β and then imprecisely by γ - secretase to yield intact A β peptides, which may be present as soluble A β oligomers or aggregated with other proteins to form senile plaques. Modified from Hicks, Nalivaeva & Turner 2012.

namely α -, β - and γ - secretases, by either the amyloidogenic pathway or non-amyloidogenic pathway (Wilson et al., 1999). These pathways are regulated by factors such as diet, hormonal status, and genetic mutations (Gandy and Petanceska, 2001; Verdile et al., 2004). Under normal circumstances, APP is processed via the non-amyloidogenic pathway wherein the α - and γ -secretases cleave APP within the A β domain resulting in the formation of non-amyloidogenic p3 fragments and the soluble N-terminal α APP fragments. The α -secretase can occur either intracellularly or at the cell surface (Haass and Selkoe, 1993). On the other hand, in the disease scenario, APP is processed via the amyloidogenic pathway involving the β -secretase APP-cleaving enzyme (BACE) which cleaves APP at the N-terminal to release soluble β APP fragments and the C99 soluble fragment, which contains the intact A β domain. This C99 soluble peptide is then further cleaved imprecisely by the heteromeric γ -secretase complex which generates A β peptides of varying lengths (Echeverria and Cuello, 2002; Wilson et al., 1999). The spectrum of A β peptides produced contain ragged N- and C- termini of which approximately 90% are the soluble A β 1-40 whereas 10% of the peptides are A β 1-42(43) species. The A β 1-42 are fibrillogenic and therefore can readily aggregate to form senile plaques (Haass and Selkoe, 1993; Price et al., 1998a).

1.1.2 A β peptide as a driver of neurotoxicity

The A β peptide has been proposed to play a central role in the onset and progression of AD (Findeis, 2007). A β is produced in numerous cell types including neurons, astrocytes, neuroblastoma cells, hepatoma cells, fibroblasts, and platelets (Atwood et al., 2003). Under normal circumstances, A β produced in low concentrations may have a role in neural development (Sadigh-Eteghad et al., 2014) and in the regulation of cholinergic transmission (Harkany et al., 2000). A β produced at physiological levels is neuroprotective by reducing both the excitatory activity of potassium channels and neuronal apoptosis. Additionally, it is proposed to protect the neurons in a concentration-dependent manner due to antioxidant properties demonstrated *in vitro* (Nunomura et al., 2006). Picomolar concentrations of A β are shown to have protective effects such as antimicrobial activity, blocking leaks in the blood-brain barrier, assisting in recovery from posttraumatic brain injury, and cancer suppression (Brothers et al., 2018). The A β peptide



Figure 1.2: The amyloid (or A β) cascade hypothesis.

Gradual changes in the steady-state levels of amyloid β -protein (A β) in the brain are thought to initiate the amyloid cascade. A β levels can be elevated by enhanced production and/or reduced clearance. In particular, the A β 42/A β 40 ratio can be augmented by mutations in three different genes (β -amyloid precursor protein (*APP*), presenilin-1 (*PS1*) and *PS2*) that cause familial forms of Alzheimer's disease. The relative increase of A β 42 enhances oligomer formation, which cause subtle and then increasingly severe and permanent changes of synaptic function. In parallel, A β 42 forms microscopically visible deposits in the brain parenchyma, first as relatively benign diffuse (non-fibrillar) plaques. As the diffuse plaques begin to acquire fibrils of A β , local inflammatory responses (microgliosis and astrocytosis) are observed. Synaptic spine loss and neuritic dystrophy also occur. Over time, these events result in oxidative stress, altered ionic (for example, calcium) homeostasis and a host of additional biochemical changes. Neurofibrillary tangles are induced by altered kinase and phosphatase activities and contribute to additional defects, including some in axonal transport. The cascade culminates in widespread synaptic/neuronal dysfunction and cell death, leading to progressive dementia associated with extensive A β and tau pathology (Haass & Selkoe, 2007).

has also been shown to enhance synaptic plasticity, learning and memory in mouse models (Morley et al., 2019). However, under pathological conditions, there is an imbalance between the production and clearance of A β that ultimately leads to the accumulation of A β (Harkany et al., 2000; Qiu et al., 2009). This accumulation of A β triggers a pathological cascade leading to synaptic dysfunction and disease.

The A β peptides released in the cytosol as monomers can assemble in distinct ways based on length, microscopic dimensions, and molecular weight (Sadigh-Eteghad et al., 2015). The A β monomers can self-assemble into different forms ranging from dimers to nonfibrillar oligomers; however, they can also aggregate to form insoluble fibrillar senile plaques (Walsh and Selkoe, 2007). Initially, the senile plaques were thought to be the toxic form of A β , inducing neurotoxicity by disrupting synaptic function (Moreira et al., 2010; Shankar and Walsh, 2009). However, subsequent studies confirmed that the amount of A β deposition does not correlate well with the severity of the disease (Dickson et al., 1995; Katzman, 1986; Terry et al., 1991). Although the presence of senile plaques is an important pathological indicator of the disease, they are also found in individuals that do not have the disease (Link, 2005). On the other hand, *in vitro* studies have shown the A β monomers can assemble into three types of A β oligomers: (i) short oligomers ranging from dimer to hexamers (Bitan et al., 2003; Levine, 1995), (ii) A β -derived diffusible ligands (ADDLs) that are small oligomers ranging from 17 to 42 kDa (Lambert et al., 1998), and (iii) protofibrils that are short fibril intermediates of < 8 nm in diameter and <150 nm in length (Harper et al., 1997; Walsh et al., 1997; Yong et al., 2002). A β protofibrils also appear prior to the formation of mature senile plaques and are known as prefibrillar assemblies (Kirkkitadze and Kowalska, 2005; Shankar and Walsh, 2009). Numerous studies have emphasized that all A β oligomers play a critical role in neuronal dysfunction by disrupting the cellular membranes of digestive organelles resulting in ions and digestive enzymes leaking into the cytoplasm (Hepler et al., 2006; Li et al., 2012; Park et al., 2016; Takahashi et al., 2002a; Tew et al., 2008). Furthermore, it has been suggested that oligomeric A β species are 10 times more toxic than the A β fibrils (Bucciantini et al., 2002; Dahlgren et al., 2002; Kirkkitadze et al., 2002; Resende et al., 2008; Walsh et al., 2002). In addition, biochemical analysis of human AD brains reveals a robust correlation between levels of soluble A β species and severity of cognitive decline and synaptic dysfunction (Lemere et al., 2002; Lue et al., 1999; McLean et al., 1999;

Wang et al., 1999). Thus, A β oligomers are a likely therapeutic target for AD (De Felice et al., 2004). There are several possible ways in which the A β peptide exerts its neurotoxic effects, including causing changes in the distribution and/or activity of neurotransmitters and their receptors, disruption of intracellular calcium homeostasis, causing disruption of axonal transport and impairment of mitochondrial function (Huang and Mucke, 2012).

1.1.3 Amyloid cascade hypothesis

The amyloid cascade hypothesis is one of the central hypotheses to explain the pathogenesis of AD and has continued to dominate the field for decades (Kametani and Hasegawa, 2018). The hypothesis posits that the abnormal accumulation and aggregation of A β in the various regions of the brain are the causative agents of AD and the other symptoms such as neurofibrillary tangles, cell loss, vascular damage and dementia follow as a result of this deposition (Figure 1.2) (Hardy and Higgins, 1992). Although some studies have suggested that A β itself exerts its toxic effects in the neurons, others suggest that A β alone is not intrinsically neurotoxic but the presence of A β makes the neurons vulnerable to excitotoxic damage as it causes calcium-mediated neuronal death (Koh et al., 1990)

Several genetic studies and biomarker evaluations support the amyloid cascade hypothesis. The APP gene was discovered to be on chromosome 21 and autosomal dominant mutations in genes encoding APP and PS1, and PS2 are associated with early onset AD (Kang et al., 1987). In addition, mutations in APP that are in close proximity to the β - and γ -secretase cleavage sites result in an increase in the production of A β ₄₂ thereby altering the ratio of A β ₄₂/40 and leading to aggregate formation (Kametani and Hasegawa, 2018). For instance, individuals that carry the Osaka variant, an APP mutation that enhances the production of A β oligomers, show limited plaque pathology and, develop early cognitive symptoms of AD (Tomiya et al., 2008). Similarly, another APP mutation known as the Arctic variant results in an increase in the production of A β protofibrils and lower amyloid plaque burden; it is also associated with early onset AD (Nilsberth et al., 2001; Scholl et al., 2012). In contrast, the Icelandic mutation, an APP genetic variant resulting in approximately 40% decrease in amyloid production, is

associated with decreased AD risk. Conversely, individuals with Down syndrome, whose extra copy of chromosome 21 causes overexpression of APP, show clinical manifestations of AD at about 40 years of age (Ricciarelli and Fedele, 2017). In these individuals, the amount of APP was shown to increase to 1.5 times the normal amount and consequently the A β production was also increased (Kolata, 1985). In contrast, individuals with Down syndrome involving only the distal part of chromosome 21 telomeric to APP do not get AD (Prasher et al., 1998). A few, rare individuals have only the APP gene micro-duplicated (i.e., not the entire chromosome 21) and do not have Down's syndrome but do get AD, typically in their mid-50s (Rovelet-Lecrux et al, 2006). These studies suggest that either increased A β production or its decreased clearance are the initial triggers of AD pathogenesis (Jonsson et al., 2012).

However, the amyloid cascade hypothesis has never been universally accepted. Firstly, extensive amyloid deposits have been found in several cognitively normal individuals whereas some AD individuals have shown very few amyloid deposits in the brain (Edison et al., 2007; Li et al., 2008). Strikingly, the amyloid deposition in the cognitively normal individuals was sometimes as extensive as that of dementia patients (Davis et al., 1999; Fagan et al., 2009; Price et al., 2009). Secondly, none of the clinical trials targeting A β have been successful. However, the failures of these clinical trials could be attributed to several reasons:

- (i) Many trials were targeting either the amyloid monomers or plaques neither of which are not associated with neurotoxicity. None of the trials address the critical pathogenic role of soluble amyloid oligomers which could be potential therapeutic targets.
- (ii) The drugs being administered were not able to cross the blood brain barrier and achieve the optimum concentrations required for the desired biological response. Specifically, the antibody therapies trialled had very low brain barrier penetration with only <1.5% of an administered dose entering the brain (Cummings et al., 2018; Honig et al., 2018; Logovinsky et al., 2016; Ostrowitzki et al., 2017; Salloway et al., 2014; Sevigny et al., 2016). This is below the concentration required for the continuous removal or prevention of the formation of A β oligomers.

- (iii) Patients enrolled in the clinical trials have had concomitant neuropathology other than amyloid or tau which results in higher variability in response to the treatment
- (iv) Finally, there have been some arguments suggesting that the treatment is being administered at the wrong stage of the disease.

Therefore, the design of these trials is not rigorous enough to adequately test the hypothesis and do not invalidate the rationale for selectively targeting A β oligomers (Tolar et al., 2020).

1.2 Animal models of AD

In general, animal models have been beneficial in dissecting the underlying molecular mechanisms leading to the disease state (Gotz and Ittner, 2008). The important rationale behind using model organisms is that many of the cellular signalling pathways and genes associated with the disease are evolutionarily conserved and therefore discoveries made in the model system may give insights into more complex organisms (Di Carlo, 2012; Markaki and Tavernarakis, 2010). Table 1.1 lists the selective advantages and limitations of commonly used vertebrate and invertebrate model organisms in AD research. For instance, some of the vertebrate model systems such as zebrafish and mouse enable researchers to understand the basic biology of neurodegenerative diseases (Link, 2001).

Danio rerio, commonly known as zebrafish, is a tropical freshwater and aquarium fish named for the uniform pigmented, horizontal blue stripes on its body. The zebrafish has a fast development and generation time of 3-4 months and short lifespan of 3.5 years (Saleem and Kannan, 2018). In addition, the nervous system is structurally similar to other vertebrates and consists of special neuronal populations such as dopaminergic neurons, astrocytes, oligodendrocytes, cerebellar Purkinje cells, myelin and motor neurons (Di Carlo, 2012). The development of the nervous system has also been well characterised in zebrafish (Kimmel et al., 1995). Hence, zebrafish is an ideal choice to study neuronal development and neurodegeneration. The zebrafish genome has several gene orthologs similar to those mutated in early onset AD such as the *appa* and *appb* (APP) and presenilin related genes *psen1* (*PSEN1*) and *psen2* (*PSEN2*). In addition, co-

orthologs of the human tau gene (*mapta* and *maptb*) and the APOE gene (*apoea* and *apoeb*) have also been identified in zebrafish (Newman et al., 2014). Researchers have studied behaviours in zebrafish like feeding, learning, hearing, vision, touch and emotions like fear, pain helplessness, courtship, social interactions, anxiety and decision making (Saleem and Kannan, 2018). Although there is some degree of conservation between the human and zebrafish A β domain, the presence of the A β peptide has not been reported (Xi et al., 2011). Strikingly, zebrafish injected with A β 1-42 showed regeneration of neurons. The regeneration induced by the A β 1-42 peptide results in the activation of the microglia to prevent synaptic degeneration and promotes neurogenesis (Saleem and Kannan, 2018). Although pharmacological modifications are possible in fish, it is difficult to quantify the amount of the chemical compound that goes into the fish through the gills and skin as these substances are added in the water tanks (Rubinstein, 2006).

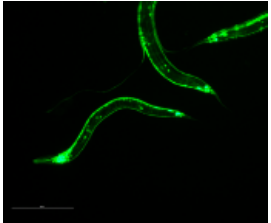
Mice have been utilized extensively in the field of AD research for several reasons. Firstly, they have a close evolutionary relationship to humans relative to other animal models, and there is structural similarity between the human and mouse brain. Secondly, there are several behavioural tests available to test specific forms of neuronal dysfunction in mice (Eriksen and Janus, 2007). However, these behavioural tests may not recapitulate the dysfunction seen in human AD precisely. Mouse models of AD, such as the Tg2756 and APP^{swe}/PS1 dE9 (APP/PS1) transgenic mice over-express human mutant APP or APP/PS1, have human A β in the brain that is deposited in amyloid plaques, and show cognitive decline, synaptic plasticity alterations, synaptic loss, and memory impairment (Hsiao et al., 1996; Jankowsky et al., 2001; Puzzo et al., 2014). Furthermore, genetic, pharmacological, and immunological approaches aimed at reducing the cerebral A β load in mouse models show reduction in synaptic loss and rescue of memory deficits (Gotz et al., 2004; Li et al., 2013). However, there are several caveats associated with these models. Although some of the mouse models show accumulation of A β amyloid fibrils, tau accumulation and neuronal loss were absent (Bryan et al., 2009; Kametani and Hasegawa, 2018). Therefore, there was no cognitive impairment in these models (Kim et al., 2013; Kim et al., 2007). In addition, the spatiotemporal distribution of A β observed in the human AD brain has not been replicated in the mouse models (Gotz et al., 2004). Another important disadvantage is that these animals accumulate A β variants that are different from those found in the human brain (Kalback et al., 2002). The mouse A β

peptides lack the extensive N-terminal degradations, posttranslational modifications, and cross-linkages that are abundant in stable human A β peptide deposits found in humans. In addition, there is a difference in the oligomeric A β species found in the mouse and human AD brain, as the ones found in mice are not formic acid stable (Kalback et al., 2002). Therefore, these peptides may not recapitulate all aspects of the human disease as they may have different physiochemical properties and therefore different pathogenic properties *in vivo*. In addition, the mouse A β peptide is less prone to aggregation as compared to the human A β peptide as a result of three amino acid substitutions in the N-terminal region, Arg5Gly, Tyr10Phe, and His13Arg (Fraser et al., 1992; Yamada et al., 1987). A further limitation is that creating mouse models is labour intensive, time consuming and expensive (Hart and Chao, 2010).

Various immunotherapies that led to a decrease in the amyloid plaque in mouse models did not show improvement in cognitive symptoms such as memory in human clinical trials (Doody et al., 2014; Giacobini and Gold, 2013; Ostrowitzki et al., 2012; Salloway et al., 2014). Therefore, none of the strategies successful in mice have translated to clinical outcomes in AD patients (Ameen-Ali et al., 2017). The reasons are complex and multifactorial, but include differences in mechanisms of drug action and metabolism, in addition to the fundamental differences of the neuronal network of human and mice (Van Dam and De Deyn, 2011). For instance, targeting β -secretase in Tg2576 mice by administering the non-peptidic BACE1 inhibitor TAK-070 reduced the soluble and insoluble A β and led to a reduction in cognitive impairments (Fukumoto et al., 2010). On the other hand, verubecestat a promising BACE1 inhibitor, recently failed to show any improvement in a human clinical trial (Mullard, 2017). Although mice are more closely related to humans than invertebrates, invertebrate models may be more easily manipulated so that they recapitulate the progression of AD in humans. Alternative approaches have focussed on invertebrate model systems to recapitulate specific molecular and cellular aspects of the disease (Di Carlo, 2012; Link, 2001). The two invertebrate model systems used extensively for AD studies are the vinegar fly *Drosophila melanogaster* and the nematode *Caenorhabditis elegans*. Use of these model organisms takes advantage of their well understood genetics, relative ease of gene

Table 1.1: Suitability and limitations of commonly utilized model organisms to study AD. Adapted and modified from (Gotz et al., 2004)

Species	Selective advantages	Selective limitations	Modelled aspects of AD
Vertebrate model organisms			
 <p><i>Mus musculus</i></p>	<ul style="list-style-type: none"> • Brain anatomy similar to humans. • NFT and plaque staging, regional vulnerability can be addressed. • Sophisticated behavioural tests possible. • Therapeutic treatments possible; monitored by histopathology and behavioural tests. 	<ul style="list-style-type: none"> • Production and breeding of transgenic mice; time-consuming, laborious, inefficient and expensive. • Ethical considerations limit animal numbers and prohibit certain experiments. • High throughput drug screening (HTS) not possible. • No neuronal loss. • Aβ species different from the ones found in the human brain. 	<ul style="list-style-type: none"> • Proof of role of FAD genes in AD pathology. • Role of lipid metabolism and inflammation in AD confirmed. • Histopathology: plaques, NFT, synapse loss, glial pathology; but no massive neuronal losses. • Behavioural impairment associated with region-specific pathology.
 <p><i>Danio rerio</i> (Saraceno et al., 2013)</p>	<ul style="list-style-type: none"> • Development of the nervous system is well characterized, therefore possible to analyse complex brain functions characteristics of vertebrates (Kimmel et al., 1995; Panula et al., 2006). • Significant homology to mammals, including humans (Esch et al., 1990). • Faster development and longer lifespan compared to mice. • High reproductive rate. • Embryos transparent and development externally. 	<ul style="list-style-type: none"> • Expensive to maintain. • Difficult to modify genetically. 	<ul style="list-style-type: none"> • Several aspects of presenilin gene biology revealed using zebrafish model (Newman et al., 2014).

Invertebrate model organisms			
 <p><i>Caenorhabditis elegans</i></p>	<ul style="list-style-type: none"> • Easy and fast to breed, cheap, no ethical limitations. • Powerful genetics. • Suppressor and enhancer (modifier) screens possible, drug screening possible. • RNA interference allows inactivation of thousands of genes in parallel. • Well established behavioural assays that can serve as direct readout. • The worm ortholog <i>apl-1</i> does not contain an Aβ domain and does not have β-secretase, which ensures faithful expression of transgenic human Aβ peptide. • Possible to study the <i>in vivo</i> toxicity of a single Aβ peptide at a time in isolation from other confounding factors. 	<ul style="list-style-type: none"> • Genome does not encode for all the human genes. • Behavioural abnormalities of AD difficult to address. • NFT and plaque staging, regional vulnerability impossible to address. 	<ul style="list-style-type: none"> • Isolation of AD-related genes. • Behavioural and synaptic abnormalities.
 <p><i>Drosophila melanogaster</i></p>	<ul style="list-style-type: none"> • Easy and fast to breed, cheap and no ethical limitations. • Modifier screens and drug screenings possible. • Powerful genetics. • UAS GAL 4 reporter systems. 	<ul style="list-style-type: none"> • Brain anatomy different from humans. • Behavioural abnormalities in AD difficult to address. • NFT and plaque staging, regional vulnerability impossible to address. 	<ul style="list-style-type: none"> • Analysis of the physiological role of APP with implications for pathological role such as impaired axonal transport. • Neurodegeneration in the absence of NFT formation.

manipulations, and the availability of experimental tools that are not available in mammalian systems (Di Carlo, 2012; Gama Sosa et al., 2012; Link, 2001). An advantage of *D. melanogaster* is availability of tools such as the GAL4-/UAS-system used in reverse genetic approaches to express human or fly proteins in a tissue- and time-dependent manner (Brand and Perrimon, 1993; Jeibmann and Paulus, 2009). Additionally, the fly has inducible promoters to allow for spatiotemporal regulation of gene expression (Dietzl et al., 2007; Matthews et al., 2005; Venken and Bellen, 2005). Conversely, the biggest advantage of using the nematode *C. elegans* as a model system is the presence of single-cell resolution for the molecular and cellular basis of specific behaviours (described in detail below).

1.3 *Caenorhabditis elegans* as a model to study age-related neurodegeneration

The free-living nematode *C. elegans* is a powerful experimental *in vivo* system to study the molecular and cellular events associated with human disease such as AD. The *C. elegans* genome has been sequenced, with 80% of the genes predicted to have human orthologs (Harris et al., 2004). Of those human genes that cause diseases, approximately 42% have an ortholog in *C. elegans* (Markaki and Tavernarakis, 2010). This high degree of conservation has facilitated numerous unbiased forward and reverse genetic screens employed to unravel complex molecular and cellular mechanisms, and disease phenotypes (Link, 2006; Markaki and Tavernarakis, 2010). Mutant strains that lack a gene can be easily identified and rapidly phenotyped (Hariharan and Haber, 2003). Protein-protein interactions, mutant and/or RNA interference (RNAi) phenotypes, and microarray data are all available on a public data repository, WormBase (www.wormbase.org) (Chen et al., 2005).

Since *C. elegans* is optically transparent throughout its life cycle, *in vivo* imaging of GFP tagged proteins is possible. For instance, GFP tagging of specific proteins allows the imaging of neuronal cell dystrophy through the lifetime of the animal (Teschendorf and Link, 2009). Furthermore, strains can be stored indefinitely in liquid nitrogen allowing large mutant repositories to be set up (Stiernagle, 2006). Therefore, *C. elegans* is a

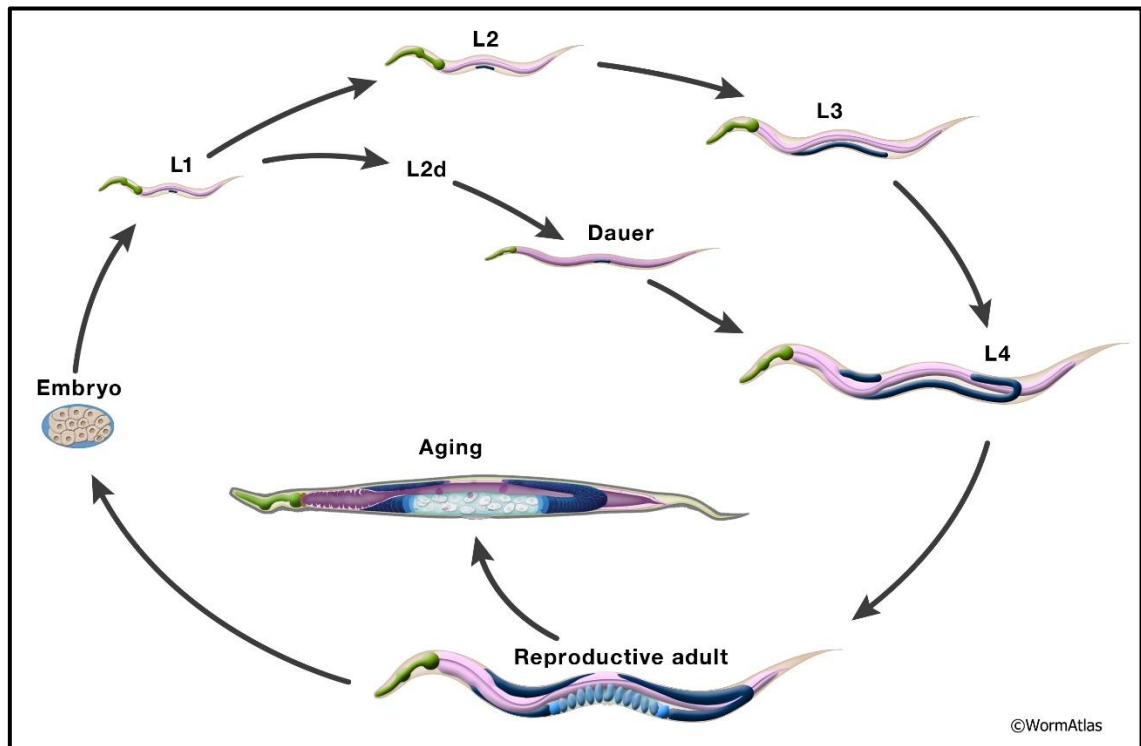


Figure 1.3: Life cycle of the nematode *Caenorhabditis elegans*.

C. elegans larval development proceeds through 4 larval stages (L1 through L4). L4 larvae moult into adults that survive for approximately 3 weeks under normal laboratory conditions; age-associated declines can be measured as various aging "phenotypes" over adult life. L1 larvae may proceed through the alternate dauer pathway under harsh environmental conditions. Dauer larvae are adapted for long-term survival and dispersal to new environments. Once in a more favourable environment, dauer larvae re-enter reproductive development by moulting into the L4 larval stage and progressing through the rest of the life cycle normally.

convenient and useful model to obtain a better understanding of the fundamental aspects of neuroscience, development, signal transduction, ageing, cell death, and mechanisms of drug action (Standaert and Yacoubian, 2010; Wang et al., 2011).

Another important advantage of using *C. elegans* for studying aging is that it has a short lifespan of about 2-3 weeks and a generation time of 3.5 days at 20 °C proceeding from larval stages (L1-L4) through to adulthood (Figure 1.3). This facilitates the rapid generation of transgenic strains thereby allowing quick evaluation of experimental interventions (Di Carlo, 2012). The adult worm is 1 mm in length, 80 µm in diameter and can either be male or hermaphrodite. The adult hermaphrodite is made up of 959 somatic nuclei and is optically transparent, allowing identification of specific cells. Each hermaphrodite can produce up to 300 progeny if self-fertilized and even more if crossed with males, which occur at a frequency of 0.1-0.2% in normal populations of Bristol N2 (Brenner, 1974; Hart and Chao, 2010). Several behavioural and physiological phenotypes of the worm undergo age-related decline during the post reproductive stage, ultimately leading to death.

C. elegans is an excellent model organism to study AD and other neurodegenerative diseases. The well-characterised nervous system of *C. elegans* consists of only 302 neurons, and the position and identity of each neuron is reproducible from animal to animal (White et al., 1986). As shown in Figure 1.4, *C. elegans* neurons are organised into several ganglia in the head and the tail, and into the ventral and dorsal nerve cords (Hobert, 2003). The pattern of synaptic connections has been reconstructed by serial electron microscopy (White et al., 1986). According to their topology and synaptic connection patterns, neurons have been grouped into different classes including chemosensory, mechanosensory, and thermosensory neurons. (Di Carlo, 2012). Moreover, 75 motor neurons innervate the body wall muscles (excluding the head), 56 of which are cholinergic and 19 GABAergic. Additionally, *C. elegans* larvae contain 4 serotonergic and 8 dopaminergic neurons (Teschendorf and Link, 2009). It is still the first and currently the only organism with a largely complete neural connectome, with neurons being connected by approximately 7800 synapses and 900 gap junctions (Byrne et al., 2017). Since robust behavioural assays are available, they have been beneficial in the identification of many genes affecting the development and function of the nervous

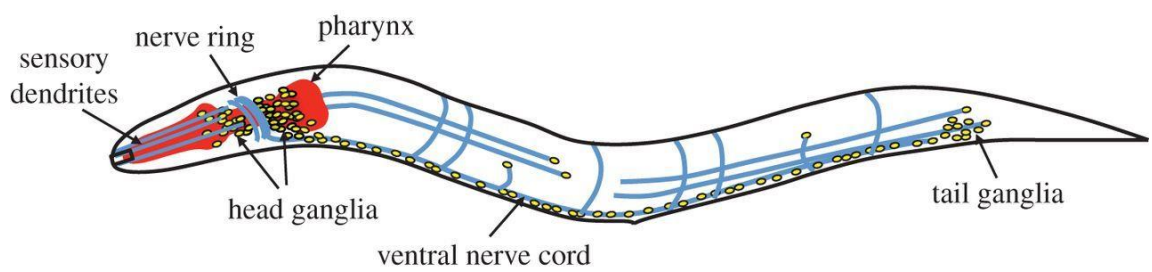


Figure 1.4: Overview of the *C. elegans* nervous system.

The majority of neurons are located in several ganglia near the nerve ring (Adapted from Fang-Yen, Alkema, & Samuel, 2015).

system, proving to be predictable output of neuronal health (Byrne et al., 2017; Griffin et al., 2017). Not only are the cellular and molecular mechanisms of these behaviours understood but also the underlying genetic basis have been identified. Ion channels, receptors, classic neurotransmitters (acetylcholine, glutamate, γ -aminobutyric acid (GABA), serotonin, and dopamine), vesicular transporters and the neurotransmitter release machinery are similar in both structure and function between vertebrates and *C. elegans* (Barclay et al., 2012; Hardaway et al., 2012). Therefore, there is a rich contextual background cellular information that can be overlaid with transgene expression and phenotype at single-cell resolution to understand not only how a transgene functions in particular cell types but also how the expression of that transgene may affect other aspects of neuronal function.

1.4 *C. elegans* behaviours to study age-related neurodegeneration

Neurodegenerative diseases are characterised by the progressive loss of neuronal function. This loss is a result of deterioration of the structure and function of specific neuronal subsets that can then present as behavioural deficits (Chen et al., 2015). Several well-established neuronally-controlled behaviours have been used to assess age-related neurodegeneration in *C. elegans*, and the effect of genetic manipulations or drugs on the survival and function of specific neuronal populations in the *C. elegans* nervous system can be readily studied *in vivo* (Chen et al., 2015).

Since aging is the greatest risk factor for neurodegenerative diseases, one of most commonly used assays to study the aging process in *C. elegans* is the life span assay (Amrit et al., 2014). Although the terms “lifespan” and “aging” tend to be used interchangeably, they are not equivalent (Tissenbaum, 2012). Lifespan is a single parameter that measures the amount of time an organism survives. It does not indicate the health (physiological and functional status) of the animal (Tissenbaum, 2015). Hence, it is crucial to define the quantitative changes associated with physiological aging to better understand the process of aging and expedite the development of therapies (Son et al., 2019). Healthspan can be defined as the time that an individual is active, productive and free from age-associated diseases (Tissenbaum, 2015).

Measuring healthspan, in addition to lifespan, is feasible in *C. elegans*. *C. elegans* exhibits several behaviours that are important for its survival and reproduction, and are therefore potentially useful indicators of healthspan because those behaviours are indicative of functionality: locomotion (crawling and swimming), feeding (pharyngeal pumping), defecation, egg-laying, mating, and its ability to sense and respond to chemical, mechanical and thermal stimuli. *C. elegans* motility is a useful marker to assess healthspan (Bansal et al., 2015). The classic sinusoidal pattern of movement is controlled and coordinated by the dorsal and ventral muscles, and is influenced by the presence or absence of food and exposure to mechanical or chemical stimuli (Croll, 1975; Donnelly et al., 2013; Omura et al., 2012). Additionally, some studies have shown that genetic mutations or exposure to environmental toxins can also change the motility of the worms, resulting in irregular body bends (Ali and Rajini, 2012; Cooper et al., 2015; Liu and Sternberg, 1995). *C. elegans* maximum speed is an indicator of healthspan of the animal and is strongly correlated with longevity (Hahm et al., 2015). About 130 neuron and muscle specific genes have been identified that affect locomotion. These include *myo-3* (myosin heavy chain structure 3) in muscle formation, *unc-18* (uncoordinated 18) in neural function, *unc-6* in neuronal pathfinding, *cha-1* (abnormal choline acetyl transferase 1) in acetylcholine function, *unc-47* in γ -aminobutyric acid (GABA) function, and *snb-1* (synaptobrevin 1) in synaptic release mechanisms. The muscle contraction that leads to complete bending of either the dorsal or ventral side of the animal is defined as a single body bend (Ghosh and Emmons, 2008). On the other hand, the term “thrashing” is defined as the movement of worms in liquid determined either by measuring the frequency of lateral movements or the direction of mid-body bending (Buckingham and Sattelle, 2009). Previous studies have showed that movement on solid and liquid media measure different aspects of health and behaviour since the kinematics of swimming is distinct from that of crawling (Rollins et al., 2017). Since decline in motility is an early effect of aging, it may eventually compromise other behavioural responses (Glenn et al., 2004). Pharyngeal pumping across age has also been positively correlated with lifespan in *C. elegans* (Luo et al., 2009). The rhythmic contraction and relaxation of the neuromuscular pharynx enables worms to ingest bacteria. This rate of pharyngeal pumping varies between individual worms and among environments that the worms are in and declines progressively with age (Luo et al., 2009). The age-related decline in motility

and pharyngeal pumping are positively correlated with lifespan and are also essential for the survival of the organism. There may be a common regulatory mechanism mediating these processes and therefore declines in these important parameters may cause reduced life expectancy (Huang et al., 2004).

Reproduction is an excellent indicator of the organism's general physiological health. When reproduction is affected adversely, physiological decline starts early because reproduction in *C. elegans* hermaphrodites is completed while the animal is relatively young, whereas most of what lifespan assays measure is post-reproductive. Reproductive aging in *C. elegans* hermaphrodites is characterized by a progressive age-related decline of physiological function beginning on the 5th day and ceasing on 10th-14th day of adulthood (Andux and Ellis, 2008; Hughes et al., 2007; Mendenhall et al., 2011). Egg-laying is a well-studied aspect in *C. elegans* physiology and an important reproductive indicator of healthspan (Maulik et al., 2017). *C. elegans* eggs are fertilized internally: a mature oocyte is ovulated and passed on to the spermatheca where it is fertilized either by self-sperm generated during the L4 larval stage or by male sperm deposited after copulation (Greenstein, 2005). The hermaphrodite accumulates fertilized eggs for ~ 2.5 hours, containing about 10-15 eggs *in utero* at any given time. Once laid into the environment, they hatch after ~10 hours (Pickett and Kornfeld, 2013; Schafer, 2005). Egg-laying occurs via a simple motor program in which the smooth muscle cells contract thereby releasing the eggs by opening the vulva and compressing the uterus. The egg-laying circuit consists of the uterine muscles, vm1 and vm2 muscles, the HSN motor neurons, and the VC motor neurons (Schafer, 2006). Egg-laying occurs in a specific temporal pattern consisting of two distinct phases: active and inactive. In the active phase, eggs are laid frequently in short bursts of 1-2 minutes, separated by the longer quiescent inactive phase wherein eggs are retained (Schafer, 2005). This distinct egg-laying behaviour is modulated by specific subset of neurons and neurotransmitters, with the HSN motor neurons employing serotonin, acetylcholine, and neuropeptides (Desai and Horvitz, 1989; Horvitz et al., 1982; Schafer, 2006). Mutants with decreased brood size have low levels of dopamine (Maulik et al., 2017). That said, reproductive span was not correlated with the age-related declines in motility, pharyngeal pumping, or survival probability, which suggests that reproductive span may be regulated independently of these processes (Huang et al., 2004). Perhaps this correlation may change if the

hermaphrodite worms are mated with males, which replenishes their sperm thereby increasing progeny production 3-4 fold and doubling the reproductive span. Thus, although fecundity is accepted as a measure of healthspan, it may not necessarily correlate with specific age-related neuronal deficits. Furthermore, fecundity is sensitive to a range of biological and environmental influences, and both endogenous and exogenous factors can contribute to changes in fecundity. Therefore, even though fecundity is a good measure of overall healthspan, it does not allow the determination of the underlying causes of changes in those measures of healthspan.

There are other neurodegenerative phenotypes which may or may not affect either healthspan or lifespan but are mediated by specific neuronal subsets that can be manipulated or tested. The ability of *C. elegans* to respond to chemosensory stimuli is one of the most extensively studied behaviour in the worms. *C. elegans* use chemosensation to locate food, avoid toxic conditions, to progress in stages of development and for mating (Hart and Chao, 2010). The worms have a highly-developed chemosensory network consisting of 16 pairs of anatomically bilateral symmetric neurons which respond to a wide range of soluble and volatile odorants (Bargmann et al., 1993). The four visible types of chemosensory neurons are the amphid, phasmid, inner labial, and outer labial neurons with each consisting of sheath and socket cells forming a pore through which the sensory neurons are exposed to the external environment (Hart and Chao, 2010; Ward, 1973; White et al., 1986). The amphid pores are located at the tip of the head and are critical for the animal's ability to respond to chemical stimuli. The phasmid pores located near the tail, although being structurally similar to the amphid pores, are smaller and contain sensory endings of PHA and PHB neurons, which are implicated in chemosensory avoidance (Hart and Chao, 2010). Chemosensory neurons directly or indirectly synapse onto the command interneurons that control locomotion through synapses with motor neurons, which in turn control body wall muscles (Chalfie et al., 1985). Of the chemosensory neuron pairs, AWA and AWC detect volatile attractants; ASE neurons detect soluble attractants; ASH, ADL, and AWB detect volatile (and soluble) repellents; ASI, ADF, and ASJ are involved in dauer formation, along with minor roles in soluble attractant and are the sensory neurons involved in the detection of O₂ and CO₂ (Hart and Chao, 2010). The worm's ability to sense chemical stimuli in the environment is measured using a well-established chemotaxis assay. Chemotaxis towards a particular

odorant is measured by establishing a gradient of attractant/repellent from a point source and counting the number of animals at the point after a fixed time (Bargmann et al., 1993). The amphid sensory AWA neurons, detect at least three volatile odorants (diacetyl, pyrazine, and 2,4,5-trimethylthiazole) whereas the AWC neurons detect at least five attractive odours (benzaldehyde, butanone, isoamyl alcohol, 2,3-pentanedione, and 2,4,5-trimethylthiazole) (Hart and Chao, 2010). Previous studies have established a link between chemotaxis behaviour and deficits in motility in day 8 adult worms: although sensory abilities appear to be similar in young (day 2) and middle-aged (day 8) worms, the decrease in chemotaxis response on day 8 may be attributed to a decline in motility (Glenn et al., 2004).

Interestingly, *C. elegans* are capable of learning about mechanosensory, chemosensory and thermosensory inputs and integrating this learnt sensory behaviour to approach or avoid tastes, odours, or temperatures (Hedgecock and Russell, 1975; Mori, 1999; Rose and Rankin, 2001; Wen et al., 1997). Additionally, they are capable of associative and non-associative forms of learning such as classical conditioning and habituation (Rankin, 2004). For instance, when worms are provided with food at a specific temperature and then transferred to a thermal gradient, they locate and crawl along the gradient to the corresponding feeding temperature (Hedgecock and Russell, 1975). Moreover, *C. elegans* possess both short- and long-term memory (Rankin et al., 1990). Food is a fundamental environmental cue, the presence or absence of which profoundly influences *C. elegans* behaviour (Sasakura et al., 2013). *C. elegans* movement changes in the presence or absence of food and with changes in feeding status (satiety vs starvation). When well-fed, wild-type animals move more slowly in the presence of bacteria in comparison to movement in the absence of bacteria. This is a form of foraging behaviour which is dependent on dopamine, and which detects the presence and availability bacterial food. Locomotion of well-fed worms slows in the presence of food (Sawin et al., 2000). This slowing response is known as the basal slowing response, and deficits in dopaminergic signalling lead to diminished slowing response (Yao et al., 2013), (Chen et al., 2013). Starved *C. elegans* slow even further in the presence of bacteria, and this response, known as enhanced slowing response, ensures that the worms do not leave the food source (Rivard et al., 2010; Sawin et al., 2000). The enhanced slowing response is modulated by serotonin (Sawin et al., 2000). Slowing response requires that the worms are able to sense

food and are able to integrate that sensory signal of presence or absence of food with behaviour, modifying their movement in the light of their previous experience. This requires that they have intact neuronal sensory capability along with the neuronal capacity for processing and integrating information. Because this complex behaviour involves different kinds of neuronal function in different neurons, it is a good indicator of neuronal health. Although the behaviour requires neuronal complexity to function, the behavioural output is a simple phenotype that is easy to measure and gives insights into a relatively complex neuronal process.

1.5 *C. elegans* models for AD research

The two possible methods by which *C. elegans* model systems for disease research can be developed are either (i) by manipulating the *C. elegans* gene orthologs known to be involved in the disease-causing pathway or (ii) by expressing the human-disease related variant in the model organism (Mhatre et al., 2013).

C. elegans as a model provides useful information about disease progression and the function of genes involved in the disease-causing neuronal pathway because of the simplicity of the wiring diagram of the nervous system. Furthermore, the advantage of *C. elegans* being amenable to genetic manipulation makes it possible to dissect which step is crucial in the disease-causing pathway that is leading to neuronal dysfunction/neuronal death thereby presenting as a behavioural defect. Therefore, orthologs of genes that are involved in the production of the aberrant A β peptides may be upstream genes such as APP and the components of the secretases, whereas orthologs of tau may be acting downstream of the accumulation and aggregation of A β .

1.5.1 Analysis of *C. elegans* orthologs of human AD genes

A powerful approach to elucidate the *in vivo* function of a protein is to inactivate the gene orthologs and observe the defects caused in the organism. Several *C. elegans* strains have been generated by mutating the worm orthologues of human genes implicated in AD (Table 1.2). The *C. elegans* genome encodes an APP ortholog *apl-1* (amyloid precursor

protein like-1). The *apl-1* gene is expressed in multiple cell types and is necessary for several developmental processes including moulting and morphogenesis. Loss of the *apl-1* gene causes 100% larval lethality, which can be rescued by neuronal expression of *apl-1* (Hornsten et al., 2007). However, APL-1 is not thought to be further processed to yield an A β -like peptide (Daigle and Li, 1993).

Mutations in the *C. elegans* presenilin genes *sel-12* and *hop-1* lead to the disruption of morphology and function of two cholinergic interneurons, thereby causing defects in temperature memory (Wittenburg et al., 2000). The gene *sel-12* was identified as a suppressor of Notch signalling (Levitan and Greenwald, 1995). Notch signalling has an important role in cell fate determination during development (Greenwald, 2005).

Moreover, presenilins mediate the activities of other proteins in addition to APP and Notch; therefore, utilizing presenilins as therapeutic targets may be problematic as it could possibly disrupt other cellular processes in addition to APP processing (Ewald and Li, 2010). Furthermore, the two α -secretase encoding genes, *sup-17* and *adm-4*, are orthologous to the mammalian *ADAM10* and *ADAM17/TACE* (Jarriault and Greenwald, 2005). Although the *C. elegans* genome encodes proteins that make up the γ -secretase complex, it lacks an ortholog of BACE (β -secretase) (Dimitriadi and Hart, 2010). Hence, while the worm contains orthologs of APP and secretases, it is not only missing the β -secretase but is also missing the A β domain. Furthermore, components of the secretase complex are most likely upstream genes that are not only involved in the aberrant processing of APP but are also involved in other cellular processes. Therefore, these genes may not have neuronal phenotypes as they are part of other cellular processes.

The tau ortholog in *C. elegans* is *ptl-1* (protein with tau-like repeats), which functions to promote microtubule binding assembly (Goedert et al., 1996; McDermott et al., 1996). The tau gene is possibly involved in downstream events after APP processing and therefore may have neuronal phenotypes such as mechanosensory defects (Gordon et al., 2008). In addition to the above-mentioned genes, *C. elegans* orthologs of several genes implicated in late onset AD—including *CLU* (clusterin), *BINI* (bridging integrator 1), and *PICALM* (phosphatidylinositol binding clathrin assembly protein) have been shown to play a role in cellular cytoskeletal dynamics, clathrin-mediated endocytosis, and postsynaptic exocytosis

Table 1.2: Knockouts of *C. elegans* orthologues of human AD genes. Adapted from (Ewald and Li, 2010)

Human		<i>C. elegans</i>			References
Role	Gene	Gene	Knockout alleles	Phenotypes of null alleles	
Amyloid Precursor protein family (APP)	APP/APLP1/APLP2	<i>apl-1</i>	<i>yn10, yn23, yn28, yn29, yn30, yn31, yn32</i>	Larval lethal; molting defect; vacuoles; morphological defects	(Hornsten et al., 2007)
Processing enzymes of APP					
α - secretase	ADAM10	<i>sup-17</i>	<i>n1306, n1315, n1316, n1318, n1319am, n1320</i>	Lethal	(Tax et al., 1997)
	ADAM17/TACE	<i>adm-4</i>	<i>ok265</i>	Wild type; functional redundancy between SUP-17 and ADM-4	(Jarriault and Greenwald, 2005)
β – secretase	BACE			No endogenous β – secretase activity that cleaves human APP found in transgenic <i>C. elegans</i>	(Link, 2006)
γ – secretase complex					
Presenilins	PSEN1 or 2	<i>sel-12</i>	<i>ar171, ty11</i>	Disrupted vulva morphogenesis; egg-laying defective	(Cinar et al., 2001; Levitan and Greenwald, 1995)
	PSEN1 or 2	<i>hop-1</i>	<i>ar-179</i>	Functionally redundant with <i>sel-12</i>	(Li and Greenwald, 1997)
APH-1	APH-1	<i>aph-1</i>	<i>ep140, ep169, ep170, ep216, ep411, ep413, zu123, or28</i>	No anterior pharynx; maternal effect embryonic lethal; egg-laying defective; APH-2 localized to cytoplasm rather than cell surface	(Francis et al., 2002), (Goutte et al., 2002)
Nicastrin	APH-2	<i>aph-2</i>	<i>zu181</i>	No anterior pharynx; maternal effect embryonic lethal	(Goutte et al., 2000)

PEN-2	PEN-2	<i>pen-2</i>	<i>ep219, ep220, ep221, ep336, ep412, ep423</i>	No anterior pharynx; maternal effect embryonic lethal; hypodermis fails to enclose body; egg-laying defective	(Francis et al., 2002)
<i>Physical interactors with APP</i>					
Fe65	FE65	<i>feh-1</i>	<i>gb561</i>	Embryonic/larval lethal and larval arrest	(Napolitano et al., 2008), (Zambrano et al., 2002)
Mena	MENA	<i>unc-34</i>	<i>e951, gm104, gm114</i>	Uncoordinated, axon guidance; reduced brood size	(Kraemer and Schellenberg, 2007), (Withee et al., 2004)
<i>Tau and suppressors of tau pathogenesis</i>					
Tau	TAU	<i>ptl-1</i>	<i>ok621</i>	Incompletely penetrant embryonic lethal, escapers have mechanosensory defect	(Gordon et al., 2008)
		<i>sut-1</i>	<i>bk79</i>	Suppresses tau pathogenesis	(Kraemer and Schellenberg, 2007)
MSUT-2	MSUT-2	<i>sut-2</i>	<i>bk741</i>	Suppresses tau pathogenesis	(Guthrie et al., 2009)

ADAM9 and *APOE4*, since no orthologues have been identified in *C. elegans*

(Bao et al., 2005; Dickman et al., 2006; Mathew et al., 2003; Nonet et al., 1999). Although *C. elegans* has orthologs of genes involved in APP processing, it is missing the key element: the aberrantly processed A β peptides. Hence, worm models may be useful to study the downstream events leading to the disease pathogenesis because it is possible to express the A β peptide in this already existing cascade, thereby allowing the study of the downstream effects of aberrantly processed APP products.

1.5.2 Transgenic *C. elegans* models of A β and tau toxicity

Transgenic *C. elegans* strains are constructed by expressing the human disease-associated genes in specific tissues using cell type-specific promoters (Gama Sosa et al., 2012). Numerous transgenic *C. elegans* strains have been constructed based on the amyloid cascade hypothesis by expressing the A β peptide in the body wall muscle, or the neurons (Table 1.3). One important consideration is that A β expression should result in an interpretable phenotype without affecting worm viability (Link, 2006). The first transgenic worm strains expressing A β (CL2006 and descendants CL2010, CL2109, & CL3115) used the *unc-54* promoter, a constitutive body wall muscles promoter, largely because its activity has been well characterized. The A β transgene in these strains had a signal peptide upstream of the A β coding region for efficient cleavage and secretion of A β peptide. The CL2006 and CL2120 transgenic worms showed a progressive paralysis phenotype and intracellular cytoplasmic A β deposits that co-localized with amyloidogenic dyes (Link, 1995). These worm models that constitutively express A β have been utilised to study A β structure/function and protein interactions; however, their utility has been limited for forward and reverse genetic screens due to the incomplete penetrance of the paralysis phenotype and variation in the age of onset of paralysis (Link, 2006). Subsequently, another muscle-specific promoter, *myo-3*, was used for temperature-inducible expression of the transgenic strain (CL4176) that displays a completely penetrant paralysis phenotype (Wu et al., 2006). The model was constructed by re-engineering the construct containing A β 1-42 gene by adding an abnormally long 3' untranslated region and then introducing the modified transgene into a *C. elegans* strain that has a temperature-sensitive mutation in *smg-1*, an essential component of the mRNA surveillance system. In a *smg-1* genetic background, the mRNA surveillance system is

Table 1.3: *C. elegans* toxicity models of human proteins implicated in AD (adapted and modified from (Ewald and Li, 2010))

Human protein/peptide	<i>C. elegans</i> promoter	Expression in <i>C. elegans</i>	Phenotypes	Strain/transgene name/(plasmid)	References
Expression of the human β-amyloid peptide					
A β 3-42	<i>unc-54</i>	Constitutively in muscles	Age-dependent progressive paralysis; forms amyloid deposits; increased oxidative stress	CL2005, CL2006, CL1019, CL1118, CL1119, CL1120, CL1121, CL2120	(Fay et al., 1998), (Link, 1995, 2001), (Yatin et al., 1999)
A β 1-40	<i>unc-54</i>	Constitutively in muscles	No SP cleavage	CL2010	(Fay et al., 1998)
Dimer A β 3-42	<i>unc-54</i>	Constitutively in muscles	No formation of amyloid deposits	CL2109, CL3109	(Fay et al., 1998), (Link, 2001),
Met ³⁵ Cys A β 3-42	<i>unc-54</i>	Constitutively in muscles	No formation of amyloid deposits; no increase in oxidative stress	CL3115	(Fay et al., 1998), (Yatin et al., 1999)
A β 3-42	<i>myo-3</i>	Inducible A β 3-42 in body wall muscles	Rapid paralysis, oxidative stress precedes amyloid deposition; autophagosome accumulation	CL4176	(Drake et al., 2003), (Link et al., 2003), (Florez-McClure et al., 2007)
A β 3-42	<i>snb-1</i>	Inducible A β 3-42 in all neurons	Normal movement, forms amyloid deposits, reduced chemotaxis toward benzaldehyde, hypersensitive to serotonin	CL2241, CL2355	(Link, 2006), (Wu et al., 2006), (Dosanjh et al., 2010)
A β 3-42	<i>eat-4</i>	Constitutively expressed in all glutamatergic neurons	Loss of GFP-marked glutamatergic neurons in an age-related manner. No gross visible phenotype	UA166	(Chen et al., 2015; Treusch et al., 2011)

A β 3-42	<i>unc-54</i>	Constitutively in muscles	Expresses human A β peptide and accumulates A β fibrils. Toxicity of A β is enhanced at higher temperatures.	PE873	(Lagido et al., 2009; Lagido et al., 2008; McLaggan et al., 2012)
A β 1-42	<i>unc-54</i>	Constitutively in muscles	Shifting L4 larvae or young adult from 20 °C to 25 °C causes severe and fully penetrant paralysis	GMC101	(McColl et al., 2012)
A β 1-42	<i>unc-119</i>	Constitutively expressed in all neurons	Impaired neuromuscular and sensorimotor behaviour	GRU102	(Fong et al., 2016)
A β 1-42	<i>flp-17</i>	Constitutively expresses A β 1-42 in the two BAG neurons	Subtle modulation of the response to CO ₂	CMD01	(Sinnige et al., 2019)
Expression of components of the γ-secretase complex					
PSEN1	<i>sel-12</i>	Constitutively in most cell types, except intestine	Rescues <i>sel-12</i> null phenotypes	PS1 (pBY146)	(Levitan et al., 1996), (Wittenburg et al., 2000)
Mutant PSEN1 variants			Fails to rescue <i>sel-12</i> null phenotypes	PS1 Δ E9, PS1M146L, PS1H163R, PS1L266V, PS1A286E, PS1C410Y, A246 (pBY147)	(Levitan et al., 1996), (Wittenburg et al., 2000)
PSEN2			Rescues <i>sel-12</i> null phenotypes	PS2	(Levitan et al., 1996)
Nicastrin			Rescues egg-laying defect of <i>aph-2</i> null	hNCT FL	(Levitan et al., 2001)

Mutant Nicastrin variants			Partially rescues egg-laying defect of <i>aph-2</i> null	DYIGS, AAIGS, Δ340, Δ369, EC	(Levitan et al., 2001)
APH-1			Human APH-1 is unable to rescue egg-laying defect of <i>aph-1</i> null worms ; can partially rescue egg-laying defect of <i>aph-1</i> null only in mixture with <i>Hpen-2</i> , <i>Haph-1a</i> , <i>Haph1b</i> and <i>HPSENI</i>	Haph-1a, Haph1b	(Francis et al., 2002)
PEN-2			Partially rescues egg-laying defect of <i>pen-2</i> null (with long 3' UTR) only in mixture with <i>Hpen-2</i> , <i>Haph-1a</i> , <i>Haph1b</i> and <i>HPSENI</i>	Hpen-2	(Francis et al., 2002)
Expression of human tau and variants					
Tau (4R1N isoform, most abundant form in human brain)	<i>aex-3</i>	Constitutively in all neurons	Age-dependent progressive unco-ordination and accumulation of tau; neurodegeneration; reduced lifespan compared to non-transgenic worms	N-1, N-2	(Kraemer et al., 2003)
V337M tau (4R1N) (FTDP-17 mutation)	<i>aex-3</i>	Constitutively in all neurons	Stronger age-dependent progressive unco-ordination and accumulation of insoluble tau; neurodegeneration; reduced lifespan compared to non-transgenic worms	337M-1, 337M-2	(Kraemer et al., 2003)
P301L tau (4R1N) (FTDP-17 mutation)	<i>aex-3</i>	Constitutively in all neurons	Strong age-dependent progressive uncoordination and accumulation of insoluble tau; neurodegeneration; reduced lifespan compared to non-transgenic worms	301L-1, 301L-2	(Kraemer et al., 2003)
Tau WT4R (wild type)	<i>mec-7</i>	Touch neurons (ALML/R, AVM, PLML/R, PVM); weak in FLP, PVD, BDU	Age-dependent progressive impairment in touch response;	tmls82, tmls83, tmls84, tmls85, tmls171	(Miyasaka et al., 2005)

			neurodegeneration; little tau accumulation in PLM neuron		
Tau WT3R (wild type)	<i>mec-7</i>	Touch neurons (ALML/R, AVM, PLML/R, PVM); weak in FLP, PVD, BDU	Age-dependent progressive impairment in touch response, neurodegeneration	tmIs110, tmIs173	(Miyasaka et al., 2005)
P301L tau (FTDP-17 mutation)	<i>mec-7</i>	Touch neurons (ALML/R, AVM, PLML/R, PVM); weak in FLP, PVD, BDU	Strong age-dependent progressive impairment in touch response; neurodegeneration; strong tau accumulation in PLM neuron (as wild-type tau WT4R)	TmIs81, tmIs178, tmIs179	(Miyasaka et al., 2005)
R406W tau (FTDP-17 mutation)	<i>mec-7</i>	Touch neurons (ALML/R, AVM, PLML/R, PVM); weak in FLP, PVD, BDU	Strong age-dependent progressive impairment in touch response; neurodegeneration; strong tau accumulation in PLM neuron (as wild-type tau WT4R)	TmIs146, tmIs147, tmIs148, tmIs149,	(Miyasaka et al., 2005)
Tau ₃₅₂ (=fetal, 352aa isoform) wild type	<i>rgef-1</i>	Constitutively in all neurons	Age-dependent progressive unco-ordination ; neurodegeneration	VH255, VH1016, VH1018	(Brandt et al., 2009)
Tau ₃₅₂ PHP (pseudo-hyperphosphorylated)	<i>rgef-1</i>	Constitutively in all neurons	Strong age-dependent progressive unco-ordination; neurodegeneration	VH254, VH1014, VH1015	(Brandt et al., 2009)
Tau ₃₅₂ Ala (10 Ser/ Thr phosphorylation sites substituted with Ala)	<i>rgef-1</i>	Constitutively in all neurons	Early onset of age-dependent progressive unco-ordination and reduced lifespan compared to wild-type tau ₃₅₂	VH418, VH421	(Brandt et al., 2009)
Pro-aggregating human tau F3(delta)K280	<i>rab-3</i>	Constitutively in all neurons	Severe locomotion defect and slow growth	BR5270	(Fatouros et al., 2012)

Anti-aggregating tau F3(delta)K280 I277P I380P	<i>rab-3</i>	Constitutively in all neurons	Strain has a mild phenotype serving as a control for BR5270	BR5271, BR6516	(Fatouros et al., 2012)
Anti-aggregating tau + full length tau (h4R1NtauV337M)	<i>rab-3</i> + <i>aex-3</i>	Constitutively in all neurons	Pronounced uncoordinated phenotype	BR5486,	(Fatouros et al., 2012)
Pro-aggregating human tau F3(delta)K280 + full length human tau (hTau V337M)	<i>rab-3</i> + <i>aex-3</i>	Constitutively in all neurons	Worms grow slowly and have a severe locomotion defect	BR5706	(Fatouros et al., 2012)
Tau anti-aggregation double transgenic line (hTau V337M)	<i>rab-3</i>	Constitutively in all neurons	Normal locomotion	BR6427	(Fatouros et al., 2012)
Full length human tau	<i>aex-3</i>	Constitutively in all neurons	Severe locomotory defect, slow growth and neurodegeneration	CK10	(Brandt et al., 2009)
Expression of tau variants and Aβ					
F3 pro-aggregating tau + A β 3-42	<i>rab-3</i> + <i>snb-1</i>	Constitutively in all neurons	Shorter lifespan, reduced progeny viability, learning deficits, impaired cholinergic, serotonergic and dopaminergic signalling.	UM0001	(Wang et al., 2018)
F3 anti-aggregating tau + A β 3-42	<i>rab-3</i> + <i>snb-1</i>	Constitutively in all neurons	Shorter lifespan and learning deficits	UM0002	(Wang et al., 2018)

functional at low temperatures and expression of A β is poor because the Smg pathway targets the “abnormal” 3’ UTR for degradation. When shifted to the restrictive temperature, mRNA surveillance is inactive and there is a significant increase in transgene mRNA stability. The subsequent translation of A β results in a completely penetrant phenotype causing rapid paralysis. The strains described above express A β in muscle and provide insight into the biochemical and some cell biological features of A β -mediated defects. However, since AD is a neurodegenerative disorder, it is important to express A β in the neurons in order to understand how the biochemistry and cell biology of A β are translated into specific neuronal and behavioural deficits. The promoter of the *snb-1* gene, which encodes synaptobrevin, a synaptic vesicle protein required by all neurons, was used for pan-neuronal expression of the transgene in CL2355. CL2355 shows intraneuronal A β deposits along with subtle deficits in chemotaxis, associative learning, thrashing in liquid, and hypersensitivity to serotonin (Dosanjh et al., 2010; Hart and Chao, 2010; Wu et al., 2006). Another strain was created to express A β exclusively in the glutamatergic neurons using the promoter of the *eat-4* gene. The *eat-4* gene has L-glutamate transmembrane transporter activity and glutamate: sodium symporter activity. Although the strain did not show any gross visible phenotype, there was an age-related loss of GFP expression in the glutamatergic neurons. At day 3, only 48% of the worms had intact glutamatergic neurons and on day 7 it was reduced to 25% (Treusch et al., 2011). In 2009, McColl and colleagues reported that all *C. elegans* strains constructed using the original A β transgene express a truncated version of β -amyloid: a A β 3-42 peptide instead of an A β 1-42 peptide. This was because the A β 1-42 translation product was processed aberrantly due to the presence of a cryptic signal peptide cleavage site at +3 of the A β 1-42 (McColl et al., 2009). A mass spectrometry analysis carried out to find the nature and abundance of A β peptides in the human AD brain showed that the two equally abundant major are A β 1-42 and A β 4-42, with A β 3-42 peptide species being completely absent (Roberts et al., 2017). Consequently, the worm strains made prior to 2009 actually expressed A β 3-42 which has different physicochemical properties to A β 1-42 and may not recapitulate the *in vivo* characteristics of the A β peptides present in the human AD brain. A new *C. elegans* transgenic strain (GMC101) was constructed that

expressed A β 1-42 correctly in the body wall muscles using the promoter of *unc-54* (McColl et al., 2012).

The new A β 1-42 expression plasmid was designed by inserting two amino acids Asp-Ala (DA) at the N-terminal end of the A β sequence of the previous A β 3-42 construct. This re-engineered plasmid was then used to create the new transgenic *C. elegans* strain (GMC101). The identity of the expressed peptide was confirmed by immunoprecipitation, MS, and immunoblotting. The targeting of the A β to the body wall muscle was confirmed by amyloid dyes and immunohistochemistry. It was possible to compare GMC101 with a previous A β 3-42 expressing transgenic strain (CL2120) since both make use of the same promoter (*unc-54*) for A β expression. When compared to older strain, GMC101 showed a more severe and fully penetrant paralysis phenotype (McColl et al., 2012). Consequently, a neuronal strain expressing the rectified A β 1-42 peptide using the pan-neuronal *unc-119* promoter was developed (Fong et al., 2016). The transgene is mainly expressed in the body wall muscles, ganglia, neurons, somatic nervous system. The new strain GRU102 showed reduced lifespan in addition to several behavioural deficits such as abnormal head oscillatory movements, middle-age sensorimotor deficits, constipation, internal hatching and defects in pharyngeal pumping (Fong et al., 2016). In addition, a strain containing a single copy of the A β 1-42 transgene was prepared, expressing the A β 1-42 peptide in a single pair of glutamatergic sensory neurons, the BAG neurons. This strain (CMD01) showed subtle modulation in its response to CO₂ (Sinnige et al., 2019).

Transgenic *C. elegans* strains have also been developed that overexpress human tau, its variants, and components of the γ -secretase complex in the *C. elegans* nervous system. All of these strains have been described in Table 1.3. The transgenic strains expressing the human presenilin genes in mutant presenilin background show rescue specifically of egg-laying. On the other hand, transgenic strains expressing tau and its variants show neurodegeneration and strong age-dependent unco-ordinated locomotory phenotype, with the severity of the phenotype dependent on the tau form being expressed. Most of these strains were engineered to express the tau transgenes in the *C. elegans* nervous system. Additionally, transgenic *C. elegans* strains generated by crossing the temperature sensitive A β 3-42 expressing strain (CL2355) with either the anti-aggregating tau strain (BR5271) or the pro-aggregating tau strain have been developed and characterized in

detail. The new strain that expresses A β 3-42 in combination with the pro-aggregating tau fragment (UM0001) displays shorter lifespan, egg-laying defect along with reduced progeny viability, and impaired cholinergic, serotonergic, and dopaminergic signalling. On the other hand, the strain that expresses A β 3-42 and the anti-aggregating tau fragment (UM0002) displays shorter lifespan and less severe learning deficits than the strain UM0001 (Wang et al., 2018).

1.6 Aims and scope of the thesis

Despite significant advances made in the field of AD research, the amyloid cascade hypothesis remains controversial and a number of questions remain unanswered. Firstly, the molecular and cellular mechanisms underlying A β toxicity remain unclear: neuronal toxicity could either be due to the aggregated A β deposits or to soluble oligomers or a combination of both. Secondly, the roles of the different N- and C- terminal truncated A β peptides that have been recorded as present in the human AD brain are relatively unexplored. To answer these questions (or propose a path towards answers), this study proposes to develop new *C. elegans* models of A β toxicity. Although *C. elegans* may not recapitulate all aspects of AD, it is an excellent system in which to study the pathogenesis of AD, because the fundamental cellular pathways required for neuronal development, function and survival are highly conserved between humans and worms. Moreover, there is no APP processing, cleavage, and breakdown in *C. elegans*, so the only A β peptide present is A β 1-42 (McColl et al., 2012): the analysis of A β peptides in transgenic *C. elegans* is not confounded by endogenous A β nor by processing variants derived from A β 1-42. This offers a huge advantage for *in vivo* study of a single A β species in isolation. In addition, the majority of the literature has focussed on A β expression in the *C. elegans* body wall muscle and thus does not address directly the connection between A β 1-42 and neuronal deficits. Furthermore, all the transgenic *C. elegans* AD strains generated until 2012 were expressing an aberrant A β 3-42 peptide which does not significantly contribute to the A β distribution found in human AD brain. It is only relatively recently that neuronal A β expression of the full length A β 1-42 is beginning to be investigated.

The hypothesis tested in this thesis is that the expression of the A β 1-42 transgene in the *C. elegans* neurons will result in disease relevant age-related behavioural deficits, and that these behavioural deficits will serve as a direct readout of the A β -induced neuronal toxicity. Additionally, the generation of new strains will be beneficial in understanding the molecular mechanisms of A β toxicity and will aid in the development of large drug screening platforms to test potential therapeutic strategies against AD. Therefore, the aims of this thesis are:

-
1. Generate a transgenic *C. elegans* strain expressing the A β 1-42 transgene in the neurons;
 2. Generate transgenic *C. elegans* strains expressing different levels of A β 1-42 transgene (via transgene copy number and varying the strength of promoter, but with same pan-neuronal spatial pattern) and compare behavioural phenotypes between strains that differ in A β expression level;
 3. Investigate the *in vivo* effect of varying A β peptide identity; and
 4. Manipulate the genetic background of A β transgene expression.

The first experimental chapter introduces a new transgenic *C. elegans* strain expressing the full length A β 1-42 transgene in the nervous system using the pan-neuronal *snb-1* promoter and describes the behavioural deficits that are the result of this neuronal A β expression (**Aim 1**). According to the amyloid cascade hypothesis, the level of A β expression is an important factor contributing to the severity of the behavioural deficit and so far, there are few studies expressing the A β peptide in the *C. elegans* neurons. Therefore, the second experimental chapter compares the severity of the behavioural deficits in transgenic A β 1-42 expressing *C. elegans* strains generated using pan-neuronal promoters that differ in activity, so that these strains show quantitative differences in the level of A β expression (**Aim 2**). The third experimental chapter discusses the generation and behavioural analysis of transgenic *C. elegans* strains expressing different versions of the A β peptide in neurons to compare the *in vivo* toxicity associated with these peptides with the full length A β 1-42 (**Aim 3**). The fourth experimental chapter explores a link between the expression of the A β peptide and the pathogenesis of AD in a *ptl-1* null genetic background (**Aim 4**). To conclude, the final chapter summarizes the key findings of all the chapters and describes future directions utilizing these transgenic strains to understand the underlying mechanisms of AD pathogenesis, and evaluate therapeutic strategies targeting the A β peptides.

Chapter Two

Molecular and behavioural characterisation of a transgenic *C. elegans* strain expressing the human amyloid-beta protein in neurons

2.1 Introduction

The primary pathological hallmark of Alzheimer's disease (AD) is the presence of extracellular senile plaques composed of aggregates of fibrillar A β peptides, derived from the proteolytic processing of Amyloid Precursor Protein (APP) (Glennner and Wong, 1984; Masters et al., 1985). The transmembrane protein APP is cleaved sequentially by β -secretase at the N-terminal amino acids 1 and 11 followed by imprecise cleavage by γ -secretase to give rise to a family of A β peptides varying between 39-43 amino acids in length (Takahashi et al., 2002b). One of the most abundant A β peptides in the human AD brain is the hydrophobic A β 1-42 peptide (Haass and Selkoe, 1993; Selkoe, 2013). The amyloid cascade hypothesis suggests that the progressive and abnormal accumulation and aggregation of the A β peptides in the human AD brain is the primary cause of the disease, and this precedes the other disease symptoms such as formation of intracellular neurofibrillary tangles, cognitive decline and dementia (Barage and Sonawane, 2015; Hardy and Higgins, 1992; Reitz, 2012). However, the molecular and cellular mechanisms underlying AD pathology remain contentious and unclear (Alexander et al., 2014; Di Carlo, 2012; Schon and Area-Gomez, 2010).

The nematode *Caenorhabditis elegans* is an excellent *in vivo* model system to study the toxicity associated with these A β peptides. The simple and compact nervous system of *C. elegans* consists of 302 neurons. It has well-mapped synaptic connections determined by serial electron micrographs (Chalfie et al., 1985; de Bono and Maricq, 2005; White et al., 1986), and a number of robust behavioural phenotypes that have been used to study neuronal function such as chemotaxis, locomotion, egg-laying, pharyngeal pumping and defecation (Bargmann and Horvitz, 1991; Croll, 1975; Hobert, 2003; Schafer, 2006). The

worm is not only capable of displaying a wide range of behavioural phenotypes but also shows behavioural plasticity, including learning behaviours (Byrne et al., 2017).

Several *C. elegans* strains have previously been generated by expressing the A β 1-42 in different cell types and a number of behavioural phenotypes have been correlated with A β 1-42 expression. For instance, the *C. elegans* strain expressing A β 1-42 peptide in the body wall muscle cells shows a severe, fully penetrant and age-dependent progressive paralysis phenotype (McColl et al., 2012). Since AD is a neurodegenerative disorder, a more disease-relevant strain expressing A β 1-42 in the nervous system using the pan-neuronal promoter *unc-119* was reported and showed reduced lifespan and subtle age-associated decline in behavioural functions such as internal hatching, pharyngeal pumping and abnormal head movements (Fong et al., 2016). Another study attempted to show the phenotype associated with A β 1-42 expression from a single inserted copy of the transgene, in a single pair of glutamatergic sensory neurons, the BAG neurons. However, there was no significant behavioural phenotype reported in this strain (Sinnige et al., 2019). Although there is a limited number of *C. elegans* strains expressing the relevant full length A β 1-42 peptide in the neurons, expression of A β is associated with subtle behavioural deficits in these strains.

I sought to evaluate the effects of pan-neuronal A β 1-42 expression on several different behavioural phenotypes in worms by developing a new *C. elegans* model of A β toxicity. This new *C. elegans* AD model expressing high levels of A β 1-42 transgene driven by the promoter of the pan-neuronal SynaptoBrevin-1 related gene, *snb-1* was developed and extensive behavioural analysis was performed to see if A β transgene expression correlated with any robust progressive age-associated disease-relevant phenotypes. This would allow testing of neuronal effects of human A β expression in *C. elegans* neurons that otherwise express no A β , thereby exploring the inherent toxicity of A β , its *in vivo* propensity to form amyloid, and the underlying amyloid cascade hypothesis. Thus, the aims of this chapter are as follows: (i) describe the construction of a pan-neuronal A β 1-42 expressing *C. elegans* strain, confirm the presence of the A β 1-42 transgene using a quantitative copy number PCR assay, and quantify the expression using RT-qPCR, (ii) characterize the age-associated effects of A β 1-42 expression in *C. elegans* and (iii) explore the severity of any behavioural defects as a result of neuronal A β 1-42 expression.

2.2 Materials and Methods

2.2.1 Materials

The composition of all reagents used in this study is listed in Supplementary Table 1. The HPLC grade water used for all the reactions was obtained from Sigma-Aldrich. Genomic DNA from *C. elegans* strains was extracted using ISOLATE II Genomic DNA kit (Bioline, Inc.). The Petri plates used were from Thermo Fisher Scientific, Australia. All primers used in the study were ordered from Integrated DNA Technology (IDT) (Supplementary Table 2). The Wizard® SV Gel and PCR Clean-Up kit from Promega was used to extract DNA fragments from agarose gels and purify PCR products. All transgenic *C. elegans* strains developed in this study were viewed and analysed under an epifluorescence microscope Olympus SZX16 containing standard GFP and RFP filters.

2.2.2 Maintenance of *C. elegans* strains

Standard protocols were employed for the maintenance of *C. elegans* strains (Stiernagle, 2006). All worm strains were cultured on standard nematode growth media (NGM) plates (Refer to Supplementary Table 1) seeded with *E. coli* OP50 culture at 20 °C, unless otherwise stated (Brenner, 1974).

2.2.2.1 Obtaining age synchronous worm populations

Age-synchronous nematodes were obtained by treating gravid adult hermaphrodites with alkaline hypochlorite (2:5 v/v 4.2% NaClO:1N NaOH) for 3 min. Adult worms dissolve in the alkaline hypochlorite solution, leaving behind eggs that are resistant to the treatment. The reaction was stopped by adding 10 ml M9 buffer (Refer to Supplementary Table 1) to the sample, mixing and centrifuging at 500 g for 5 min at room temperature. The supernatant was discarded, and the previous step was repeated twice to remove all the residual bleach from the sample. The sample was then resuspended in 3 ml M9 buffer and placed on a shaker at room temperature for 20 h. Newly hatched L1 larvae in the sample were passed through a 40-µm filter to remove debris, counted, and then transferred to a clean NGM plate seeded with *E. coli* OP50. Alternatively, 10-15 gravid adults were

picked onto a few freshly seeded plates and allowed to lay eggs for about 4-6 h at 20 °C. At the end of 4-6 h, the adults were removed, and the eggs were allowed to develop into an age-synchronous population at 20 °C. Day of the egg-lay was considered to be day 0. In order to obtain worms for day 4 (young adults), day 8 (middle-aged) and day 12 (old adults) time points, the age synchronous L4 staged worms (48-50 h post-hatch) were transferred to FUdR (Fluorodeoxyuridine; 25 µM) containing NGM plates. The FUdR plates were seeded with 10% *E. coli* OP50 (w/v).

2.2.3 Preparation of *C. elegans* transgenic strains

Transgenic *C. elegans* strains were generated by microinjecting varying concentrations of the expression plasmids pSNB1AB42 and pSNB1GFP into the gonad of young adult wild-type worms. Plasmid pAV1944 (*myo-2::mCherry::unc-54* 3'UTR) was used as co-injection marker. pAV1944 expresses mCherry specifically in the pharyngeal muscles (Miedel et al., 2012). This plasmid was a gift from Gary Silverman at the Washington University School of Medicine in St. Louis (Addgene plasmid #37830; <http://n2t.net/addgene:37830>; RRID: Addgene_37830). The injection mix also contained fragmented *C. elegans* wild type genomic DNA in varying concentrations such that the total concentration of DNA microinjected was maintained as 100 ng/µl regardless of plasmid concentration. The genomic DNA was digested with the 4-base cutting restriction enzyme, *Sau3A* (New England Biolabs, Inc.). The progeny obtained from worms microinjected with pSNB1AB2 and pAV1944 were selected on the basis of pharyngeal mCherry expression, whereas the progeny of worms obtained from pSNB1GFP microinjection were selected on the basis of pan-neuronal GFP expression. No marker plasmid was co-injected with pSNB1GFP as the transgene itself expresses GFP which can be easily viewed via epifluorescence microscopy. Refer to Supplementary Table 3 and Supplementary Table 4 for details on the concentrations of the plasmids used for microinjections for all the strains generated in this study.

2.2.3.1 Stable integration of extrachromosomal arrays in *C. elegans* genome using X-ray irradiation

One hundred age synchronous L4 stage hermaphrodites were placed on an unseeded 6 cm NGM agar plate and were irradiated with X-rays (3000-4000 rad) for 4 min using the RS 2000 Biological Research Irradiator (Rad Source Technologies, Inc.). The worms were then transferred to seeded plates and allowed to recover overnight in an incubator set at 15 °C. These X-ray irradiated adults, also known as P0s, were then allowed to lay eggs. About 400 F1 progeny were picked individually on 6 cm seeded NGM agar plates and analysed for increased transgene transmission in the F2s. For an F1 that is heterozygous for an integrated array, the percentage of F2s showing the presence of an integrated array upon self-fertilization is approximately 75% and only one third of the 75% will be homozygous. About eight F2 progeny from each F1 parent showing >75% fluorescent progeny were picked individually to 6 cm NGM plates and were analysed for 100% transmission of the transgene (Mariol et al., 2013). Approximately four F3 progeny from candidate F2 homozygotes were individually picked to confirm genomic integration of transgene and to avoid selecting sterile worms. The integrated strain was then outcrossed at least three times to the wild type strain to remove any background mutations introduced during the irradiation procedure.

2.2.3.2 Freezing worm strains

A subset of worms from each transgenic *C. elegans* strain were frozen after they were generated using previous described methods (Stiernagle, 2006). About 2-3 large NGM plates (9 cm) containing a high number of starved L1-L2 worms were washed with S buffer (Refer to Supplementary Table 1), after which the worms in solution were collected in a sterile tube. An equal volume of Freezing buffer (S buffer + 30% glycerol) (Refer to Supplementary Table 1) was added to the worm sample, mixed and transferred to four 1.8 ml cryovials labelled with the strain name and date. The cryovials were then packed in an isopropanol freezing container Mr Frosty™ at room temperature and placed in -80 °C freezer overnight. The cryovials were transferred to their designated boxes at -80 °C the following day. One of the four cryovials was tested to check for the recovery of

the worm strains after freezing. The remaining vials were either stored in -80°C or in liquid nitrogen.

2.2.3.3 Microscope details for imaging the pan-neuronal GFP expressing strain.

Glass microscope slides were prepared with agarose pads by pipetting 300 µl of 2% agarose in M9 buffer (Supplementary Table 1) onto the slide and flattening slightly using a coverslip, before allowing the agarose to cool and gel. Once the agarose pad was formed, the coverslip was removed. Several worms were picked on each agarose pad and immobilised by heating the slide on a block at 55 °C for 10 s. The agarose pad was then covered with a coverslip. For imaging WG625 (*Prgef-1:GFP*) worms, images were acquired using either an Upright microscope Nikon Eclipse Ci equipped with Nikon DS-U3 Digital Camera or Zeiss LSM 510 laser scanning confocal microscope with a Plan Apochromatic 20X/0.8 NA objective. Excitation was achieved with an argon multiline laser at 488 nm (eGFP) and DPSS laser of 561 nm (mCherry). A long pass LP575 filter was used for detection of mCherry. Z stacks were obtained using Zen software. For imaging the WG700 (*Psnb-1:GFP*) strain, an inverted microscope Nikon Ti Eclipse microscope was used. The FITC filter was used to visualise GFP fluorescence (~495 nm) in the worms.

2.2.3.4 Strains used in this chapter

Details of all transgenic *C. elegans* strains used in this study have been listed in Supplementary Table 5. The strains described in this chapter include: **N2**, Wild-type Bristol strain; **WG731**, [*Pmyo2::mCherry*]; **WG643**, [*Pmyo2::mCherry +Psnb-1::huAβ1-42*]; **CB1124**, *che-3(e1124)*; **CB1141**, *cat-4 (e1141)*; **CB1112**, *cat-2 (e1112)*; **MT8943**, [*bas-1(ad446)* III; *cat-4(e1141)* V]; **MT7988**, *bas-1(ad446)* III; **RB888**, *casy-1(ok739)* II; **KP4**, *glr-1(n2461)* III.

2.2.4 Construction of expression plasmids

The plasmid pPD49.26 was used as the backbone to construct the pan-neuronal human DA-A β 1-42 expression plasmid. As seen in Figure 2.1A, pPD49.26 contains a synthetic intron and a 3' UTR region from the *unc-54* gene, which are essential elements required for appropriate transgene expression in the worm, as well as three polylinker (MCS) regions for cloning exogenous DNA (Fire et al., 1990). The expression plasmid containing the human amyloid β (A β) 1-42 gene driven by the pan-neuronal promoter of the *snb-1* gene was assembled in two steps. First, the signal peptide and the DA-A β 1-42 were extracted from pCL354 (McColl et al., 2012). The fragment containing the signal peptide and hu-DA-A β 1-42 was digested using NheI and SacI from pCL354 (McColl et al., 2012) and cloned into the MCSII of pPD49.26 to generate the promoter-less plasmid, pAB42 (Figure 2.1A). Briefly, pCL354 is an expression plasmid that consists of the peptide/DA-A β 1-42 driven by the muscle-specific promoter *unc-54* (Supplementary Table 3). This generated a promoter-less *DA-A β 1-42* containing vector pAB42. This newly constructed promoter-less A β 1-42 expressing plasmid could be used as a template for future plasmid construction, to drive the expression of A β 1-42 in specific subsets of neurons using different neuronal promoters. Secondly, a 2 kb region upstream of the *snb-1* gene (thought to contain the promoter-enhancer sequence) was amplified from *C. elegans* wild-type genomic DNA with *snb-1* promoter-specific forward and reverse primers that add XbaI (5') and XmaI (3') sites respectively (shown in Figure 2.1B) (Nonet et al., 1998). Immolase enzyme (Bioline, Inc.) was used for amplifying the *snb-1* promoter fragment in a 10 μ l PCR reaction [1 μ l DNA template, 0.5 μ l Primer mix (10 μ M), 0.4 μ l dNTPs, 1 μ l Buffer (10X), 0.6 μ l MgCl₂ solution (50 mM), 0.1 μ l Immolase enzyme, 6.4 μ l HPLC grade water] and using the following PCR conditions: denaturation at 95 °C for 10 min, 35 cycles of denaturation at 95 °C for 15 s, annealing at 61.2 °C for 40 s, elongation at 72 °C for 2.5 min followed by final extension at 72 °C for 5 min. Refer to Supplementary Table 2 for the list of primers used in the study.

The *snb-1* fragment PCR product was digested with XbaI and XmaI and cloned into the complementary XbaI (5') and XmaI (3') sites of MCSI of plasmid pAB42, resulting in transgene expression plasmid pSNB1AB42 (Figure 2.1C). Additionally, the *snb-1* promoter fragment was also cloned into the vector backbone pPD49.46 for future plasmid

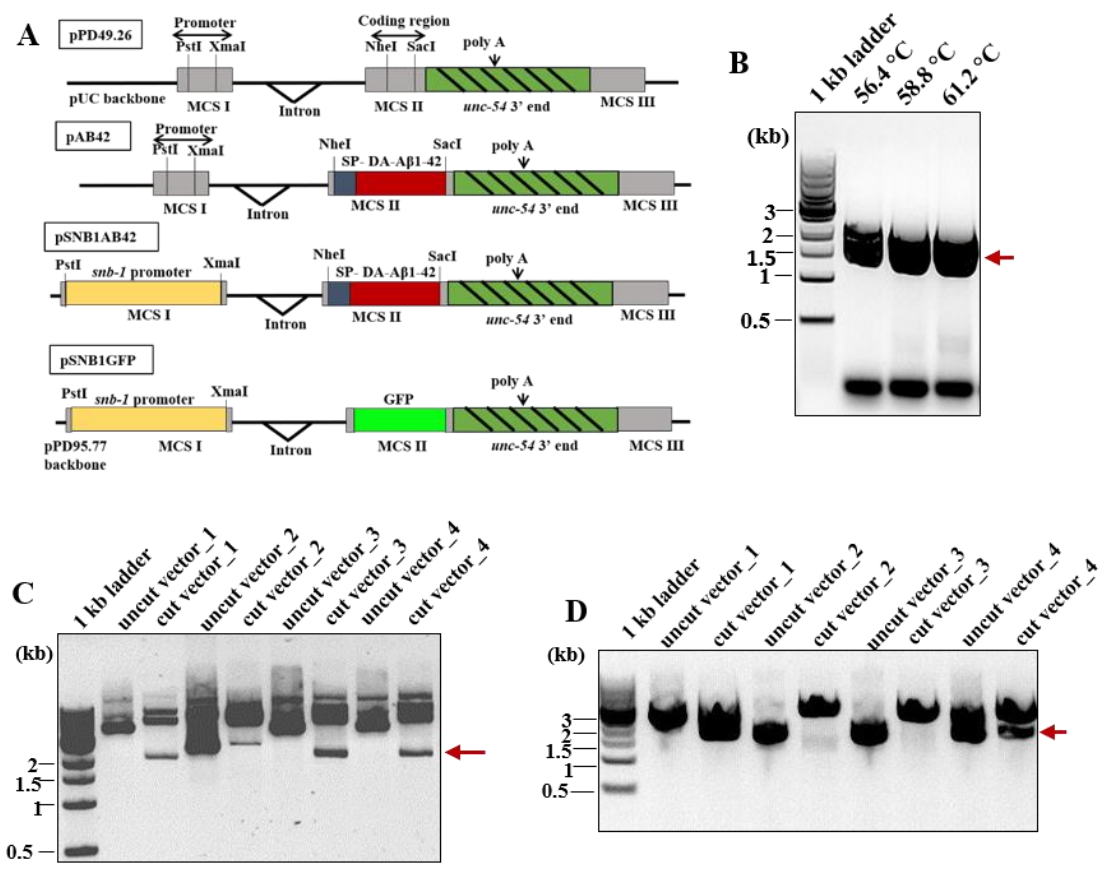


Figure 2.1: Cloning of *snb-1* fragment.

A) Schematic representation of the expression plasmids used in this chapter. The template plasmid was pPD49.26 from Fire vector kit 1995 (Fire, Harrison, & Dixon, 1990). Promoter-less plasmid pAB42 was constructed by cloning hu-DA-A β 1-42 gene into MCS II of pPD49.26. The pan-neuronal A β expression plasmid pSNB1AB42 was prepared by cloning *snb-1* promoter enhancer fragment into MCS I of pAB42, and the pan-neuronal GFP expressing plasmid pSNB1GFP was constructed by inserting the *snb-1* promoter fragment into MCS I of promoter-less GFP-containing plasmid pPD95.77. B) The gradient PCR optimisation of *snb-1* promoter fragment. C) The digestion of clones to confirm the presence of *snb-1* promoter fragment in the pPD95.77 vector backbone. D) Digestion of clones to confirm the presence of *snb-1* promoter fragment in the pAB42 vector backbone. All DNA fragments were run on a 1% agarose gel. The expected DNA fragments are indicated with a red arrow.

constructions containing different transgenes driven by *snb-1*. As a control for appropriate pan-neuronal expression, the same *snb-1* promoter fragment was also inserted into the complementary sites XbaI (5') and XmaI (3') of the promoter-less GFP containing plasmid, pPD95.77 (Fire vector kit 1995) (Fire et al., 1990), resulting in pan-neuronal GFP expression plasmid pSNB1GFP (Figure 2.1D).

The presence of the insert in the transgene expression plasmids (also listed in Supplementary Table 3) was confirmed by restriction enzyme digestion and all clones were finally verified by Sanger sequencing (Macrogen, Inc, Korea). For pAB42, the presence of the A β gene was confirmed by sequencing a portion of the vector containing A β gene using vector-specific M13 reverse primer. For pSNB1AB42 and pSNB1GFP, the presence of *snb-1* promoter was confirmed using primers specific to the *snb-1* promoter sequence (Supplementary Table 2).

2.2.5 Generating standard curves from plasmid and genomic DNA for copy number PCR assay

Genomic DNA isolated from GMC101 (using ISOLATE II Genomic DNA kit from Bioline, Inc.) was used as template DNA to generate standard curves for two PCR reactions for the target A β 1-42 gene and a single-copy reference gene, *Y45F10D.4*, which encodes a putative iron sulphur-containing protein (Zhang et al., 2012). Gradient PCR was performed to optimize annealing temperature of the primers on a CFX96 Real-Time PCR system (Bio-Rad Laboratories, Inc.). Each 10 μ l PCR reaction consisted of 2 μ l DNA template (0.5 ng/ μ l), 1 μ l Primer mix (10 μ M), 2 μ l HPLC grade water and 5 μ l Sso Advanced SYBR Green Super mix (Bio-Rad Laboratories, Inc.). The PCR conditions were : initial denaturation at 98 $^{\circ}$ C for 2 min, 40 cycles of denaturation at 98 $^{\circ}$ C for 5 s, annealing at 50-70 $^{\circ}$ C gradient for 15 s, elongation at 72 $^{\circ}$ C for 15 s followed by melt curve analysis from 65-95 $^{\circ}$ C, 0.5 $^{\circ}$ C increment for 5 s to verify the specificity of the amplicons. Once the PCR conditions were optimized, standard curves were obtained for A β 1-42 gene and *Y45F10D.4* by generating a 10-fold dilution series (DNA concentration range: 1 ng to 1×10^{-7} ng) of the template DNA. A no-template negative control (NTC) was included in all the PCR reactions.

2.2.6 Single worm lysis for PCR

Single worm lysis was performed by picking individual worms from each transgenic strain into 20- μ l lysis buffer (Supplementary Table 1). Samples were incubated for 16 h at 55 °C followed by 1 h at 85 °C. Worm lysates diluted 10-fold with HPLC grade water were used as DNA template for qPCR of all test samples.

2.2.7 Copy number PCR assay

The putative A β containing transgenic strains, selected based on pharyngeal mCherry expression, were analysed for A β 1-42 transgene copy number. Average efficiencies obtained from the standard curves were used to normalise the Cq value of the test samples. The relative copy number of A β 1-42 gene to reference gene *Y45F10D.4* was calculated using $\Delta\Delta$ Ct method with the formula (Rao et al., 2013)

Equation 1: Relative copy number: delta delta Ct method

$$\text{Relative copy number} = 2^{[Cq(A\beta) * E(A\beta)] - [Cq(Y45F10D.4) * E(Y45F10D.4)]}$$

where Cq = quantitation cycle and E= reaction efficiency.

qPCR reactions for all samples were performed in duplicate. The relative copy number of A β 1-42 in each transgenic strain was calculated by averaging the copy number of A β 1-42 gene of the at least eight worms for that particular transgenic strain.

2.2.8 Total RNA isolation and cDNA synthesis

Total RNA was isolated from wild type and transgenic worms using Trizol (Invitrogen). The frozen worm pellets were homogenized in 500 μ l Trizol and incubated at room temperature for 10 min, to which 0.1 volumes of 1 –bromo 3 –chloropropane (Sigma) were added, mixed thoroughly, and incubated for another 10 min. The sample was centrifuged at 12,000 g for 20 min at 4 °C The aqueous phase containing RNA was transferred to a fresh tube and 0.8 volumes of isopropanol (Sigma-Aldrich, Inc.) was added to it. The samples were incubated at room temperature for 15 min and centrifuged

at 12000 g for 15 min at 4 °C. The pellet obtained was washed with 75% ethanol and centrifuge for 5 min at 7500 g. The pellet was then air dried and resuspended in nuclease free water (NFW) by heating at 60 °C for 10 min to dissolve the RNA. Following RNA extraction, the samples were treated with DNase I and purified (New England Biolabs, Inc.) according to the manufacturer's instructions to remove any residual genomic DNA contamination. cDNA was synthesised using Tetro cDNA synthesis kit (Bioline, Inc.) according to manufacturer's instructions.

2.2.9 RT-qPCR

Standard curves for reference genes *cdc-42* and *Y45F10D.4* were generated using 10-fold serial dilutions of N2 cDNA and for Aβ GMC296 cDNA was used as template. RT-qPCR was performed using the same PCR reaction and conditions for qPCR as described above. The real time quantitative RT-PCR data was normalised by geometric averaging of multiple internal control genes as previously described and is a modification of the Pfaffl method (Bustin et al., 2009; Hellemans et al., 2007; Hoogewijs et al., 2008; Vandesompele et al., 2002). The equation used for calculating the relative gene expression using multiple reference genes is as follows:

Equation 2: Equation for calculating relative gene expression in RT-qPCR

$$\text{Relative gene expression} = \frac{(E_{GOI})^{\Delta Ct_{GOI}}}{\text{GeoMean}[(E_{REF})^{\Delta Ct_{REF}}]}$$

2.2.10 Lifespan analysis

Age-synchronous worm populations were obtained by setting up an egg lay for 4-6 h on 6 cm NGM plates seeded with *E.coli* OP50. The eggs obtained were incubated at 20 °C for three days. young worms on the first day of adulthood were used for all lifespan assays. At day 3, about 20 worms were picked on each 6 cm seeded NGM plate, for a total of 120 worms used for each assay. The number of alive and dead worms were counted. The worms were transferred to fresh plates every day until the end of the reproductive period to avoid overlapping generations and to separate them from the larvae and transferred to

new plates every second day during the post-reproductive period. A worm was scored as dead if there was no touch provoked movement. In addition, the worms that were lost either by crawling off the plate, resulting in drying out, or due to internal hatching (bagging) were scored as censored and not incorporated into the analysis. The assay for each strain was repeated at least three times. Survival curves or Kaplan Meier (KM) curves were generated and analysed in GraphPad Prism 8 software (GraphPad Software, Inc., La Jolla, USA). The log rank (Mantel-Cox) test was used to analyse the differences between the survival curves and to determine the p values. Furthermore, the maximal lifespans for all the strains were analysed by OASIS2 using the modified version of the Mann-Whitney U Test, which determines the differences in the distribution tails of survival data which affects the lifespan. This test also determines the differences in the proportion of the longevity outliers (Gao et al., 2008; Han et al., 2016; Wang et al., 2004). Mortality curves were plotted using the commonly used Gompertz equation (Yen et al., 2008).

Equation 3: Gompertz equation

$$h(t) = Ae^{Gt}$$

The initial mortality rate is A and G is the exponential mortality rate co-efficient. The best-fit values were determined by the performing a maximum-likelihood ratio test using the flexsurv package in R (Bansal et al., 2015; Yen et al., 2008).

2.2.11 Brood size assay

Age-synchronous L4 staged worms (day 2 post hatch) were picked individually to seeded NGM plates and incubated at 20 °C for 24 h. About 5-7 worms per strain were used for each experiment and the worms were transferred to fresh plates every 24 h until the cessation of egg-laying. Any worms that crawled off the plate or showed internal hatching were removed from the experiment. The plates containing the eggs were incubated at 20°C for 3 days and then the progeny counted. The experiment was repeated at least twice for each strain.

2.2.12 Egg retention assay

The egg-in-worm assay was performed according to the protocol described in (Gardner et al., 2013) with a few modifications. Briefly, 15-20 L4 staged worms per strain were picked to seeded NGM plates and incubated at 20 °C for 40 h. One the day of the assay, 10 drops of bleach (2:5 v/v 4.2% NaClO:1N NaOH) were dropped on different locations of a petri dish lid. Individual worms were transferred into each bleach drop and allowed to disintegrate for about 10 min. This gives enough time for the worm cuticle to dissolve and the eggs to remain. The eggs *in utero* were counted using a dissecting microscope.

2.2.13 Rate of egg production assay

Rate of egg production was determined for all the strains using the protocol described in (Teshiba et al., 2016) with few modifications. Briefly, 15-20 L4 staged worms per strain were picked on seeded NGM plates and incubated at 20 °C for 40 h. Approximately 88-90 h post hatch, five young adult worms were transferred to a new NGM plate with a total of six plates per strain. The adult worms were removed from the plates after 6 h and the progeny allowed to develop for 2-3 days. The number of progeny on each plate was then counted and the number of eggs laid/worm/h was determined. The experiment was repeated at least three times.

2.2.14 Chemotaxis assay

Age-synchronous worm populations were obtained by bleaching gravid adults as described above. The newly hatched L1 larvae in M9 buffer were counted and about 500 L1s were transferred to seeded 9 cm NGM plates. This time point was considered to be day 1. Once the worms reached L4 stage, the plates were washed, and the worms were transferred to FUdR (25 µM) containing NGM plates seeded with 10% (w/v) *E.col.* OP50. Chemotaxis was performed according to a standard protocol (Bargmann et al., 1993) with few modifications. Adult worms on day 4 and day 8 were used for chemotaxis. The worms were washed off the plates with M9 buffer and transferred to a 15 ml tube. The worms were then allowed to settle, and the supernatant was removed. The washing step

was repeated for a total of three times to remove all residual bacteria. The worms were not centrifuged as it could affect chemotaxis. The volatile odorants diacetyl and benzaldehyde were used as test odorants for the assay. Diacetyl was diluted 1:1000 [1 μ l in 999 μ l ethanol (100%)] and benzaldehyde was diluted 1:200 [1 μ l in 199 μ l ethanol (100%)]. To set up a chemotaxis assay plate, the volatile odorant (1 μ l) was spotted at one end of the plate, about 3 cm from the centre of the plate. The vehicle control (1 μ l) [100% ethanol] was spotted on the opposite end of the plate, 3 cm from the centre, similar to the odorant spot. In addition, 5% sodium azide (1 μ l) was spotted at the odorant and the control spot to immobilise the worms 15 min prior to the assay. To ensure that the worm motility towards the odorant spot was not an artefact, two plates were set up for each assay by spotting the odorant on the right side of one plate and on the left side of the other plate. The worms in buffer solution were transferred to a small piece of Whatman filter paper (grade 1), which was then inverted onto the assay plate to spot the worms at the centre of the plate. After the worms were transferred on the agar, the Whatman paper was removed using forceps, taking care to not damage the agar surface. The plates were incubated at 20 °C for 1 h after which they were scored, and the chemotaxis index calculated as follows:

Equation 4: Equation for calculating chemotaxis index (CI)

$$\text{Chemotaxis index (CI)} = \frac{\# \text{ worms (test)} - \# \text{ worms (control)}}{\text{Total \# worms} - \# \text{ worms (origin)}}$$

The chemotaxis index (CI) was calculated using Excel 2010 (Microsoft, Inc.) and the bar graph for chemotaxis index was plotted in GraphPad Prism 8 software (GraphPad Software, Inc., La Jolla, USA) to allow for comparison between the different *C. elegans* strains.

2.2.15 Associative learning assay

Age-synchronous worm populations were obtained by bleaching gravid adults. day 4 adult worms were washed three times with M9 buffer and transferred to an unseeded NGM plate. The worms were conditioned for 2 h by placing 2 μ l of odorant (diacetyl) on the lid of the plates. In addition, another group of worms were simultaneously starved in

the absence of diacetyl. Moreover, a naïve group of worms was incubated on an NGM plate in the presence of food without any odorant. At the end of the starvation period, chemotaxis assays towards diacetyl were performed on the both the naïve and the conditioned groups as described above in section 2.2.14.

2.2.16 Memory loss assay

The butanone associative memory assay was performed according to a previously described protocol with a few modifications (Kauffman et al., 2011). Age-synchronous worm populations were obtained using the bleach protocol described above. On day 4, the worms were washed off the NGM plates and transferred to a 15 ml tube. The supernatant was removed after the worms settled by gravity. The wash procedure was repeated for a total of three times. The chemotaxis assay was performed according to the protocol described above. The test odorant used for the assay was butanone 10% (v/v) [100 µl diluted in 1000 µl ethanol (100%)]. The chemotaxis assay for the naïve group was carried out immediately after the worms were washed. The remaining worms were allowed to starve in M9 buffer for 1 h in the 15 ml tube after which they were transferred to conditioning plates (seeded 6 cm NGM plates spotted with 2 µl 10% butanone on the lid) for 1 h. The trained worms were washed off the conditioning plates. Some of the trained worms were used for chemotaxis (CI_{0hr}) immediately after training to estimate the learning index. For measurements of short-term associative memory, the remaining worm population was transferred onto 3 seeded NGM plates and allowed to incubate for 30 min, 1 h and 2 h. The chemotaxis assay for each of the time points was performed at the end of the incubation period. The learning index is estimated from the equation:

Equation 5: Learning index

$$\textit{Learning Index (LI)} = CI_{0h} - CI_{naive}$$

The short-term associative memory (STAM) for the particular time point was calculated using the equation:

Equation 6: Short-term associative memory (STAM)

$$\text{Short – term associative memory (STAM)} = CI_{\text{time point}} - CI_{0h}$$

2.2.17 Motility assays

Worm locomotion was measured on solid and in liquid media. To measure motility on solid media, age-synchronous worms were washed thrice with M9 buffer and placed onto unseeded NGM plates (6 cm). The excess buffer was wicked away using a Kimwipe. The worms were allowed to acclimatize on the plates for 5 min after which worm motility was recorded using an iPhone 7 Plus through Labcam from iDu Optics (New York, USA), which is a microscope adaptor for the iPhone. The videos of worm motility on solid media were recorded at 25 FPS and scale of 4.39 $\mu\text{m}/\text{pixel}$ whereas the motility in liquid media was recorded at 25 FPS, 8.8 $\mu\text{m}/\text{pixel}$. Motility in liquid media was measured according to the protocol described in (Bansal et al., 2015) with few modifications. Briefly, about 10-15 worms were washed at least three times with M9 buffer and transferred to 24 well plates containing 1 ml M9 buffer in each well. The worms were allowed to acclimatize in the liquid for 1 min after which the thrashing was recorded. Adult worms on day 4 (young), day 8 (middle-aged) and day 12 (old worms) were used for all the motility assays. Video recordings were of approximately 45 s-1 min duration. All the videos were then transferred to the computer, converted to .avi format and analysed using the Wormlab software system version 4.0 (MBF Bioscience, Williston, VT USA). The default track settings were used to analyse the videos with a few exceptions. The swimming or crawling option was selected depending on the type of video being analysed and the threshold was adjusted manually for every video.

2.2.18 Basal and enhanced slowing response assays

The basal and enhanced slowing response assays were performed according to an established protocol with few modifications (Sawin et al., 2000). Each 6 cm NGM assay plate consisted of a ring-shaped bacterial lawn of *E. coli* strain HB101 with an inner diameter of 1 cm and outer diameter of 3.5 cm. The basal slowing response (BSR) assay

was performed on well-fed worms and enhanced slowing response (ESR) was measured on starved worms. For BSR, well-fed worms were washed off seeded NGM plates and half of the worms in the buffer solution were transferred to an unseeded NGM plate. The remaining half were placed at the centre of the bacterial ring in the assay plate. All the excess buffer was removed using a Kimwipe after which the worms were allowed to acclimatize for 5 min. The worm movement on unseeded and seeded plates was recorded. The videos were recorded for 45 s - 1 min. To measure the enhanced slowing response assay, worms were washed off seeded NGM plates and transferred to an unseeded NGM plate. The worms were then allowed to starve for 30 min to 2 h after which some of the worms from the starved plate were picked to the centre of the bacterial ring on an assay plate and allowed to acclimatize for 5 min. The worm movement of starved worms on food and off food was recorded for 45 s to 1 min. All videos were analysed using the Wormlab software. The slowing responses were measured on day 4 (young), day 8 (middle-aged) and day 12 (old) adult worms.

2.2.19 Statistical analysis

All data are reported as mean \pm standard error of the mean (SEM). To analyse age-associated data, two-way ANOVA was used with post-hoc pairwise comparisons tests. All other data were analysed using either Unpaired Student's t-test or 1-way ANOVA followed by post-hoc Tukey multiple comparison test. All the data were plotted and analysed in GraphPad Prism 8 software (GraphPad Software, Inc., La Jolla, USA). A p-value < 0.05 was considered statistically significant.

2.3 Results

2.3.1 Construction of a pan-neuronal A β containing transgenic strain

To generate transgenic *C. elegans* strains required for this study, the expression plasmids were introduced into the *C. elegans* gonads by microinjection. The transgenic progeny obtained contain extrachromosomal arrays of these plasmids that are meiotically and mitotically unstable. To ensure stable integration and propagation of the transgene, the transgenic worms were irradiated with X-rays to integrate the array into the worm genome. All the transgenic strains generated using the microinjection marker plasmid pAV1944 were identified by pharyngeal expression of mCherry (Supplementary Figure 2.1A). The transgenic neuronal GFP strain WG700 expressing GFP driven by the *snb-1* promoter was obtained as shown in Supplementary Figure 2.1B. The GFP expression is evident in the head and tail neurons in addition to the entire neuronal network throughout the length of the worm which confirms pan-neuronal expression by *snb-1*. The GFP signal appears diffused because this construct does not include a nuclear localization signal.

2.3.2 Pan-neuronal strain WG643 shows multiple copies of the A β transgene

Transgenic *C. elegans* strains expressing pharyngeal mCherry were confirmed for the presence of *snb-1::DA-A β 1-42::unc-54 3' UTR* transgene by copy number PCR. A segment of a putative iron-sulphur cluster assembly enzyme, *Y45F10D.4*, was used as a reference sequence as it has been previously shown to be a single copy gene per haploid genome (Zhang et al., 2012). In order to obtain the range of the copy number PCR assay, a standard curve was generated using the A β copy number derived from 10-fold serial dilutions of known concentrations of an A β plasmid. The concentration and size of the plasmid was used to estimate the number the copies of the A β transgene in the plasmid DNA sample used for PCR. As can be seen in Figure 2.2A, the copy number ranges from 1-2560 copies per PCR reaction. In addition, standard curves for *Y45F10D.4* and A β were generated using serial dilutions of *C. elegans* genomic DNA (Supplementary Figure 2.2) and A β containing plasmid DNA (Supplementary Figure 2.3), respectively. The reaction efficiency of A β gene (E=95.8%, R²=0.996) and *Y45F10D.4* (E=101.4%, R²=0.993) was

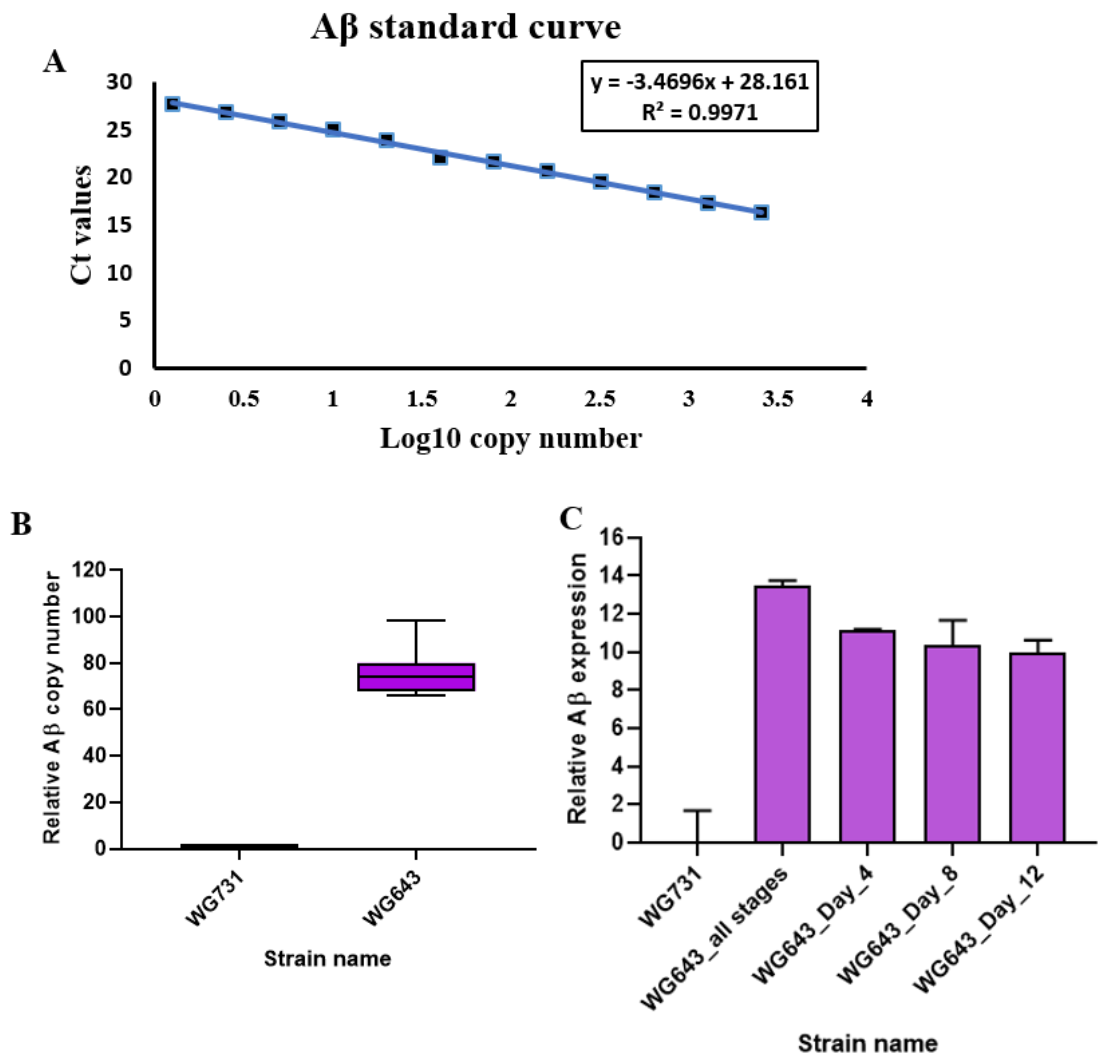


Figure 2.2: Transgenic stable integrated strain WG643 showing presence and expression of A β minigene.

A) Standard curve obtained from 2-fold dilutions of A β containing plasmid DNA ranging from copy number (1-2560 copies) per reaction. Data represented as \log_{10} of the plasmid copy number versus the cycle threshold (C_t) value. This shows the range of the PCR assay. B) Copy number assay showing ~75 copies of the integrated A β transgene relative to the reference gene *Y45F10D.4* (consists of copy number 1 per haploid genome). C) Relative A β expression at the transcript level in the nematodes, normalized to reference genes *Y45F10D.4* and *cdc-42*. day 4: young adults; day 8: middle-aged adults; day 12: old adults. (N=3 for all stages and N=2 for time points day 4, day 8 and day 12 consisting of 200-300 worms per replicate). **WG731**, [*Pmyo2:mCherry*]; **WG643**, [*Pmyo2:mCherry + Psnb-1::huA β 1-42*].

obtained. As can be seen in the box and whiskers plot (Figure 2.2B), the negative transgenic control strain WG731 does not show any evidence of the A β transgene. On the contrary, the transgenic strain WG643 shows the presence of ~75 copies of the A β transgene per haploid genome. The next step was to determine the relative levels of A β transgene expression at the transcript level in the strain WG643 for which RT-qPCR was performed. The stable reference genes *Y45F10D.4* and *cdc-42* were used for normalization as internal control as the expression is shown to be relatively stable at all stages of development (Hoogewijs et al., 2008; Zhang et al., 2012). Moreover, the data generated using multiple reference genes for normalizing A β expression is more reliable (Bustin et al., 2009; Hellemans et al., 2007; Hoogewijs et al., 2008; Vandesompele et al., 2002). The standard curves for A β gene (E=99.4%, R²=0.995) (Supplementary Figure 2.4), *Y45F10D.4* (E=102.9%, R²=0.993) (Supplementary Figure 2.5) and *cdc-42* (E=100.2%, R²=0.898) (Supplementary Figure 2.6) were performed using a cDNA as template. As can be seen in Figure 2.2C, there is A β expression in this WG643 strain. Furthermore, three different time points were selected, which represented adult worms of different ages, day 4 indicates ‘young’, day 8 ‘middle-aged’ and day 12 ‘old adults. The level of A β transgene expression measured was similar at each of these time points.

2.3.3 Subtle decrease in growth rate of the A β -expressing transgenic strain WG643

In order to assess if the expression of the A β transgene in *C. elegans* neurons causes changes in the growth of the worms, the amount of time the worms took to develop to L4 from an egg was initially measured. As can be seen in Figure 2.3A, there was no difference in the time taken to develop to L4s between the wild type N2 and the transgenic control strain WG731 ($p > 0.9999$). However, there was a significant increase in the time taken by the A β -expressing worms to develop to L4 stage when compared to transgenic control strain WG731 and the wild type ($p < 0.0001$). Additionally, the length and the width of the A β -expressing strain WG643 was compared to the transgenic control strain WG731 on day 4 (young), day 8 (middle-aged) and day 12 (old) adults in order to assess the growth rate of the worms, using the Worm lab software. As seen in Figure 2.3, the difference in the length and width of the A β -expressing strain WG643 in comparison

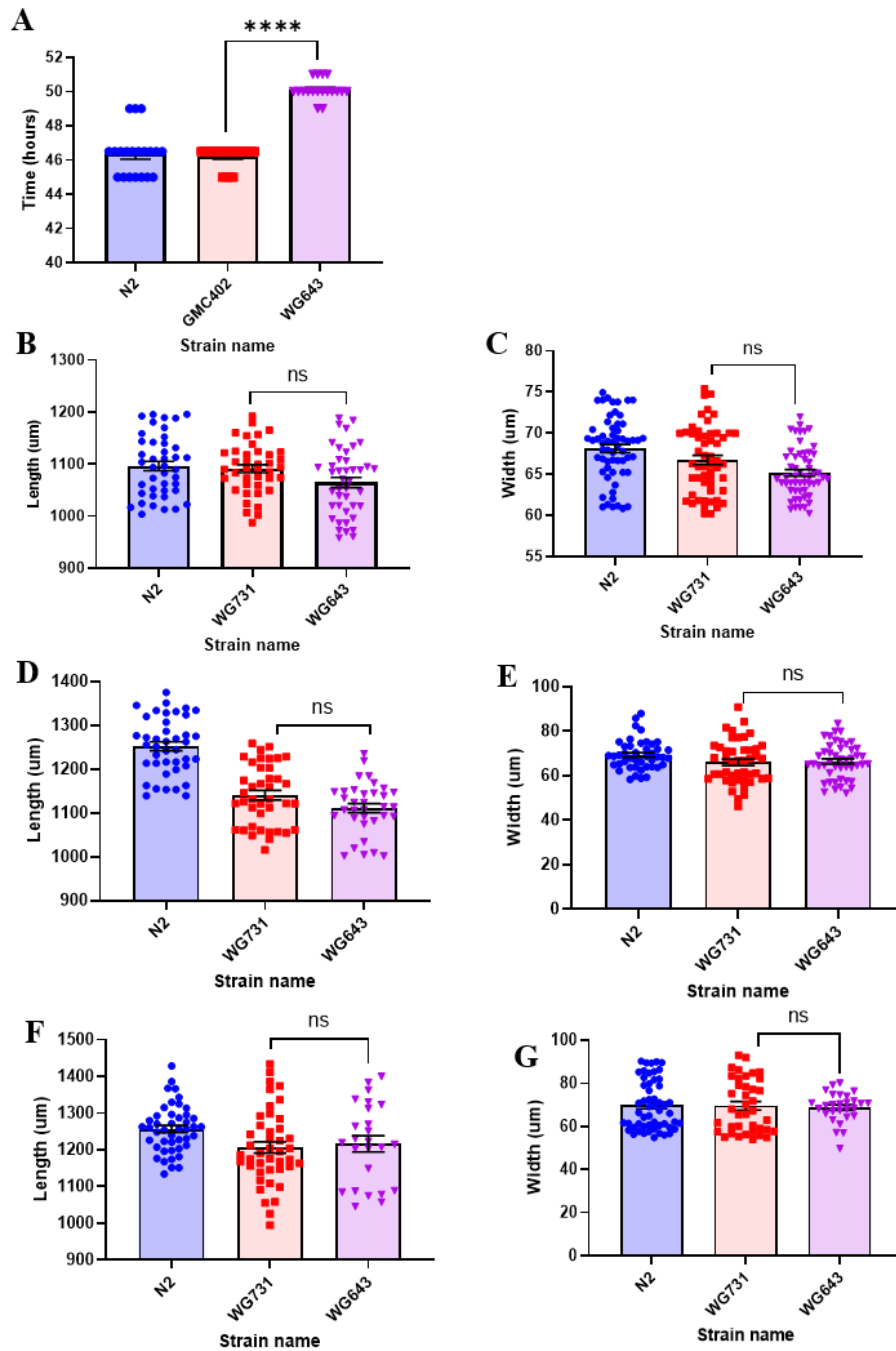


Figure 2.3: *C. elegans* growth estimated by body size measurements of early (day 4), middle-aged (day 8) and old (day 12) worms.

A) Time taken for worms to reach L4. B) Body length of day 4 worms. C) Body width of day 4 worms. D) Body length of day 8 worms. E) Body width of day 8 worms. F) Body length of day 12 worms. G) Body width of day 12 worms. (n = 15 - 45). Each data point represents a single animal. All data analysed using one-way ANOVA followed by post hoc Tukey multiple comparisons test. ns not significant and ****p < 0.0001 N2, Wild type Bristol strain; **WG731**, [*Pmyo2:mCherry*]; **WG643** [*Pmyo2:mCherry* + *Psnb-1::huAβ1-42*].

to transgenic control strain WG731 was not significant on day 4, day 8, or day 12 ($p > 0.05$). In addition, there was no difference in the length and width of the wild type N2 strain and the transgenic control strain WG731 in all age groups. Although the A β -expressing worms showed a slight delay in the initial development to L4, the adult transgenic A β -expressing strain did not show significant change in the growth rate when compared to the transgenic control strain WG731.

2.3.4 Pan-neuronal A β strain shows reduction in lifespan

Since premature death is one of the symptoms of AD, the survival of the A β -expressing strain WG643 was analysed. As can be seen in Figure 2.4A, the A β -expressing strain WG643 shows a sharp decline in the survival in comparison to the transgenic control strain WG731. The log-rank test showed a significant difference between the transgenic control WG731 and A β -expressing strain WG643 ($p < 0.0001$). The survival curves for the remaining biological replicates have been plotted in Supplementary Figure 2.7. Furthermore, there is a significant decrease in the median lifespan of the worms in the A β -expressing strain WG643 (25.8%) compared to the transgenic control strain WG731 ($p < 0.0001$). In addition, the median lifespan of the transgenic control strain WG731 was lower when compared to the wild type N2 strain ($p = 0.018$), which may be due to the presence of the co-injection marker transgene (*Pmyo-2::mCherry*) (Figure 2.4B). The survival data was also used to evaluate the differences in the rate of aging between these strains by calculating the initial mortality rate (A) and the Gompertz rate coefficient (G) from the Gompertz equation using maximum likelihood estimation. The cumulative hazard plot for three strains are shown in Supplementary Figure 2.8. A lower G value indicates lower rate of aging. As can be seen in Table 2.1, there is a significant increase in the Gompertz rate coefficient (G) of the A β -expressing strain WG643 as compared to the transgenic control strain WG731. Therefore, the mortality rate doubling time (MRDT) shows the chance of the A β -expressing worms dying after sexual maturity doubles every 2 days, which is higher than the transgenic control strain that shows a MRDT value of ~4 days.

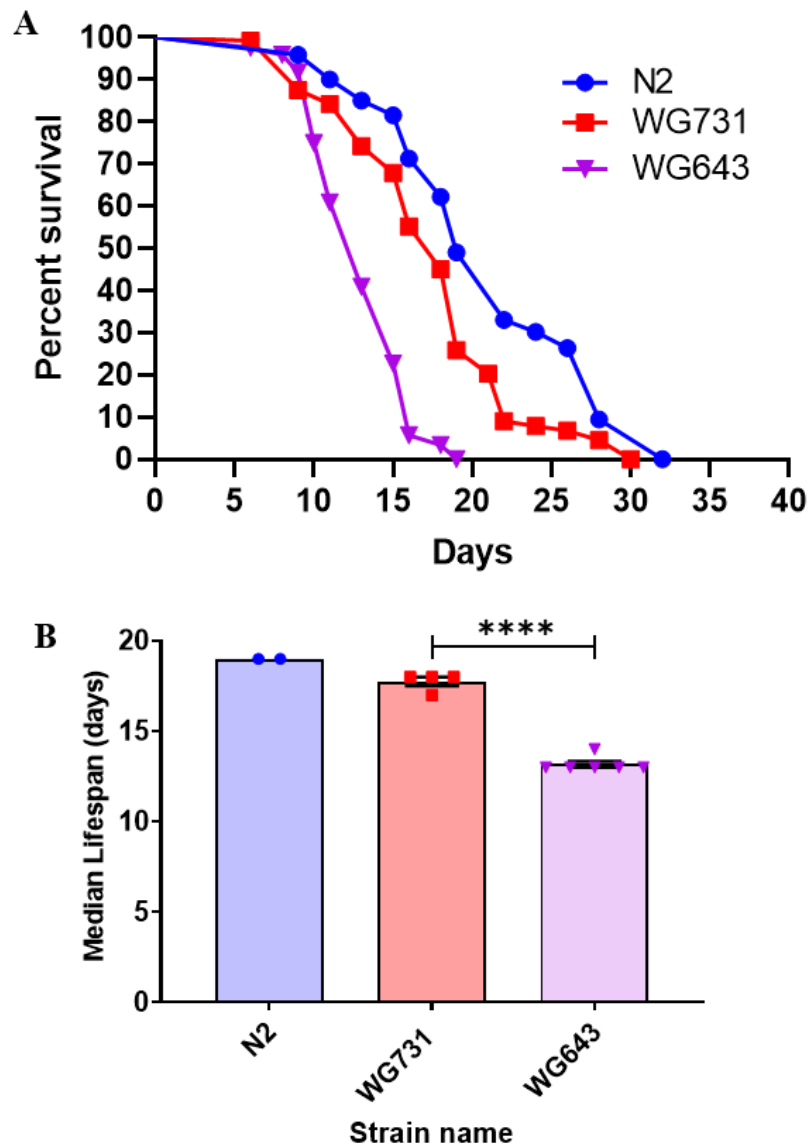


Figure 2.4: Pan neuronal A β -expressing strain shows reduced longevity.
 A) Representative survival curves of one biological replicate (n =120 worms/replicate). B) Median life span (n =2-4, 120 worms/replicate). ns not significant. ****p < 0.0001, N2, wild type Bristol strain; WG731 [*Pmyo-2::mCherry*];WG643 [*Pmyo-2::mCherry* + *Psnb-1::huA β 1-42*]

Table 2.1: Values for G and A obtained by using the Gompertz equation

Strain name	Initial mortality rate (A)	Gompertz value(G)	Rate of aging (MRDT)
N2	3.65E-03	0.1667	4.15
WG731	6.00E-03	0.1677	4.13
WG643	3.89E-03	0.3217**	2.16

2.3.5 Pan-neuronal A β -expressing strain shows age-related deficits in locomotion

Several studies have shown that functionally distinct neuronal circuits regulate *C. elegans* crawling and swimming behaviours. Movement on solid media (crawling) is characterized by a sinusoidal posture, whereas in liquid worms show a C-shaped posture (Mesce and Pierce-Shimomura, 2010; Pierce-Shimomura et al., 2008; Vidal-Gadea et al., 2011). To determine if there were any age-related behavioural deficits associated with A β expression, motility of the worms was measured on both solid and liquid media on day 4 (young worms), day 8 (middle-aged worms), and day 12 (old worms). Movement of worms on solid media was measured using several different motility parameters. As can be seen in Figure 2.5A, the number of body bends was similar between the A β -expressing worms WG643 and the transgenic control strain WG731 on day 4 ($p = 0.82$). However, there was a sharp decline in the body bends of the A β -expressing worms on day 8 ($p < 0.0001$) and day 12 ($p < 0.0001$), being significantly lower than the transgenic control strain WG731. Similarly, the mean speed showed a significant decline in comparison to the transgenic control on day 8 ($p < 0.0001$) and day 12 ($p < 0.0001$) (Figure 2.5B). However, there was an age-related decline in body bends and mean speed for all the strains. Additionally, maximum speed is an important indicator of healthspan and was also measured in the A β -expressing strain WG643 (Hahm et al., 2015). As can be seen in Figure 2.5C, there was a significant age-related decline in the maximum speed in the A β -expressing worms compared to the control strain on day 12 ($p = 0.038$, unpaired t test). Furthermore, the amplitude of the body bend, defined as the amplitude of the sine wave that best fits the worm posture or the depth of the body bends was measured. As can be seen in Supplementary Figure 2.9A, there was a significant decrease in the amplitude of the A β -expressing worms on day 8 ($p < 0.0001$) compared to the transgenic control strain WG731. The wavelength that is defined as the period of the sine wave that best fits the

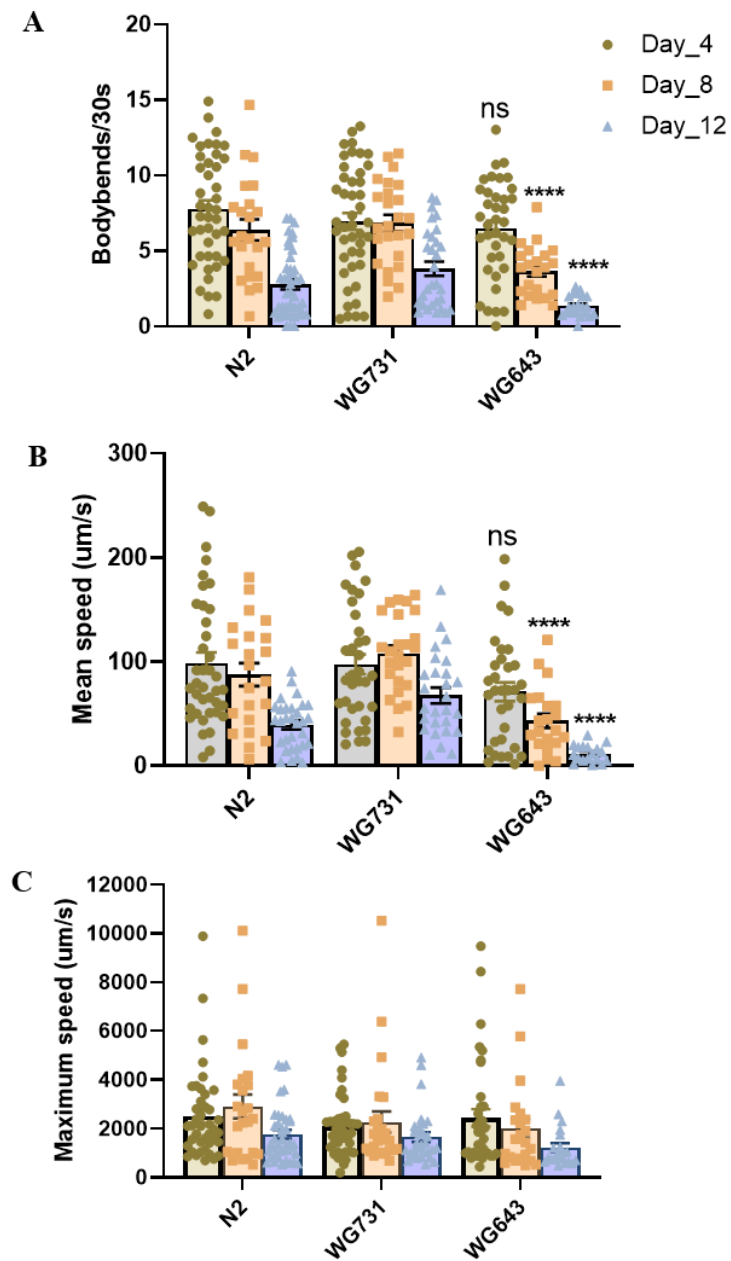


Figure 2.5: Age-related changes in worm motility parameters in solid media.

A) Bodybends/30s. B) Mean speed (um/s). C) Maximum speed. (um/s) Headbends/30s. All data analysed by two-way ANOVA followed by post hoc Tukey multiple comparisons test. Significance values represent pairwise comparison between transgenic control WG731 and Aβ-expressing strain WG643. ns not significant, ** $p < 0.01$, *** $p < 0.001$, **** $p < 0.0001$ (n=3, 5-15 worms/replicate). N2, wild type Bristol strain; WG731 [*Pmyo-2::mCherry*]; WG643 [*Pmyo-2::mCherry + Psnb-1::huAβ1-42*].

worm posture showed a significant overall increase from day 4 to day 12 in all the strains, while the difference in wavelength between the A β -expressing strain and the transgenic control strain was statistically insignificant on day 4 ($p = 0.99$), day 8 ($p = 0.83$), and day 12 ($p = 0.96$) (Supplementary Figure 2.9B). Furthermore, the number of head bends measured in a 30s interval, an indicator of foraging behaviour, showed no difference between strains (Supplementary Figure 2.9C). Pairwise correlations were performed using R to evaluate which of the parameters are significantly correlated with each other and if there were any changes in the correlation as the worms get older. As can be seen in Supplementary Figure 2.10A and Supplementary Figure 2.11A, several parameters are significantly correlated in young adults on day 4 in the transgenic control strain WG731 and the A β -expressing strain WG643. For instance, the correlation of body bends with distance travelled diminishes in WG643 but not in WG731 on day 8. Similarly, the body bends and mean speed correlations in the A β -expressing strain diminishes on day 12. In summary, the correlation between the motility parameters diminishes in the transgenic A β -expressing strain WG643 on day 8 and day 12.

Worm motility on liquid media is usually characterized by a C-shaped posture (Pierce-Shimomura et al., 2008). As shown in Figure 2.6A, there was no difference in the body bends/30s (thrashes/30s) between the A β -expressing strain WG643 and the transgenic control WG731 on day 4 ($p = 0.98$). However, there was a significant reduction in the body bends/30s of the A β -expressing strain WG643 on day 8 ($p = 0.0068$) and day 12 ($p < 0.0001$) in comparison to the transgenic control WG731. Furthermore, there was a significant reduction in the mean swimming speed of the A β -expressing strain WG643 when compared to the transgenic control strain on day 4 ($p = 0.004$), day 8 ($p < 0.0001$) and day 12 ($p < 0.0001$) (Figure 2.6B). In addition, the activity index which is a measure of how vigorously the worms bend while swimming over time was also analysed. In comparison to the transgenic control WG731, the transgenic A β -expressing strain WG643 showed a significant decline in activity on day 4 ($p = 0.048$), day 8 ($p = 0.0004$) and day 12 ($p = 0.0003$) (Figure 2.6C). The wave initiation rate which is defined as the number of body waves initiated from the head or tail per minute was also measured (Figure 2.6D). There was a significant decrease in the wave initiation rate of A β -expressing strain

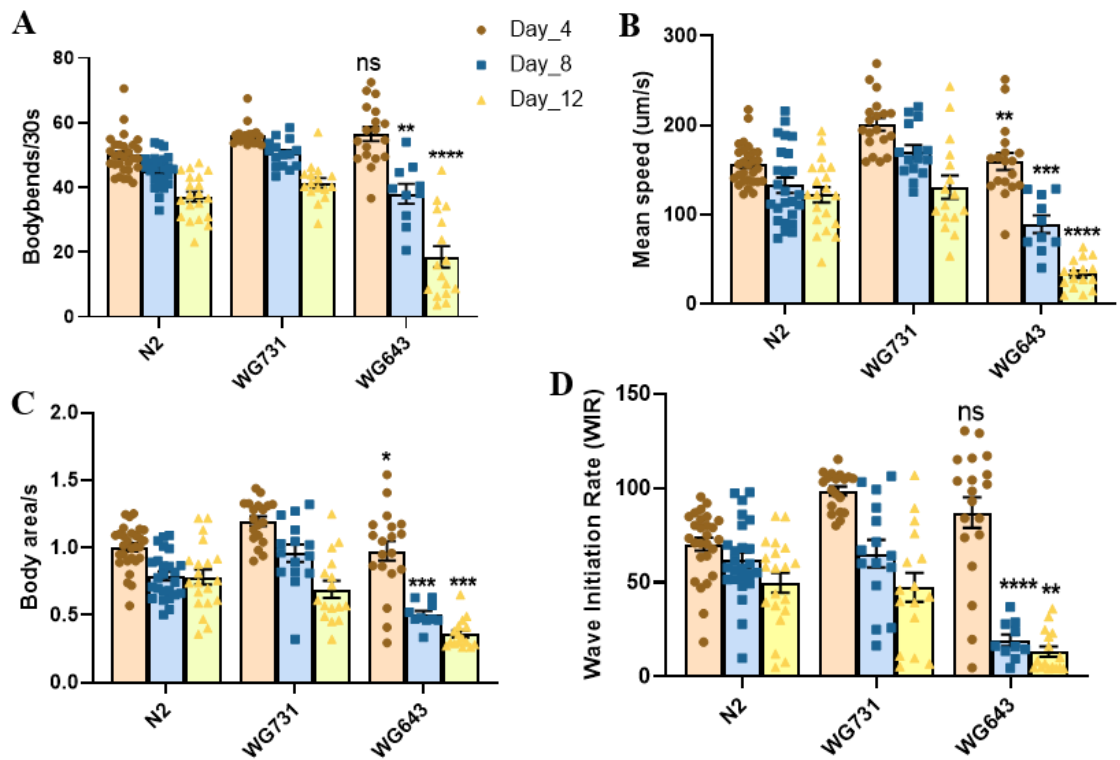


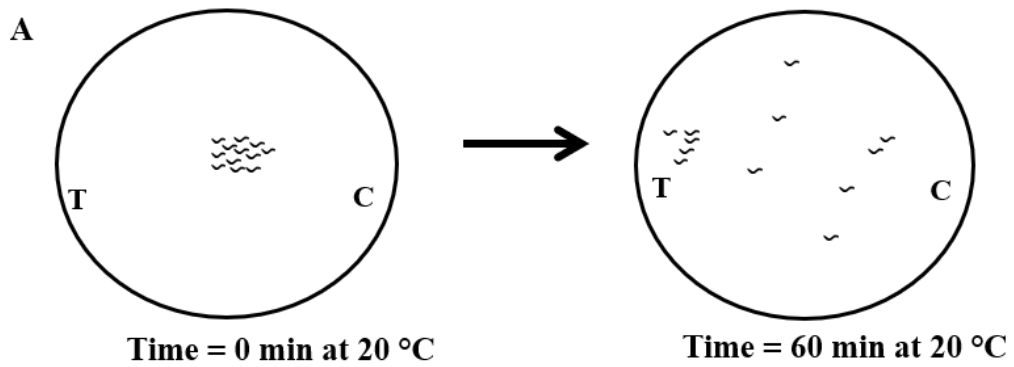
Figure 2.6: Age-related changes in worm swimming parameters

A) Average number of thrashes/30s B) Mean speed (um/s) C) Activity (body area/s) D) Wave Initiation rate (WIR)(n=2, 5-15 worms/replicate).. All data analysed by two-way ANOVA followed by post hoc Tukey multiple comparisons test. Significance values represent pairwise comparison between transgenic control WG731 and A β -expressing strain WG643 at each timepoint. ns not significant, *p < 0.05 **p < 0.01, ***p < 0.001, ****p < 0.0001. N2, Wild type Bristol strain;WG731 [*Pmyo-2::mCherry*];WG643 [*Pmyo-2::mCherry* + *Psnb-1::huA β 1-42*].

WG643 in comparison to the transgenic control on day 8 ($p < 0.0001$) and day 12 ($p = 0.0015$), but not on Day 4 ($p = 0.38$). Curvature-based motility analysis using parameters such as the brush stroke, dynamic amplitude and curling of the worms was performed. The brush stroke gives an indication of the depth of the worm movement and extent to which the worms has stretched in a given body bend. As shown in Supplementary Figure 2.12A, although the brush stroke of the A β -expressing strain WG643 remains similar to the transgenic control on day 4 ($p = 0.94$) and day 8 ($p = 0.52$), there is a significant reduction in the brush stroke on day 12 ($p = 0.03$). Furthermore, the dynamic amplitude gives a sense of whether the body bends are deep or flat and how much stretching effort occurs in a single body bend. In contrast to the brush stroke, there is a significant increase in the stretching effort by the A β -expressing strain WG643 in comparison to the transgenic control strain WG731 on day 4 ($p = 0.025$) and day 12 ($p = 0.024$) (Supplementary Figure 2.12B). Additionally, the curling parameter determines the percentage of time the animal spends in the bent state and can detect changes in curl pattern of swimming worms, and that there was no significant difference between the transgenic A β -expressing strain WG643 and the transgenic control WG731 on day 8 ($p = 0.85$), and day 12 ($p = 0.99$) but was on Day 4 ($p = 0.038$) (Supplementary Figure 2.12C).

2.3.6 Pan-neuronal A β -expressing strain shows changes in chemotactic response towards volatile odorants

Another behaviour used to assess age-associated neuronal dysfunction is olfaction. Since olfaction in the worms is mediated by specific subsets of chemosensory neurons, two well-characterised volatile odorants, diacetyl and benzaldehyde, were used for chemotaxis assays (Bargmann et al., 1993). The chemotaxis index of the worms towards both the odorants were measured in young (day 4) and middle-aged (day 8) adults. A schematic illustration of a chemotaxis assay is shown in Figure 2.7A. Chemotaxis assays measure the fraction of the worms that are attracted towards a particular chemical in a given time interval. This fraction is represented as a chemotaxis index (calculated using Equation 4) and the values obtained range from +1 to -1, wherein +1 indicates maximum attraction and -1 indicates maximum repulsion. As can be seen in Figure 2.7B, there was a



$$\text{Chemotaxis Index (CI)} = \frac{\# \text{ worms at point T} - \# \text{ worms at point C}}{\# \text{ total worms} - \# \text{ worms at origin}}$$

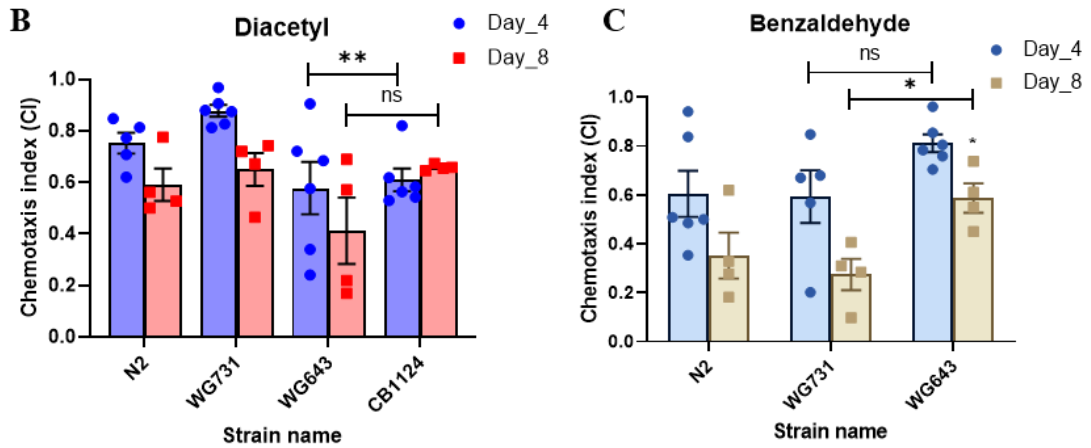


Figure 2.7: A β -expressing strain WG643 shows a change in chemotactic response.
 A) Schematic illustration of a chemotaxis assay. Bar graph showing the chemotaxis index of *C. elegans* strains for Diacetyl (B) and Benzaldehyde (C) on Day 4 and Day 8. (n=4-6, 100-200 worms/ replicate). ns non-significant, *p<0.05, **p<0.01. **N2**, Wild type Bristol strain; **WG731** [*Pmyo-2::mCherry*]; **WG643** [*Pmyo-2::mCherry* + *Psnb-1::huA β 1-42*].

significant decrease in the chemotaxis index of the A β -expressing strain WG643 (CI 0.57) in comparison to the transgenic control WG731 on day 4 ($p < 0.01$, unpaired t test). Although the A β -expressing strain does show a reduced chemotaxis index towards diacetyl on day 8 (CI 0.41) compared to the control group, the difference was not statistically significant. The *che-3* mutant strain CB1124 was used as a negative control of chemotaxis towards diacetyl and showed reduced chemotaxis on day 4 (CI 0.60) and day 8 (CI 0.65). On the other hand, the A β -expressing strain WG643 showed a significant increase in its ability to sense benzaldehyde compared to the transgenic control strain WG731 on day 8 ($p = 0.022$, unpaired t test) (Figure 2.7C). In addition, the wild type strain N2 and the transgenic control strain WG731 showed similar chemotaxis index towards both odorants on day 4 and day 8. These findings suggest that the expression of A β peptide affects neuronal function *in vivo*.

The motility of the worms was estimated by calculating the % worms that moved from the origin at the end of chemotaxis assay. As can be seen in Supplementary Figure 2.13, although there was a decrease in the motility of the A β -expressing worms on chemotaxis plates on day 8 in comparison to the transgenic control strain WG731, it was statistically significant only for benzaldehyde ($p = 0.0005$).

2.3.7 Pan-neuronal A β -expressing strain shows decrease in fecundity

Egg-laying in *C. elegans* has been used extensively to study the genetics of the nervous system (Schafer, 2006). In order to assess if the expression of A β in the worms results in egg-laying defects, egg-laying assays were performed. Firstly, the number of progeny laid per day per worm was counted during the reproductive span of the worm as shown in Figure 2.2.8A. There was a significant reduction in the progeny of the A β -expressing worms on Day 6 ($p < 0.0001$) and Day 7 ($p = 0.016$) of adulthood in comparison to the transgenic control strain WG731. In addition, the fecundity or total brood size was measured by counting the total number of progeny produced during the entire reproductive span of the worm. The overall brood size of the A β -expressing strain

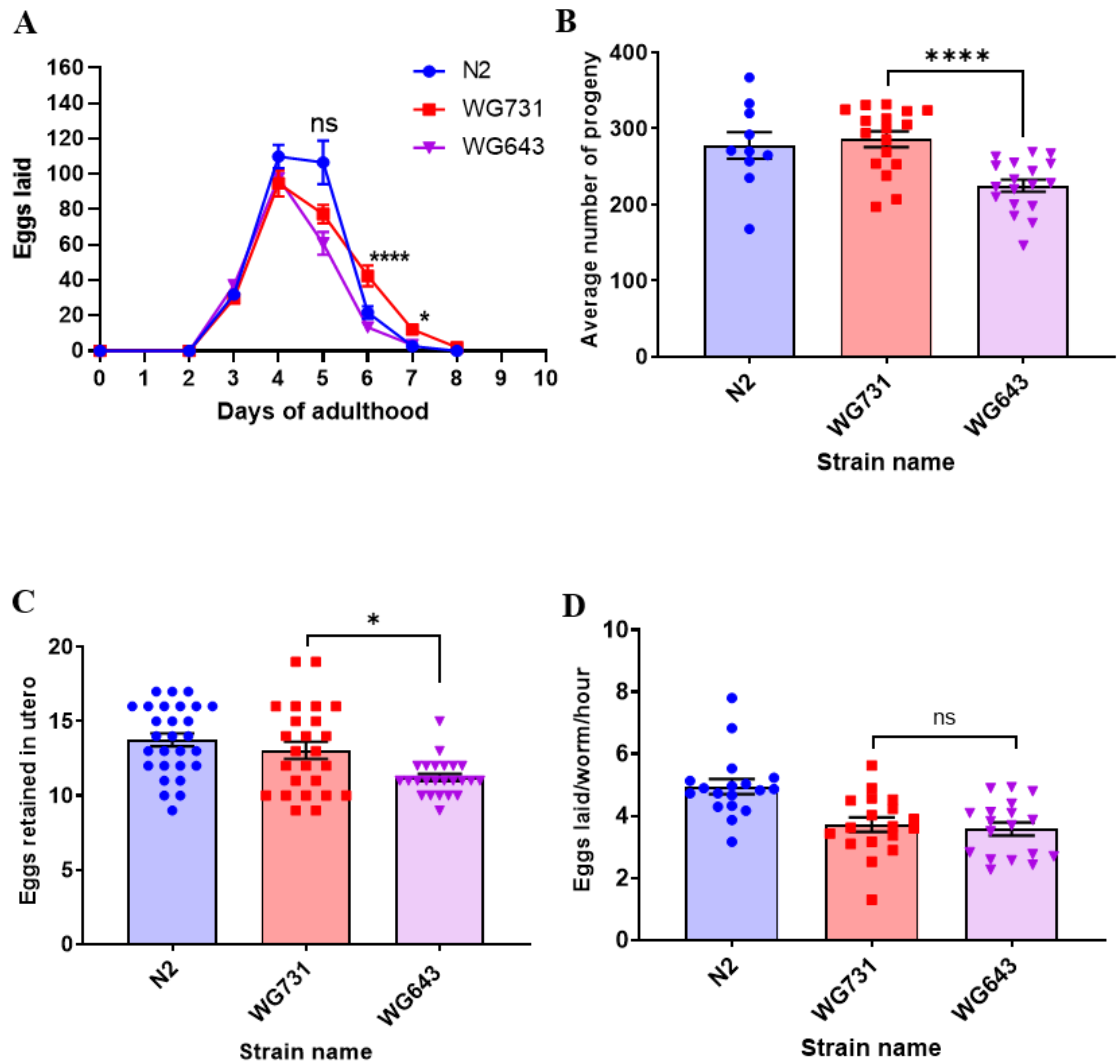


Figure 2.2.8: Pan-neuronal A β expression results in impaired egg-laying.

A) Average number of eggs laid per day during the reproductive span of the worm. B) Brood size assay (n = 3, 5-7 worms/replicate). C) Egg-retention assay measuring the average number of eggs retained *in utero* (n=3, 15-20 worms/replicate). D) Average number of eggs laid per worm per hour (n=3, 15-20 worms/replicate). All data analysed using one-way ANOVA followed by post hoc Tukey multiple comparisons test, ns not significant *p < 0.05, **p < 0.01, ***p < 0.001, ****p < 0.0001. **N2**, wild type Bristol strain; **WG731** [*Pmyo-2::mCherry*]; **WG643** [*Pmyo-2::mCherry* + *Psnb-1::huA β 1-42*].

WG643 was significantly lower ($p < 0.0001$) in comparison to the transgenic control WG731 (Figure 2.2.8B). Moreover, the total brood size of the transgenic control WG731 was similar to the wild type N2 strain.

Secondly, an egg-retention assay was performed to measure the number of eggs retained in the uterus of the worm. It was found that the number of eggs retained *in utero* of the A β -expressing strain WG643 was significantly lower (~11 eggs/worm) than the control transgenic strain WG731 (~13 eggs/worm) ($p < 0.05$) (Figure 2.2.8C). Additionally, there was no difference in the number of eggs retained *in utero* between the transgenic control strain WG731 and the wild type N2 strain.

Thirdly, the progeny laid per worm per hour was calculated and there was no change in the egg-laying rate between the transgenic A β -expressing strain WG643 (3.6 eggs/worm/h) and the transgenic control strain WG731 (3.7 eggs/worm/h) (Figure 2.2.8D) ($p = 0.24$). Overall, these data suggest that there may be a defect in the rate of egg production which results in reduced number of eggs *in utero* and ultimately leads to a decrease in brood size in the A β -expressing strain WG643.

2.3.8 Pan-neuronal A β -expressing strain showed deficits in dopaminergic signalling

Experience-based locomotion assays are used to study defects in neurotransmission. The behaviour of worms has been shown previously to change in the presence of food in the environment. For instance, well-fed worms slow down when reintroduced into a bacterial lawn. This slowing response also known as basal slowing response (BSR), is experience-based and shown to be dependent on the dopaminergic neuronal pathway (Ranganathan et al., 2001; Sawin et al., 2000). The diminished slowing response of well-fed worms on food suggest deficits in dopaminergic signalling. As shown in Figure 2.9A, the transgenic A β -expressing strain WG643 showed a statistically significant slowing response in the presence of food on day 4 ($p < 0.0001$) similar to the the control strain WG731 and the wild type N2 strain; on the contrary, as predicted, the control strain CB1112 (*cat-2(e1112)*) shows diminished slowing response even at day 4. The mutant strain CB1112 has defects in dopaminergic signalling as the mutation in the *cat-2* gene, which encodes a

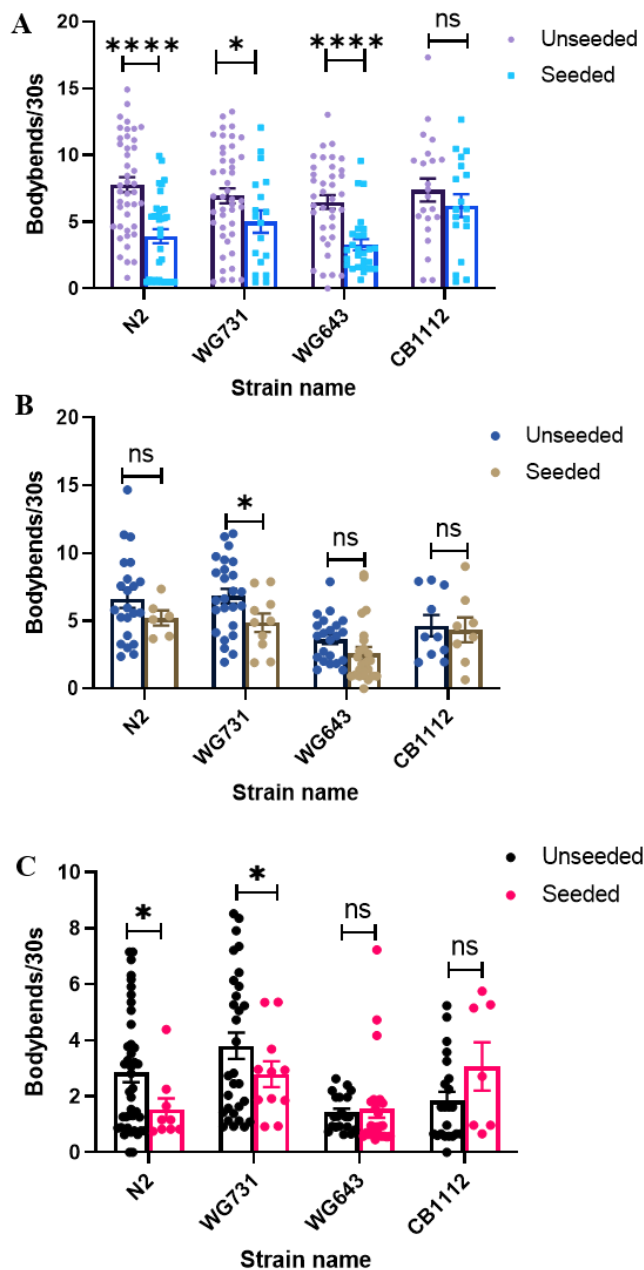


Figure 2.9: Pan-neuronal Aβ-expressing strain shows deficits in dopaminergic signalling.

A) Day 4. B) Day 8. C) Day 12 (n = 3, 5-15 worms/replicate). An unpaired t test was performed to test for significance in slowing response, ns not significant, *p < 0.05, **p < 0.01, ***p < 0.001, ****p < 0.0001. **N2**, wild type Bristol strain; **WG731** [*Pmyo-2::mCherry*]; **WG643** [*Pmyo-2::mCherry* + *Psnb-1::huAβ1-42*], **CB1112** [*cat-2 (e1112) II*].

tyrosine hydroxylase known to be involved several processes including dopamine biosynthesis (Sawin et al., 2000). However, the A β -expressing strain showed diminished slowing response on day 8 ($p = 0.24$) and day 12 ($p = 0.72$), which suggests deficits in dopaminergic signalling as the worms grow older. On the contrary, the transgenic control strain WG731 show statistically significant slowing responses even at later time points on day 8 ($p = 0.049$) and day 12 ($p = 0.038$) whereas the control strain CB1112 showed diminished slowing responses on day 8 and day 12 as expected. Although wild type N2 worms do slowdown in the presence of food on day 8 and day 12, the slowing response is only significant on day 12 (Figure 2.9B,C). Since the A β -expressing strain WG643 show diminished slowing responses on Day 8 and Day 12, these results indicate that these animals may be defective in dopaminergic signalling.

Another experience-based locomotion assay is the enhanced slowing response assay (ESR) mediated by serotonin. The ESR measures the slowing response of starved worms when reintroduced onto a bacterial lawn. Mutant strains defective in neurotransmission were used as positive controls for this experiment. The mutant strain CB1141(*e1141*) has a mutation in the gene *cat-4*, which encodes an enzyme that synthesises the co-factor required for dopamine and serotonin biosynthesis (Weinshenker et al., 1995). The mutant strain MT7988 (*bas-1(ad446)*) has reduced serotonin levels due to a mutation in an aromatic amino acid decarboxylase, an enzyme needed for the biosynthesis of serotonin and dopamine (Loer and Kenyon, 1993.). As can be seen in Supplementary Figure 2.14A, on day 4, the wild type N2 strain ($p < 0.0001$), the transgenic control strain W731($p = 0.0048$) and A β -expressing strain WG643 ($p = 0.0004$) slow down significantly in the presence of bacteria. However, the positive control strains MT7988 ($p = 0.52$) and CB1141($p = 0.024$) do not slow down in the presence of bacteria. Although the wild type N2 strain ($p = 0.29$) and the transgenic control strain ($p = 0.32$) slowdown in the presence of food on day 8, the slowing response is not statistically significant. However, the A β -expressing strain WG643 showed diminished slowing response on day 8 ($p = 0.54$) similar to the control strains MT7988 and CB1141 (Supplementary Figure 2.14B). On day 12, none of the worm strains show significant slowing response in the presence of food (Supplementary Figure 2.14C). Based on these data, no evidence was found that the A β -expressing strain WG643 shows a defect in serotonergic signalling.

2.3.9 Pan-neuronal A β -expressing strain showed deficits in associative learning and short-term memory

In order to study the effects of A β expression on learning and memory of the worms, food-odorant association-based learning assays were conducted. In the first associative learning assay, young adult worms on day 4 were starved in the presence of the attractant diacetyl for 2 h and standard chemotaxis assays towards diacetyl were performed after the incubation period. The naïve group consisted of well-fed worms incubated in the absence of the odorant. The groups starved in the absence and presence of diacetyl have been denoted as diacetyl ‘-’ and diacetyl ‘+’ in Figure 2.10A. The wild type N2 strain and the transgenic control strain WG731 show an aversive response by a significant reduction of chemotaxis towards diacetyl after the starvation period. Although the transgenic A β -expressing strain group starved in the presence of diacetyl shows a moderate reduction in chemotaxis towards diacetyl after the starvation, the difference between the groups that were starved in the presence and absence of the odorant is not significant.

The second associative learning and memory assay utilised the AWC neuron-sensed volatile chemoattractant butanone at a concentration that should result in a low chemotactic response. On day 4, briefly starved worms were fed in the presence of butanone and then the chemotaxis of these conditioned worms towards butanone was tested. The AWC pair of chemosensory neurons sense butanone, and pairing butanone with food changes the chemotactic response of *C. elegans* towards butanone, known as butanone enhancement (Torayama et al., 2007). This associative learning assay was performed to evaluate the cognitive decline associated with A β expression. In addition, the memory of this food-butanone association was also tested. The controls used in the experiment that showed associative learning defects were KP4 *glr-1(n2461)* and RB888 *casy-1(ok739)*. The gene *glr-1* belongs to the glutamate receptor family and *casy-1* is a CAISYntenin/AIcadein homolog. As can be seen in Figure 2.10B, the learning index (LI) at time T0 of the A β -expressing strain WG643 was 0.2, which is an increment in the chemotactic response of the conditioned worms in comparison to the naïve group. This increase in chemotactic response was similar to that seen in the transgenic control strain WG731. The memory of this learned association was measured after specific time

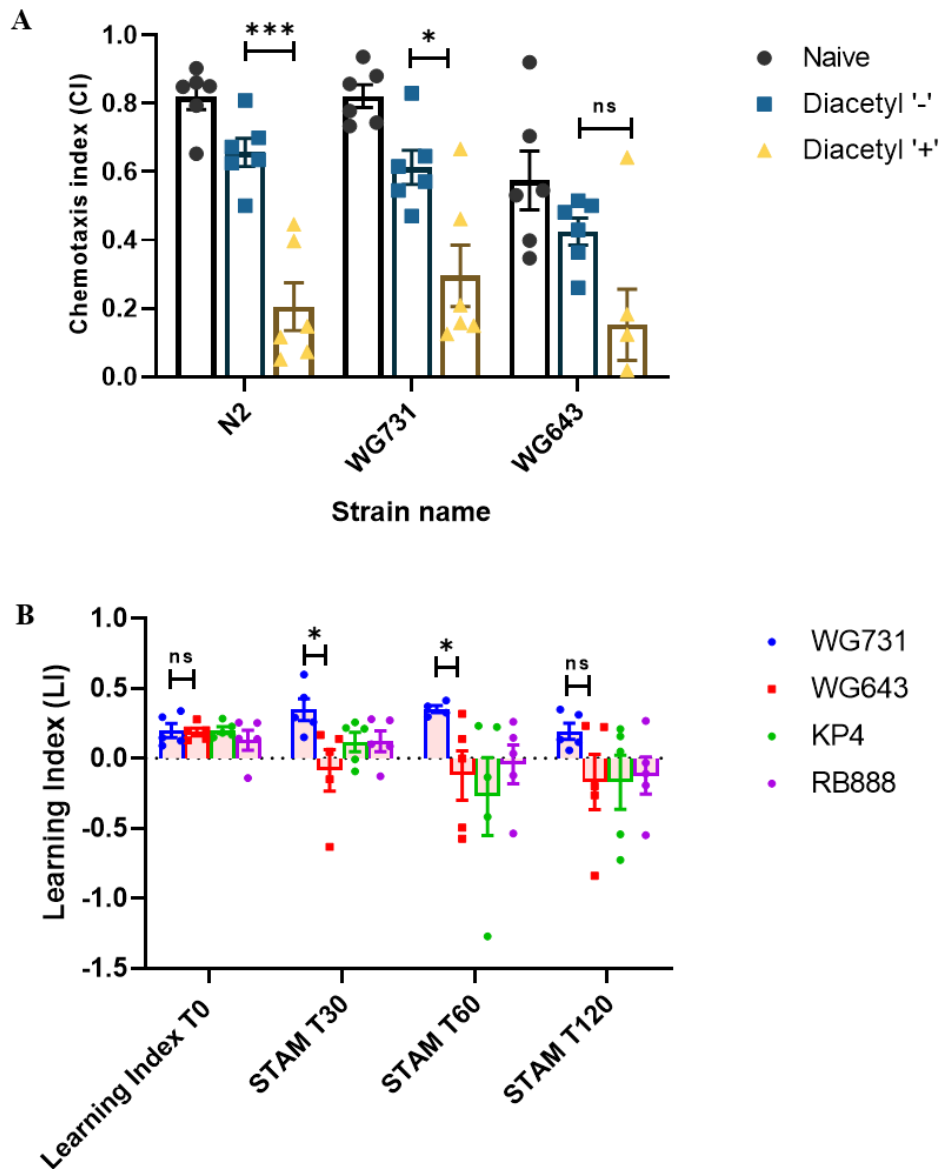


Figure 2.10: Pan-neuronal A β -expressing strain shows deficits in learning and memory.

A) Associative learning assay using volatile odorant Diacetyl. (n=6, 100-200 worms per biological replicate). An unpaired t test was used to test for significant difference in chemotactic response to odorant between control and conditioned worms within strains. B) Short term memory loss assay using butanone (n =6, 100-200 worms per replicate). An unpaired t test was used to test for significant difference in STAM between strains at specific timepoints.

ns not significant *p < 0.05, ***p < 0.001. **N2**, wild type Bristol strain; **WG731** [*Pmyo-2::mCherry*]; **WG643** [*Pmyo-2::mCherry* + *Psnb-1::huA β 1-42*].

intervals known as the short-term associative memory (STAM). STAM is measured by the difference between the chemotaxis index towards butanone after conditioning at specific time intervals (30 min, 1 h, and 2 h) and chemotaxis at T0. The STAM measured after conditioning declines to -0.08 after 30 min, -0.12 after 1 h, and -0.16 after 2 h. Moreover, the decline in short term associative memory is significantly lower than the transgenic control strain WG731 at 30 min ($p < 0.05$) and 60 min ($p < 0.05$). This implies that although the A β -expressing worms are able to form the association between butanone and food, they are unable to retain the information, resulting in the decline of the learning index after 30 min of conditioning.

2.4 Discussion

The aim of this chapter was to develop a new *in vivo* model of AD by expressing the human A β 1-42 peptide in the *C. elegans* nervous system, using the pan-neuronal promoter *snb-1*. The new transgenic *C. elegans* strain described here shows high levels of expression of the A β transgene and displays a wide range of behavioural deficits, thereby making an important addition to the already existing strains. Behavioural phenotypes include reduced longevity, impaired motility in solid and liquid media, defects in chemotactic response towards diacetyl, reduced brood size and deficits in short term associative memory. This strain can be used to test the hypothesis that expression of human A β 1-42 in the *C. elegans* nervous system causes a behavioural change in the worms that may be relevant to the disease symptoms seen in human AD patients.

2.4.1 Successful integration and expression of A β in the transgenic *C. elegans* strain WG643

The new strain WG643 described in this chapter was constructed using a plasmid containing the modified version of the human A β 1-42 transgene that had an extra sequence GACGCG at its 5' end. Several of the previously reported transgenic *C. elegans* AD strains were shown to express a truncated version of the human amyloid β -peptide, A β 3-42, which is not abundantly expressed in the human AD brain. This error occurred due to an unexpected post-translational N-terminal truncation of the synthetic signal peptide (McColl et al., 2009). The transgene sequence was repaired by inserting the sequence GACGCG (-DA-) to the 5' region of the human A β gene between the synthetic signal peptide and A β minigene (Fong et al., 2016; McColl et al., 2012). The amino acid residues (-DA-) were selected based on the empirical rules known for the substrate specificity of the signal peptidase. The first rule predicts that the signal peptidase requires small hydrophobic residues like alanine at positions at -1 and -3 with respect to the cleavage site. The second rule predicts that the peptide bond located at a distance of six residues C-terminal to the end of the hydrophobic core of the signal peptide will mainly be cleaved (Dalbey and Von Heijne, 1992; Lichtenthaler et al., 1999; von Heijne, 1983).

The pan-neuronal promoter *snb-1* was used to drive the expression of the A β transgene in the *C. elegans* nervous system. Synaptobrevins are proteins associated with synaptic vesicles, have a role in synaptic transmission, and are expressed predominantly in the neurons. Previous reports indicate that majority of SNB-1 expression was restricted to the major process bundles such as the nerve ring, ventral cord and dorsal cords, with some expression seen in neuronal cell bodies but no expression detected in commissural and dendritic processes (Nonet et al., 1998). There is evidence that transgenes driven by the *snb-1* promoter may be expressed in other non-neuronal cells such as the spermatheca and the pharynx but that the expression is predominantly neuronal (Hunt-Newbury et al., 2007; McKay et al., 2003). The neuronal A β 3-42 expressing strain also used the promoter *snb-1* to drive the expression of the A β transgene in the neurons (Dosanjh et al., 2010).

All the transgenic *C. elegans* strains were generated by microinjection of the expression plasmids at different concentrations together with a visible marker plasmid and fragmented genomic DNA into the worm gonad. Microinjected DNA is assembled into a large, mitotically and meiotically unstable extrachromosomal, multicopy arrays by non-homologous recombination. Genomic DNA fragments in the injection mixture allow the genomic DNA to assemble into the array with the plasmid DNA, thereby preventing germline silencing of the array that can occur when there are tandemly repeated plasmid sequences without any intervening DNA (Kelly et al., 1997; Praitis and Maduro, 2011), and the copy number of the transgene in the assembled array depends on the ratio of the genomic “carrier” DNA to the transgene plasmid. The arrays assemble independently in each F1 progeny, so that the copy number of the transgene and the stability of extrachromosomal arrays are different in each transgenic F1 individual; and each strain derived from F1 animals that transmit the array is an independent transgenic strain carrying a unique array. Extrachromosomal arrays are of varying lengths, and stability of inheritance of the array is roughly proportional to its length (Mello and Fire, 1995). There are a few copies of the arrays present in a cell and they segregate in a non-mendelian fashion during cell division, thereby having varying degrees of meiotic and mitotic instability (Mello et al., 1991) (Stinchcomb et al., 1985).

As a result of this instability, not all progeny of a transgenic worm inherit the array, thereby giving rise to transgenic and non-transgenic progeny. Apart from that,

extrachromosomal arrays that contain a high copy number of a transgene that is toxic for the worms are silenced or selected against, resulting in few progeny inheriting the array and a decrease in transmission frequency (Praitis and Maduro, 2011). In addition to meiotic instability, arrays are also mitotically unstable and thus quickly lost over subsequent generations. Further, each worm will contain a unique array containing a unique number of copies of the transgenes; therefore, the effect of the transgene is confounded by differences between individual worms.

To overcome this problem, it is important to integrate the array into the genome by irradiation. This causes DNA damage in the worm that is subsequently repaired by non-homologous end-joining and includes random insertion of the arrays at the sites of repair. This means that arrays in different integrated F1s will be inserted in different locations, and at different numbers of locations, generating stable inter-strain variation in copy number and thus expression, eliminating within-worm mosaicism of expression. The generation of a family of related strains with variable transgene copy number is a distinct advantage of microinjection and integration over alternative methods, such as Mos1 mediated single copy insertion (MosSCI) and clustered regularly interspaced short palindromic repeats (CRISPR) (Dickinson et al., 2013; Frokjaer-Jensen et al., 2008). Moreover, it is possible to obtain isogenic animals for further analysis after the transgene has been integrated (Praitis and Maduro, 2011). All the strains in this study are integrated, ensuring all the cells in every worm inherit the array at each generation. A limitation of this approach for generating transgenic strains is that the insertion of the multicopy array occurs at a random chromosomal location and there may be potential mutations and genome rearrangements due to irradiation (Nance and Frokjaer-Jensen, 2019). Therefore, it is important to obtain multiple integrants and outcross them repeatedly to the wild type to remove any background mutations.

The presence and expression of the A β transgene in the new transgenic strain described here, WG643, was characterized and validated at the genomic and transcript level (Figure 2.2). Immunoblotting was attempted to detect the expression of A β peptide in transgenic A β -expressing strain WG643 (data not shown). However, no clear evidence of A β peptide expression was determined from this experiment. This may be due to the technical difficulties associated with detecting the hydrophobic A β peptide using Western blot

combined with the fact that neurons make up a very small proportion of the total protein mass of a worm. Confirmation that this strain accumulates human A β 1-42 is an essential follow up. Therefore, immunohistochemistry experiments performed on this strain would ensure there is A β expression and accumulation in this strain.

2.4.2 Reduced lifespan and healthspan in the A β -expressing strain

Although the growth of the A β -expressing worms is similar to the transgenic control strain, there was a rapid increase in mortality after middle age (Figure 2.4). In other words, this implies that the worms did not have stunted or enhanced growth early in their lifespan, but instead aged and died faster. Healthspan, described as the period when an individual is functional and free of disease, was also assessed (Fuellen et al., 2019; Luyten et al., 2016). Maximum movement velocity is correlated with healthspan and longevity and has been shown to decline with age (Hahm et al., 2015). In this context, the age-related decline in maximum velocity of the A β -expressing worms compared to the transgenic control may suggest a decline in healthspan at middle age (Figure 2.5C). In addition, there was an overall reduction in brood size, and the number of eggs retained *in utero* is lower as a result of reduced rate of egg production. There was a sharp decline in the number of progeny on day 6 of the reproductive fertility period in the A β -expressing worms suggesting a decline in healthspan at middle age compared to the transgenic control (Figure 2.2.8). Egg-laying behaviour has been shown to be affected by disruptions to the cellular homeostasis and defective neurotransmission (Fang et al., 2019), and this likely also explains the results presented here.

2.4.3 A β expression impacts locomotion in transgenic strain WG643

Motility was analysed on both solid and liquid media since crawling differs from swimming in both kinematics and neuromuscular activity (Pierce-Shimomura et al., 2008). For instance, worms that carry mutations in the *unc-79* or *unc-80* genes were reported to be defective in swimming, but showed normal locomotion in solid media (Pierce-Shimomura et al., 2008). This observation might be due to the fact that swimming

in liquid requires more energy than crawling, and because any abnormal movement may be easier to detect in liquid since there is an increase in the freedom of movement (Fang-Yen et al., 2010; Korta et al., 2007; Laranjeiro et al., 2017; Schreiber et al., 2010). In this study, the A β -expressing worms showed similar motility in solid media as the transgenic control on day 4, while crawling parameters, including body bends and mean speed, start to decline at middle age on day 8 (Figure 2.5). In liquid media, parameters such as wave initiation rate and activity have been previously shown to decline with age even in the most favourable genetic backgrounds (Ibanez-Ventoso et al., 2016; Restif et al., 2014). In line with the current knowledge, there was an age-related decline in these parameters in all the strains. However, the decline in the activity and wave initiation rate of the A β -expressing worms in liquid was much more severe starting at day 8. Furthermore, motility in liquid showed a decline in the number of thrashes starting at day 8, as well as a significant decline in mean swimming speed even on day 4 (Figure 2.6). These motility measures are highly sensitive and have been utilized to define functional declines in longevity mutants such as *age-1(hx546)* and *daf-16(mgDf50)* (Ibanez-Ventoso et al., 2016).

Experience based motility of the A β -expressing worms was also explored. The basal slowing response modulated by dopamine and the enhanced slowing response modulated by serotonin are behaviours with associative learning properties (Hobert, 2003). Several studies have reported that serotonergic and dopaminergic neurons are susceptible to aging in humans, specifically in age-related diseases such as AD (Mattson, 2004). The A β -expressing strain WG643 shows a diminished basal slowing response starting at day 8 which suggests that A β expression results in deficits in dopaminergic signalling in mid-late adulthood (Figure 2.9B, C). An enhanced slowing response was observed in the A β -expressing strain as early as day 4 (Supplementary Figure 2.14). However, no enhanced slowing responses were observed for any of the strains on day 8 and day 12. It has been previously shown that differences in the basal and enhanced slowing response between diminishes with age, which may be due to an increase in the basal slowing response with age among all strains (Murakami et al., 2008). Moreover, the ESR assays are sensitive to motility defects and this will affect the ability to detect a serotonin defect. Thus, it is not

possible to determine if the A β -expressing worms are deficient in serotonergic signalling using the enhanced slowing response assay alone.

2.4.4 A β -expressing transgenic *C. elegans* strain WG643 has disease relevant phenotypes

Despite of having a simple nervous system, *C. elegans* is able to display complex behaviours such as the ability to discriminate and move towards or away from chemicals, odorants, temperatures and food sources and it is possible to correlate neuronal function with certain behavioural responses (Bargmann, 2006; de Bono and Maricq, 2005). For example, worms can detect attractant and repellent compounds using chemosensory neurons: response to these chemicals is mediated by the activation of sensory and interneurons that, in turn, stimulate the motor neurons that induce the worm to move (Hobert, 2003). The AWA neurones detect diacetyl and the AWC pair detects butanone and benzaldehyde (Bargmann et al., 1993). The A β -expressing worms showed a decline in chemotactic ability towards diacetyl on day 4 (Figure 2.7A). In contrast, the worms showed an increase in their chemotaxis towards benzaldehyde relative to the control strain (Figure 2.7B). These responses may be due to the specific loss of AWA neurons associated with the expression of A β . Since the motility of the A β -expressing worms is similar to the transgenic control on day 4, the defect in chemotaxis is a primary defect and not a secondary defect arising due to loss in motility (Supplementary Figure 2.13). Furthermore, the neuronal A β 3-42-expressing strain has previously been shown to have a reduced chemotactic ability towards benzaldehyde and no change in chemotaxis towards diacetyl (Dosanjh et al., 2010). The A β 3-42 peptide may have different physiochemical properties *in vivo* than the A β 1-42, which may result in variation in the behavioural phenotype observed. Furthermore, the inability to identify odours is a common symptom observed in aging humans and is the best-known predictor of AD dementia (Rahayel et al., 2012; Ship et al., 1996; Sun et al., 2012; Velayudhan et al., 2013; Wehling et al., 2016). Previous studies have suggested odour identification may be an earlier indicator of accumulated pathology before the onset of other symptoms (Lafaille-Magnan et al., 2017).

Since the most visible symptoms of AD are memory loss and cognitive decline, quantitative measurement of differences in learning and memory in the A β -expressing worms is important to assess its utility as a model for AD. High-level cognitive abilities across *C. elegans* strains are lost much earlier than basic motility and chemotaxis abilities. Therefore, deficiencies in the worm's learning behaviour can be detected early on (Herndon et al., 2002; Kauffman et al., 2011; Kauffman et al., 2010; Morrison and Hof, 1997). All the memory assays were performed on young adults (day 4) since the chemoreception abilities should be intact on day 4 before the loss of chemotaxis. Food-odour associative learning is a food-dependent behaviour mediated by serotonin, which informs the food status of the environment to the nervous system (Nuttley et al., 2002). The first associative-learning assay used adaptation suppression, as starving wild-type worms in the presence of diacetyl reduces the chemotaxis of the worms towards the odorant. Studies have shown that high and low concentrations of diacetyl induce distinct learning mechanisms (Bernhard and van der Kooy, 2000). The A β -expressing worms show reduction in adaptation suppression and therefore defects in associative learning (Figure 2.10A). Another study performed the same assay using benzaldehyde and found this associative learning behaviour to be mediated by serotonergic signalling (Nuttley et al., 2001). A similar learning defect was reported for the A β 3-42-expressing strain when using diacetyl in the learning assay (Dosanjh et al., 2010).

The second learning assay conditioned the worms with food in association with butanone at a concentration of this chemical that is known to result in a low chemotactic response when it is presented alone. The combination of food with this low concentration of butanone, increases the chemotaxis towards this odor, a phenomenon known as butanone enhancement (Kauffman et al., 2011; Kauffman et al., 2010). Butanone enhancement requires butanone sensation, food sensation, followed by integration of the butanone and food signals, and formation of memory, which occurs when butanone is sensed by the AWC neurons (Bargmann et al., 1993). Pairing food and butanone produces a short-term memory response that lasts for about 2 hours in wild type worms (Kauffman et al., 2011; Kauffman et al., 2010). Although the A β -expressing worms showed associative learning immediately after conditioning, there was a more rapid decline in the short-term associative memory in the A β -expressing worms after 30 min of conditioning which

implies deficits in memory (Figure 2.10B). Similar results were reported for mouse models of AD (Ashe, 2001; Chiba et al., 2009).

2.5 Conclusion

The new transgenic *C. elegans* strain WG643 has been extensively characterised for A β transgene integration and expression, and behavioural phenotyping has been carried out to analyse diverse worm behaviours that are regulated by different subsets of neurons. These worms showed rapid age-related decline in behavioural phenotypes that are regulated by the neurotransmitters, dopamine and serotonin. The severe and robust behavioural phenotypes demonstrated makes this strain important for the study of the disease. In addition, it should provide an important tool to test the amyloid cascade hypothesis which posits that A β plays a major role in initiating the cascade of events leading to AD. Therefore, greater the accumulation of A β may result in an increase in the severity of the phenotype. The next chapter describes strains that express the A β transgene at different concentrations and correlates this expression with severity of the disease phenotype.

Chapter Three

Behavioural phenotyping of strains expressing varying levels of amyloid β transgene driven by three different pan-neuronal promoters

3.1 Introduction

Despite genetic evidence and the demonstrated involvement of A β in inducing synaptic dysfunction, disrupting neural connectivity, and association with neuronal death in a brain-region specific manner, the amount and distribution of extracellular A β deposition are only weakly correlated with the clinical expression and severity of the disease (Murphy and LeVine, 2010). This weak correlation between the plaque burden and disease severity has been used to criticise the amyloid cascade hypothesis. Furthermore, in many cases the level of the soluble A β correlates with the disease burden better than the insoluble A β version (McLean et al., 1999; Yu et al., 2019). Additionally, it has been suggested that the soluble A β protein is associated with faster cognitive decline, supporting the role of soluble A β as a neurotoxic agent of aging (Yu et al., 2019). The insoluble A β appears only to signify the presence of the disease. Although a low concentration of A β may have a role in neural development and in the regulation of cholinergic transmission (Harkany et al., 2000; Sadigh-Eteghad et al., 2014), it appears that A β in higher concentration causes neurotoxicity, impairs blood flow within the cerebral structure, and accelerates neuronal dysfunction (Sadigh-Eteghad et al., 2015). Thus, the exact relationship between A β concentration and neuronal dysfunction is unclear and more studies need to be done to clarify it (Sadigh-Eteghad et al., 2015).

In the previous chapter, I introduced a pan-neuronal A β 1-42 expressing transgenic *C. elegans* strain driven by the *snb-1* gene promoter. In doing so, I showed that the expression of human A β 1-42 in the *C. elegans* neurons resulted in neuronal-controlled behavioural deficits in worms relevant to the disease symptoms observed in humans. In

this chapter, I explore whether the severity of the disease phenotypes is correlated with the levels of A β 1-42 expression. Therefore, the aims of this chapter are as follows:

1. Create transgenic *C. elegans* strains that vary in the A β expression level.
2. Analyse how varying levels of A β correlate with the severity of the relevant disease phenotypes.

To do this, additional transgenic *C. elegans* strains were generated to achieve variation in A β expression. Differences in transgene expression can be mediated by the promoters integrated with the plasmid, as well as the number of copies of the transgene. A new transgenic strain expressing the A β 1-42 transgene in the nervous system driven by another pan-neuronal promoter, *rgef-1*, was generated and compared to the previously described neuronal strain that uses the promoter *snb-1* (Chapter 2). The gene *rgef-1* encodes a human ortholog of RAS guanyl-releasing protein 3 and is expressed exclusively in the nervous system (Altun-Gultekin et al., 2001; Chen et al., 2011). The median FPKM (fragments per kilobase of transcript per million mapped reads) expression value for the *rgef-1* gene in all life-stages is 4.5 which is quite low (Grun et al., 2014). In comparison, the *snb-1* promoter shows higher levels of activity in all life stages with a median FKPM expression value of 192.8 (Grun et al., 2014). In addition, I also tested a previously published neuronal A β 1-42 expressing strain, GRU102, in which the *unc-119* promoter drives A β 1-42 expression. The *unc-119* gene is expressed in several tissues, including the head, the muscular system, and the nervous system (Materi and Pilgrim, 2005). The median FKPM expression value in all life stages for the *unc-119* gene is 22.9 (Grun et al., 2014) and so it is intermediate between *rgef-1* and *snb-1* promoter activities (although not restricted specifically to the nervous system). Amongst the three promoters, the *rgef-1* promoter has the lowest activity, the *unc-119* promoter has higher activity than *rgef-1*, and the *snb-1* promoter is the strongest pan-neuronal promoter in the list. Furthermore, variation in A β expression levels may result from variation in the number of copies of the A β transgene. Hence, A β transgene copy number was also measured in these transgenic strains.

These strains (which I show vary in transgene transcript level) may provide an opportunity to test the relationship between A β concentration (or expression) and

dysfunction. I hypothesise that the severity of the disease phenotype correlates with the levels of A β expression in these transgenic strains, assuming that transcript concentration is correlated positively with protein translation and/or accumulation. Key behaviours in *C. elegans* include lifespan, growth rate, egg-laying and retention, chemotaxis, and motility. If the level of A β expression in the nervous system drives differences in disease severity, then I expect that as A β expression increases, so does the impact on each of the life and health span measurements as worms get older.

3.2 Methods

All materials and methods used in this chapter are described in Section 2.2 with a few exceptions (described below).

3.2.1 Construction of expression plasmids and generation of transgenic *C. elegans* expressing pan-neuronal transgenes by microinjection

The promoter region 2670 bp upstream of the *rgef-1* gene was amplified from the *C. elegans* wild-type genomic DNA using the *rgef-1* promoter-specific forward and reverse primers by long range PCR Go Taq enzyme (Promega Corporation, Madison, Wisconsin, USA) (Chen et al., 2011). The PCR reaction was 10 μ l (1 μ l DNA template, 0.5 μ l Primer mix (10 μ M), 3.5 μ l HPLC grade water, and 5 μ l GoTaq Master mix (2X)), and the PCR conditions were (initial denaturation at 94 °C for 2 min, 35 cycles of denaturation at 94 °C for 30 s, annealing at 69.7 °C for 30 s, elongation at 70 °C for 3 min, followed by final extension at 72 °C for 10 min). See Supplementary Table 2 for a list of primers used in the study. The amplified *rgef-1* promoter fragment was then digested with PstI and XmaI and cloned into the complementary PstI and XmaI sites of promoter-less A β plasmid pAB42, resulting in the expression plasmid pEXAB42 containing the human A β 1-42 transgene driven by pan-neuronal promoter *rgef-1* (F25B3.3). The *rgef-1* promoter fragment was also inserted into the complimentary PstI and XmaI sites of the promoter-less GFP-containing plasmid pPD95.77, resulting in transgene expression plasmid pEXGFP. Details of the transgene expression plasmids are listed in Supplementary Table 3. All clones were digested with restriction enzymes PstI and XmaI to confirm the presence of the *rgef-1* promoter insert (Supplementary Figure 3.1) and were verified by Sanger sequencing (Macrogen, Korea). For pEXAB42 and pEXGFP, the presence of *rgef-1* promoter was confirmed using *rgef-1* specific primers internal to the promoter sequence.

To generate the transgenic *C. elegans* strains (refer to Supplementary Table 4 for details all transgenic strains generated in this study), the expression plasmids were introduced into the *C. elegans* gonads by microinjection, performed at the Florey Institute of Neuroscience and Mental Health by Kirsten Grant. The A β -containing plasmid pEXAB42

was micro-injected at a concentration of 25 ng/μl along with marker plasmid pAV1944 (2.5 ng/μl) and sheared genomic DNA (50 ng/μl). Furthermore, the plasmid pEXGFP was microinjected along with sheared genomic DNA (50 ng/μl pEXGFP and 50 ng/μl genomic DNA). Details of the plasmids used for microinjections to generate the strains described in this study are listed in Supplementary Table 4.

3.2.2 Microscope details for pan-neuronal GFP-expressing strain WG625

Glass microscope slides were prepared with agarose pads by pipetting 300 μl of 2% agarose solution (in HPLC water) onto the slide and flattening slightly using a cover slip, before allowing the agarose to cool and gel. Once the agarose pad solidified, the cover slip was removed. Several worms were picked on to each agarose pad and immobilised by heating the slide on a block at 55 °C for 10 s. The agarose pad was then covered with a cover slip. Images were acquired using either an Upright microscope Nikon Eclipse Ci equipped with Nikon DS-U3 Digital Camera or Zeiss LSM 510 laser scanning confocal microscope with a Plan Apochromatic 20X/0.8 NA objective. Excitation was achieved with an argon multiline laser at 488 nm (eGFP) and DPSS laser of 561 nm (mCherry). A long pass LP575 filter was used for detection of mCherry. Z stacks were obtained using Zen software.

3.2.3 Strains used in this chapter

The strains described in this chapter are as follows: **WG731** [*Pmyo-2::mCherry*]; **WG643** [*Pmyo-2::mCherry +Psnb-1::huAβ1-42*]; **WG663** [*Pmyo-2::mCherry +Prgef-1::huAβ1-42*]; **GRU101** *gnaIs1*[*Pmyo-2::YFP*]; GRU102 *gnaIs2*[*Pmyo-2::YFP + Punc-119::huAβ1-42*]; **CB1124** [*che-3(e1124)*]; **CB1141** [*cat-4 (e1141)*]; **CB1112** [*cat-2 (e1112)*]; **MT8943** [*bas-1(ad446) III; cat-4(e1141) V*]; **MT7988** [*bas-1(ad446) III*]. Details of all transgenic *C. elegans* strains used in this study have been listed in Supplementary Table 5.

3.2.4 Statistical analysis

All data have been reported as mean \pm SEM values. To compare the strains WG643 and WG663 with the control strain WG731, an ordinary one-way ANOVA was used followed post-hoc Tukey multiple comparisons test unless otherwise stated. To determine differences between GRU101 and GRU102, an unpaired-t test was used unless otherwise stated. A Shapiro-Wilk test was used to test normality and if the data were not normally distributed, then non-parametric tests were used to determine whether differences were significant.

3.3 Results

3.3.1 Pan neuronal A β 1-42 expressing strains show variation in copy number and expression

I hypothesised that the expression levels of A β 1-42 in these transgenic strains would depend on the number of copies of the A β transgene integrated into the *C. elegans* genome in addition to the intrinsic promoter activity. Therefore, a copy number assay was performed to quantify the number of copies of the A β 1-42 transgene in each transgenic strain. The transgenic strain WG663 contains A β 1-42 driven by the promoter *rgef-1*, WG643 contains A β 1-42 driven by the *snb-1* promoter, and the transgenic strain WG731 was used as a control for these strains since all three were constructed using the same transgenic marker *Pmyo-2::mCherry*. On the other hand, the strain GRU102 contains A β 1-42 driven by the promoter *unc-119* and the strain GRU101 was used as a control for this strain as both contain the transgenic marker *Pmyo2::YFP*. Figure 3.1A shows the relative A β 1-42 transgene copy number per haploid genome, normalised to a single-copy reference gene *Y45F10D.4*. The average relative A β 1-42 copy number in WG643 (*Psnb-1::A β*) is 85.67 ± 3.65 copies, the strain WG663 (*Prgef-1::A β*) contains 75.86 ± 2.58 and GRU102 (*Punc-119::A β*) contains 3.59 ± 0.68 copies. As expected, the control strains do not show any copies of the A β 1-42 transgene.

Furthermore, the expression levels of the A β 1-42 transgene were measured in these transgenic strains using an RT-qPCR assay. Figure 3.1B illustrates the relative log-fold expression of A β 1-42 transgene in these strains normalised to reference genes *Y45F10D.4* and *cdc-42*. The strain WG643 shows the highest levels of A β 1-42 expression (13.47 ± 0.28) in comparison WG663 (11.67 ± 0.26) and GRU102 (5.197 ± 0.91). The strain WG663 shows relatively higher A β 1-42 expression than GRU102 even though the A β transgene driven by a weak promoter *rgef-1*. As a result, we have a panel of pan-neuronal A β 1-42 expressing strains showing variation in the A β expression levels due to both different pan-neuronal promoter activity and variation in the number of A β 1-42 copies in each of these strains. For easier explanation of the results, the WG643 strain will be denoted as *Psnb-1::A β* , the WG663 strain as the *Prgef-1::A β* and the transgenic control strain WG731 as the mCherry control. In addition, the GRU101 control strain will be

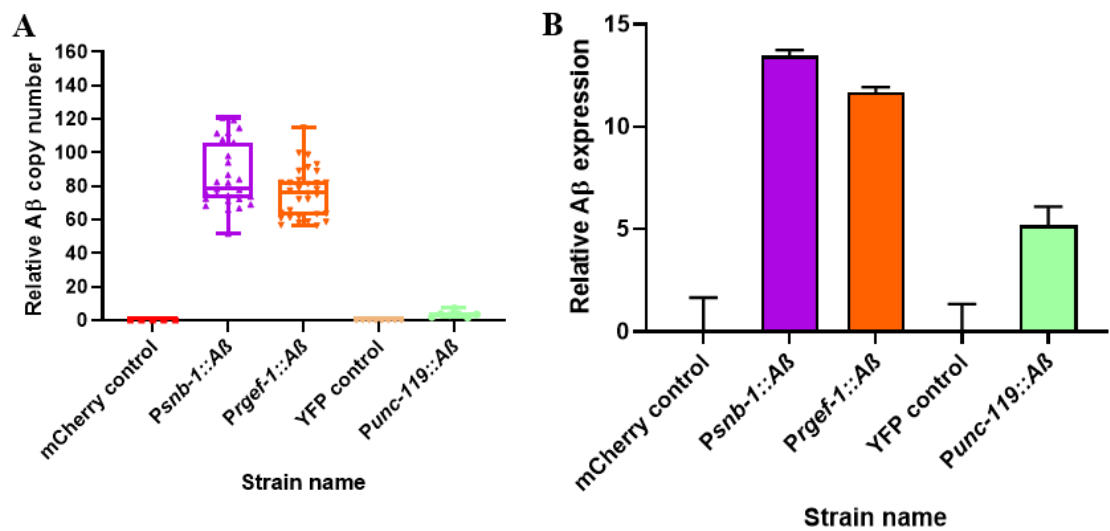


Figure 3.1: Comparison of A β expression levels in the pan-neuronal A β strains. A) Copy number assay showing the number of copies of the A β transgene in the strains per haploid genome. B) RT-qPCR showing relative expression of the A β transgene normalized to reference genes *cdc-42* and *Y45F10D.4*.

referred to as the YFP control and the GRU102 strain as the *Punc-119::A β* . Since the strain WG643 shows the highest levels of A β 1-42 expression among the pan-neuronal strains, this strain was expected to show a more severe behavioural defect in comparison to the other strains. On the other hand, the GRU102 strain showed the lowest levels of A β 1-42 expression and therefore it was expected to display more moderate behavioural defects.

3.3.2 Pan-neuronal A β 1-42-expressing transgenic *C. elegans* strains show significant reduction in lifespan

To assess whether variation in the expression of A β 1-42 in these strains correlates with the severity of the disease phenotype, the lifespan of these transgenic strain was initially measured. The representative survival curves of the transgenic *C. elegans* strains are shown in Figure 3.2A and the Mantel-Cox (log rank) test was used to determine the difference in the distribution of these survival curves. In addition, the survival curves for the remaining biological replicates have been shown in Supplementary Figure 3.2. The transgenic strains *Psnb-1::A β* and *Prgef-1::A β* showed a significant reduction in lifespan in comparison to the mCherry control strain WG731 ($p < 0.0001$). In addition, the strains *Psnb-1::A β* and *Prgef-1::A β* showed a median lifespan of 13.17 ± 0.17 and 14 ± 0.58 (S.E.) compared to the control WG731 (17.75 ± 0.25). The reduction in median lifespan was 26% for *Psnb-1::A β* and 21% for *Prgef-1::A β* . The transgenic strain *Punc-119::A β* also showed a significant reduction in lifespan compared to the YFP control strain ($p < 0.0001$). The median lifespan of *Punc-119::A β* is 15 days compared to 16 days for the YFP control strain thereby showing a ~6.25% reduction in median lifespan in comparison to the control (Figure 3.2B). Furthermore, the lifespan data was also used to estimate the rate of aging in these strains. Table 3.1 lists the Gompertz rate coefficient (G) and the initial mortality rate (A) values derived from the Gompertz equation for all the transgenic *C. elegans* strains as an estimate of the rate of aging. A lower value of G indicates lower rate of aging. There was a significant increase in the Gompertz rate coefficient (G) of the A β -expressing strains *Psnb-1::A β* and *Prgef-1::A β* in comparison to

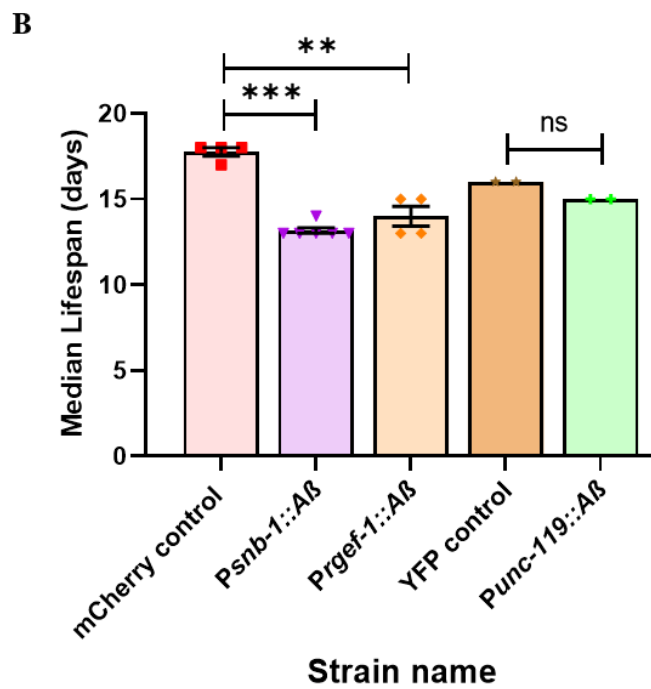
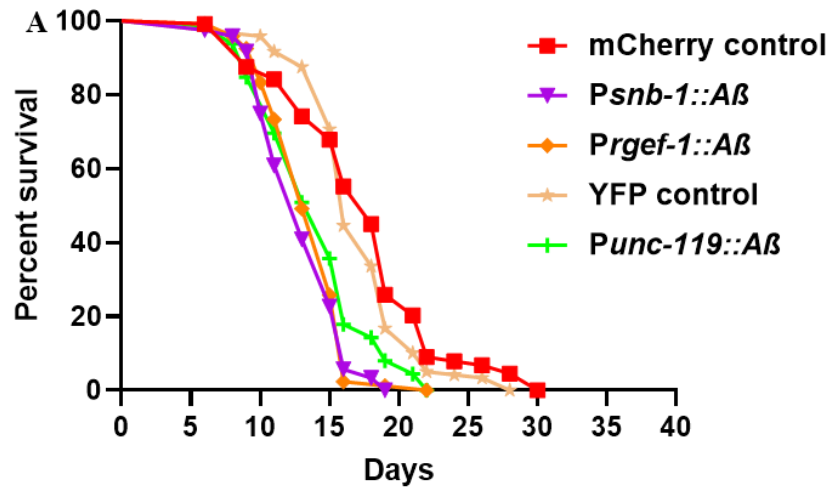


Figure 3.2: Transgenic *C. elegans* strains expressing A β peptide in the neurons show reduction in life span.

A) Representative Kaplan-Meier survival curves of one biological replicate (n = 120). B) Bar graphs showing the Median life span (n = 4, 120 worms/biological replicate). ns not significant, **p < 0.01, ***p < 0.001.

the mCherry control strain. This indicates that the rate of aging in the A β -expressing strains is higher than the control strain. The mortality rate doubling time calculated using the formula (MRDT) shows the chance of worms dying after sexual maturity doubles every 2.16 days for *Psnb-1::A β* and 1.79 in case of *Prgef-1::A β* strain. On the contrary, there was no significant difference in the rate of aging between YFP control strain and *Punc-119::A β* .

Table 3.1: Values for G and A obtained by using the Gompertz equation

Strain name	Initial mortality rate (A)	Gompertz value (G)	Rate of aging (MRDT)
mCherry control	6.00E-03	0.1677	4.13
<i>Psnb-1::Aβ</i>	3.89E-03	0.3217**	2.16
<i>Prgef-1::Aβ</i>	1.91E-03	0.3881*	1.79
YFP control	3.06E-03	0.2274	3.05
<i>Punc-119::Aβ</i>	3.95E-03	0.2602	2.66

3.3.3 The strains *Prgef-1::A β* and *Punc-119::A β* show reduction in length on day 12

The growth rate of the worm strains was determined by measuring their length and width of the worms on day 4 (young adults), day 8 (middle-aged) and day 12 (old adults) to test whether variation in the A β expression results in differences in the growth of the A β -expressing worms. Although the Day 4 data indicate growth of the worms, the body measurements at later time points measure decrease in body size due to aging. A one-way ANOVA, used to test for differences in the animal's length and width of the transgenic A β -expressing strains, showed that *Psnb-1::A β* ($p = 0.0947$) and *Prgef-1::A β* ($p = 0.051$) do not differ significantly from the mCherry control strain on day 4 and day 8. Although the transgenic strain *Psnb-1::A β* did not show any differences in worm length on day 12, there was significant reduction in the length of *Prgef-1::A β* strain on day 12 ($p = 0.0039$) compared to the mCherry control strain. In addition, an unpaired t-test was used to determine significant differences between YFP control strain and the *Punc-119::A β* strain. In young adults on day 4, there was no difference in the length between the two strains, whereas on day 8 the length of the A β 1-42 expressing worms was higher than the YFP control strain ($p = 0.0144$). In contrast, *Punc-119::A β* worms showed significant

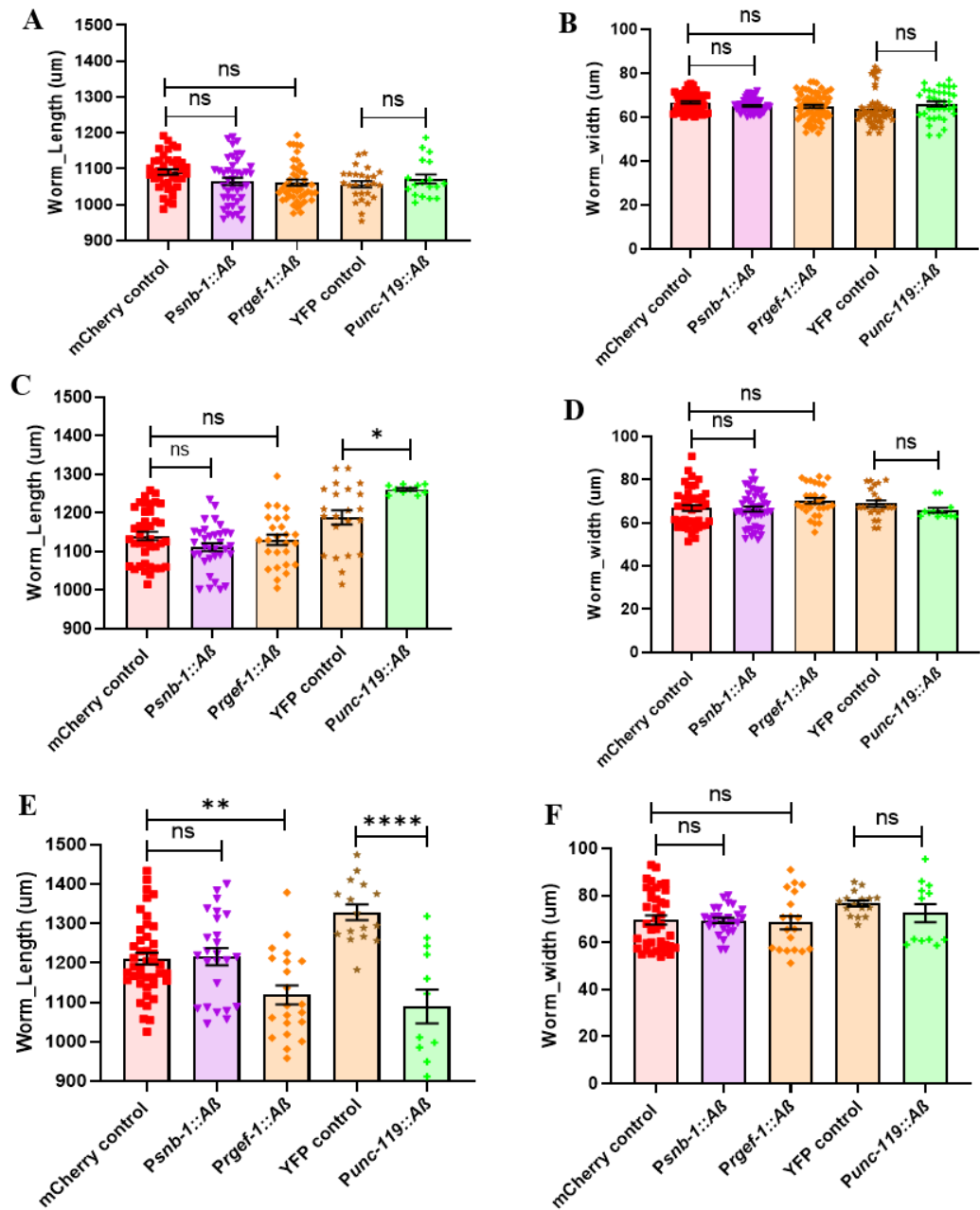


Figure 3.3: *C. elegans* growth and aging estimated by body size measurements of early (day 4), middle-aged (day 8), and old (day 12) worms.

A) Body length of day 4 worms. B) Body width of day 4 worms. C) Body length of day 8 worms. D) Body width of day 8 worms. E) Body length of day 12 worms. F) Body width of day 12 worms (n = 15 - 45). Each data point represents a single animal. ns not significant, *p < 0.05, **p < 0.01, ***p < 0.001, ****p < 0.0001.

reduction in length on day 12 ($p < 0.0001$). The length and width of all the transgenic strain on day 4, day 8, and day 12 have been shown Figure 3.3. The differences in the width of the transgenic A β strains and the control strains was not significant at all time points. Therefore, all the strains grow at the same rate (non-significant comparisons at Day 4), but they age at different rates shown as differences in sizes as they age. There was no difference in the rate of aging of the *Psnb-1::A β* and the control transgenic strain WG731 in terms of the body length at all timepoints. On the contrary, the *Prgef-1::A β* and *Punc-119::A β* show reduced length on Day 12, which suggests that these A β expressing worms senesce and shrink faster in comparison to the controls .

3.3.4 Pan-neuronal A β 1-42-expressing strains show defects in egg-laying behaviour

To assess whether variation in the expression of A β 1-42 influenced the severity of the egg-laying deficit in these transgenic strains, three egg-laying assays were performed. First, the total number of progeny produced per day during the reproductive span of a worm was counted (Figure 3.4A) and the total brood size estimated from this data (Figure 3.4B). The *Psnb-1::A β* strain showed a significant reduction in the number of progeny produced on day 6 ($p = 0.0001$) and day 7 ($p = 0.0034$) thereby leading to a significant reduction in the total brood size (225 ± 8.053) in comparison to the mCherry control strain (286 ± 10.37). Although the *Prgef-1::A β* strain showed a significant reduction in the number of progeny produced on day 6 ($p = 0.0119$) and day 7 ($p = 0.0251$), and there was a moderate reduction in the total brood size of *Prgef-1::A β* (265 ± 12.44) in comparison to the mCherry control strain WG731, the difference in total brood size was not statistically significant ($p = 0.76$). Similarly, the strain *Punc-119::A β* shows a reduction in brood size (248.8 ± 14.72) when compared to the YFP control strain GRU101 (282.8 ± 11.79); however, the difference was not statistically significant ($p = 0.87$).

Second, the egg-laying rate was measured in these worms. As shown in Figure 3.4C, there were no significant difference in the rate of egg-laying in any of the A β 1-42-expressing strains compared to the transgenic controls. Lastly, the number of eggs retained *in utero* was measured (Figure 3.4D). The number of eggs retained is

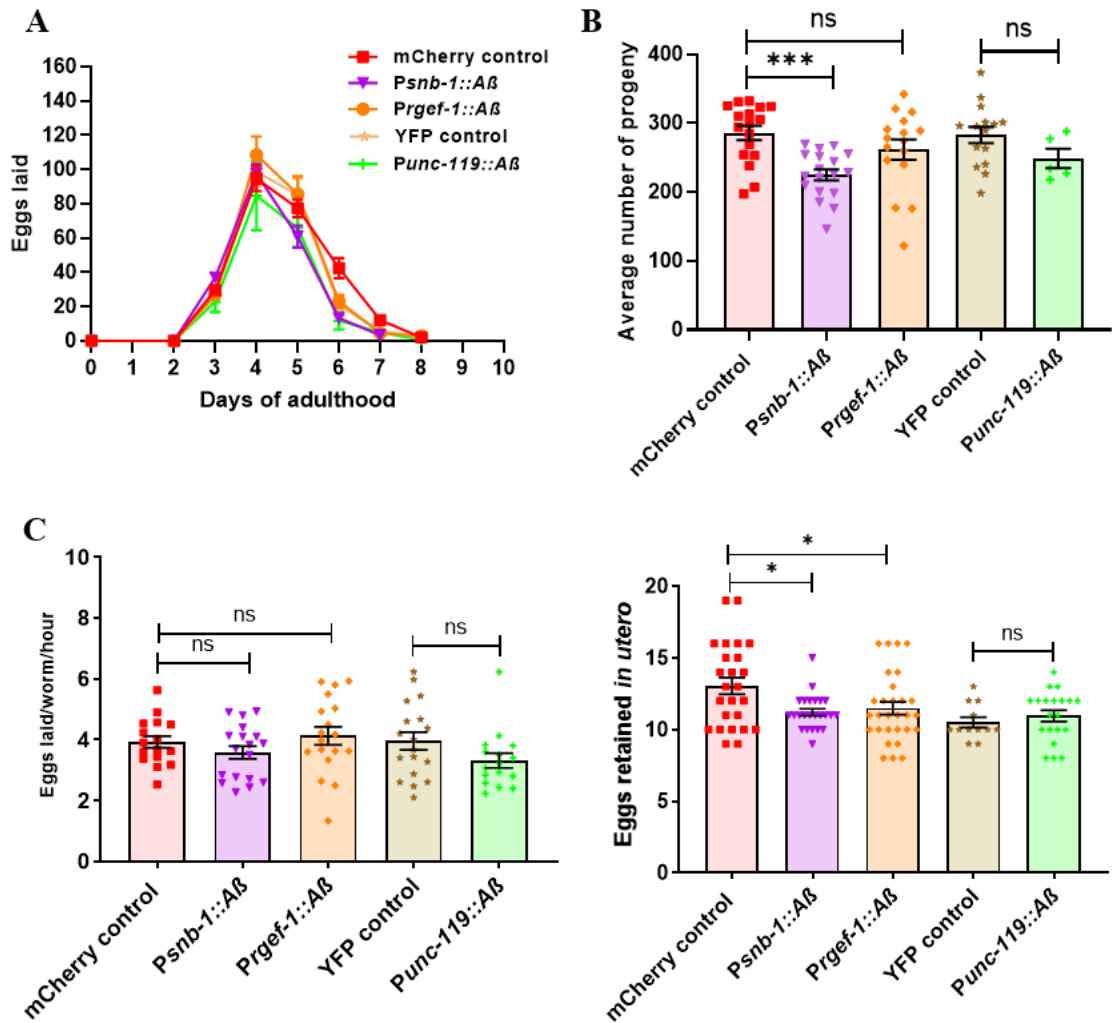


Figure 3.4: Comparison of egg-laying assays in transgenic Aβ-expressing *C. elegans* strains.

A) Number of eggs laid per worm per day during the reproductive span of the animal. B) Total brood size (n=3, 5-7 worms/replicate). C) Rate of egg production calculated by counting the number of eggs laid/worm/hour (n = 3, 15-20 worms/replicate). D) Mean number of eggs retained *in utero* per worm (n = 3, 15-20 worms/replicate). ns. not significant *p < 0.05, ***p<0.001.

significantly reduced in *Psnb-1::Aβ* ($p = 0.0192$) and *Prgef-1::Aβ* ($p = 0.0419$) in comparison to the mCherry control strain, whereas no difference was seen in the Aβ1-42 expressing strain *Punc-119::Aβ* ($p = 0.447$) compared to the YFP control strain GRU101. Therefore, the ability to lay eggs is not affected, but the rate of egg production is reduced, which results in an overall reduction in brood size in the *Psnb-1::Aβ* and *Prgef-1::Aβ* transgenic strains.

3.3.5 Pan-neuronal Aβ1-42-expressing strains show subtle changes in chemotactic abilities

Chemotaxis assays were performed using two volatile odorants, diacetyl and benzaldehyde, on the Aβ1-42-expressing strains to measure any differences in the chemotactic responses between these strains as a result of variation in Aβ1-42 expression. Chemotaxis towards diacetyl and benzaldehyde is mediated by the AWA and AWC pair of chemosensory neurons, respectively. As can be seen in Figure 3.5A, there was a significant reduction in chemotactic ability of the Aβ1-42 expressing strain *Psnb-1::Aβ* towards diacetyl on day 4 (0.57 ± 0.075) in comparison to the transgenic control WG731 (0.89 ± 0.022). Although the *Psnb-1::Aβ* strain also showed a reduction in the chemotaxis index towards diacetyl on day 8 (0.41 ± 0.13) compared to the transgenic control WG731 (0.65 ± 0.063), the difference is not statistically significant. In comparison, the transgenic strain *Prgef-1::Aβ* does show reduced chemotactic ability on day 4 (0.66 ± 0.085) and day 8 (0.37 ± 0.10), although the data are not statistically significant compared to the mCherry control strain WG731. While both the Aβ-expressing strains show reduced chemotaxis towards diacetyl on day 4, the reduction is significant only in the case of *Psnb-1::Aβ* strain. Furthermore, the Aβ1-42 expressing strain *Punc-119::Aβ* shows a significant reduction in the chemotactic ability towards diacetyl in middle-aged worms on day 8 (0.50 ± 0.082) compared to the transgenic control GRU101 (0.77 ± 0.07) ($p = 0.045$, unpaired t test), but not on day 4 ($p = 0.36$). The strain CB1124 shows reduced chemotaxis index towards diacetyl and serves as a negative control.

As shown in Figure 3.5B, the strain *Prgef-1::Aβ* shows a moderate increase in the chemotactic response towards benzaldehyde on day 4 ($p = 0.12$) and day 8 ($p = 0.066$),

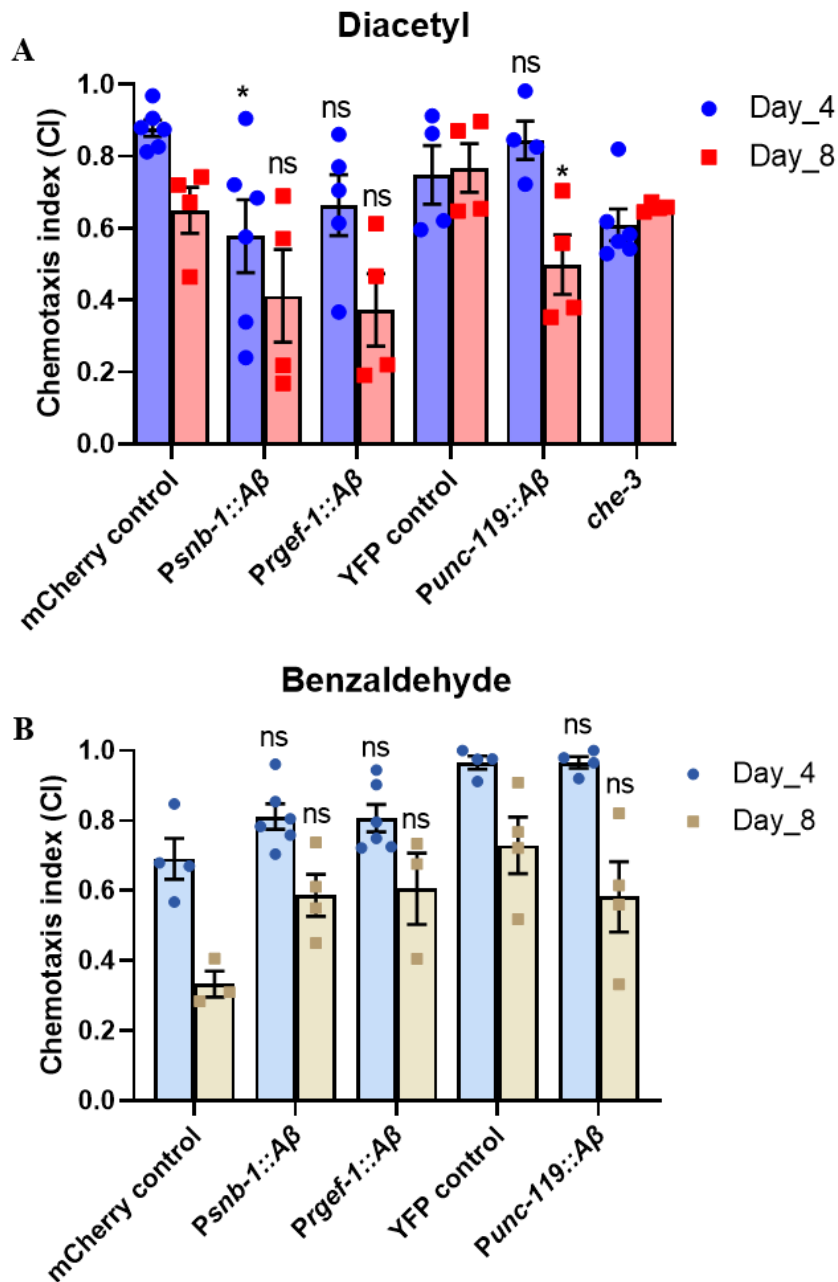


Figure 3.5: Variation in chemotactic response of Aβ-expressing transgenic *C. elegans* strains towards volatile odorants on Day 4 and Day 8

Bar graph showing chemotaxis index towards Diacetyl (A) and Benzaldehyde (B) (n= 4-6, 100-200 worms). One way ANOVA was used to compare the *Psnb-1::Aβ* and *Prgef-1::Aβ* to the transgenic mCherry control strain at each time point. An unpaired t test was used to compare the *Punc-119::Aβ* with the YFP control strain for each timepoint. ns not significant *p < 0.05.

similar to the transgenic strain *Psnb-1::Aβ* when compared to the mCherry control strain WG731. Although the strain *Punc-119::Aβ* showed a decrease in the chemotaxis index towards benzaldehyde on day 8 ($p = 0.30$), it was not statistically different from the transgenic YFP control strain GRU101.

Worm mobility was measured on the chemotaxis plates by calculating the percentage of worms that moved away from the origin after 1 hour (Supplementary Figure 3.3). All the transgenic Aβ1-42-expressing strains moved similar to the transgenic controls on the chemotaxis plates. Although there was an age-related decline in the mobility of all the worm strains on day 8, there was no significant difference between the mobility of the transgenic Aβ1-42 expressing strains in comparison to the controls for either of the volatile odorants. Therefore, the differences in the chemotaxis obtained between the strains is due to the chemotactic defects and not due to movement *per se*. It is important to note that these mobility data only indicate the ability of the worms to move towards the odorant in a given time period, but do not detect any motility defects between worm strains.

3.3.6 The transgenic Aβ1-42 expressing strains show a significant reduction in motility parameters

Several motility parameters were measured in the Aβ-expressing transgenic strains to determine if differences in the levels of Aβ expression result in variation in the severity of the motility defect. Firstly, motility parameters on solid media were assessed. As can be seen in Figure 3.6A and B, there is an age-related decline in the body bends/30s and mean speed in all the transgenic strains. When comparing between strains, there was a significant reduction in the body bends of the *Psnb-1::Aβ* and *Prgef-1::Aβ* starting at day 8 in comparison to the mCherry control. However, the *Prgef-1::Aβ* shows a significant reduction in mean speed even in young adult animals on day 4 ($p < 0.0001$). In addition, the *Psnb-1::Aβ* and *Prgef-1::Aβ* show a drastic reduction in mean speed on day 8 and day 12. Maximum speed (Figure 3.6C), considered to be an indicator of health span, was also measured in these strains (Hahm et al., 2015). The strain *Prgef-1::Aβ* did not show differences in maximum speed in comparison to the mCherry control. In contrast, the

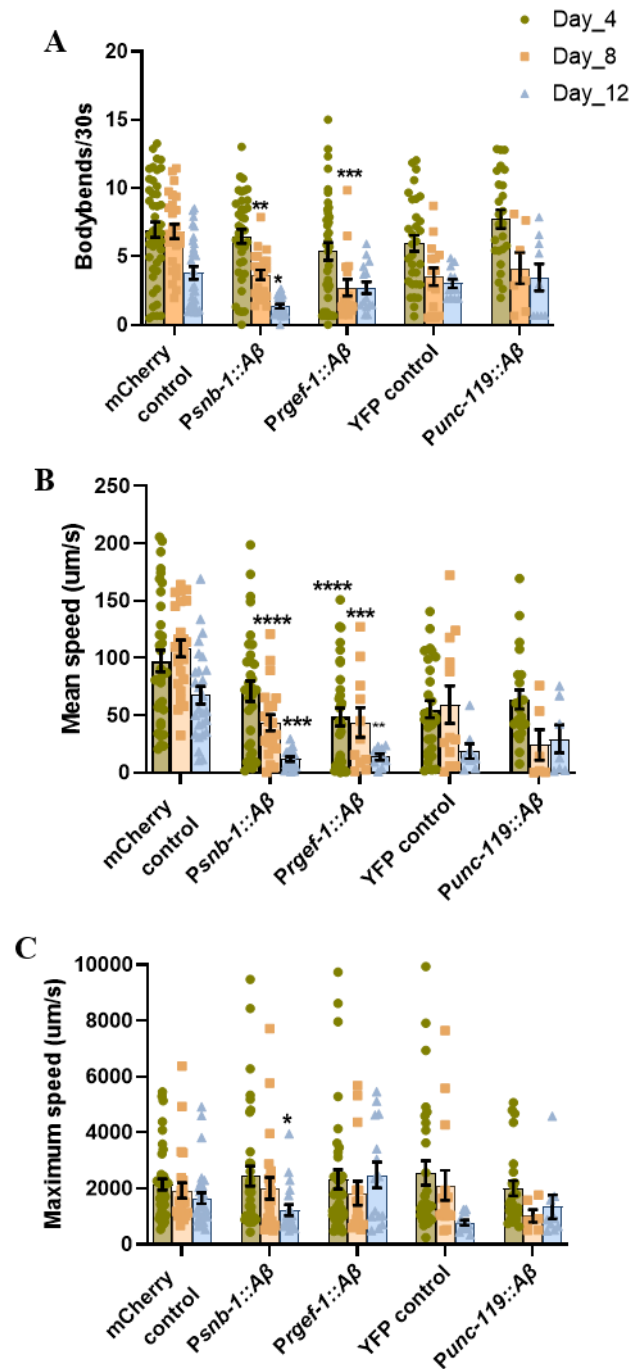


Figure 3.6: P an-neuronal A β -expressing strains show age-dependent reduction in motility on solid media.

A) Body bends/30s. B) Mean speed ($\mu\text{m/s}$). C) Maximum speed. All data analysed by two-way ANOVA followed by post hoc Tukey multiple comparisons test. ns not significant, ** $p < 0.01$, *** $p < 0.001$, **** $p < 0.0001$ ($n=3, 5-15$ worms/replicate). The *Psnb-1::A β* and *Prgef-1::A β* have been compared to the transgenic mCherry control and *Punc-119::A β* has been compared to the YFP control strain.

Psnb-1::Aβ does show a significant reduction in maximum speed on day 12 ($p = 0.039$) by the non-parametric Mann-Whitney test. Therefore, the moderate and high Aβ-expressing strains show age-related motility defects on solid media on Day 8 and Day 12 in comparison to the control. On the other hand, the low Aβ-expressing strain *Punc-119::Aβ* does not show changes in any of the three motility parameters when compared to the YFP control strain. Therefore, the decline in motility is more severe (relative to transgenic control) in Aβ1-42-expressing strains *Psnb-1::Aβ* and *Prgef-1::Aβ* but not in *Punc-119::Aβ*. Other motility parameters, such as mean wavelength, mean amplitude and head bends/30s, were also compared between the strains (Supplementary Figure 3.4). The *Psnb-1::Aβ* strain did not show any significant differences in the mean wavelength compared to the mCherry control WG731 in all age groups. In contrast, there was a significant decrease in the mean wavelength of the *Prgef-1::Aβ* strain ($p = 0.0093$) on day 12 relative to the mCherry control. Similarly, there was a significant reduction in the mean wavelength of *Punc-119::Aβ* strain ($p < 0.0001$) in comparison to the YFP control strain (Supplementary Figure 3.4A). Another parameter that displayed a variation in the severity in the different Aβ-expressing strains was mean amplitude. As seen in Supplementary 3.4B, there was a significant reduction in the mean amplitude on day 8 ($p = 0.013$) and day 12 ($p = 0.038$) for the *Psnb-1::Aβ* strain and on day 8 ($p = 0.043$) for the *Prgef-1::Aβ* strain compared to the mCherry control strain WG731. The YFP control strain and the *Punc-119::Aβ* strain do not show any significant differences in mean amplitude (Supplementary Figure 3.4B). In addition, no significant differences in foraging behaviour, measured as frequency of head bends, was observed in the Aβ1-42-expressing transgenic strains in comparison to the transgenic controls (Supplementary Figure 3.4C).

Secondly, motility in liquid was also assessed in these strains. There was a significant decline in the number of thrashes in the *Prgef-1::Aβ* strain on day 12 ($p = 0.0007$) in comparison to the mCherry control strain. However, in the *Psnb-1::Aβ* strain, the decrease in the number of thrashes started on day 8 ($p = 0.0131$) and day 12 ($p < 0.0001$). In addition, there was a significant reduction in the number of thrashes in the *Punc-119::Aβ* strain relative to the YFP control strain on day 8 ($p = 0.038$) (Figure 3.7A). As shown in Figure 3.7B, the mean speed was significantly lower in day 4 ($p = 0.0348$), day 8 ($p = 0.0001$)

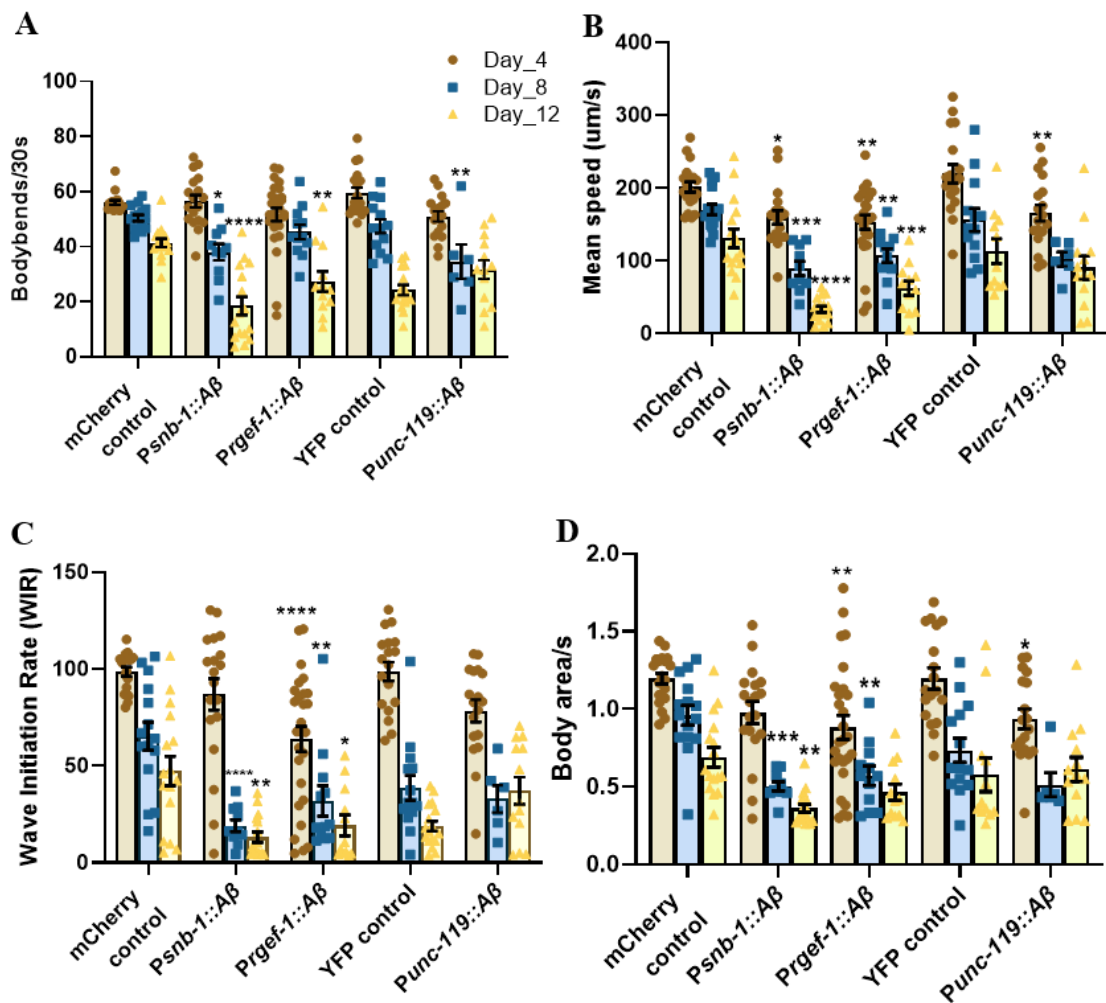


Figure 3.7: Pan-neuronal A β -expressing strains show age-dependent reduction in motility on liquid media.

A) number of thrashes in liquid (Body bends/30s). B) Mean swimming speed ($\mu\text{m/s}$). C) Wave initiation rate. D) Activity in liquid (body area/s) (n=2, 5-15 worms/replicate). All data analysed by two-way ANOVA followed by post hoc Tukey multiple comparisons test. The *Psnb-1::A β* and *Prgef-1::A β* have been compared to the transgenic mCherry control and *Punc-119::A β* has been compared to the YFP control strain. *p < 0.05 **p < 0.01, ***p < 0.001, ****p < 0.0001

and day 12 ($p < 0.0001$) in the transgenic A β 1-42 expressing strain *Psnb-1::A β* compared to the mCherry control strain WG731. Similarly, the *Prgef-1::A β* strain showed a significant age-related decline in mean swimming speed on day 4 ($p = 0.0032$), day 8 ($p = 0.0025$) and day 12 ($p = 0.0006$) relative to the mCherry control strain. On the other hand, the *Punc-119::A β* strain showed a significant decline in the mean swimming speed only on day 4 ($p = 0.0028$) when compared to the YFP control strain. In addition, there was rapid decline in the wave initiation rate of the *Prgef-1::A β* on day 4 ($p < 0.0001$), day 8 ($p = 0.0051$) and day 12 ($p = 0.026$) in comparison to the mCherry control strain. However, the *Psnb-1::A β* strain showed a rapid decline in the wave initiation rate on day 8 ($p < 0.0001$) and day 12 ($p = 0.0010$). In contrast, there was no difference in the wave initiation rate between the YFP control strain and *Punc-119::A β* (Figure 3.7C). As can be seen in Figure 3.7D, there was a decline in the activity of all the A β 1-42 expressing strains. The *Prgef-1::A β* showed a significant decline in activity starting on day 4 ($p = 0.0018$) in comparison to the *Psnb-1::A β* that showed a reduction in activity on day 8 ($p = 0.0005$) relative to the mCherry control. In addition, there was a decline in the activity of the *Punc-119::A β* worms on day 4 ($p = 0.037$), but not on day 8 ($p = 0.35$) or day 12 ($p > 0.9999$). All other parameters such as the dynamic amplitude (curvature), curling, and the brush stroke (shown in Supplementary Figure 3.5) do not show any significant differences between the A β 1-42-expressing strains *Psnb-1::A β* and *Prgef-1::A β* and the transgenic control WG731. The *Punc-119::A β* showed a significant reduction in curling on day 12 ($p < 0.0001$) as compared to the YFP control strain (Supplementary Figure 3.5B). In summary, all the A β -expressing strains show an age-related decline in motility parameters in liquid media and the severity of the phenotype correlates with the levels of A β -expression.

3.3.7 Pan-neuronal A β -expressing strains *Psnb-1::A β* and *Prgef-1::A β* show diminished basal slowing response mediated by dopamine

Two types of experienced-based learning assays were performed to compare deficits in learning behaviour. The basal slowing response is mediated by dopaminergic signalling, displayed by slowing of well-fed worms in the presence of food (Sawin et al., 2000). An

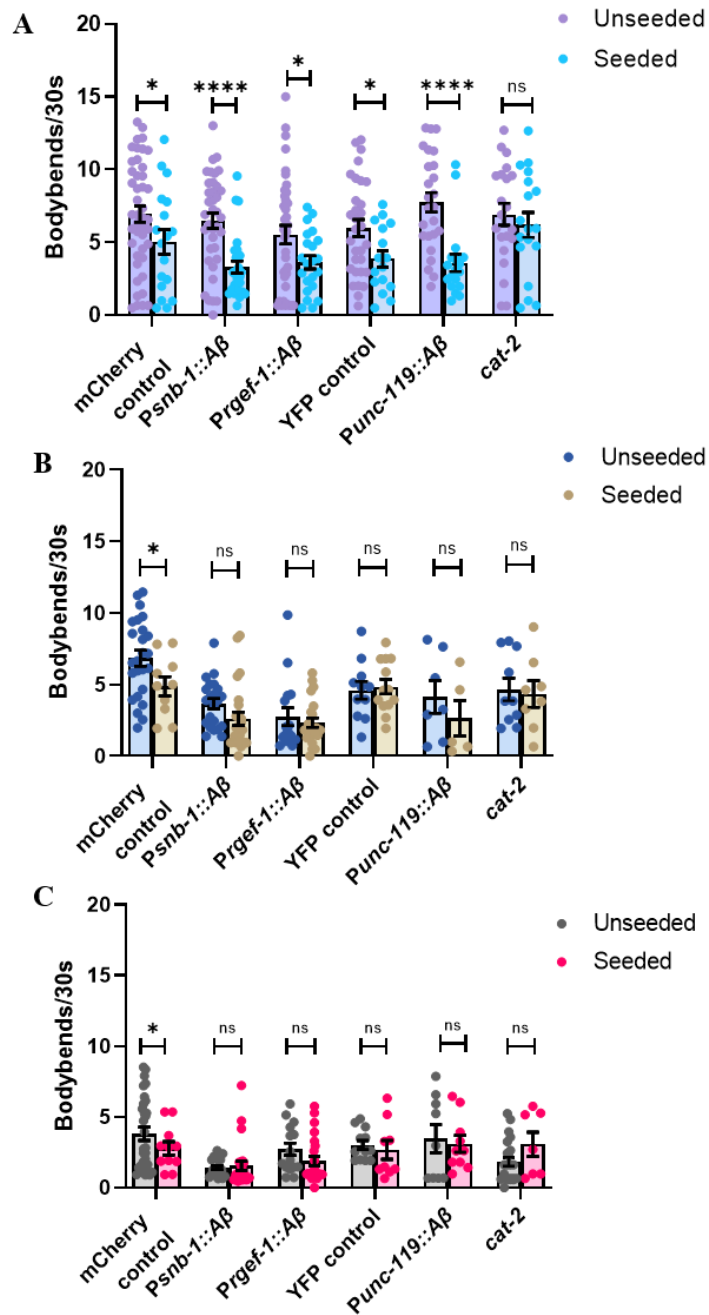


Figure 3.8: Pan-neuronal A β -expressing strains show diminished basal slowing response mediated by dopamine.

A) Day 4. B) Day 8. C) Day 12 (n=3, 5-15 worms/replicate). An unpaired t test is used to test for significant differences in worm movement on seeded and unseeded plates. ns not significant, *p < 0.05 **p < 0.01, ***p < 0.001, ****p < 0.0001.

unpaired t-test was used to determine significant differences between the animals on seeded and unseeded plates. In young adults on day 4, all the transgenic *C. elegans* strains showed a significant reduction in body bends in the presence of food except the control strain *cat-2*. The control strain *cat-2* is defective in dopamine synthesis and does not slow down in the presence of food. However, this slowing response diminishes on day 8 and day 12 for the A β 1-42 expressing strains *Psnb-1::A β* and *Prgef-1::A β* in comparison to the mCherry control strain. These results indicate that there may be a deficit in dopaminergic signalling in the A β -expressing strains *Psnb-1::A β* and *Prgef-1::A β* as the worms age. On the other hand the YFP control strain and the *Punc-119::A β* strains also display slowing response on day 4, however, the slowing response is diminished on day 8 and day 12 in both these strains (Figure 3.8). Although these preliminary data indicate that the *Punc-119::A β* strain possibly has a defect dopaminergic signalling, they are difficult to interpret as the basal slowing response of the YFP control strain is not statistically significant on Day 8 and Day 12.

An enhanced slowing response is displayed by starved worms in the presence of food and is mediated by serotonergic signalling (Supplementary Figure 3.6). In young worms on day 4, all transgenic strains showed a significant reduction in body bends in the presence of food following a period of starvation, as determined by an Unpaired t-test. The control strains *cat-4* and *bas-1* did not show any slowing responses in the presence of food. On day 8, the slowing response is diminished in all the transgenic strains. Surprisingly, the enhanced slowing response is still evident in *Punc-119::A β* on day 8. On day 12, none of the worm strains show enhanced slowing responses including the controls.

3.4 Discussion

Although the A β peptide has been proposed to play a role in the pathogenesis of AD, direct evidence that quantitatively links A β concentration to disease severity is lacking. Here, I have compared strains expressing varying levels of A β 1-42 in *C. elegans* neurons. The strains have been constructed by a conventional transgenesis approach to show variation in A β peptide expression using two different pan-neuronal promoters *snb-1* and *rgef-1*. A new transgenic *C. elegans* strain expressing the A β 1-42 transgene in the nervous system using the promoter *rgef-1* was generated and characterised (*Prgef-1::A β*). This strain was compared to the previously described strain WG643 (Chapter 2) that utilised the pan-neuronal promoter *snb-1* to drive the expression of the A β 1-42 transgene (*Psnb-1::A β*). In addition, a published pan-neuronal A β 1-42 expressing strain, which uses the *unc-119* promoter to drive the A β 1-42 transgene expression, was also used (*Punc-119::A β*) (Fong et al., 2016). These strains were used to test the hypothesis that the severity of the disease phenotype is correlated with the levels of A β 1-42 expression in these strains. The pan-neuronal A β 1-42 expressing transgenic *C. elegans* strains described in this study showed varying levels of the A β 1-42 expression and also showed variation in the severity of some, but not all, of behavioural phenotypes that were measured. Overall, all the A β -expressing strains showed reduced longevity, impaired egg-laying, and age-related decline in motility in liquid media accompanied by subtle defects in chemotaxis and deficits in dopaminergic signalling. The phenotypic variation may be correlated with the level of A β 1-42 transcript abundance measured by RT-qPCR. However, it is difficult to make direct comparisons between the *Psnb-1::A β* or the *Prgef-1::A β* strains that express mCherry as a reporter and the *Punc-119::A β* strain because the *Punc-119::A β* strain was made in a different genetic background and expresses a different transgenic marker YFP.

3.4.1 Transgenic A β 1-42 expressing *C. elegans* strains show variation in A β expression

All strains were generated using conventional transgenesis involving microinjection of the A β 1-42 containing plasmid combined with a transgenic marker plasmid to obtain

transgenic progeny containing the A β 1-42 transgene on an extrachromosomal array. This transgenic progeny obtained after microinjection were followed by irradiation to integrate the extrachromosomal array randomly into the *C. elegans* genome. One possible limitation of this approach is that this random integration can sometimes lead to germline silencing of the array. In addition, there is limited control on the number of copies of the A β 1-42 transgene integrated into the *C. elegans* genome (Mello et al., 1991). There were ~ 80 copies of the A β 1-42 transgene integrated in the *Psnb-1::A β* and *Prgef-1::A β* strains and ~ 5 copies of the A β 1-42 transgene integrated in the *Punc-119::A β* strain (Figure 3.1A). Hence, the copy number of the *Psnb-1::A β* and *Prgef-1::A β* strains is approximately 16-fold higher in comparison to the *Punc-119::A β* . If the copy number and the FPKM values were utilised to generate an index of expected expression by multiplying the copy number and FPKM values, this would mean *Psnb-1::A β* has the highest A β expression of 16388 units, *Prgef-1::A β* shows expression of 337.5 units and *Punc-119::A β* shows the lowest expression of 80.15 units. In other words, if it were a simple relationship between intrinsic activity and copy number, the *Punc-119::A β* would have 20-25% the expression of the *Prgef-1::A β* strain despite somewhat higher intrinsic promoter activity. When comparing the A β expression levels by RT-qPCR, there was a 100-fold difference in A β expression between the *Psnb-1::A β* and *Prgef-1::A β* . In addition, the *Prgef-1::A β* shows 200% higher A β expression than *Punc-119::A β* which shows the lowest levels of A β expression (Figure 3.1B). However, it is difficult to compare a FPKM value, which is a direct measure of transcript abundance, to A β expression as measured by RT-qPCR, because the latter is a relative measure of transcript abundance and thus dependent on the “housekeeping” transcript(s) that is/are used. In addition, direct comparisons of *Psnb-1::A β* and *Prgef-1::A β* strains with *Punc-119::A β* strain is complicated because it was constructed in a different genetic background, has a different transgenic marker which mediates the quantitative variation in A β expression, and variation in intrinsic promoter activity. In addition, there may be other factors influencing the A β expression in these transgenic strains such as integration sites. In order to control the variation in A β expression, the same promoter construct could be microinjected at different concentrations to generate strains containing different copies of the A β transgene thereby resulting in variation of A β expression. In addition, gene editing tools such as MosSCI

and CRISPR could be utilized to insert specific number of copies of the A β transgene at specific sites in the *C. elegans* genome (Nance and Frokjaer-Jensen, 2019). Regardless of the quantitative differences in expression (or their cause), if the *Psnb-1::A β* strain with the highest levels of A β expression shows a more severe behavioural deficit than the *Prgef-1::A β* and the *Punc-119::A β* strains shows only subtle behavioural deficits, this would support the hypothesis that levels of A β expression correlate with the severity of the disease phenotype.

3.4.2 Pan-neuronal A β 1-42-expressing strain show premature death and reduction in fecundity

All the transgenic A β 1-42-expressing strains showed a significant reduction in median lifespan (Figure 3.2). However, *Psnb-1::A β* strain, with the highest A β expression, showed the most significant reduction in median lifespan (~ 25%). The *Prgef-1::A β* strain shows ~21% reduction in median lifespan. On the other hand, the *Punc-119::A β* strain with the lowest A β expression showed subtle reduction in median lifespan in comparison to the control (~6%). Therefore, the reduction in median lifespan correlates with the levels of A β expression. The rate of aging, measured by the Gompertz equation, is greater in the high A β -expressing strains *Psnb-1::A β* and *Prgef-1::A β* (Table 3.1). These results indicate that increased levels of A β in the *C. elegans* neurons cause the worms to age faster, whereas low levels of A β influences lifespan but does not necessarily lead to a change in the rate of aging. Several previous studies have showed that although there are individuals that do not show any symptoms of AD, their brains have profuse plaques at autopsy known as high pathology controls or preclinical AD (Arriagada et al., 1992b; Dickson et al., 1992). Moreover, the level of soluble A β in these individuals is lower than that seen in AD patients. They also do not show presence of neurofibrillary tangles which may indicate that the level of A β in these individuals is unable to trigger the pathogenic cascade that ultimately leads to neuronal dysfunction and death (Lue et al., 1999).

All the A β -expressing strains show reduction in brood size (Figure 3.4B). However, this reduction in brood size was only significant for the highest A β -expressing strain *Psnb-1::A β* . In addition, there was possibly an impairment in rate of egg production in these

strains which would result in a reduction in the brood size. It is also important to note that all the young adult A β -expressing worms lay eggs at the rate close to wild type and the rate of egg production is lower than the transgenic control only on day 6 and day 7 of adulthood. Further experimentation is required to validate these results. For instance, ectopic expression of serotonin to stimulate egg-laying and could be used to test whether the worms response to the treatment restores the egg-laying deficit (Trent et al., 1983; Waggoner et al., 1998).

3.4.3 Pan-neuronal A β 1-42-expressing strains *Psnb-1::A β* and *Prgef-1::A β* show a severe decline in motility

There was a rapid age-related decline in motility parameters in all the A β -expressing strains; however, the defect was more severe in the *Psnb-1::A β* strain (Figure 3.6). When comparing motility on solid media, only the high A β -expressing strains *Psnb-1::A β* and *Prgef-1::A β* showed significant declines in crawling parameters such as body bends and mean speed. However, only the *Psnb-1::A β* strain showed a significant declines in maximum speed, which is a measure that has been correlated with healthspan. The low A β -expressing strain did not show any significant difference in the motility on solid media relative to the control strain. On solid media, there is mechanical resistance that the worm encounters when crawling on the agar surface and this is 10,000-fold greater than that encountered while swimming. Moreover, worms also display other engaging behaviours such as foraging or pharyngeal pumping on solid media (Laranjeiro et al., 2017; Vidal-Gadea et al., 2011). Therefore, any subtle defects in motility will be harder to detect on solid media.

It is easier to detect motility defects in liquid as the worms are able to move freely. Moreover, it has been previously reported that swimming in liquid is more energetically demanding than crawling and there is increase in the metabolic rate of the worms while swimming (Laranjeiro et al., 2017). When looking at motility parameters in liquid media, the *Psnb-1::A β* and *Prgef-1::A β* strains show a decline in swimming parameters such as the mean swimming speed, activity, number of thrashes and wave initiation rate (Figure 3.7). The low A β -expressing strain *Punc-119::A β* also shows a decline in all of these

swimming parameters, except for the wave initiation rate. Although the wave initiation rate in this strain shows a decline from day 4 to day 8, the change is similar to the one seen in the transgenic control (Figure 3.7C). Consistent with the defects in swimming parameters for the *Punc-119::A β* strain, the low A β -expressing strain *Punc-119::A β* has been reported to show ATP deficit at young age (Fong et al., 2016).

3.4.4 Defects in chemotaxis observed in all A β 1-42-expressing strains

Olfaction is affected in AD and is a primary early indicator of the disease. All the pan-neuronal A β 1-42 expressing strains show subtle defects in chemotaxis towards diacetyl (Figure 3.5). The *Psnb-1::A β* strain shows reduced chemotaxis towards diacetyl on day 4 whereas the *Punc-119::A β* strain showed decreased chemotactic response on day 8 . Therefore, the *Psnb-1::A β* strain with the highest A β expression, has earlier onset of chemotaxis impairment than the *Punc-119::A β* strain, which has the lowest A β expression. One possible explanation for this observation is that there is a threshold of A β expression at which the phenotype arises and *Psnb-1::A β* reaches this threshold for chemotaxis defect earlier because it accumulates A β faster. The chemotaxis assay does not demonstrate an increase in the severity of the behavioural defect as A β expression increased but does show a defect if there is any expression of A β . Thus, changes in olfaction are early indicators of age-related cognitive decline due to A β in worms as in humans because olfaction is sensitive to the presence of low concentrations of A β (Sun et al., 2012).

3.4.5 Pan-neuronal A β 1-42-expressing strains show deficits in dopaminergic signalling.

Synaptic dysfunction in AD is considered to be an early hallmark of the disease (Dosanjh et al., 2010). In *C. elegans*, the basal slowing response is sensitive to even small amounts of A β : all the A β -expressing strains showed a diminished basal slowing response on day 8 and day 12, these results support the idea that A β causes synaptic dysfunction, thereby leading to neurotransmitter deficits, in this case dopaminergic signalling (Figure 3.8).

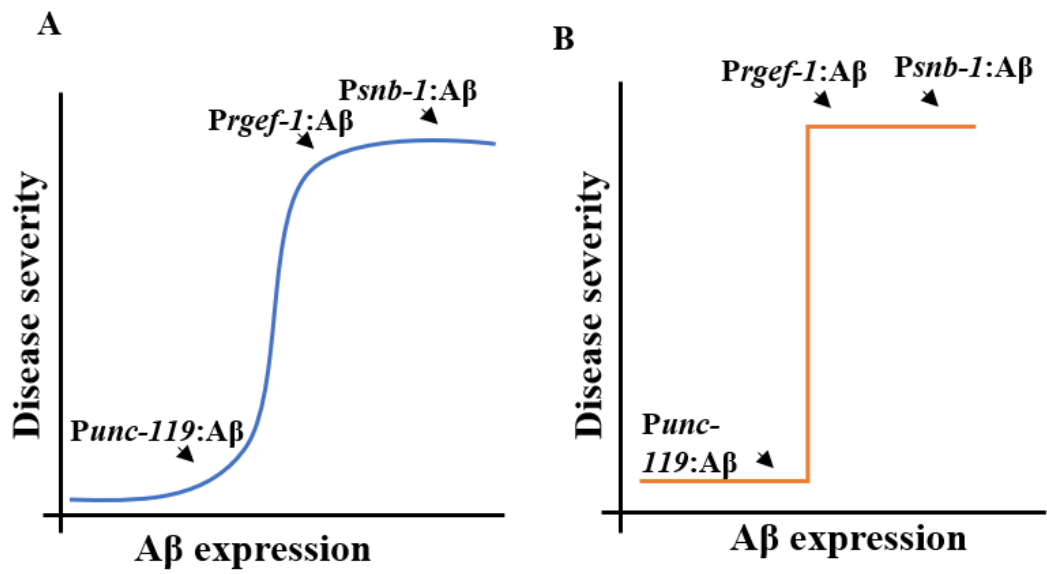


Figure 3.9: Dose response curves explaining the correlation between the levels of Aβ expression and the severity of disease.

A) Gradual dose response curve. B) Fixed dose response curve.

These motility related behaviours are noisy, and preliminary experiments to reveal subtle defects that may be the first signs of A β toxicity will require large sample sizes. Previous studies suggest that the insoluble plaques do not correlate with disease severity, and the soluble A β 1-42 oligomers may be more toxic *in vivo* (McLean et al., 1999). A strain expressing the A β 1-42 peptide in the body wall muscle showed A β exists as a high order oligomer (McColl et al., 2012). To verify the version of A β in these strains, a liquid chromatography experiment would need to be performed on the pan-neuronal A β 1-42-expressing strains reported here. Several other studies have suggested that soluble A β oligomers are more toxic *in vivo* compared to the insoluble A β (Cohen et al., 2006; Roberts et al., 2012; Shankar et al., 2008). As shown in Figure 3.9, the relation between A β concentration and disease severity could possibly be explained in two ways: (i) Using gradual dose response curve in which there is gradual increase in disease severity with the concentration of A β and there is visible phenotype after a particular threshold; (ii) Fixed dose response in which there is a range of A β concentration that shows a phenotype. The next step would be to construct strains that fall in between these high and low A β -expressing strains to understand this relationship better.

3.5 Conclusion

This is the first study to demonstrate that varying expression levels using different promoters and variable copy number of different integrated arrays does offer the possibility of establishing a quantitative dose response between A β expression and AD related phenotypes. These data support the conclusion that there is a correlation between A β concentration and the initiation and progression of the disease, rather than the end point of the disease. Therefore, *C. elegans* serves as a good model to study the relationship between disease progression and A β expression because the severity of these behavioural deficits is correlated with the quantitative expression of A β . Additionally, these data provide preliminary support for the hypothesis that some behaviours are more sensitive indicators of the disease, such as the basal slowing response assay in which all the A β -expressing strains show diminished slowing response irrespective of the A β concentration.

Chapter Four

Comparison of transgenic strains expressing different versions of the A β transgene in the *C. elegans* nervous system

4.1 Introduction

Early onset familial forms of AD are caused by mutations in genes involved in the processing of amyloid precursor protein (APP), causing enhanced production of amyloid β (A β) peptides. This has ultimately led to the hypothesis that amyloid β is involved in the AD pathogenic process (Haass and Selkoe, 1993). In this hypothesis, accumulation of A β is a result of enhanced production and reduced clearance from the cerebrospinal fluid in AD patients and this deposition starts many years before the cognitive deficits become evident (Mawuenyega et al., 2010). The A β peptides proposed to play a critical role in the pathogenesis of AD, released after the imprecise proteolytic cleavage of the APP by β and γ secretases, are usually about 38-43 amino acids in length (Haass and Selkoe, 1993; Portelius et al., 2010). Extractions of amyloid deposits from the AD brain are composed of heterogenous species of A β 1-42, A β 1-40, and shorter N- and C- terminal truncated peptides (Kalback et al., 2002). Although studies have reported that the oligomeric A β species constituting mainly of the full length A β 1-42 impair synaptic function, the amyloid fibrils are also a toxic form of A β (Haass and Selkoe, 2007; Harmeyer et al., 2009; Klein, 2002; Selkoe, 2001; Wilcox et al., 2011). Furthermore, it has been reported that several high and low oligomeric species, rather than a specific type of oligomer, could trigger neuronal dysfunction (McLean et al., 1999). Although the presence of A β oligomers have been correlated with disease severity and are suggested to be the toxic form of A β , the mechanism of toxicity remains unclear (Kayed et al., 2003; Lambert et al., 1998; Podlisny et al., 1998).

Since the A β 1-40 and A β 1-42 peptides are found most abundantly in the human AD brain, the majority of studies have focussed on the role of these peptides in the pathogenesis of the disease (Naslund et al., 1994; Piccini et al., 2005). A β 1-40 is the

predominant form secreted from cultured cells (Asami-Odaka et al., 1995) and biological fluids, such as blood (Lewczuk et al., 2004) and cerebrospinal fluid (Wiltfang et al., 2002). However, they are observed in later stages of the disease (Delacourte et al., 2002). On the other hand, the longer form A β 1-42 is thought to be a major contributor in the pathogenesis of AD due to its higher propensity to aggregate (Jarrett and Lansbury, 1993). Surprisingly, it was found that majority of the A β peptides that make up the A β oligomers were amino-truncated (Sergeant et al., 2003). Moreover, the A β peptides containing ragged N- and C-termini have been overlooked and an estimated 64% of these amino truncated peptides are A β 4-X (Masters et al., 1985; Portelius et al., 2010). The relative contribution of these A β species in the pathology of the disease has not been fully understood and was ignored for almost 30 years since it was first discovered. However, evidence suggests that these N-truncated peptides play a key role in AD, either the A β X-42 species starting at positions 4,5,8,9 or with a pyroglutamate residue at position 3 (Jawhar et al., 2011; Sergeant et al., 2003). Figure 4.1 shows all the N-truncated A β peptides in the human AD brain. In addition, *in vitro* studies on these amino-truncated A β species have shown that they are both more fibrillogenic at physiological pH and more toxic than the full length A β 1-42. These N-terminal truncations enhance the A β aggregation, which may initiate the pathological cascade that leads to A β deposition and ultimately to disease (Pike et al., 1995; Russo et al., 2002). Since these amino-truncated A β species are found in people with Down syndrome and in preclinical AD, they are implicated in the very first step of amyloidosis (Liu et al., 2006; Russo et al., 2001; Sergeant et al., 2003).

One of the first N-truncated A β species reported was the A β 4-42, which is relatively abundant in AD, aged individuals, and those with vascular dementia (Lewis et al., 2006; Masters et al., 1985). These findings were further supported by evidence from immunoprecipitation and mass spectrometry experiments showing that A β 4-42 is one of the major fractions in the hippocampus and cortex of AD patients (Portelius et al., 2010). Short-term exposure of primary cortical cultures to aggregated A β 4-42 peptides triggers neuronal loss. Furthermore, intracerebral fusion of A β 4-42 oligomers affects hippocampus-dependent behaviour as assessed by working memory behavioural testing in mice. These A β 4-42 oligomers have detrimental effects comparable to the A β 1-42

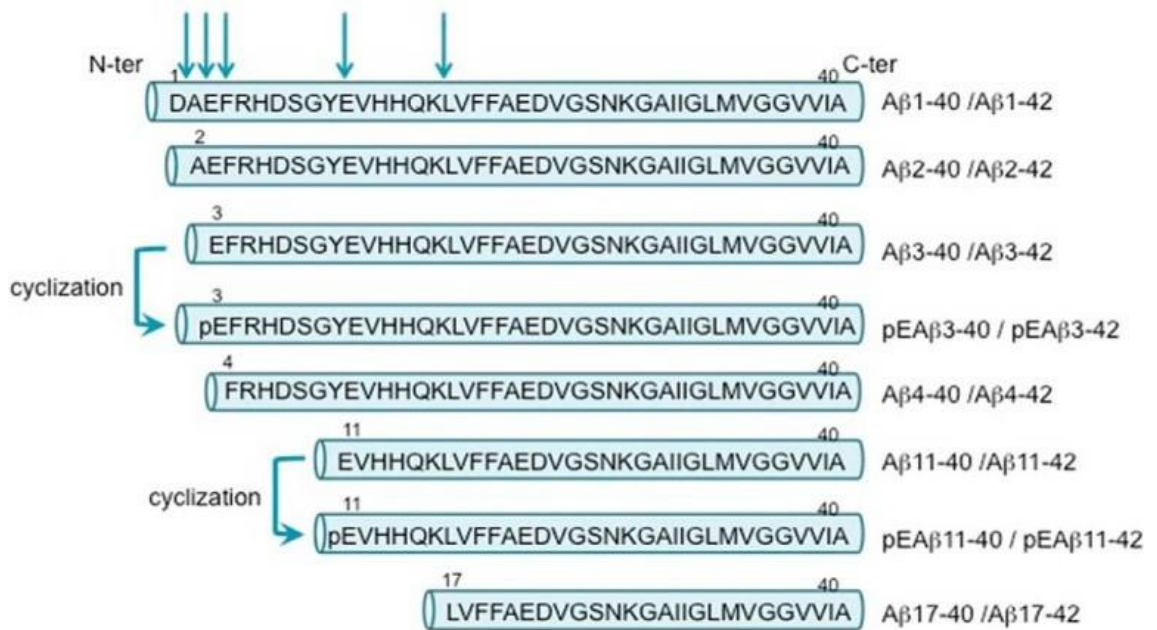


Figure 4.1: N-terminally truncated Aβ peptides.

Representation of all the N-terminally truncated Aβ variants. Arrows represent sites of cleavages (Dunys, Valverde, & Checler, 2018).

oligomers (Bouter et al., 2013). In addition, an *in vivo* mouse model of AD overexpressing A β 4-42 suffer from massive CA1 pyramidal neuronal loss accompanied by memory dysfunction (Bouter et al., 2013). However, the mode of A β 4-42 toxicity remains unclear. For instance, bapineuzumab is used in antibody-based immunotherapy directed against the amino-terminus of A β 1-42, and is proposed to bind to A β in the brain and facilitate its clearance (Bard et al., 2000; Schroeter et al., 2008). Although the antibody was successful in lowering the brain amyloid after 78 weeks of clinical trial, there was no improvement in cognition (Rinne et al., 2010). Since bapineuzumab potentially only binds to A β 1-42, it ignores the majority of the other A β peptides in the AD brain that may play an important role in cognitive decline and disease pathogenesis. Therefore, it is critical to determine the *in vivo* toxicity associated with these amino-truncated A β species found in the human AD brain.

Comparative studies of the relative toxicity of these specific A β peptides (amino truncated, post-translationally modified or otherwise) have not been performed in canonical mouse models of AD such as Tg2576 (Hsiao et al., 1996) or APP^{swe}/PS1^{dE9} (APP/PS1) transgenic mice (Jankowsky et al., 2001). Although these mice overexpress human A β , deposit amyloid plaques, and show cognitive deficits, the spectra of A β peptides found in the mouse brain are different from those found in the human AD brain and is limited to A β 1-40/42/43 (Adlard et al., 2008; Kalback et al., 2002). This suggests differences in mechanisms driving the deposition of A β in mouse and humans (Schieb et al., 2011). Furthermore, the toxic effects associated with A β peptides have been linked to peroxide generation in cell cultures through metal ion reduction (Huang et al., 1999). The metal ion binding site of A β has been mapped to the N- terminus amino acids 1-28 (Bush et al., 1993; Bush et al., 1994). The A β peptide found in mice contains three amino acid substitutions within this metal binding domain (Arg5Gly, Tyr10Phe, His13Arg), which significantly decreases the metal binding activity and peroxide production (Huang et al., 1999). In addition, mice do not develop amyloid deposition with age even when A β 1-42 is overexpressed in the brains of familial AD-linked mutant presenilin transgenics, which suggests that the mouse A β is not as intrinsically pathogenic as the human A β (Duff et al., 1996). Moreover, the mouse A β peptides lack the extensive N-terminal degradations, posttranslational modifications and cross-linkages abundant in

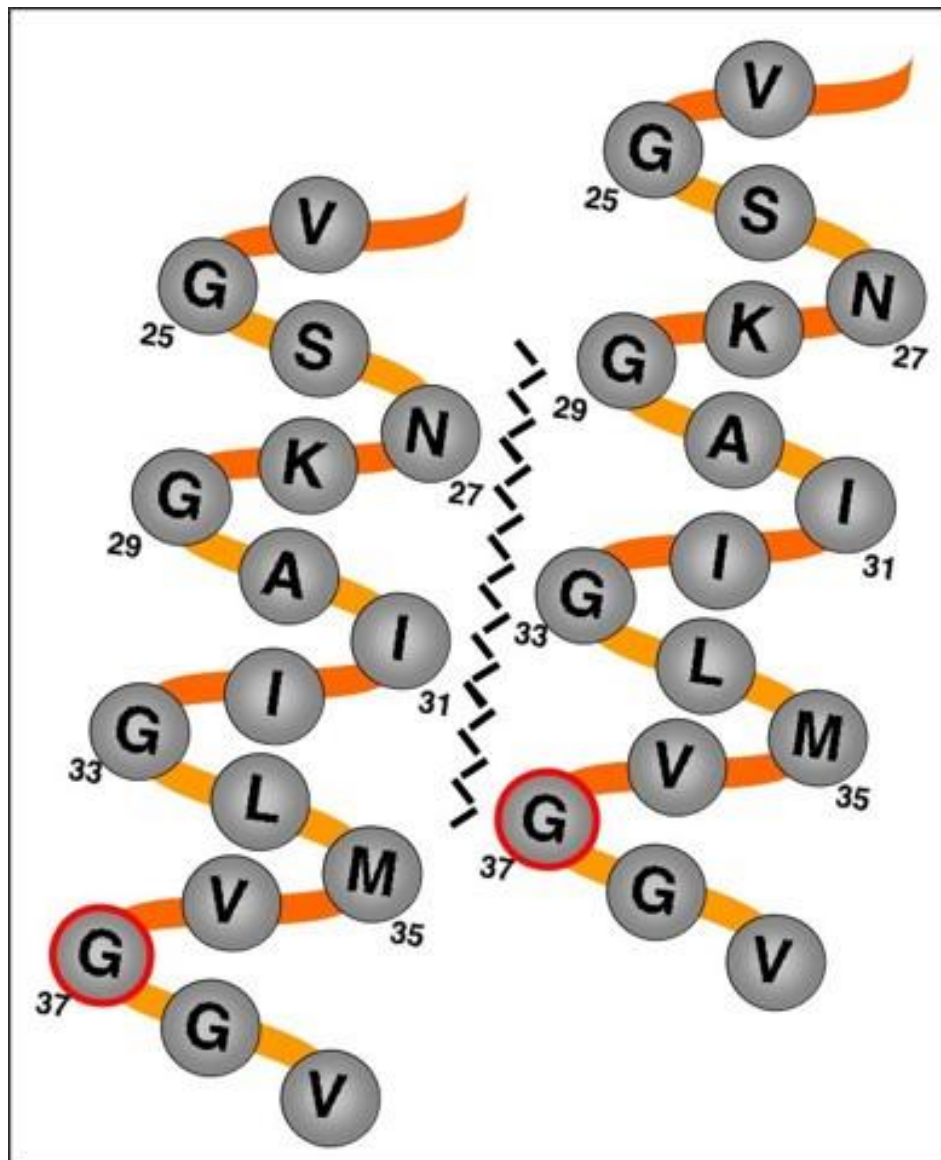


Figure 4.2: Schematic model of hypothetical glycine zipper-mediated interaction between A β helical regions.

Model of possible packing arrangement between C-terminal regions (residues 24-39) of neighbouring A β molecules. The glycine zipper interface is represented by the jagged line; residue G37 is highlighted in red. Adapted from (Fonte et al., 2011).

the stable A β peptide deposits. Finally, the oligomeric A β species found in mouse AD brain are not formic acid stable, while those in the human AD brain are (Kalback et al., 2002). However, the *in vivo* toxicity of mouse A β compared to human A β has not been directly explored in other animals.

Study of mutations that result in changes to the *in vivo* neurotoxicity of these A β peptides may be beneficial. Transgenic strains expressing A β peptides with amino acid substitutions have been generated to study different aspects of A β toxicity (Fay et al., 1998; Link, 1995). For instance, the hydrophobic C-terminal motif -Gly-XXX- Gly-XXX-Gly- motif in A β (residues 24-39) which forms a glycine zipper, has been identified as being important for the oligomerization and toxicity of A β (Fonte et al., 2011; Kim et al., 2005). Previous studies have shown that these glycine zippers assist in the packing of A β peptides into transmembrane α -helices (Figure 4.2), and G-to-L substitutions in these glycine zipper motifs reduce A β toxicity in cultured cells and in primary mouse cortical neurons; G37L substitutions were particularly shown to have greater reduction in toxicity (Hung et al., 2008; Kim et al., 2005). Addition of A β G37L to neuronal cells led to reduction of A β toxicity, which may be due to a direct interaction between the A β and A β variant causing the G37L mutation to interfere with the formation of A β oligomers, or due to an indirect effect such as competing for a common target (Fonte et al., 2011).

Furthermore, these glycine zipper motifs play an important role in the dimerization of APP, and also in production of A β by APP processing (Munter et al., 2010; Munter et al., 2007). The role of the glycine zipper motif in processing means that using transgenic mouse models expressing human APP containing these glycine zipper substitutions may be difficult as these substitutions interfere with the proteolytic processing of APP into A β peptides. In contrast, a transgenic *C. elegans* strain expressing the A β 1-42G37L in the body wall muscles does not require peptide processing and showed significant reduction in the rate of paralysis compared to the A β 1-42-expressing strains (Fonte et al., 2011). Expressing this A β 1-42G37L peptide in the *C. elegans* nervous system will make this model more disease-relevant. Moreover, expressing this A β 1-42G37L peptide in the already established neuronal A β 1-42-expressing strain will give further insight into the *in vivo* toxicity of these A β 1-42G37L peptides.

In this chapter, I test the hypothesis that the expression of each of these different A β species in the *C. elegans* nervous system (one peptide at a time) will show differences in behavioural deficits when compared to the strains expressing the pan-neuronal A β 1-42 transgene. To test this hypothesis, I aim to do the following:

1. Characterise the *in vivo* toxic effects of the neuronal expression of the amino-truncated A β 4-42 transgene on *C. elegans* behaviour, and determine any differences between the *in vivo* toxicity of this amino-truncated transgene and the full length A β 1-42 transgene.
2. Examine the *in vivo* toxic effects of the mouse A β transgene by expressing this transgene in the *C. elegans* neurons and comparing the behavioural phenotypes between the mouse A β and human A β -expressing strains.
3. Determine the *in vivo* effects of the concurrent expression of a mutant A β transgene containing a G37L substitution and the full length A β 1-42 transgene, by generating double transgenic *C. elegans* strains expressing both the A β transgenes simultaneously in the neurons and comparing the behavioural phenotypes of this strain with the single A β 1-42-expressing transgenic strain.

4.2 Methods

All materials and methods used in this chapter are described in Section 2.2 with a few exceptions (described below).

4.2.1 Construction of transgenic *C. elegans* expressing A β variants in the neurons

The expression plasmid *pSNB-1* was constructed by cloning the *snb-1* promoter fragment into the MCS I of the pPD49.26 vector backbone. This plasmid was then used to construct expression plasmids containing different A β transgenes driven by the *snb-1* promoter. The A β 4-42, A β 1-42G37L, and mouse A β fragments were extracted from the plasmids pGMC104, pGMC107, and pGMC110, respectively, using the restriction enzymes NheI and SacI and cloned into the MCS II of pSNB1 vector backbone. These pGMC plasmids were obtained from Dr. Gawain McColl at the Florey Institute of Neuroscience and Mental Health. The presence of the insert in these new expression plasmids pSNB1AB442, pMouseAB, and pA β 42G37L was confirmed by restriction enzyme digestion and all clones were verified by Sanger sequencing (Macrogen, Korea).

The expression plasmids were then introduced into the *C. elegans* gonads by microinjection, performed by Kirsten Grant at the Florey Institute of Neuroscience and Mental Health. Details of the plasmid concentrations used for microinjections are listed in Supplementary Tables 1-5. Briefly, all the expressed plasmids were initially microinjected at a concentration of 25 ng/ μ l, with marker plasmid pAV1944/pAV119 (2.5 ng/ μ l) and sheared genomic DNA (50 ng/ μ l). Transgenic strains were obtained for A β 1-42G37L and mouse A β containing expression plasmids. After multiple unsuccessful attempts to obtain transgenic A β 4-42 expressing strains, even at lower concentrations of the expression plasmid, the A β 4-42 fragment was cloned into a plasmid containing *rgef-1* pan-neuronal promoter. The new expression plasmid pEXAB442 was microinjected at a concentration of 10 ng/ μ l along with marker plasmid pAV1944 (2.5 ng/ μ l) and sheared genomic DNA (100 ng/ μ l) to successfully obtain pan-neuronal A β 4-42 expressing transgenic strains. Since all these transgenic strains contain extrachromosomal arrays of these plasmids, the strains were irradiated using X-rays to integrate the array into the

worm genome. Subsequently, all the integrated transgenic strains were backcrossed three times to the wild type animals in order to remove background mutations.

4.2.2 Strains used in this chapter

The strains used in this chapter are as follows: **WG731** [*Pmyo-2::mCherry*], **WG643** [*Pmyo-2::mCherry* + *Psnb-1::huAβ1-42*], **WG663** [*Pmyo2::mCherry* + *Prgef-1::huAβ1-42*], **WG709** [*Pmyo-2::mCherry* + *Prgef-1::huAβ4-42*]; **WG724** [*Pmyo-2::mCherry* + *Psnb-1::mouseAβ1-42*], **WG657** [*Pmyo2::GFP* + *Psnb-1::huAβ1-42G37L*], **WG664** [*Pmyo2::mCherry* + *Prgef-1::huAβ1-42*; *Pmyo2::GFP* + *Psnb-1::huAβ1-42G37L*], **WG666** [*Pmyo2::mCherry* + *Psnb-1::huAβ1-42*; *Pmyo2::GFP* + *Psnb-1::huAβ1-42G37L*], **CB1112** [*cat-2 (e1112)* II], **MT7988** [*bas-1 (ad446)* III] (Loer and Kenyon, 1993), **CB1141** [*cat-4 (e1141)* V] (Sulston et al., 1975), **MT8943** [*bas-1(ad446)* III; *cat-4 (e1141)* V].

4.2.3 Statistical analysis

All data have been reported as mean ± SEM values. The Shapiro-Wilk test was used to test normality and if the data were not normally distributed, then appropriate non-parametric tests were used to determine significant differences. A two-way ANOVA using age and genotype was used as variables for all motility assays, whereas a one-way ANOVA was used for all other assays (unless otherwise stated).

4.3 Results

4.3.1 Copy-number PCR assay shows a range of A β copies in the transgenic strains

A copy-number PCR assay was performed to quantify the number of the copies of the A β transgene in the transgenic *C. elegans* strains containing A β variants. As shown in Figure 4.3A, the mouse A β strain WG724 has the lowest number of A β copies per haploid genome (0.82 ± 0.03), while the A β 1-42G37L transgene-containing strains WG666 and WG664 showed very high copy numbers of the A β transgene when compared to the other strains. In addition, there was a lot of variation in the copy number of A β 1-42G37L transgene within each strain. The transgenic *C. elegans* strain WG664, obtained by crossing the strain WG663 (*Prgef-1::huA β 1-42*) with WG657 (*Psnb-1::A β 1-42G37L*), showed a copy number of 383 ± 29 . The strain WG666 showed the highest copy number of ~400 copies (418 ± 74) amongst all the strains. This strain was obtained by crossing the strain WG643 (*Psnb-1::huA β 1-42*) with the strain WG657 (*Psnb-1::A β 1-42G37L*). The A β copy number in the strain WG664 and WG666 was due to the A β 1-42 and A β 1-42G37L transgenes. The transgenic A β 4-42 expressing strain WG709 showed ~30 copies of the A β transgene per haploid genome.

4.3.2 Transgenic *C. elegans* strains containing the A β variant transgenes show low levels of A β transgene expression in comparison to the human A β 1-42 expressing strains.

To allow for better comparison of the *in vivo* effects of A β transgene expression, all the transgenic strains described in this chapter are divided into three groups. The first group consists of the mouse A β expressing strain WG724 (*Psnb-1::mouseA β 1-42*) compared to the human A β 1-42 expressing strain WG643 (*Psnb-1::huA β 1-42*) as they are driven by the same pan-neuronal promoter *snb-1*. The second group compares the *in vivo* toxicity between the A β 1-42 and the truncated A β 4-42 peptide, thereby utilising the transgenic strains WG709 (*Prgef-1::huA β 4-42*) and WG663 (*Prgef-1::huA β 1-42*) as these strains contain the A β transgene being driven by same pan-neuronal promoter *rgef-1*. Lastly, the third group comprises of the double transgenic strains WG664 and WG666 expressing both the A β 1-42 and the mutant A β 1-42G37L peptide, wherein different promoters are

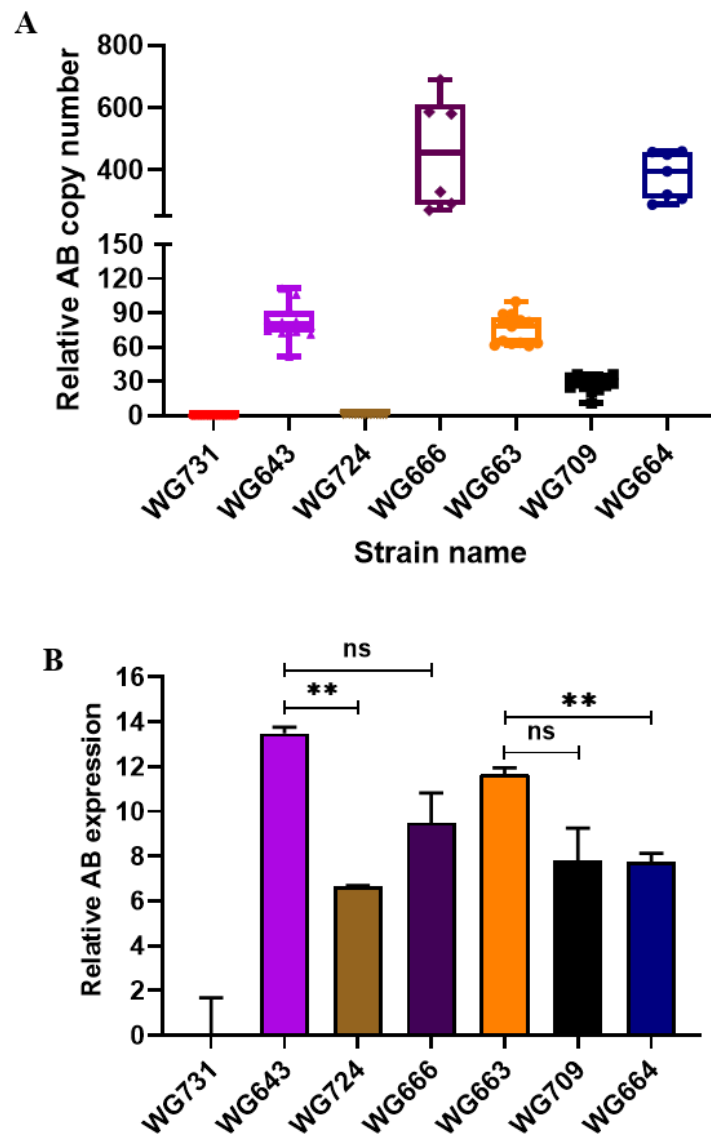


Figure 4.3: Comparison of A β expression levels in the pan neuronal A β strains.

A) Copy number assay showing the number of copies of the A β transgene in the strains per haploid genome. B) RT-qPCR showing the relative expression of the A β transgene in the strains normalized to reference genes *cdc-42* and *Y45F10D.4*. An unpaired t test was used to compare between two strains, ns not significant, * $p < 0.05$, ** $p < 0.01$. **WG731** [*Pmyo-2::mCherry*], **WG643** [*Pmyo-2::mCherry + Psnb-1::huA β 1-42*], **WG663** [*Pmyo2::mCherry + Prgef-1::huA β 1-42*], **WG709** [*Pmyo-2::mCherry + Prgef-1::huA β 4-42*]; **WG724** [*Pmyo-2::mCherry + Psnb-1::mouseA β 1-42*], **WG657** [*Pmyo2::GFP + Psnb-1::huA β 1-42G37L*], **WG664** [*Pmyo2::mCherry + Prgef-1::huA β 1-42*; *Pmyo2::GFP + Psnb-1::huA β 1-42G37L*], **WG666** [*Pmyo2::mCherry + Psnb-1::huA β 1-42*; *Pmyo2::GFP + Psnb-1::huA β 1-42G37L*].

utilised to express the A β 1-42 transgene. The transgenic *C. elegans* strain WG664 was obtained by crossing the strain WG663 (*Prgef-1::huA β 1-42*) with WG657 (*Psnb-1::huA β 1-42G37L*). Additionally, the transgenic strain WG666 was obtained by crossing the strain WG643 (*Psnb-1::huA β 1-42*) with WG657 (*Psnb-1::huA β 1-42G37L*). The double transgenic strains WG664 and WG666 are compared to the single A β 1-42 expressing transgenic strains WG663 and WG643 respectively. The WG731 strain expressing *mCherry* in the pharynx was used as a transgenic control.

To characterize the A β transgene expression in these strains, an RT-qPCR assay was performed. As can be seen in Figure 4.3B, the mouse A β -expressing strain WG724 showed the lowest expression (6.65 ± 0.03) amongst all the transgenic strains and was significantly lower ($p = 0.0017$) compared to A β 1-42 strain WG643 (13.47 ± 0.28) as determined by an unpaired t-test. Although the A β 4-42 expressing strain WG709 showed lower A β expression (7.81 ± 1.43) compared to A β 1-42 expressing strain WG663 (11.67 ± 0.26), the difference in level of expression was not statistically significant ($p = 0.057$, unpaired t test). Surprisingly, the level of A β expression in the double transgenic strain WG666 (9.5 ± 1.33) was moderately lower as compared to the A β 1-42 expressing strain WG643 (13.47 ± 0.28) ($p = 0.105$, unpaired t test). Furthermore, the strain WG664 (7.75 ± 0.37) showed significant reduction in A β expression as compared to A β 1-42 expressing strain WG663 (11.67 ± 0.26) ($p = 0.001$, unpaired t test). The A β expression levels in the double transgenic strain WG664 and WG666 did not show any statistically significant differences between these strains. In addition, levels of A β expression analysed in young (day 4), middle-aged (day 8) and old worms (day 12) showed lower levels of expression when comparing to transgene expression levels from RNA obtained from mixed life-stages (Supplementary Figure 4.1).

4.3.3 Pan-neuronal mouse A β -expressing strain WG724 is longer lived than the human A β -expressing strain.

Life span assays were performed to determine the *in vivo* effects of the A β variant transgenes on the longevity of the worms. As can be seen in Figure 4.4A, Kaplan-Meier survival curves were plotted, and a log rank test was used to compare the survival curves

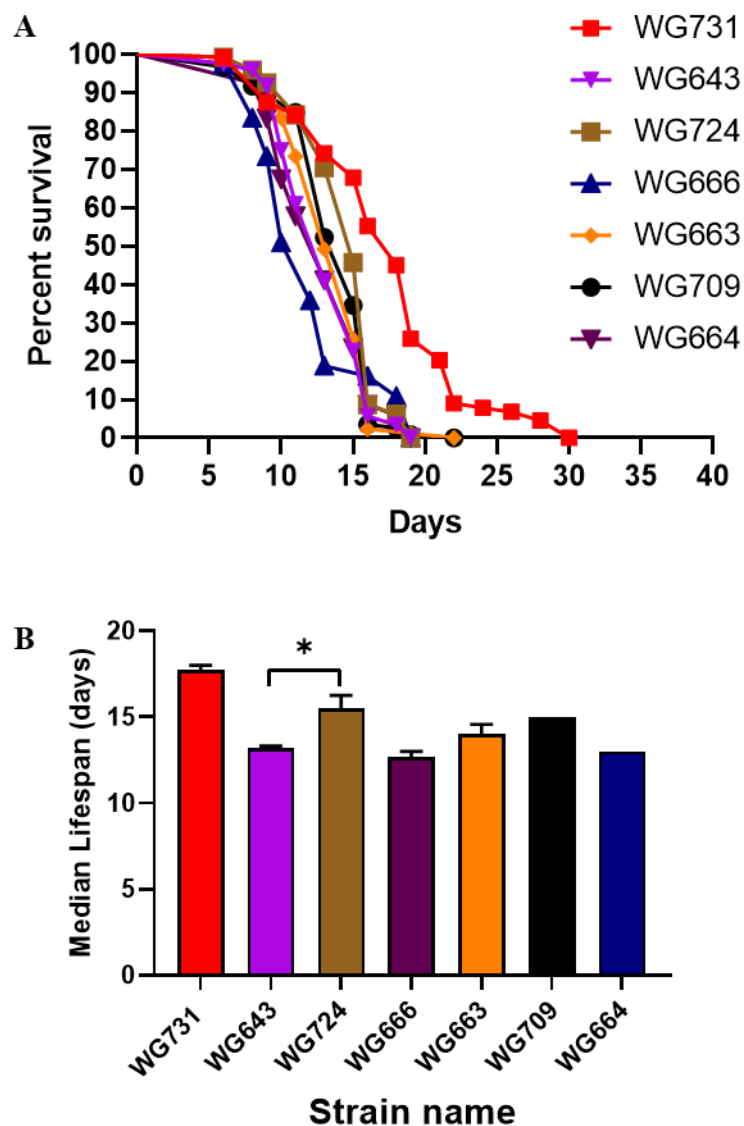


Figure 4.4: Transgenic *C. elegans* strains expressing A β variants in the neurons show reduction in the lifespan.

A) Representative Kaplan-Meier survival curves of one biological replicate (n=120 worms/replicate). B) Median lifespan (n=4, 120 worms/biological replicate). The median lifespan data were analysed using one-way ANOVA followed by post hoc Tukey multiple comparisons test. **WG731** [*Pmyo-2::mCherry*], **WG643** [*Pmyo-2::mCherry* + *Psnb-1::huA β 1-42*], **WG663** [*Pmyo2::mCherry* + *Prgef-1::huA β 1-42*], **WG709** [*Pmyo-2::mCherry* + *Prgef-1::huA β 4-42*]; **WG724** [*Pmyo-2::mCherry* + *Psnb-1::mouseA β 1-42*], **WG657** [*Pmyo2::GFP* + *Psnb-1::huA β 1-42G37L*], **WG664** [*Pmyo2::mCherry* + *Prgef-1::huA β 1-42*; *Pmyo2::GFP* + *Psnb-1::huA β 1-42G37L*], **WG666** [*Pmyo2::mCherry* + *Psnb-1::huA β 1-42*; *Pmyo2::GFP* + *Psnb-1::huA β 1-42G37L*].

of all the A β -expressing strains. The survival curves of the remaining biological replicates are shown in Supplementary Figure 4.2. In addition, the median lifespan was calculated from the survival data, and one-way ANOVA was used to test for significant differences in the median lifespan between the A β -expressing strains (Figure 4.4B). Table 4.1 shows the median and maximum life span values and the decrease of the life span of the A β -expressing strains compared to the transgenic control strain WG731. The Gompertz equation was used to calculate the initial mortality rate (A) and the Gompertz value (G). A lower Gompertz value (G) indicates low rate of aging. The mortality rate doubling time was calculated using the formula $MRDT = 0.693/G$ (

Table 4.2). When comparing the transgenic strains utilising *snb-1* as the pan-neuronal promoter to drive A β transgene expression, there was a significant difference in the survival curves of the mouse A β 1-42 strain WG724 and the human A β 1-42 expressing strain WG643 ($p = 0.0002$). Additionally, the median life span of the mouse A β -expressing strain WG724 was significantly higher than the human A β -expressing strain WG643 ($p=0.0119$). Hence, these data show that the survival of the mouse A β 1-42 expressing strain WG724 is higher than the human A β 1-42 expressing strain WG643. In the second group, there was no difference in the survival curves ($p = 0.18$) and median lifespan ($p>0.9999$) of the truncated A β 4-42 expressing strain WG709 and the A β 1-42 expressing strain WG663 ($p = 0.18$).

Furthermore, the survival curve of the double transgenic strain WG666 was significantly lower from the A β -expressing strain WG643 ($p = 0.03$) as determined by log rank test. However, there was no difference in the median lifespan. On the other hand, the double transgenic strain WG664, expressing both the A β 1-42 and A β 1-42G37L transgenes, and the human A β 1-42 expressing strain WG663 did not show significant differences in survival curves ($p = 0.12$) and median lifespan ($p = 0.2031$). There was a reduction in median and maximum lifespan of all A β wildtype and variant expressing transgenic strains in comparison to the transgenic control strain WG731 (Table 4.1). As seen in Table 4.2, the rate of aging was similar for all the transgenic A β -expressing strains and was higher than the transgenic control WG731. Hence, these data suggest that expressing

both the wild type and variant A β peptides in the nervous system accelerates the rate of aging in *C. elegans*.

Table 4.1: Median and maximum life span values (Mean \pm SEM)

Strain name	Median Lifespan (days)	% decrease in median lifespan	Maximum Lifespan (days)	% decrease in maximum lifespan
WG731(Tg control)	17.75 \pm 0.25		24 \pm 1.15	
WG643 (<i>Psnb-1::huAβ1-42</i>)	13.17 \pm 0.17	-25.8%	16.67 \pm 0.61	-30.54%
WG724 (<i>Psnb-1:mouseAβ1-42</i>)	15.5 \pm 0.76	-12.68%	19.33 \pm 1.26	-19.46%
WG663 (<i>Prgef-1::huAβ1-42</i>)	14.00 \pm 0.58	-21.12%	17.25 \pm 0.75	-28.12%
WG709 (<i>Prgef-1:huAβ4-42</i>)	15.00 \pm 0.00	-15.49%	17.33 \pm 0.67	-27.79%
WG664 (<i>Prgef-1::huAβ1-42 + Psnb-1::huAβ1-42G37L</i>)	13.00 \pm 0.00	-26.76%	16 \pm 0.00	-33.33%
WG666 (<i>Psnb-1::huAβ1-42 + Psnb-1::huAβ1-42G37L</i>)	12.67 \pm 0.33	-28.62%	17 \pm 1.16	-29.17%

Table 4.2: G and A estimates derived from Gompertz equation

Strain name	Gompertz value (G)	Initial mortality rate (A)	MRDT
WG731(Tg control)	0.17	6.003E-3	4.08
WG643 (<i>Psnb-1::huAβ1-42</i>)	0.40	1.591E-3	1.75
WG724 (<i>Psnb-1:mouseAβ1-42</i>)	0.41	5.66E-4	1.67
WG663 (<i>Prgef-1::huAβ1-42</i>)	0.32	3.894E-3	2.16
WG709 (<i>Prgef-1:huAβ4-42</i>)	0.39	1.917E-3	1.77
WG666 (<i>Psnb-1::huAβ1-42 + Psnb-1::huAβ1-42G37L</i>)	0.32	5.076E-3	2.2
WG664 (<i>Prgef-1::huAβ1-42 + Psnb-1::huAβ1-42G37L</i>)	0.37	1.262E-3	1.87

4.3.4 Measurement of growth rate of variant A β -expressing transgenic strains

To investigate if the expression of the A β variant transgene has any effect on the growth and aging of these worms, the body size of all transgenic strains was measured in terms of length and width on day 4 (young), day 8 (middle-aged), and day 12 (old) (Figure 4.5). One-way ANOVA was performed to test for differences in the length and width between these animals. When comparing the mouse A β -expressing strain WG724 with the human A β 1-42 expressing strain WG643 and the control strain WG731, there was no difference in the growth rate of the worms in terms of the length and width on day 4, day 8 and day 12. Amongst the young adult worms on day 4, the length of the A β 4-42 expressing strain WG709 was significantly lower than the transgenic control WG731 ($p = 0.0009$) unlike WG663 ($p = 0.25$). However, on day 8 and day 12, there was no difference in the length and width of the WG709 (A β 4-42), WG663 (A β 1-42), and the control strain WG731. This indicates that there is a difference in the growth rate of these strains on Day 4, but this difference in growth diminishes in middle-aged adults on Day 8

Further, the length of the A β 1-42G37L strain WG664 strain was significantly lower as compared to the control strain WG731 ($p = 0.01$), but not different from A β 1-42 expressing strain WG663 ($p = 0.31$) on day 4. The differences in length between these strains diminishes on Day 8 and Day 12. In contrast, the strain expressing two A β transgenes A β 1-42 and A β 1-42G37L driven by the same promoter *snb-1* was slow growing and did show significant differences in the length on day 4 and day 12 compared to the A β 1-42 expressing strain WG643 and the transgenic control strain WG731. However, there were no differences in the width between all the worm strains at all time points. Overall, these data suggest that there is no difference in the growth rate of the A β expressing worms and the transgenic control strain WG731 except for the slow growing double transgenic strain WG666.

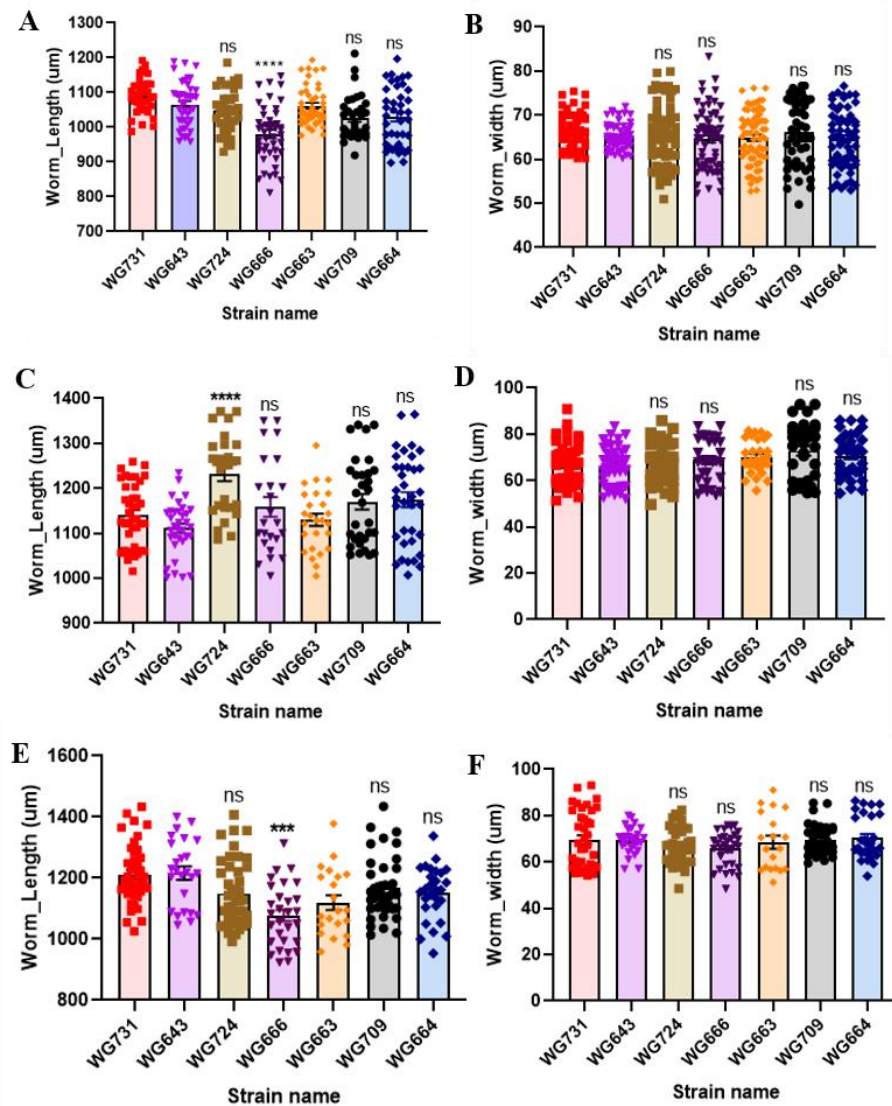


Figure 4.5: Double transgenic *C. elegans* strain WG666 expressing A β and A β shows slow growth as estimated by body size measurements of early (day 4), middle-aged (day 8) and old (day 12) adults.

A) Body length of day 4 worms. B) Body width of day 4 worms. C) Body length of day 8 worms. D) Body width of day 8 worms. E) Body length of day 12 worms. F) Body width of day 12 worms. All data analysed using One-way ANOVA followed by post hoc Tukey multiple comparisons test, ns not significant, * $p < 0.05$, ** $p < 0.01$, *** $p < 0.001$, **** $p < 0.0001$. The strains WG666 and WG724 were compared to the WG643 strain whereas the strains WG709 and WG664 were compared to the WG663 strain. **WG731** [*Pmyo-2::mCherry*], **WG643** [*Pmyo-2::mCherry + Psnb-1::huA β 1-42*], **WG663** [*Pmyo-2::mCherry + Prgef-1::huA β 1-42*], **WG709** [*Pmyo-2::mCherry + Prgef-1::huA β 4-42*]; **WG724** [*Pmyo-2::mCherry + Psnb-1::mouseA β 1-42*], **WG657** [*Pmyo-2::GFP + Psnb-1::huA β 1-42G37L*], **WG664** [*Pmyo-2::mCherry + Prgef-1::huA β 1-42; Pmyo-2::GFP + Psnb-1::huA β 1-42G37L*], **WG666** [*Pmyo-2::mCherry + Psnb-1::huA β 1-42; Pmyo-2::GFP + Psnb-1::huA β 1-42G37L*].

4.3.5 A β variant expressing strains show differences in egg-laying behaviour compared to the human A β 1-42 expressing strains

In order to determine differences in egg-laying behaviour between the transgenic A β variant expressing strains, egg-laying behaviour was measured using three different assays. Firstly, brood size was measured by counting the total number of progeny per worm and the number of progeny produced per day during the reproductive span of each worm (Figure 4.6A,B). Secondly, the number of eggs retained *in utero* was measured in young adult worms (Figure 4.6C). Thirdly, the rate of egg production was measured by counting the number of progeny per worm per hour (Figure 4.6D).

Strikingly, the A β 4-42 expressing strain WG709 showed significantly reduced brood size (~117 progeny/worm) compared to the A β 1-42 expressing strain WG663 (~265 progeny/worm, $p = 0.0063$). Additionally, there was a significant reduction in the number of progeny produced between WG709 and WG663 on day 4 ($p = 0.02$) and day 5 ($p < 0.0001$) but not on day 6 ($p = 0.85$) or day 7 ($p = 0.97$). There was also a drastic reduction in the rate of egg production in the strain WG709 (1.49 ± 0.12) compared to WG663 (4.29 ± 0.26 , $p < 0.0001$). Hence, the A β 4-42 strain WG709 shows a drastic reduction in brood size and rate of egg production.

The mouse A β 1-42 expressing strain WG724 (~268 progeny/worm) showed no significant difference in the brood size when compared to the transgenic control strain WG731 (~286 progeny/worm) or the A β -expressing strain WG643 (~225 progeny/worm). However, when the progeny number per worm per day during the reproductive span of the worm was measured, the mouse A β strain produced significantly fewer on day 6 ($p = 0.0002$) and day 7 ($p = 0.0047$) compared to the control strain WG731. In contrast, when compared to the human A β -expressing strain WG643 (60.92 ± 6.44), the mouse A β strain WG724 produced more progeny on day 5 (91.17 ± 5.63 , $p = 0.0077$). There was no difference in the eggs retained *in utero* or the rate of egg production between the human A β and mouse A β -expressing strains. These results suggest that although there are differences in the developmental profile of reproduction neither egg production (brood size) nor egg-laying (egg retention) are affected in the mouse A β expressing strain WG724.

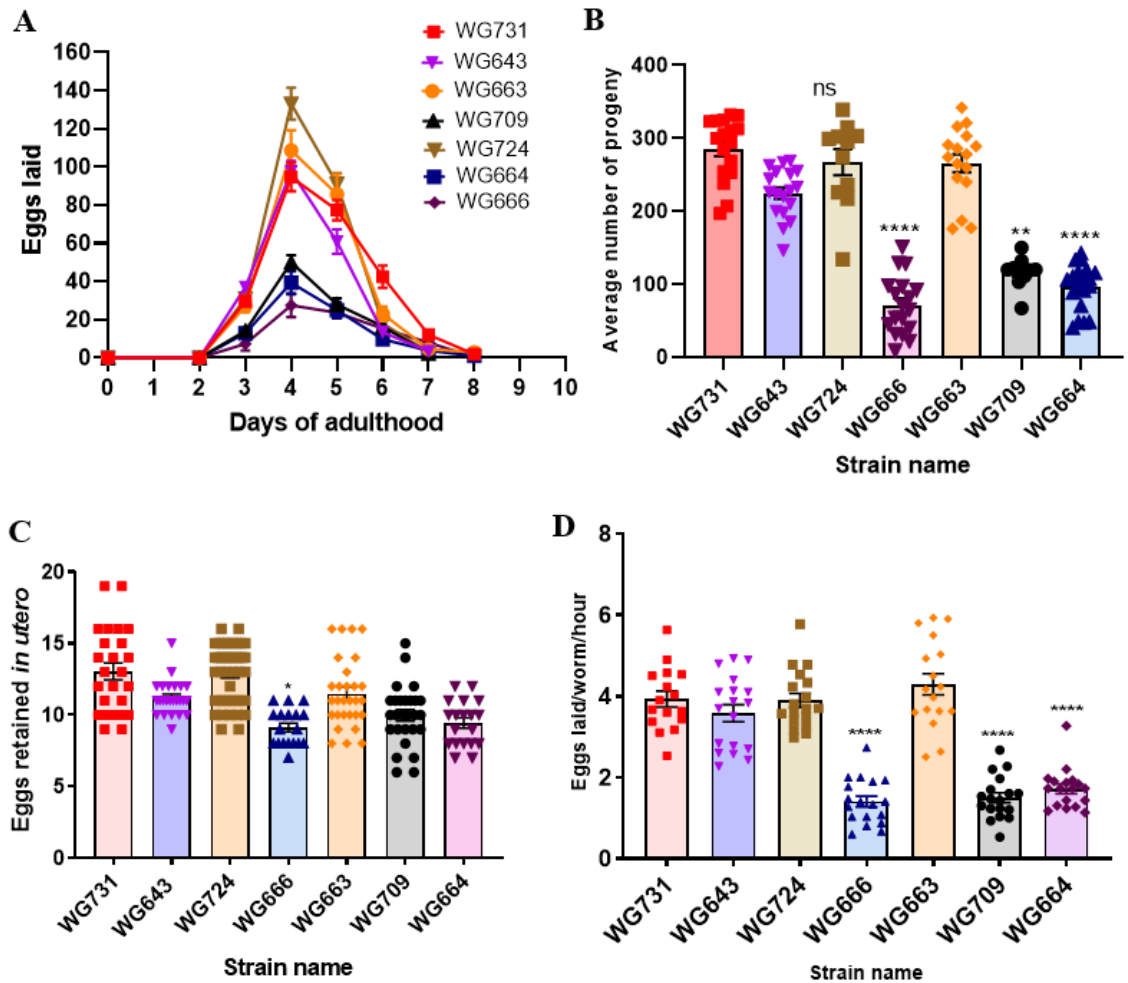


Figure 4.6: Transgenic *C. elegans* strains expressing different versions of the A β peptide show egg-laying defects.

A) Number of eggs laid per worm per day during the reproductive span of the worm. B) Total brood size (n=3, 5-7 worms/replicate). C) Mean number of eggs retained *in utero* per worm (n=3, 15-20 worms/replicate). D) Rate of egg production calculated by counting the number of eggs laid/worm/hour (n=3, 15-20 worms/replicate). All data analysed using One-way ANOVA followed by post hoc Tukey multiple comparisons test, ns not significant, *p < 0.05, **p < 0.01, ***p < 0.001. The strains WG666 and WG724 were compared to the WG643 strain whereas the strains WG709 and WG664 were compared to the WG663 strain. **WG731** [*Pmyo-2::mCherry*], **WG643** [*Pmyo-2::mCherry + Psnb-1::huA β 1-42*], **WG663** [*Pmyo2::mCherry + Prgef-1::huA β 1-42*], **WG709** [*Pmyo-2::mCherry + Prgef-1::huA β 4-42*]; **WG724** [*Pmyo-2::mCherry + Psnb-1::mouseA β 1-42*], **WG657** [*Pmyo2::GFP + Psnb-1::huA β 1-42G37L*], **WG664** [*Pmyo2::mCherry + Prgef-1::huA β 1-42; Pmyo2::GFP + Psnb-1::huA β 1-42G37L*], **WG666** [*Pmyo2::mCherry + Psnb-1::huA β 1-42; Pmyo2::GFP + Psnb-1::huA β 1-42G37L*].

The double transgenic strain WG666 expressing both the A β 1-42 and A β 1-42G37L driven by pan-neuronal promoter *snb-1* showed severe egg-laying defects as seen by reduced brood size (\sim 72 progeny/worm, $p < 0.0001$), low rate of egg production (1.4 ± 0.13 , $p < 0.0001$) and lower egg retention (9.11 ± 0.30 , $p = 0.0169$) compared to the A β 1-42 expressing strain WG643. On the other hand, the double transgenic strain WG664 expressing both the A β 1-42 and A β 1-42G37L transgenes showed a drastic reduction in the total brood (\sim 96 progeny/worm) relative to the A β 1-42 expressing strain WG663 (\sim 266 progeny/worm, $p < 0.0001$). Furthermore, the WG664 strain laid significantly fewer eggs on day 4 ($p = 0.0018$) and day 5 ($p < 0.0001$) when compared the strain WG663. Although there was a significant reduction in the rate of egg production between the two strains ($p < 0.0001$), the number of eggs retained *in utero* was similar to that of WG663 ($p = 0.07$). Therefore, the double transgenic strain WG666 and WG664 show severe impairment in egg laying.

4.3.6 A β variant expressing strains WG709 and WG664 show subtle differences in crawling compared to the A β 1-42 expressing strain WG663

In order to examine whether the A β variant expressing strains had an age-related locomotion phenotype and to test whether these phenotypes were different from those seen in human A β 1-42 expressing strains, motility was measured on solid and liquid media in young (day 4), middle-aged (day 8) and old (day 12) worms. Several motility parameters were assessed on solid media: body bends, mean speed, maximum speed, mean wavelength, mean amplitude, and head bends (Figure 4.7 and Supplementary Figure 4.3). Two- way ANOVA followed by Tukey's multiple comparisons test was used to analyse the data set using age and genotype as independent factors. The p-values of the comparison of motility parameters on solid media between the A β -expressing strains have been listed in Table 4.3.

The A β 4-42 expressing strain WG709 showed significant age-related decline in body bends ($p < 0.0001$), mean speed ($p < 0.0001$), maximum speed ($p = 0.012$), mean wavelength ($p < 0.0001$) and head bends ($p = 0.002$) from day 4 to day 12.

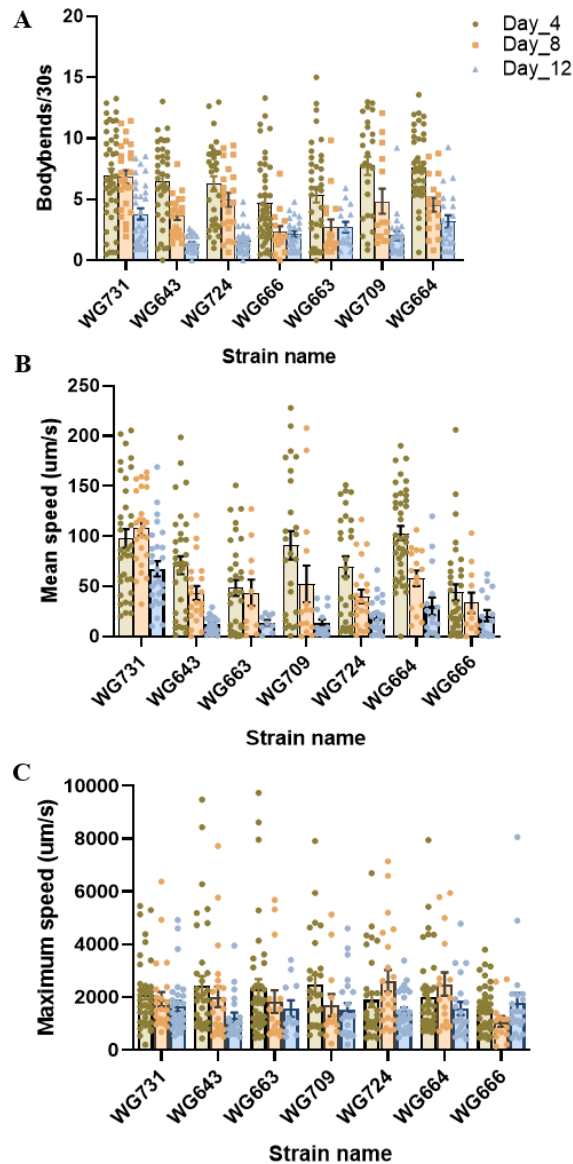


Figure 4.7: Age-related changes in motility of transgenic A β -expressing strains on solid media.

A) Body bends/30s. B) Mean speed ($\mu\text{m/s}$). C) Maximum speed ($\mu\text{m/s}$).

All data analysed by two-way ANOVA followed by post hoc Tukey multiple comparisons test (n=3, 5-15 worms/replicate). The strains WG666 and WG724 were compared to the WG643 strain whereas the strains WG709 and WG664 were compared to the WG663 strain. **WG731** [*Pmyo-2::mCherry*], **WG643** [*Pmyo-2::mCherry* + *Psnb-1::huA β 1-42*], **WG663** [*Pmyo2::mCherry* + *Prgef-1::huA β 1-42*], **WG709** [*Pmyo-2::mCherry* + *Prgef-1::huA β 4-42*]; **WG724** [*Pmyo-2::mCherry* + *Psnb-1::mouseA β 1-42*], **WG664** [*Pmyo2::mCherry* + *Prgef-1::huA β 1-42*; *Pmyo2::GFP* + *Psnb-1::huA β 1-42G37L*], **WG666** [*Pmyo2::mCherry* + *Psnb-1::huA β 1-42*; *Pmyo2::GFP* + *Psnb-1::huA β 1-42G37L*].

Although the body bends ($p = 0.019$) and the mean speed ($p = 0.005$) of the strain WG709 (A β 4-42) were significantly higher than WG663 (A β 1-42) on day 4, these differences diminished in older worms on day 8 and day 12. None of the other motility parameters showed significant differences between the two strains.

The mouse A β -expressing strain WG724 showed age-related decline in body bends ($p < 0.0001$), mean speed ($p = 0.0001$), mean wavelength ($p = 0.0001$), and head bends ($p < 0.0001$) from day 4 to day 12. None of the motility parameters show significant differences between the mouse A β WG724 and human A β WG643 expressing strains (Table 4.3).

Further, the double transgenic strain WG666 expressing A β 1-42 and A β 1-42G37L driven by pan-neuronal promoter *snb-1* showed significant age-related decline in body bends ($p = 0.0015$), mean wavelength ($p = 0.0013$), and head bends ($p < 0.0001$) from day 4 to day 12. None of the motility parameters were significantly different between the two strains WG666 and WG643. The second double transgenic strain WG664 expressing A β 1-42 and A β 1-42G37L transgenes showed significant age-related decline in body bends ($p < 0.0001$), mean speed ($p < 0.0001$), mean wavelength ($p = 0.0003$), and head bends ($p = 0.0028$) from day 4 to day 12. While the double transgenic strain WG664 expressing both A β 1-42 and A β 1-42G37L showed better movement in terms of body bends and mean speed compared to the single transgenic strain WG663 (A β 1-42) on day 4, it was not significant on day 8 or day 12. None of the other parameters showed significant differences between the two strains WG664 and WG663.

Table 4.3: Comparison of crawling parameters between transgenic A β -expressing strains

Strain comparisons	Genotype	day 4 (p value)	day 8 (p value)	day 12 (p value)
Body bends				
WG663 vs WG709	<i>Prgef-1::huAβ1-42</i> vs <i>Prgef-1::huAβ4-42</i>	0.0193* ↑	0.4101	0.9917
WG663 vs WG664	<i>Prgef-1::huAβ1-42</i> vs <i>Prgef-1::huAβ1-42; Psnb-1::huAβ1-42G37L</i>	0.0079** ↑	0.5317	0.9991
WG643 vs WG724	<i>Psnb-1::huAβ1-42</i> vs <i>Psnb-1::mouseAβ1-42</i>	>0.9999	0.7359	0.9857
WG643 vs WG666	<i>Psnb-1::huAβ1-42</i> vs <i>Psnb-1::huAβ1-42; Psnb-1::huAβ1-42G37L</i>	0.6262	0.8189	0.9667
Mean speed				
WG663 vs WG709	<i>Prgef-1::huAβ1-42</i> vs <i>Prgef-1::huAβ4-42</i>	0.0052** ↑	0.9989	>0.9999
WG663 vs WG664	<i>Prgef-1::huAβ1-42</i> vs <i>Prgef-1::huAβ1-42; Psnb-1::huAβ1-42G37L</i>	<0.0001**** ↑	0.9817	0.9716
WG643 vs WG724	<i>Psnb-1::huAβ1-42</i> vs <i>Psnb-1::mouseAβ1-42</i>	>0.9999	>0.9999	0.9973
WG643 vs WG666	<i>Psnb-1::huAβ1-42</i> vs <i>Psnb-1::huAβ1-42; Psnb-1::huAβ1-42G37L</i>	0.1545	0.9969	0.9967
Maximum speed				
WG663 vs WG709	<i>Prgef-1::huAβ1-42</i> vs <i>Prgef-1::huAβ4-42</i>	0.9995	0.9898	>0.9999
WG663 vs WG664	<i>Prgef-1::huAβ1-42</i> vs <i>Prgef-1::huAβ1-42; Psnb-1::huAβ1-42G37L</i>	0.9487	0.8860	>0.9999
WG643 vs WG724	<i>Psnb-1::huAβ1-42</i> vs <i>Psnb-1::mouseAβ1-42</i>	0.7537	0.6024	0.9982
WG643 vs WG666	<i>Psnb-1::huAβ1-42</i> vs <i>Psnb-1::huAβ1-42; Psnb-1::huAβ1-42G37L</i>	0.0634	0.6930	0.8520
Mean amplitude				
WG663 vs WG709	<i>Prgef-1::huAβ1-42</i> vs <i>Prgef-1::huAβ4-42</i>	0.9995	0.5072	0.9786
WG663 vs WG664	<i>Prgef-1::huAβ1-42</i> vs <i>Prgef-1::huAβ1-42; Psnb-1::huAβ1-42G37L</i>	0.9998	0.0991	0.9954
WG643 vs WG724	<i>Psnb-1::huAβ1-42</i> vs <i>Psnb-1::mouseAβ1-42</i>	>0.9999	0.9898	0.9961
WG643 vs WG666	<i>Psnb-1::huAβ1-42</i> vs <i>Psnb-1::huAβ1-42; Psnb-1::huAβ1-42G37L</i>	0.9243	0.9674	0.9187
Mean wavelength				
WG663 vs WG709	<i>Prgef-1::huAβ1-42</i> vs <i>Prgef-1::huAβ4-42</i>	0.9749	0.7535	0.4910
WG663 vs WG664	<i>Prgef-1::huAβ1-42</i> vs <i>Prgef-1::huAβ1-42; Psnb-1::huAβ1-42G37L</i>	0.5702	0.9959	0.6087
WG643 vs WG724	<i>Psnb-1::huAβ1-42</i> vs <i>Psnb-1::mouseAβ1-42</i>	>0.9999	>0.9999	0.9187
WG643 vs WG666	<i>Psnb-1::huAβ1-42</i> vs <i>Psnb-1::huAβ1-42; Psnb-1::huAβ1-42G37L</i>	0.6111	0.4952	0.0484*
Head bends				
WG663 vs WG709	<i>Prgef-1::huAβ1-42</i> vs <i>Prgef-1::huAβ4-42</i>	0.9916	>0.9999	>0.9999
WG663 vs WG664	<i>Prgef-1::huAβ1-42</i> vs <i>Prgef-1::huAβ1-42; Psnb-1::huAβ1-42G37L</i>	>0.9999	0.9048	0.9737
WG643 vs WG724	<i>Psnb-1::huAβ1-42</i> vs <i>Psnb-1::mouseAβ1-42</i>	0.9274	>0.9999	0.9986
WG643 vs WG666	<i>Psnb-1::huAβ1-42</i> vs <i>Psnb-1::huAβ1-42; Psnb-1::huAβ1-42G37L</i>	0.9991	0.7811	>0.9999

*Arrows indicate direction of change of motility parameter in strain 2 in comparison to strain 1.

4.3.7 A β variant expressing strains WG724 and WG666 show subtle differences in swimming compared to the A β 1-42 expressing strain WG643

Swimming parameters were also compared in young (day 4), middle-aged (day 8) and old (day 12) worms between the A β variant and A β 1-42 expressing strains, including the number of thrashes, mean swimming speed, wave initiation rate, activity, brush stroke, dynamic amplitude, mean waves, and self-contact curling distance (curling) (Figure 4.8 and Supplementary Figure 4.4). The A β 4-42 expressing strain WG709 shows an age-related decline in the number of thrashes ($p < 0.0001$), mean swimming speed ($p < 0.0001$), wave initiation rate ($p < 0.0001$), and activity ($p < 0.0001$) from day 4 to day 12. Surprisingly, when comparing the two strains WG663 (A β 1-42) and WG709 (A β 4-42), there were no statistically significant differences in any of the swimming parameters at all time points (Table 4.4).

The mouse A β -expressing strain WG724 showed significant age-related decline in the number of thrashes ($p < 0.0001$), mean swimming speed ($p < 0.0001$), wave initiation rate ($p < 0.0001$), activity ($p < 0.0001$), dynamic amplitude ($p = 0.0013$) and curling ($p < 0.0001$) from day 4 to day 12. When comparing the mouse A β strain WG724 and human A β strain WG643, there was a significant difference in number of thrashes ($p = 0.0037$) and mean swimming speed ($p = 0.024$) between the older worms on day 12. These parameters were higher in the mouse A β strain WG724 compared to the human A β strain WG643. Similarly, the wave initiation rate was higher in the mouse A β strain on day 8 ($p = 0.0006$) and day 12 ($p = 0.015$). However, none of the other swimming parameters showed significant differences between the two strains.

Lastly, the double transgenic strains WG666 and WG664 showed age-related decline in the number of thrashes, mean swimming speed, wave initiation rate, activity, dynamic amplitude, and mean waves from Day 4 to Day 12. On day 4, the double transgenic strain WG666 showed a significant decrease in number of thrashes ($p = 0.0003$), wave initiation rate ($p < 0.0001$), and activity ($p = 0.0037$) and an increased dynamic amplitude ($p < 0.0001$) compared to the single transgenic strain WG643, but none of these differences were significant on day 8 and day 12. Additionally, none of the swimming parameters showed significant differences between the double transgenic strain WG664 and the single transgenic strain WG663 (Table 4.4).

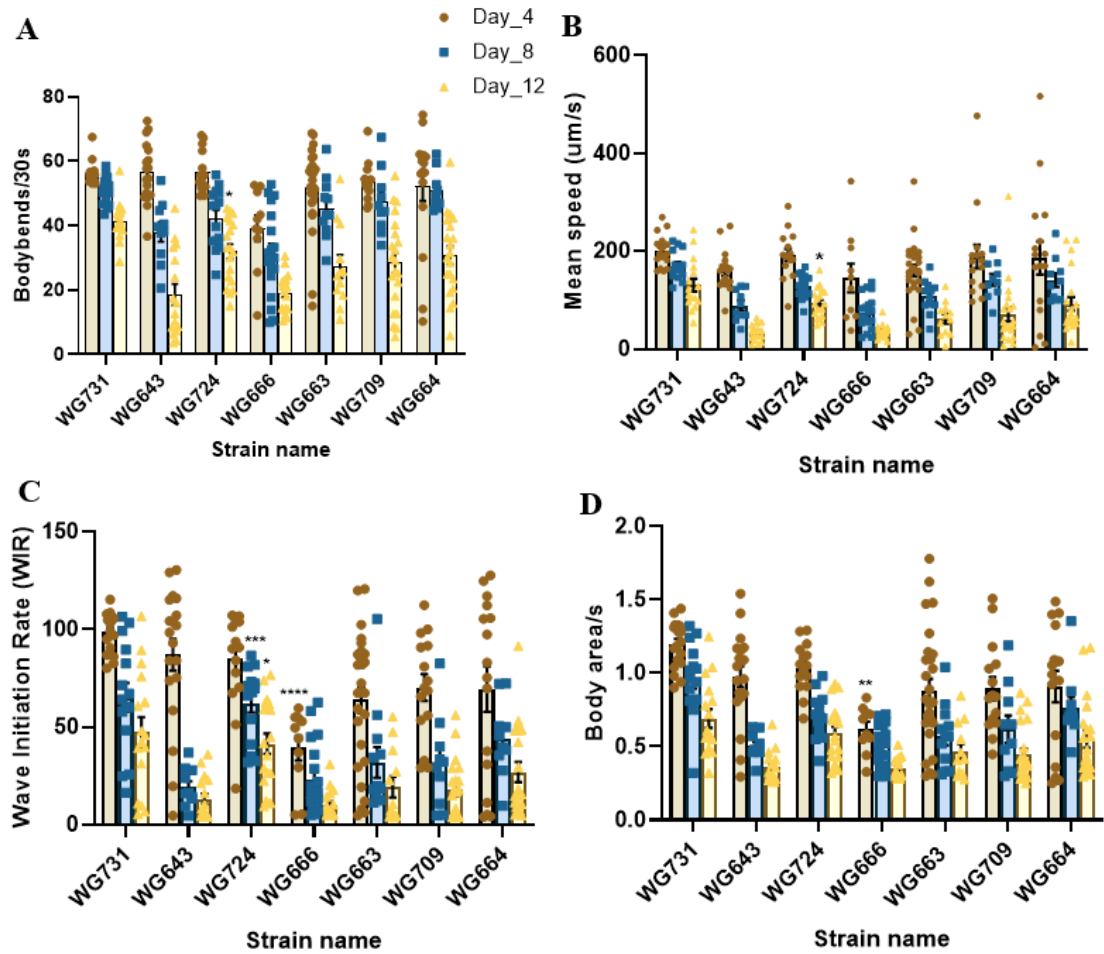


Figure 4.8: Age-related changes in motility of transgenic *C. elegans* strains in liquid media.

A) number of thrashes in liquid (Body bends/30s). B) Mean swimming speed ($\mu\text{m/s}$). C) Wave initiation rate. D) Activity in liquid (body area/s) ($\mu\text{m/s}$). All data analysed using two way ANOVA followed by post hoc Tukey multiple comparisons test, ns not significant, * $p < 0.05$, ** $p < 0.01$, *** $p < 0.001$ ($n=2, 5-15$ worms/replicate). The strains WG666 and WG724 were compared to the WG643 strain whereas the strains WG709 and WG664 were compared to the WG663 strain. **WG731** [*Pmyo-2::mCherry*], **WG643** [*Pmyo-2::mCherry + Psnb-1::huA β 1-42*], **WG663** [*Pmyo2::mCherry + Prgef-1::huA β 1-42*], **WG709** [*Pmyo-2::mCherry + Prgef-1::huA β 4-42*]; **WG724** [*Pmyo-2::mCherry + Psnb-1::mouseA β 1-42*], **WG664** [*Pmyo2::mCherry + Prgef-1::huA β 1-42; Pmyo2::GFP + Psnb-1::huA β 1-42G37L*], **WG666** [*Pmyo2::mCherry + Psnb-1::huA β 1-42; Pmyo2::GFP + Psnb-1::huA β 1-42G37L*].

Table 4.4: Comparison of swimming parameters between transgenic A β -expressing strains

Strain comparisons	Genotype	Day 4 (p value)	Day 8 (p value)	Day 12 (p value)
Number of thrashes				
WG663 vs WG709	<i>Prgef-1::huAβ1-42</i> vs <i>Prgef-1::huAβ4-42</i>	0.99	0.99	0.99
WG663 vs WG664	<i>Prgef-1::huAβ1-42</i> vs <i>Prgef-1::huAβ1-42; Psnb-1::huAβ1-42G37L</i>	>0.99	0.92	0.90
WG643 vs WG724	<i>Psnb-1::huAβ1-42</i> vs <i>Psnb-1::mouseAβ1-42</i>	>0.99	0.94	0.0037** \uparrow
WG643 vs WG666	<i>Psnb-1::huAβ1-42</i> vs <i>Psnb-1::huAβ1-42; Psnb-1::huAβ1-42G37L</i>	0.0003*** \downarrow	0.73	>0.99
Mean swimming speed				
WG663 vs WG709	<i>Prgef-1::huAβ1-42</i> vs <i>Prgef-1::huAβ4-42</i>	0.71	0.70	0.99
WG663 vs WG664	<i>Prgef-1::huAβ1-42</i> vs <i>Prgef-1::huAβ1-42; Psnb-1::huAβ1-42G37L</i>	0.82	0.95	0.56
WG643 vs WG724	<i>Psnb-1::huAβ1-42</i> vs <i>Psnb-1::mouseAβ1-42</i>	0.59	0.55	0.024* \uparrow
WG643 vs WG666	<i>Psnb-1::huAβ1-42</i> vs <i>Psnb-1::huAβ1-42; Psnb-1::huAβ1-42G37L</i>	0.99	0.99	>0.99
Wave initiation rate (WIR)				
WG663 vs WG709	<i>Prgef-1::huAβ1-42</i> vs <i>Prgef-1::huAβ4-42</i>	0.99	>0.99	>0.99
WG663 vs WG664	<i>Prgef-1::huAβ1-42</i> vs <i>Prgef-1::huAβ1-42; Psnb-1::huAβ1-42G37L</i>	0.99	0.92	0.98
WG643 vs WG724	<i>Psnb-1::huAβ1-42</i> vs <i>Psnb-1::mouseAβ1-42</i>	>0.99	0.0006*** \uparrow	0.016* \uparrow
WG643 vs WG666	<i>Psnb-1::huAβ1-42</i> vs <i>Psnb-1::huAβ1-42; Psnb-1::huAβ1-42G37L</i>	<0.0001**** \downarrow	0.99	0.99
Activity (body area/s)				
WG663 vs WG709	<i>Prgef-1::huAβ1-42</i> vs <i>Prgef-1::huAβ4-42</i>	>0.99	0.97	>0.99
WG663 vs WG664	<i>Prgef-1::huAβ1-42</i> vs <i>Prgef-1::huAβ1-42; Psnb-1::huAβ1-42G37L</i>	>0.99	0.51	0.81
WG643 vs WG724	<i>Psnb-1::huAβ1-42</i> vs <i>Psnb-1::mouseAβ1-42</i>	0.99	0.37	0.08
WG643 vs WG666	<i>Psnb-1::huAβ1-42</i> vs <i>Psnb-1::huAβ1-42; Psnb-1::huAβ1-42G37L</i>	0.0037** \downarrow	>0.99	>0.99
Dynamic Amplitude				
WG663 vs WG709	<i>Prgef-1::huAβ1-42</i> vs <i>Prgef-1::huAβ4-42</i>	>0.99	>0.99	0.94
WG663 vs WG664	<i>Prgef-1::huAβ1-42</i> vs <i>Prgef-1::huAβ1-42; Psnb-1::huAβ1-42G37L</i>	0.99	0.99	0.75
WG643 vs WG724	<i>Psnb-1::huAβ1-42</i> vs <i>Psnb-1::mouseAβ1-42</i>	0.076	0.73	0.14
WG643 vs WG666	<i>Psnb-1::huAβ1-42</i> vs <i>Psnb-1::huAβ1-42; Psnb-1::huAβ1-42G37L</i>	<0.0001**** \uparrow	0.75	0.99
Self-contact curling				
WG663 vs WG709	<i>Prgef-1::huAβ1-42</i> vs <i>Prgef-1::huAβ4-42</i>	0.94	>0.99	0.99

WG663 vs WG664	<i>Prgef-1::huAβ1-42</i> vs <i>Prgef-1::huAβ1-42; Psnb-1::huAβ1-42G37L</i>	0.63	>0.99	0.92
WG643 vs WG724	<i>Psnb-1::huAβ1-42</i> vs <i>Psnb-1::mouseAβ1-42</i>	0.99	0.08	0.19
WG643 vs WG666	<i>Psnb-1::huAβ1-42</i> vs <i>Psnb-1::huAβ1-42; Psnb-1::huAβ1-42G37L</i>	0.81	0.69	0.78
Brush stroke				
WG663 vs WG709	<i>Prgef-1::huAβ1-42</i> vs <i>Prgef-1::huAβ4-42</i>	>0.99	>0.99	>0.99
WG663 vs WG664	<i>Prgef-1::huAβ1-42</i> vs <i>Prgef-1::huAβ1-42; Psnb-1::huAβ1-42G37L</i>	0.99	0.99	0.99
WG643 vs WG724	<i>Psnb-1::huAβ1-42</i> vs <i>Psnb-1::mouseAβ1-42</i>	0.71	0.69	0.44
WG643 vs WG666	<i>Psnb-1::huAβ1-42</i> vs <i>Psnb-1::huAβ1-42; Psnb-1::huAβ1-42G37L</i>	>0.99	>0.99	>0.9999
Mean waves				
WG663 vs WG709	<i>Prgef-1::huAβ1-42</i> vs <i>Prgef-1::huAβ4-42</i>	0.99	0.82	0.99
WG663 vs WG664	<i>Prgef-1::huAβ1-42</i> vs <i>Prgef-1::huAβ1-42; Psnb-1::huAβ1-42G37L</i>	0.71	0.99	0.72
WG643 vs WG724	<i>Psnb-1::huAβ1-42</i> vs <i>Psnb-1::mouseAβ1-42</i>	0.23	0.76	0.97
WG643 vs WG666	<i>Psnb-1::huAβ1-42</i> vs <i>Psnb-1::huAβ1-42; Psnb-1::huAβ1-42G37L</i>	0.99	>0.99	0.99

*Arrows indicate direction of change of motility parameter in strain 2 in comparison to strain 1

4.3.8 A β variant expressing strains show distinct age-related changes in chemotactic ability towards volatile odorants

To compare differences in olfactory responses between A β variants and A β 1-42 expressing strains, chemotaxis assays were conducted using the volatile odorants diacetyl and benzaldehyde in young (day 4) and middle-aged (day 8) worms (Figure 4.9). The percentage mobility of all the transgenic strains on chemotaxis plates has been plotted in Supplementary Figure 4.5. Chemotaxis towards diacetyl and benzaldehyde is mediated by AWA and AWC chemosensory neurons respectively (Bargmann et al., 1993). On day 4, the A β 4-42 expressing strain WG709 showed a chemotaxis index of 0.86 ± 0.029 towards diacetyl compared to both the control strain WG731 (0.88 ± 0.023 , $p = 0.71$) and the A β 142 strain WG663 (0.66 ± 0.085 , $p = 0.04$). On day 8, the chemotaxis index (C.I) of the A β 4-42 expressing strain WG709 was 0.78 ± 0.015 when compared to the control strain WG731 (0.65 ± 0.06 , $p = 0.09$) and the A β 1-42 strain WG663 (0.37 ± 0.010 , $p = 0.0071$). In addition, the WG709 strain performed significantly better in its ability to sense diacetyl compared to the A β 1-42-expressing strain WG663 on both day 4 and day 8. Although there was an age-related decline in the CI of WG709 towards benzaldehyde from day 4 (0.86 ± 0.06) to day 8 (0.39 ± 0.11), it was not significantly different from the chemotaxis response of either the A β 1-42 expressing worm strain WG663 or the control strain WG731.

The chemotactic ability of the mouse A β -expressing strain WG724 towards diacetyl was not significantly different from the human A β -expressing strain WG643. However, there was an age-related decline in the chemotaxis index of WG724 from day 4 (0.71 ± 0.045) to day 8 (0.56 ± 0.064). In contrast, the mouse A β strain performed significantly better in its ability to sense benzaldehyde compared to the control transgenic strain WG731 on both day 4 (0.90 ± 0.028 , $p = 0.0065$) and day 8 (0.78 ± 0.02 , $p < 0.0001$). In addition, the mouse A β -expressing worms on day 8 show moderately better chemotaxis towards benzaldehyde when compared to the human A β -expressing strain WG643 (0.59 ± 0.06 , $p = 0.023$). Thus, the A β 4-42 expressing strain WG709 performed significantly better in its ability to sense diacetyl in comparison to the A β 1-42 expressing strain WG663. In addition, the mouse A β expressing strain WG724 also showed higher chemotaxis index towards both the volatile odorants when compared to the human A β expressing strain WG643 on Day 4 and Day 8.

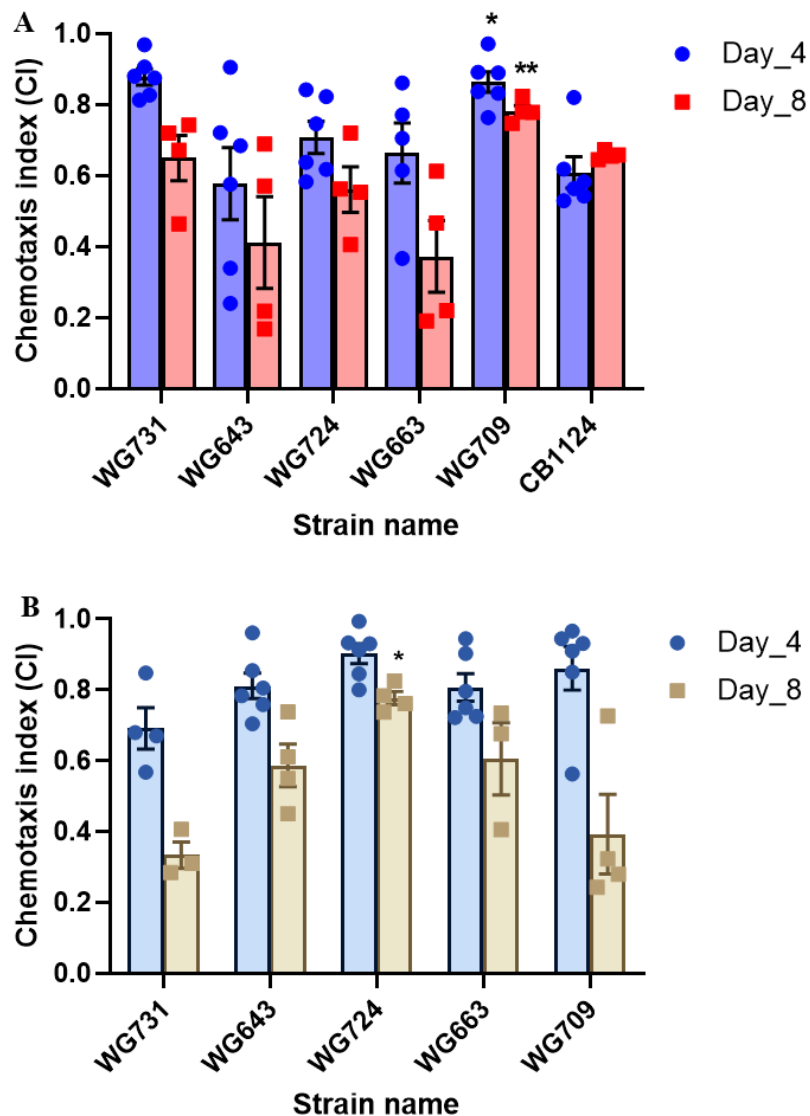


Figure 4.9: Chemotaxis of transgenic *C. elegans* strains towards A) Diacetyl B) Benzaldehyde.

An unpaired t test was used to compare between strains, ns not significant, * $p < 0.05$, ** $p < 0.01$, *** $p < 0.001$ ($n=4-6$, 100-200 worms/replicate). The strain WG724 was compared to the WG643 strain whereas the strain WG709 was compared to the WG663 strain.

WG731 [*Pmyo-2::mCherry*], **WG643** [*Pmyo-2::mCherry + Psnb-1::hu β 1-42*], **WG663** [*Pmyo-2::mCherry + Prgef-1::hu β 1-42*], **WG709** [*Pmyo-2::mCherry + Prgef-1::hu β 4-42*]; **WG724** [*Pmyo-2::mCherry + Psnb-1::mouse β 1-42*], **WG657** [*Pmyo-2::GFP + Psnb-1::hu β 1-42G37L*].

4.3.9 Double transgenic A β -expressing strains WG664 and WG666 show deficits in dopaminergic signalling starting at Day 4.

The basal and enhanced slowing response assays were performed to see if there were any deficits in dopaminergic or serotonergic signalling in the A β variant expressing strains. The slowing response of well-fed worms on seeded plates is mediated by dopaminergic signalling and is known as the basal slowing response. The slowing response of starved worms on seeded plates is enhanced due to the starvation and is mediated by serotonergic signalling (Sawin et al., 2000). The body bends/30 s of well-fed worms on seeded and unseeded plates on day 4, day 8 and day 12 have been listed in Table 4.5. The differences in body bends tested here are *within* strain differences. Although there is a strong age-related decline in body bends in all strains from Day 4 to Day 12, as in other phenotypes, it is difficult to interpret *between* strain differences in this assay. Based on an unpaired t-test, all the worm strains showed significant basal slowing response on day 4 except the double transgenic strains WG666 and WG664. The mutant strain CB1112 is used as a control for this experiment because it is deficient in dopaminergic signalling (as can be seen by the diminished slowing response). Although the transgenic control strain WG731 continues to show significant slowing response on day 8 ($p = 0.049$) and day 12 ($p = 0.038$), all of the A β -expressing strains do not show any slowing responses on day 8 and day 12 (Figure 4.10).

Similarly, the body bends/30s of the starved worms between unseeded and seeded plates was recorded in on day 4, day 8. and day 12. The data obtained has been plotted in Supplementary Figure 4.6. An unpaired t test was performed to check if the worms significantly slowed down on seeded plates. All the p-values have been listed in Table 4.6. On day 4, all the worms strains showed a significant enhanced slowing response. However, the control strains MT7988 and CB1141 do not slow down in the presence of food and are deficient in dopaminergic and serotonergic signalling (Loer and Kenyon, 1993; Sulston et al., 1975). This slowing response is completely diminished in older worms on day 8 and day 12 for all the strains assayed.

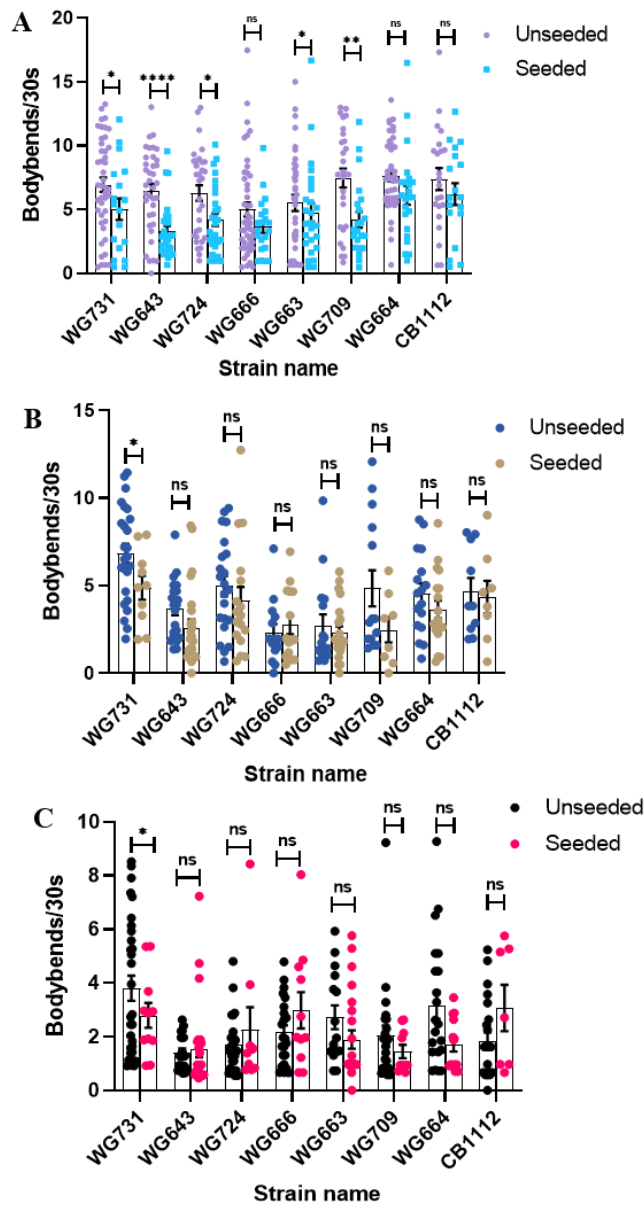


Figure 4.10: Transgenic *C. elegans* strains expressing A β peptides show diminished basal slowing response.

A) Day 4. B) Day 8. C) Day 12. An unpaired t test was used to test for significances in slowing responses, ns not significant, * $p < 0.05$, ** $p < 0.01$, *** $p < 0.001$ ($n=3, 5-15$ worms/replicate). The strains WG666 and WG724 were compared to the WG643 strain whereas the strains WG709 and WG664 were compared to the WG663 strain. **WG731** [*Pmyo-2::mCherry*], **WG643** [*Pmyo-2::mCherry + Psnb-1::huA β 1-42*], **WG663** [*Pmyo2::mCherry + Prgef-1::huA β 1-42*], **WG709** [*Pmyo-2::mCherry + Prgef-1::huA β 4-42*]; **WG724** [*Pmyo-2::mCherry + Psnb-1::mouseA β 1-42*], **WG657** [*Pmyo2::GFP + Psnb-1::huA β 1-42G37L*], **WG664** [*Pmyo2::mCherry + Prgef-1::huA β 1-42; Pmyo2::GFP + Psnb-1::huA β 1-42G37L*], **WG666** [*Pmyo2::mCherry + Psnb-1::huA β 1-42; Pmyo2::GFP + Psnb-1::huA β 1-42G37L*], **CB1112** [*cat-2 (e1112) II*].

Table 4.5: Summary of the basal slowing response assays

Strain name	Genotype	Body bends/30s on unseeded plates (mean ± SEM)	Body bends/30s on seeded plates (mean ± SEM)	p-value (unpaired t test)
Day 4				
WG731	<i>Pmyo-2::mCherry</i>	6.95 ± 0.56	4.26 ± 0.74	0.012 (*)
WG643	<i>Psnb-1::huAβ1-42</i>	6.67 ± 0.51	3.30 ± 0.42	<0.0001 (****)
WG724	<i>Psnb-1:mouseAβ1-42</i>	6.29 ± 0.6	4.2 ± 0.49	0.01(*)
WG666	<i>Psnb-1::huAβ1-42 + Psnb-1::huAβ1-42G37L</i>	5.00 ± 0.56	3.63 ± 0.47	0.30 (ns)
WG663	<i>Prgef-1::huAβ1-42</i>	5.52 ± 0.64	3.6 ± 0.45	0.04(*)
WG709	<i>Prgef-1:huAβ4-42</i>	7.46 ± 0.74	4.19 ± 0.62	0.002 (**)
WG664	<i>Prgef-1::huAβ1-42 + Psnb-1::huAβ1-42G37L</i>	7.63 ± 0.43	6.11 ± 0.74	0.06(ns)
CB1112	<i>cat-2(e1112)II</i>	7.39 ± 0.86	6.2 ± .85	0.34 (ns)
Day 8				
WG731	<i>Pmyo-2::mCherry</i>	6.84 ± 0.55	4.87 ± 0.67	0.049 (*)
WG643	<i>Psnb-1::huAβ1-42</i>	3.66 ± 0.36	2.83 ± 0.64	0.06 (ns)
WG724	<i>Psnb-1:mouseAβ1-42</i>	4.97 ± 0.58	4.14 ± 0.78	0.21 (ns)
WG666	<i>Psnb-1::huAβ1-42 + Psnb-1::huAβ1-42G37L</i>	2.32 ± 0.49	2.75 ± 0.52	0.61(ns)
WG663	<i>Prgef-1::huAβ1-42</i>	2.74 ± 0.62	2.33 ± 0.34	0.54 (ns)
WG709	<i>Prgef-1:huAβ4-42</i>	4.85 ± 1.03	2.48 ± 0.73	0.21 (ns)
WG664	<i>Prgef-1::huAβ1-42 + Psnb-1::huAβ1-42G37L</i>	4.56 ± 0.57	3.64 ± 0.5	0.24 (ns)
CB1112	<i>cat-2(e1112)II</i>	4.65 ± 0.79	4.34 ± 0.92	0.81 (ns)
Day 12				
WG731	<i>Pmyo-2::mCherry</i>	4.5 ± 0.49	2.79 ± 0.46	0.04 (*)
WG643	<i>Psnb-1::huAβ1-42</i>	1.42 ± 0.14	1.55 ± 0.32	0.18 (ns)
WG724	<i>Psnb-1:mouseAβ1-42</i>	1.69 ± 0.19	2.26 ± 0.83	0.95 (ns)
WG666	<i>Psnb-1::huAβ1-42 + Psnb-1::huAβ1-42G37L</i>	2.16 ± 0.26	2.98 ± 0.67	0.35 (ns)
WG663	<i>Prgef-1::huAβ1-42</i>	2.72 ± 0.44	1.90 ± 0.34	0.14 (ns)
WG709	<i>Prgef-1:huAβ4-42</i>	2.04 ± 0.38	1.44 ± 0.25	0.52 (ns)
WG664	<i>Prgef-1::huAβ1-42 + Psnb-1::huAβ1-42G37L</i>	3.18 ± 0.51	1.70 ± 0.25	0.09 (ns)
CB1112	<i>cat-2(e1112)II</i>	1.85 ± 0.32	3.07 ± 0.86	0.12 (ns)

Table 4.6: Summary of the enhanced slowing response assays

Strain name	Genotype	Body bends/30s on unseeded plates (mean ± SEM)	Body bends/30s on seeded plates (mean ± SEM)	p-value (unpaired t test)
Day 4				
WG731	<i>Pmyo-2::mCherry</i>	7.36 ± 0.76	4.16 ± 0.65	0.005 (**)
WG643	<i>Psnb-1::huAβ1-42</i>	4.65 ± 0.67	2.75 ± 0.75	0.0004 (***)
WG724	<i>Psnb-1::mouseAβ1-42</i>	4.79 ± 0.41	1.92 ± 0.33	<0.0001 (****)
WG666	<i>Psnb-1::huAβ1-42 + Psnb-1::huAβ1-42G37L</i>	7.08 ± 0.75	2.63 ± 0.48	<0.0001 (****)
WG663	<i>Prgef-1::huAβ1-42</i>	6.91 ± 0.69	2.75 ± 0.75	<0.0001 (****)
WG709	<i>Prgef-1::huAβ4-42</i>	5.69 ± 0.711	2.64 ± 0.53	0.0013 (**)
WG664	<i>Prgef-1::huAβ1-42 + Psnb-1::huAβ1-42G37L</i>	7.18 ± 0.97	2.18 ± 0.48	<0.0001 (****)
MT7988	<i>bas-1 (ad446) III</i>	6.19 ± 0.82	5.51 ± 0.65	0.52 (ns)
CB1141	<i>cat-4 (e1141) V</i>	4.70 ± 0.52	6.55 ± 0.56	0.025 (*)
Day 8				
WG731	<i>Pmyo-2::mCherry</i>	4.70 ± 0.66	3.90 ± 0.70	0.32 (ns)
WG643	<i>Psnb-1::huAβ1-42</i>	2.65 ± 0.36	3.14 ± 0.77	0.54 (ns)
WG724	<i>Psnb-1::mouseAβ1-42</i>	3.02 ± 0.55	3.42 ± 0.613	0.46 (ns)
WG666	<i>Psnb-1::huAβ1-42 + Psnb-1::huAβ1-42G37L</i>	2.91 ± 0.51	2.52 ± 0.55	0.65 (ns)
WG663	<i>Prgef-1::huAβ1-42</i>	2.95 ± 0.68	2.74 ± 0.59	0.82 (ns)
WG709	<i>Prgef-1::huAβ4-42</i>	2.54 ± 0.64	3.72 ± 0.94	0.73 (ns)
WG664	<i>Prgef-1::huAβ1-42 + Psnb-1::huAβ1-42G37L</i>	3.90 ± 0.71	4.02 ± 1.20	0.52 (ns)
MT7988	<i>bas-1 (ad446) III</i>	3.50 ± 0.54	3.4 ± 1.46	0.98 (ns)
MT8943	<i>bas-1(ad446) III; cat-4 (e1141) V</i>	2.42 ± 0.46	1.44 ± 0.28	0.09 (ns)
CB1141	<i>cat-4 (e1141) V</i>	1.87 ± 0.37	1.82 ± 0.48	0.96 (ns)
Day 12				
WG731	<i>Pmyo-2::mCherry</i>	1.93 ± 0.26	1.93 ± 0.44	0.99 (ns)
WG643	<i>Psnb-1::huAβ1-42</i>	1.1 ± 0.17	1.3 ± 0.18	0.77 (ns)
WG724	<i>Psnb-1::mouseAβ1-42</i>	2.39 ± 0.36	2.24 ± 0.38	0.33 (ns)
WG666	<i>Psnb-1::huAβ1-42 + Psnb-1::huAβ1-42G37L</i>	2.06 ± 0.43	2.39 ± 0.46	0.71 (ns)
WG663	<i>Prgef-1::huAβ1-42</i>	1.78 ± 0.45	1.66 ± 0.45	0.91 (ns)
WG709	<i>Prgef-1::huAβ4-42</i>	2.37 ± 0.34	1.6 ± 0.30	0.047 (ns)
WG664	<i>Prgef-1::huAβ1-42 + Psnb-1::huAβ1-42G37L</i>	2.26 ± 0.35	2.29 ± 0.38	0.68 (ns)
MT7988	<i>bas-1 (ad446) III</i>	2.63 ± 0.99	4.2 ± 1.81	0.45 (ns)
CB1141	<i>cat-4 (e1141) V</i>	3.96 ± 1.04	2.88 ± 1.10	0.49 (ns)

4.4 Discussion

In the previous chapter, transgenic *C. elegans* strains expressing different concentrations of full-length A β 1-42 peptides in the neurons were described. In this chapter, the aim was to examine the *in vivo* toxic effects of different A β variants by expressing these transgenes in the *C. elegans* neurons and comparing the phenotypes of the A β variant expressing strains with the transgenic strains expressing the full length A β 1-42. Although several studies have suggested that A β oligomers are the toxic species, a general agreement on the structure and composition of these oligomers is lacking (Fonte et al., 2011). Some studies have suggested that these oligomeric species are composed of N- and C- truncated species (Sergeant et al., 2003). Moreover, despite the abundance of the N- and C-truncated A β peptides in human AD brain, their relative importance in the pathogenesis of AD has not been well studied. The transgenic *C. elegans* strains described here express three different A β versions in the neurons and show specific behavioural deficits when compared to the strains expressing the full length A β 1-42.

4.4.1 *C. elegans* expressing A β 4-42 show deficits in egg-laying behaviour but improved movement and chemotaxis relative to A β 1-42

The N-terminal truncated A β species, beginning with phenylalanine at position 4, was discovered over 30 years ago and has been proposed to have higher amyloidogenic property and thereby higher propensity to aggregate than full-length species (Cabrera et al., 2018). This may be due to increased hydrophobicity as a result of removal of the first few N- terminal residues, thereby altering its cytotoxic properties and its interaction with other A β peptides. In addition, *in vitro* studies in primary neurons have suggested that A β 4-42 peptide is as toxic as the full length A β 1-42 (Bouter et al., 2013). Since there are currently no *C. elegans* models of A β 4-42 expression, a new transgenic *C. elegans* strain was constructed specifically expressing this transgene in the *C. elegans* neurons. I hypothesised that the expression of this transgene may be as toxic, if not more, as the full length A β 1-42 peptide. Initially, it was difficult to obtain transgenic strains using a strong pan-neuronal promoter, *snb-1*, which suggests that high levels of A β 4-42 expression in the neurons may be toxic and select against transgenic worms expressing high levels of this toxic peptide. In support of this hypothesis, transgenic strains expressing this peptide were obtained using the alternative pan neuronal promoter *rgef-1*, which is characterised

as a weaker promoter than *snb-1* (Grun et al., 2014), and thus expresses less of the toxic transgene. Scoring dead eggs or early larval death may be informative to confirm this hypothesis in future work. If embryonic death occurs around neuronal development and differentiation, then it may be due to the A β 4-42 transgene expression.

The only behaviour that was severely affected in the human A β 4-42 expressing strain was reduced brood size relative to the human A β 1-42 strain (Figure 4.6B). Egg-laying behaviour in *C. elegans* is mediated by the hermaphrodite-specific neurons (HSNs) that synapse on the vulval muscles promoting muscle contraction by serotonin signalling (Kaletta and Hengartner, 2006; Tanis et al., 2008). Either the expression of the A β 4-42 transgene exerts its neurotoxic effects by causing neuronal loss in specific subset of neurons, or it is a general indicator of poor health in the transgenic strain. The rate of egg-production was also significantly reduced in this strain which may explain the reduced brood size (Figure 4.6D). This implies that the egg-production (or even perhaps sperm production) has a neuronal regulatory circuit of some description. This may also explain why the phenotype is more pronounced later in the reproductive period.

In the *C. elegans* strains studied here, although we expected to observe greater behavioural deficits in the A β 4-42 strain, there was no difference in the lifespan, swimming parameters, or chemotaxis towards benzaldehyde between the A β 4-42 and A β 1-42-expressing strains (Figure 4.4, Figure 4.8, and Figure 4.9B). Surprisingly, the A β 4-42 expressing animals showed significantly higher motility on solid media on Day 4 in terms of body bends and mean speed (Figure 4.7A,B). In addition, the ability of these worms to sense diacetyl is significantly better than the human A β 1-42-expressing worms (Figure 4.9A). These results show that some behavioural deficits appear earlier in the full length A β 1-42-expressing strains. In contrast, the literature suggests that A β 4-42 is involved in the initial seeding step prior to *in vivo* aggregation (Cabrera et al., 2018). In fact, mice overexpressing A β 4-42 develop age-dependent memory impairments as a result of specific hippocampal neuronal loss in a gene dose-dependent manner. Moreover, young A β 4-42-expressing mice show altered excitatory synaptic transmission which precedes neuronal loss and behavioural deficits (Bouter et al., 2013; Dietrich et al., 2018; Huttenrauch et al., 2016). There are a few possible reasons to explain these contradicting results. Firstly, the concentration of A β 4-42 in this transgenic strain is considerably lower compared to the full length A β 1-42-expressing strain. This could mean that the amount of transgene expression in young worms is not enough to result in a behavioural deficit.

Secondly, it is possible that although the A β 4-42 may act as an initial stimulus for aggregation, the interaction with the full length A β 1-42 to form heterogenous oligomers is important to cause neurotoxic damage. Therefore, this transgene is either acting in a concentration dependent manner or only involved in the initial stages and is therefore toxic only in a few neuronal subsets. If the A β 4-42 toxicity is dependent on interaction with other forms of A β , such as A β 1-42, then heterozygous worms strains expressing both the transgenes may show a severe behavioural deficit as compared to the single transgenic strains. Perhaps the A β 4-42 peptide is processed differently, which complicates our understanding of what happens downstream of the generation of these peptides. Since these peptides have different physiochemical properties, these differences result in the qualitative differences in the phenotypes are that generated by these peptides.

4.4.2 Mouse A β -expressing strain does not show noteworthy behavioural deficits

The mouse A β 1-42 was anticipated to be less toxic than the human A β 1-42 due to its reduced metal binding activity and hydrogen peroxide production (Huang et al., 1999). Although the concentrations of the plasmid used for microinjections was the same as the other transgenic strains generated in the study (25 $\mu\text{g}/\mu\text{l}$), the copy number of the mouse A β transgene in the integrated strain was very low. As a result, the expression levels of mouse A β were also lower in this transgenic strain compared to the human A β 1-42 expressing strain, and this difference, rather than molecular characteristics, may be what drives its significantly higher lifespan and lack of deficits in chemotaxis and egg-laying behaviour (Figure 4.4, Figure 4.6, and Figure 4.9).

Despite the difference observed in lifespan and in expression level (Figure 4.3 and Figure 4.4), there were no clearly defined behavioural differences between the human and mouse strains. There was an age-related decline in movement in liquid media in the mouse A β -expressing strain, but the worms performed significantly better than the human A β 1-42 expressing even at day 12 (Figure 4.8). However, the difference in the movement between the two strains on solid media was statistically insignificant (Figure 4.7). This is because swimming in *C. elegans* is known to be distinct from crawling in kinematics and underlying neuromuscular activity (Pierce-Shimomura et al., 2008).

The severity of the disease phenotype increases with age in human A β -expressing strain but not in mouse A β . This observation could either be because the concentration of this

transgene does not reach a critical concentration to cause disease even in old worms, or it could also indicate that the mouse A β has different physicochemical properties and therefore less toxic than the human A β . To distinguish between these hypotheses, strains with comparable A β expression levels will be needed. This would allow to establish the relationship between concentration/expression of any A β and neuronal defects.

4.4.3 Simultaneous expression of A β 1-42 and A β 1-42G37L in *C. elegans* neurons does not causes reduction in *in vivo* A β toxicity

Synthetic A β preparations form pores in synthetic membranes, which leads to the hypothesis that the *in vivo* toxicity of A β causes or is the result of membrane damage (Kim et al., 2005). The C-terminal motif Gly-XXX-Gly-XXX-Gly-motif in A β (residues 24-39) is a glycine zipper important for A β oligomerization and toxicity, since this motif drives the packing of transmembrane α - helices and the formation of membrane pores in *C. elegans* (Fonte et al., 2011). Hung et. al showed that mutations in this glycine zipper motif results in reduced toxicity in primary mouse cortical neurons, with mutations G37L and G33L having the greatest beneficial effect (Hung et al., 2008).

To test this hypothesis, I generated a transgenic *C. elegans* strain expressing the A β G37L transgene. This strain showed a very high copy number compared to the other integrated A β -expressing strains (Figure 4.3A). In addition, there was high variation in the copy number of this transgene within the strain, despite its being integrated in the genome. Following microinjection, a process of non-homologous end joining occurs resulting in the transgene plasmids, marker DNA, and genomic DNA forming complex extrachromosomal arrays, consisting of variable numbers of 50-300 copies of the transgene which are genetically instable (Nance and Frokjaer-Jensen, 2019; Stinchcomb et al., 1985). In my study, these multicopy extrachromosomal arrays containing the A β G37L transgene were integrated in the strain, but expression was still highly variable between RNA extractions for unknown reasons. Surprisingly, the A β expression in these transgenic strains was lower than the human A β 1-42-expressing strains despite its higher copy number (Figure 4.3B). A possible explanation could be that these repetitive arrays may have undergone germline silencing which resulted in reduced expression (Kelly et al., 1997). Alternatively, the A β G37L transgene may not be toxic for the worms compared to other transgenes used in this experiment, and therefore individuals with high

copies of this transgene survived. The variation in A β expression in the double transgenic strains may be result of variation in the extent of transgene silencing between individual animals. However, it is difficult to draw definitive conclusions unless the expression of the two transgenes can be measured independently.

It has been previously shown that expression of A β G37L in the *C. elegans* body wall muscle displays reduced paralysis rates when compared with strains expressing A β 1-42 only. However, the expression of A β G37L is not non-toxic as does show a delayed paralysis phenotype (Fonte et al., 2011). To test how possible molecular interactions between A β 1-42 and A β G37L in the neurons might impact healthspan, lifespan, and behaviour, I generated a double transgenic strain expressing full length A β 1-42 and A β 1-42G37L using the *snb-1* promoter. This strain was slow growing and had shorter lifespan than the human A β 1-42 expressing strain (Figure 4.4 and Figure 4.5). Furthermore, the strain showed deficits in egg-laying behaviour as evident by reduced brood size, lower rate of egg production and reduced number of eggs retained *in utero* (Figure 4.6). The double transgenic strain also showed defects in swimming parameters such as wave initiation rate and reduced activity of the worms (Figure 4.8). In addition, the onset of motility defect in this double transgenic strain was seen prior to the single transgenic strain expressing the A β 1-42 transgene on day 4. Similarly, the double transgenic strain on day 4 showed diminished slowing response as a result of deficits of dopaminergic signalling (Figure 4.10). Thus, the simultaneous expression of the A β G37L and A β 1-42 transgene in the *C. elegans* nervous system does not result in reduction of A β toxicity *in vivo*. Although this G37L substitution does not interfere with A β driven aggregation, in a single mutant strain expressing G37L in muscle tissues, detectable amyloid formation was prevented (Fonte et al., 2011). The difference observed here with this previous research may be because neurons are more susceptible to damage as a result of *in vivo* A β aggregation. Previous studies have shown that accumulation of misfolded proteins in *C. elegans* muscle can lead to disruption of cellular protein handling (proteostasis) and expression of an aggregation-prone polyglutamine protein in *C. elegans* causes a locomotion defect (Gidalevitz et al., 2006; Gidalevitz et al., 2009; Morley et al., 2002). Additionally, the neuronal *C. elegans* strain described here is expressing both the full length A β 1-42 and A β G37L transgene rather than only the A β G37L transgene. Moreover, it has been previously reported that A β G37L readily formed oligomers *in vitro*, and

formed higher molecular weight species than the full length A β 1-42 (Harmer et al., 2009; Hung et al., 2008)

The *snb-1* promoter is a strong promoter and drives the expression of both the transgenes A β 1-42 and A β G37L in the WG666 strain; therefore, it was difficult to interpret whether the differences in the phenotypes were due to the enhanced expression or molecular interactions between transgenes. Hence, I tested a second transgenic strain WG664 that expressed the human A β 1-42 transgene using the *rgef-1* promoter and the A β 1-42G37L transgene using the *snb-1* promoter. The *snb-1* promoter, with high intrinsic activity, is known to be active in the early stages of embryonic development, while the *rgef-1* promoter has comparably lower levels of activity beginning at later stages of embryonic development (Grun et al., 2014). Unlike the double transgenic strain described above, this strain WG664 showed no difference in lifespan compared to the single A β 1-42 transgenic strain (Figure 4.4). However, this second strain shows significant reduction in brood size and rate of egg-production and diminished basal slowing response compared to the transgenic full length A β 1-42 expressing strains in young adults on day 4 (Figure 4.6B and Figure 4.10). Reduced basal slowing response may be attributed to deficits in dopaminergic signalling (Sawin et al., 2000). The results from these double transgenic strains do not support the non-toxicity of the A β G37L mutation *in vivo*. Surprisingly, the worms showed significantly higher motility on solid media in terms of mean speed and body bends in young and middle-aged worms compared to A β 1-42 (Figure 4.7A,B)

The only difference between the two double transgenic strains is the promoter used to drive A β 1-42 expression. Because of the differences in promoters, expression of A β G37L driven by *snb-1* begins before the expression of A β 1-42 driven by *rgef-1* in the second double transgenic strain WG664. Therefore, this difference in phenotype between the two double transgenic strains may be driven by the timing and level of A β 1-42 expression thereby resulting in differences in the amyloid seeding step (Harper and Lansbury, 1997). The relative expression levels/concentration of the two transgenes in double transgenic strains is clearly important when examining how the interactions of these species impact *in vivo* toxicity of the A β G37L transgene in *C. elegans* neurons. Additional transgenic *C. elegans* strains with lower copy number and variation in the A β G37L transgene would be particularly useful. If the stoichiometry of the peptide does matter, then in principle it may be possible to manipulate the ratio and concentrations of the different A β species (combination of pan-neuronal promoter and A β transgene copy number) *in vivo* in the

worm in a more controlled fashion. Phenotypic differences between the two double transgenic strains with respect to lifespan and fertility may be because different phenotypes may have different thresholds for triggering declines.

4.5 Conclusion

Research on AD has been hampered by a lack of clarity in how variation in species of A β affect disease progression. To address this need, I generated and characterised transgenic *C. elegans* strains expressing different versions of A β transgenes. The strain expressing the amino-truncated A β 4-42 variant was shown to be as toxic as the full length human A β 1-42, consistent with the previously published literature. These amino-truncated A β may be a novel biomarker to monitor the onset and progression of AD and to study the underlying mechanisms of disease-modifying drugs (Ghidoni et al., 2011). In addition, this strain shows a severe egg-laying defect which may be an outcome of poor health *per se*. The mouse A β -expressing transgenic strain did not show any noteworthy behavioural deficit which may be a result of low expression levels of the A β transgene. Lastly, double transgenic strains expressing the A β G37L and the A β 1-42 transgene using different pan-neuronal promoters to drive A β 1-42 expression showed differences in behavioural deficits. These strains can be used to study the molecular mechanisms underlying *in vivo* A β toxicity.

Chapter Five

Phenotypic consequences of amyloid β expression in a *ptl-1* null genetic background

5.1 Introduction

Alzheimer's disease is characterized by two important pathological brain lesions, the extracellular senile plaques (described in detail previously) and intracellular neurofibrillary tangles (NFTs) (Ikezu, 2008). NFTs are composed of aggregates of hyperphosphorylated protein tau occurring mainly as paired helical filaments, but may also be present as straight filaments, twisted ribbons or other conformations (Ballatore et al., 2007; Buee et al., 2000; Kidd, 1963). These tau aggregates have been implicated in several age-related neurodegenerative conditions called tauopathies (Ballatore et al., 2007; Buee et al., 2000). Moreover, these NFT aggregates are also known to significantly correlate with the severity of AD (Zhao et al., 2014).

In humans, there are six major isoforms of tau protein expressed abundantly throughout the central and peripheral nervous system that are derived from the alternative splicing of a single gene, the microtubule associated protein (*MAPT*) gene (Zhao et al., 2014). These six putative isoforms differ in the number of microtubule (MT) binding repeats consisting of either three or four of these regions, with each isoform having precise and distinct physiological roles (Ballatore et al., 2007). The carboxy terminal of the tau protein consists of a microtubule (MT) binding domain composed of repeats of a highly conserved tubulin binding motif, whereas the amino terminal consists of a basic proline rich domain known as the projection domain (Ballatore et al., 2007; Binder et al., 1985). Any mutations in the *MAPT* gene resulting in changes in the alteration of the number of repeats results in several tauopathies including AD (Gotz et al., 2013; Iqbal et al., 2010; Ittner and Gotz, 2011; Lee and Leugers, 2012; Wade-Martins, 2012). In addition to *MAPT*, there are other tau-like genes in the microtubule associated proteins (MAPs)/tau family, which includes *MAP2* and *MAP4*. *MAP2* and tau are expressed in the neurons exclusively whereas the *MAP4* are expressed in other cell types (Gordon et al., 2008; Heidary and Fortini, 2001; Rolls et al., 2007).

The main role of physiological tau is to promote the stabilization of axonal microtubules in the central nervous system and function as an enzyme anchor, helping in neurite outgrowth and in the transport of axoplasm (Avila et al., 2004). Tau modulates the microtubule network and is thereby important in maintaining the appropriate morphology of neurons as it is in a constant dynamic equilibrium associating and disassociating from the microtubules (Ballatore et al., 2007; Roy et al., 2005). This equilibrium is possibly controlled by the phosphorylation state of tau, determined by kinases and phosphatases (Ballatore et al., 2007; Churcher, 2006; Mazanetz and Fischer, 2007). Furthermore, it may also have other functions resulting from its interaction with other structures and enzymes such as the plasma membrane, the actin cytoskeleton, the src tyrosine kinases such as FYN, RNA and presenilin (Brandt et al., 1995; Buee et al., 2000; Fulga et al., 2007; Kampers et al., 1999; Lee, 2005; Maas et al., 2000). These findings indicate that tau function entails a range of poorly defined interactions and functions, making it difficult to understand the mechanism by which aggregated tau plays a role in neurodegeneration (Ballatore et al., 2007). Moreover, it is possible that tau aggregation results in a range of phenotypes occurring at various stages of disease onset and progression (Ballatore et al., 2007).

In the disease state, there is disruption of the equilibrium of tau protein binding to the microtubule network that results in increased levels of free tau. Furthermore, the increased rate and state of tau phosphorylation results in disengagement of tau from the microtubules and, thereby, aggregation (Kuret et al., 2005). In addition, tau protein undergoes modifications, such as abnormal phosphorylation, in addition to some other modifications such as nitration, ubiquitination, or truncation, thereby resulting in reduced affinity of tau to bind to microtubules and binding to other macromolecules. Collectively, this leads to aggregation of tau protein, which in turn leads to the disruption of normal structure and regulatory functions of the cytoskeleton that likely causes disturbances in axonal transport, thereby resulting in synaptic dysfunction and neurodegeneration (Arriagada et al., 1992a; Avila et al., 2004; Chen et al., 2004; Flaherty et al., 2000; Zhao et al., 2014).

There could be two possible ways in which tau aggregation results in neurodegeneration. Firstly, it could potentially be a toxic gain of function acquired by the aggregates and/or their precursors. Secondly, there could be harmful effects that arise from the loss of normal tau function resulting in a diseased state (Ballatore et al., 2007). Furthermore, a

hypothesis was established to explain the pathological role of tau-mediated neurodegeneration suggesting that reduction of tau may be beneficial (Rapoport et al., 2002; Roberson et al., 2007). However, it is difficult to understand the relative contribution of the toxic gain of function conferred by tau aggregates as compared to the potential loss of physiological tau function resulting from tau concentration being depleted and sequestered by the tau aggregates (Ballatore et al., 2007). For instance, tau is not only toxic if its levels are elevated but also results in a disease state as a result of loss of normal physiological function (Ballatore et al., 2007). Intraneuronal A β accumulation appears to trigger the cleavage of tau, and A β can interfere with tau inducing conformational changes, thereby resulting in neurodegeneration (Gouras et al., 2000; Rissman et al., 2004).

Several transgenic *C. elegans* strains have been constructed as models of tauopathy and show behavioural deficits due to neuronal dysfunction (Fatouros et al., 2012; Kraemer et al., 2003). In addition, these biochemical changes resulting in neurodegeneration can be easily followed as the worms age, thereby obtaining temporal information on the pathogenesis events (Kraemer et al., 2003). Furthermore, transgenic *C. elegans* strains expressing both A β and tau protein have been generated to study the behavioural defects associated with the toxic gain of function (Wang et al., 2018). Currently, there is no study that reports any behavioural change associated with the loss of function of physiological tau in a *C. elegans* AD model.

MAP with tau-like repeats, PTL-1, is a protein in the structural tau/MAP2 family and is the sole tau ortholog found in *C. elegans* (Goedert et al., 1996; Gordon et al., 2008). The *ptl-1* gene is composed of eight coding exons, with exons 5-7 coding for the microtubule binding domain (Chew et al., 2013). There are two isoforms derived from alternative splicing of *ptl-1* expressed in embryonic epidermal neurons from early larval to adult stages. PTL-1 binds and promotes microtubule assembly *in vitro*, like the human tau, and is thought to perform equivalent functions of MAP2 and tau (Goedert et al., 1996). Although there is a high degree of similarity between the C-terminal of the invertebrate *ptl-1* gene and the vertebrate tau sequence, the N-terminal shows considerable divergence between the vertebrate and invertebrate sequences (Gordon et al., 2008). A transcriptional reporter line for *ptl-1* showed that PTL-1 is predominantly expressed in the adult mechanosensory neurons, but is also expressed in the head neurons, cells along the ventral nerve cord, cells near the vulva, and the stomato-intestinal muscle (Gordon et al.,

2008). Although a *ptl-1* knockout worm grows and develops normally, it shows several deficits in egg hatching and reduced sensitivity to touch stimuli (Gordon et al., 2008). In addition, these worms show neuronal blebbing, which is an age-related increase in the presence of abnormal structures, and display a reduction in longevity (Chew et al., 2013). Despite of these deficits, tau is not essential for the viability of the worms (Gordon et al., 2008).

In this chapter, a new strain expressing the A β 1-42 peptide in a *ptl-1* null genetic background was generated in order to better understand the effects of A β expression in the absence of normal physiological tau. I hypothesised that the type and/or the severity of behavioural deficit in this new strain would be greater than the strain that expresses A β 1-42 in the wild type genetic background. Therefore, the aims of this chapter are as follows:

1. To characterise the expression of A β in the absence of tau. To do this, a new strain was developed expressing the A β transgene in *ptl-1* null background.
2. To determine the phenotypic impact of A β expression in the absence of tau, by comparing behavioural phenotypes between the strain expressing A β in the absence of *ptl-1* and the strain expressing A β peptide in a wild type background.

This strain would give an insight into the mechanisms underlying tau and A β mediated neurotoxicity.

5.2 Methods

All materials and methods used in this chapter are described in Section 2.2 with a few exceptions (described below).

5.2.1 Competitive PCR strategy

In order to determine whether a worm was heterozygous or homozygous for the *ptl-1* null mutation, three primers were used for the competitive PCR, with two primers flanking the regions deleted and one within the deleted the region. Worms that are homozygous for the mutation generate a PCR product of approximately 464 bp, wild type worms yield a product of 735 bp, and heterozygotic worms generate both PCR products. The details of primers used in the study have been listed in Supplementary Table 2.

5.2.2 Strains used in this chapter

The strains described in this chapter are as follows: the transgenic control strain **WG731**, [*Pmyo-2::mCherry*], the A β -expressing strain **WG643**, [*Pmyo-2::mCherry + Psnb-1::huA β 1-42*], the strain expressing A β in *ptl-1* null background **WG673** [*Pmyo-2::mCherry + Psnb-1::huA β 1-42; ptl-1*], the *ptl-1* null strain **APD004** [*ptl-1*].

5.2.3 Statistical analysis

All data have been reported as mean \pm SEM values. Shapiro-Wilk test was used to test normality and if the data were not normally distributed, then appropriate non-parametric tests were used to determine significant differences. A two-way ANOVA using age and genotype as variables for all motility assays and one -way ANOVA was used for all other assays unless otherwise mentioned.

5.3 Results

5.3.1 Generation of a transgenic *C. elegans* strain WG673 expressing pan-neuronal A β in a *ptl-1* null background

The *ptl-1* mutation (*ok621*) is a 1933 bp deletion spanning a region from the end of exon 2 through to exon 8. The *ok621* mutation was generated by the OMRF arm of the *C. elegans* Knockout Consortium (WormBase ID: WBVar00091905) (Chew et al., 2013). The *ptl-1* null strain APD004 was a kind gift from Dr Hannah Nicholas at the University of Sydney. This strain has been derived by outcrossing the mutant strain RB809 [*ptl-1(ok621)*] to the wild type strain six times. The A β 1-42-expressing worm strain WG643 was crossed with *ptl-1* null strain APD004 to obtain the new strain WG673. The heterozygous F1 progeny from this cross were screened for the presence of the transgenic pharyngeal *mCherry* marker. Worms containing only one copy of the *mCherry* transgene will show a dull fluorescence compared to their homozygous counterparts. The F1 progeny showing dull fluorescence were picked individually and allowed to reproduce. All the resulting homozygous F2 progeny that showed a bright *mCherry* expression were screened by competitive PCR for the presence of the *ptl-1* null mutation. The heterozygous and homozygous worms showing the *ptl-1* mutation were picked individually. A few F3s were then screened from each plate to test for worms that were homozygous for the *ptl-1* null mutation. The resulting new strain WG673 is homozygous for the *ptl-1(ok621)* and for the transgenic *mCherry* marker. A schematic illustration of the competitive PCR and the expected PCR products on the gel have been shown in Supplementary Figure 5.1.

To estimate the expression levels of A β in this new transgenic strain WG673 expressing neuronal A β in a *ptl-1* null background, an RT-qPCR was performed. As can be seen in Figure 5.1, although there is clear A β expression in the new strain WG673, there was a moderate but significant decrease in the A β expression levels in the new strain compared to the A β -expressing strain WG643 ($p = 0.0054$; unpaired t test). In addition, the *ptl-1* null mutant strain APD004 did not show any expression of A β as expected. To allow easier explanation of the results, the new strain WG673 expressing A β in the *ptl-1* null background will be referred to as the A β ;*ptl-1* strain, the transgenic strain WG643 expressing A β in the wild type background will be referred to as the wild type A β strain,

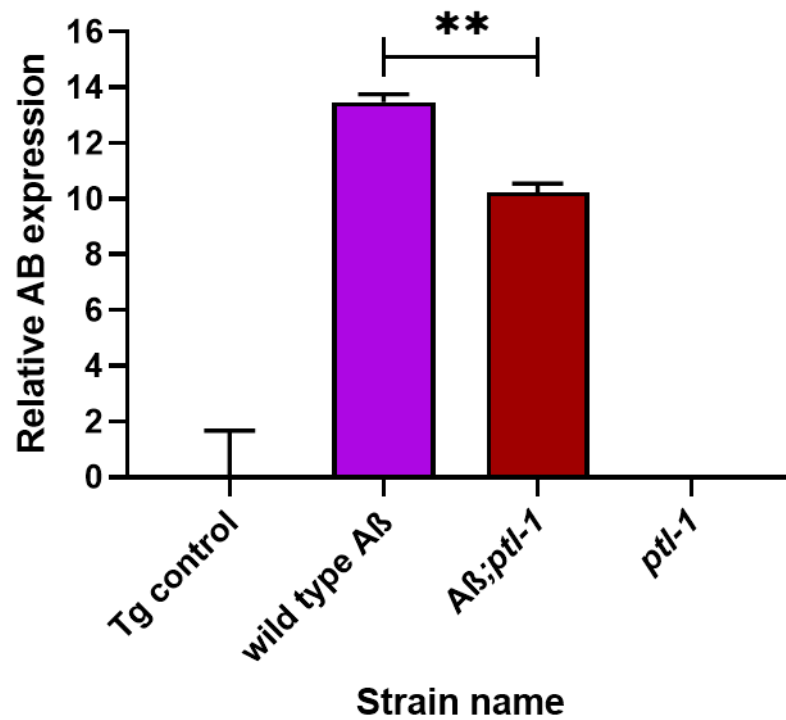


Figure 5.1: Reduction in A β transcript level when expressed in a *ptl-1* null genetic background.

The new strain WG673 (*Psnb-1::huA β 1-42; ptl-1*) strain shows a moderate but significant reduction in levels of A β expression as compared to the strain WG643 (*Psnb-1::huA β 1-42*) determined by an unpaired t test. **p < 0.001.

the control strain expressing the transgenesis marker *Pmyo-2::mCherry* only will be addressed as the transgenic control and the strain APD004 as the *ptl-1* null strain.

5.3.2 Transgenic A β ;*ptl-1* strain WG673 shows changes in growth rate

To test whether the expression of A β in a *ptl-1* mutant background has any effect on the growth of the animals, the body size was measured in terms of length and width on day 4 (young), day 8 (middle-aged) and day 12 (old worms). As can be seen in Figure 5.2A, the length of the A β ;*ptl-1* strain on day 4 was significantly lower than the transgenic control strain ($p = 0.0013$); however, when compared to the wild type A β ($p = 0.31$) and *ptl-1* null strain ($p = 0.84$), the differences in length were not statistically significant. Moreover, there were no significant differences in the width of the A β ;*ptl-1* strains on day 4 when compared to the transgenic control ($p = 0.77$), wild type A β strain ($p = 0.95$), or the *ptl-1* null strain ($p = 0.18$). On day 8, there was a significant increase in the length of A β ;*ptl-1* worms in comparison to the transgenic control ($p < 0.0001$), wild type A β strain ($p < 0.0001$), and the *ptl-1* null strain ($p = 0.0144$) (Figure 5.2C). In contrast, there was no significant difference in the width of these worms on day 8 (D). Furthermore, there was no significant difference in the length and width of the worms on day 12 (Figure 5.2E, F). The increased length of the A β ;*ptl-1* worms on day 8 suggests that A β expression in a *ptl-1* null genetic background does not decrease the growth of the worms in comparison to the slow growing strain expressing A β in the wild type background but that there is non-uniform differences in growth rates between the two strains.

5.3.3 Expression of A β in a *ptl-1* mutant background shows reduction in longevity

Lifespan assays were performed to assess if expression of neuronal A β in a *ptl-1* null background influences the longevity of the animals. The difference in the survival curves was measured using a log rank test, and the new A β ;*ptl-1* strain showed a significant reduction in lifespan when compared to the transgenic control strain ($p < 0.00001$), the wild type A β -expressing strain ($p < 0.00001$), and *ptl-1* null strain ($p < 0.00001$). The survival curves for one of the biological replicates is shown in Figure 5.3A.

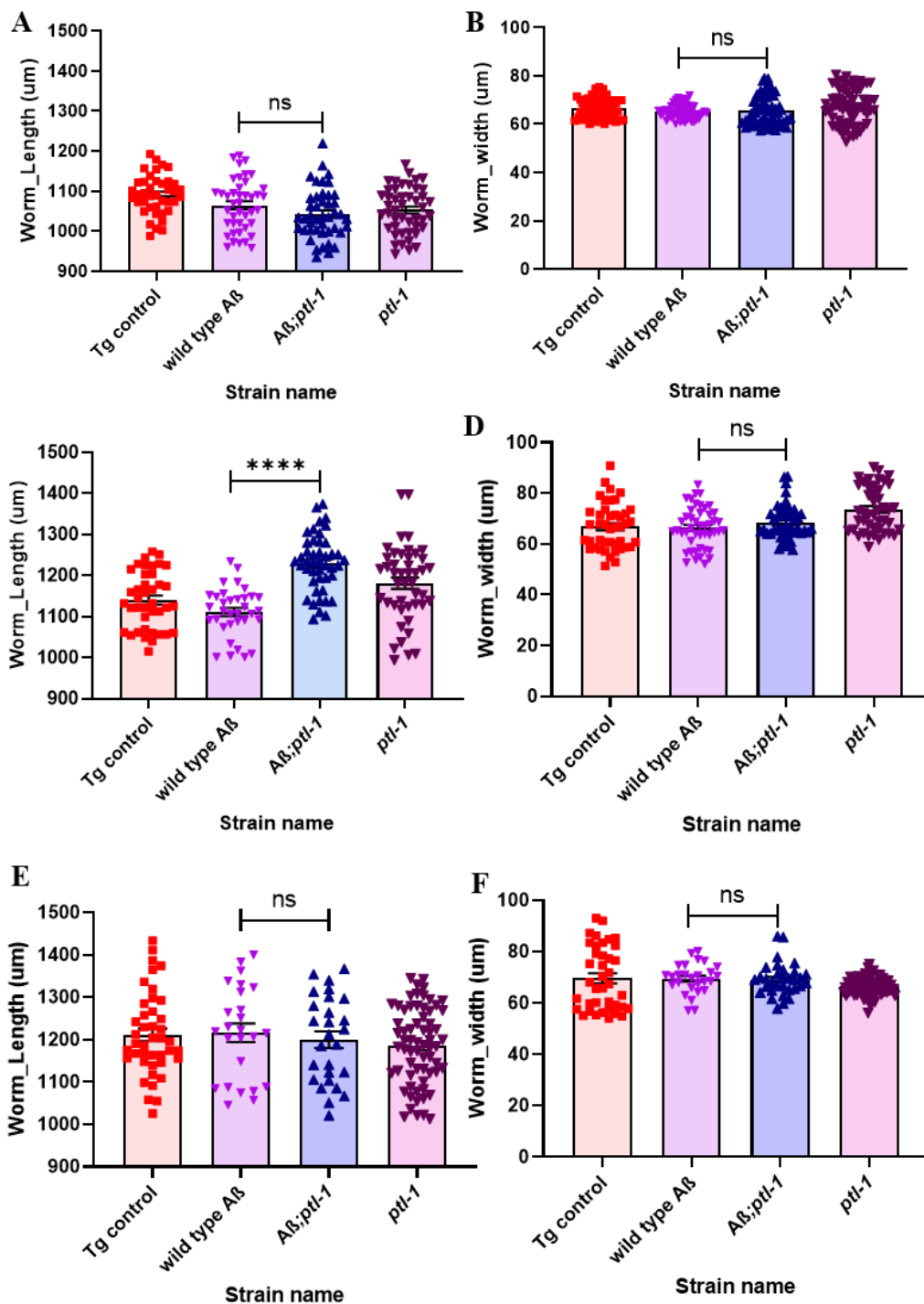


Figure 5.2: *C. elegans* growth estimated by body size measurements of early (day 4), middle-aged (day 8) and old (day 12) adults.

A) Body length of day 4 worms. B) Body width of day 4 worms. C) Body length of day 8 worms. D) Body width of day 8 worms. E) Body length of day 12 worms. F) Body width of day 12 worms. All data analysed by one-way ANOVA followed by post hoc Tukey multiple comparisons test, ns not significant, **** $p < 0.001$.

All the remaining biological replicates are shown in Supplementary Figure 5.2. Furthermore, the median lifespan of the $A\beta$;*ptl-1* strain was ~ 11 days (11 ± 0.84), significantly lower than the transgenic control strain ($p = 0.0016$). Although the median lifespan of the wild type $A\beta$ strain (~ 13 days) and *ptl-1* null strain (~ 15 days) was higher than the $A\beta$;*ptl-1* strain, the difference was not statistically significant (Figure 5.3B). In addition, the Gompertz equation was used to estimate the initial mortality rate (A) and Gompertz value (G) from the survival data in order to measure any differences in the rate of aging between these strains. A higher G value indicates higher rate of aging. The G and A values for all strains are listed as a table in Figure 5.3C. There is a significant increase in the rate of aging in the $A\beta$;*ptl-1* strain in comparison to the transgenic control ($p = 0.0008$) and *ptl-1* null mutant strain ($p = 0.0137$). In contrast, there is no significant difference in the rate of aging between the $A\beta$;*ptl-1* strain and the wild type $A\beta$ strain. Although the *ptl-1* mutation results in subtle reduction in the longevity of the worm, the expression of $A\beta$ in this *ptl-1* null mutant background greatly enhances the severity of the phenotype.

5.3.4 Transgenic *C. elegans* strain expressing $A\beta$ in a *ptl-1* null background shows impaired egg-laying

In order to study the effects of $A\beta$ expression in the *ptl-1* null background on worm fecundity, three egg-laying assays were performed. Firstly, the number of progeny laid per worm per day was calculated for the entire reproductive span of the worm (Figure 5.4A). The average brood size was also derived from these data (Figure 5.4B). When comparing the $A\beta$;*ptl-1* strain to the transgenic control strain, although there was no significant difference in the number of progeny on day 3 ($p = 0.57$), day 4 ($p = 0.39$), or day 5 ($p = 0.15$) of the reproductive period, the $A\beta$;*ptl-1* strain showed significantly reduced progeny on day 6 ($p = 0.0004$). On the other hand, the difference in the number of progeny between the $A\beta$;*ptl-1* strain and the wild type $A\beta$ strain was only significant on day 3 ($p = 0.0018$) of the reproductive span of the worm. In addition, although there was a significant reduction in the number of progeny on day 4 ($p = 0.052$) of the $A\beta$;*ptl-1* strain when compared to the *ptl-1* null strain, the difference was not statistically significant on day 5 ($p = 0.059$), day 6 ($p = 0.82$), or day 7 ($p = 0.89$). Consequently, there was a drastic reduction in the brood size of $A\beta$;*ptl-1* strain in comparison to the transgenic

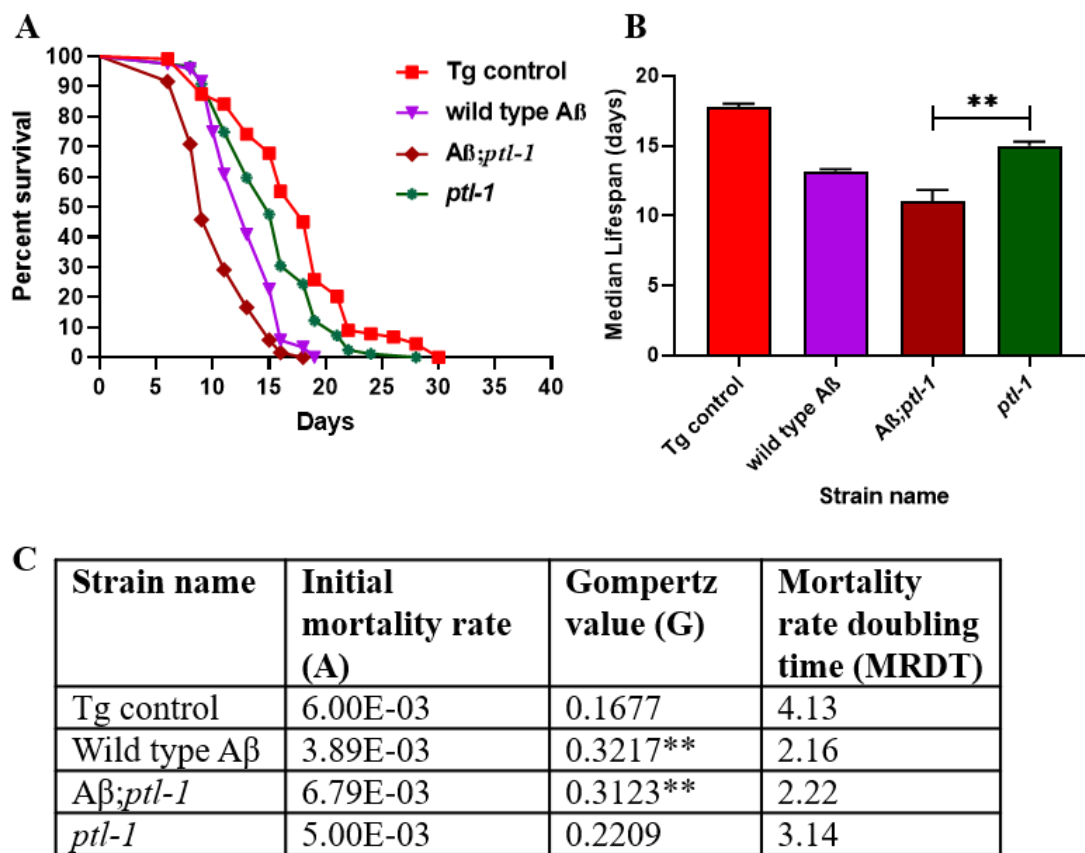


Figure 5.3: Shortened lifespan of WG673 strain expressing A β peptide in a *ptl-1* genetic background.

A) Representative Kaplan Meier survival curves of one biological replicate (n=120 worms/replicate). B) Average of Median lifespan three biological replicates (n = 3, 120 worms/replicate). **p < 0.001.

control ($p < 0.0001$), the wild type A β strain ($p = 0.024$) and the *ptl-1* mutant strain ($p = 0.0137$). To further explore this egg-laying deficit, an egg retention assay was performed to estimate the number of eggs retained *in utero*. As can be seen in Figure 5.4C, the number of eggs retained by A β ;*ptl-1* strain is about (9 ± 0.87), which is significantly lower than the transgenic control strain ($p = 0.0003$). However, there was no significant difference in the number of eggs retained *in utero* in the A β ;*ptl-1* strain when compared to the wild type A β ($p = 0.0936$) or *ptl-1* strain ($p = 0.0867$). Finally, the rate of egg-production was calculated for each of these strains. The rate of egg-production was significantly lower in the A β ;*ptl-1* strain in comparison to the transgenic control strain ($p = 0.0003$), wild type A β strain ($p = 0.0084$) and the *ptl-1* null strain ($p < 0.0001$) (Figure 5.4D). Thus, the expression of A β in a *ptl-1* genetic background leads to severe egg laying defects as demonstrated by reduced brood size, less number of eggs retained *in utero*, and decreased rate of egg production. The reduced brood size and fewer eggs retained *in utero* can both be explained by a reduction in the rate of egg production, noting that the developmental duration of fertility is the same in all strains.

5.3.5 Transgenic *C. elegans* strain expressing A β in a *ptl-1* null background shows improvement in olfactory response towards volatile odorants

To evaluate if the expression of A β in a *ptl-1* null genetic background changes the worm's chemotactic responses, chemotaxis assays were performed using the volatile odorants diacetyl and benzaldehyde on day 4 (young worms) and day 8 (middle-aged worms). An unpaired t test was used to compare the chemotactic abilities of the strains. Diacetyl and benzaldehyde are sensed by chemosensory neurons AWA and AWC, respectively. As can be seen in Figure 5.5A, on day 4, the chemotaxis index of the A β ;*ptl-1* strain (0.81 ± 0.056) towards diacetyl is similar to that of the transgenic control ($p = 0.59$) although it was significantly higher than the chemotaxis index of the wild type A β strain (0.57 ± 0.075 , $p = 0.033$). On day 8, the difference in chemotaxis index of the A β ;*ptl-1* strain in comparison to the chemotaxis index of the transgenic control strain ($p = 0.60$) and the wild type A β strain ($p = 0.20$) was not statistically significant. Hence, the A β ;*ptl-1* strain was able to sense diacetyl better than the wild type A β strain on day 4 and day 8. However, the difference in the chemotaxis index between the two strains was significant only on day 4.

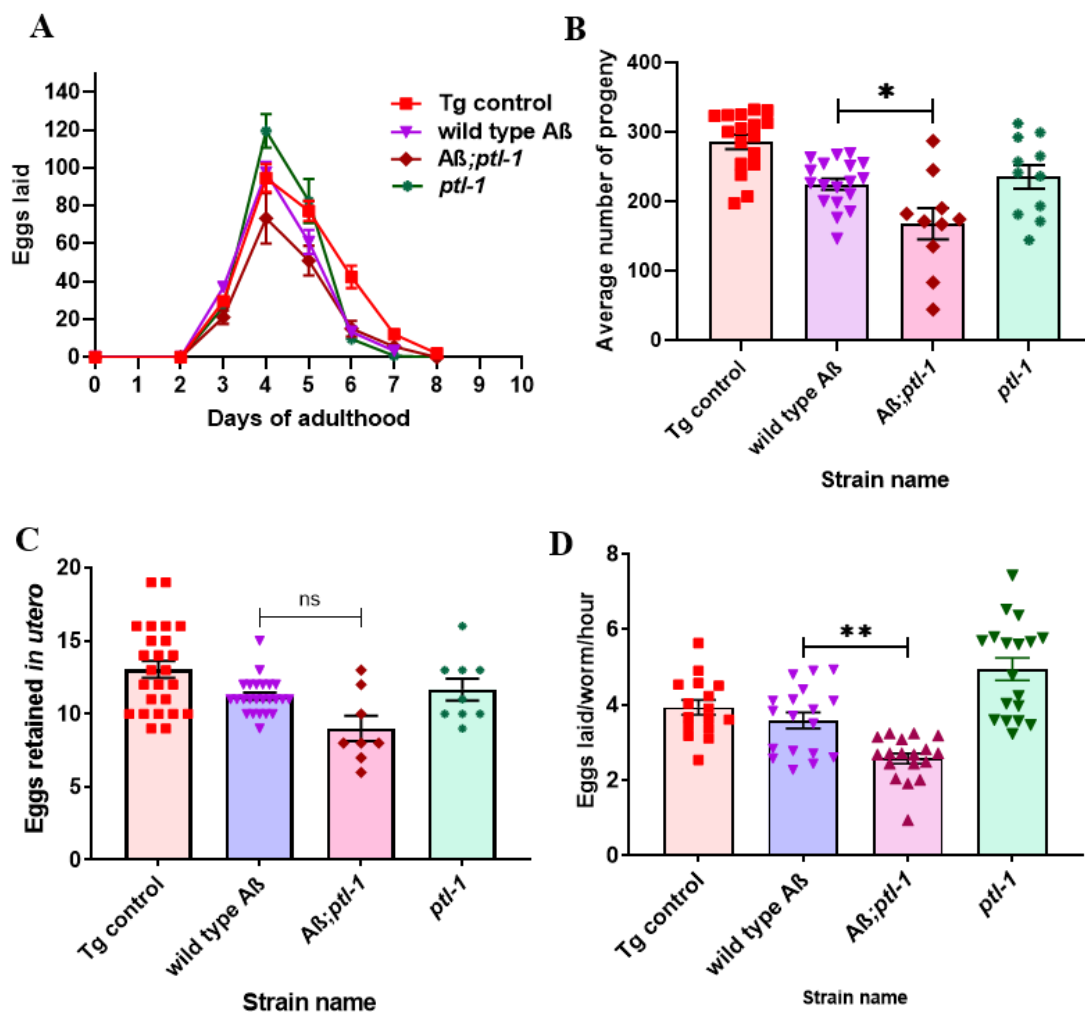


Figure 5.4: Transgenic *C. elegans* strain A β ;ptl-1 shows deficits in egg-laying behaviour.

A) Number of eggs laid per worm per day during the reproductive span of the worm. B) Total brood size (n=3, 5-7 worms/replicate). C) Mean number of eggs retained *in utero* per worm (n=3, 15-20 worms/replicate). D) Rate of egg-production calculated by counting the number of eggs laid/worm/hour (n=3, 15-20 worms/replicate). All data were analysed using one-way ANOVA followed by post hoc Tukey multiple comparisons test, ns not significant, *p < 0.05, **p < 0.01, ***p < 0.001.

Although the chemotaxis index of the *ptl-1* null strain towards diacetyl was lower than the $A\beta$;*ptl-1* strain on day 4 (0.68 ± 0.037 , $p = 0.074$) and day 8 (0.52 ± 0.088 , $p = 0.40$), the difference was not statistically significant. Furthermore, the mobility of these strains towards diacetyl on chemotaxis plates was also derived from the chemotaxis data (Supplementary Figure 5.3A). Although the strains show an age-related reduction in mobility towards diacetyl on day 8, the mobility of the $A\beta$;*ptl-1* strain in comparison to the other strains is not significantly different on day 4 and day 8.

The second volatile odorant used was benzaldehyde, the $A\beta$;*ptl-1* strain (0.90 ± 0.05) and wild type $A\beta$ (0.81 ± 0.036) show similar chemotactic indices on day 4 ($p = 0.8385$) towards benzaldehyde (Figure 5.5B). However, the chemotaxis index of the $A\beta$;*ptl-1* strain (0.77 ± 0.036) was significantly higher than the wild type $A\beta$ strain (0.59 ± 0.06) on day 8 ($p = 0.038$). In addition, the chemotaxis index of the $A\beta$;*ptl-1* strain towards benzaldehyde was significantly higher than the transgenic control strain on day 4 ($p = 0.0273$) and day 8 ($p = 0.0004$). On the other hand, there was no difference in chemotactic responses between $A\beta$;*ptl-1* and *ptl-1* null strain towards benzaldehyde on day 4 ($p = 0.82$) and day 8 ($p = 0.34$). Moreover, the percentage mobility of these strains was measured on chemotaxis plates. As can be seen in Supplementary Figure 5.3B, although the $A\beta$ -expressing strains moved slower than the transgenic control strain and the *ptl-1* null strain on benzaldehyde chemotaxis plates on day 8, the differences in the percentage mobility between the strains was not statistically significant. Therefore, these results suggest that the accuracy of chemotaxis towards both the volatile odorants is consistently higher in the $A\beta$;*ptl-1* in comparison to the wild type $A\beta$ strain.

5.3.6 Expression of $A\beta$ peptide in a *ptl-1* mutant genetic background results in impaired locomotory behaviour

Age-related changes in movement were measured in these worm strains using motility assays on solid and liquid media on day 4 (young worms), day 8 (middle-aged worms) and day 12 (old worms). All the worm strains show progressive decline in motility with age. In addition, the wild type $A\beta$ strain and the $A\beta$;*ptl-1* strain showed rapid decline in motility parameters in comparison to the transgenic control strain unless otherwise specified. Firstly, several movement parameters were measured on solid media (Figure 5.6 and Supplementary Figure 5.4). As can be seen in Figure 5.6A, the $A\beta$;*ptl-1* strain

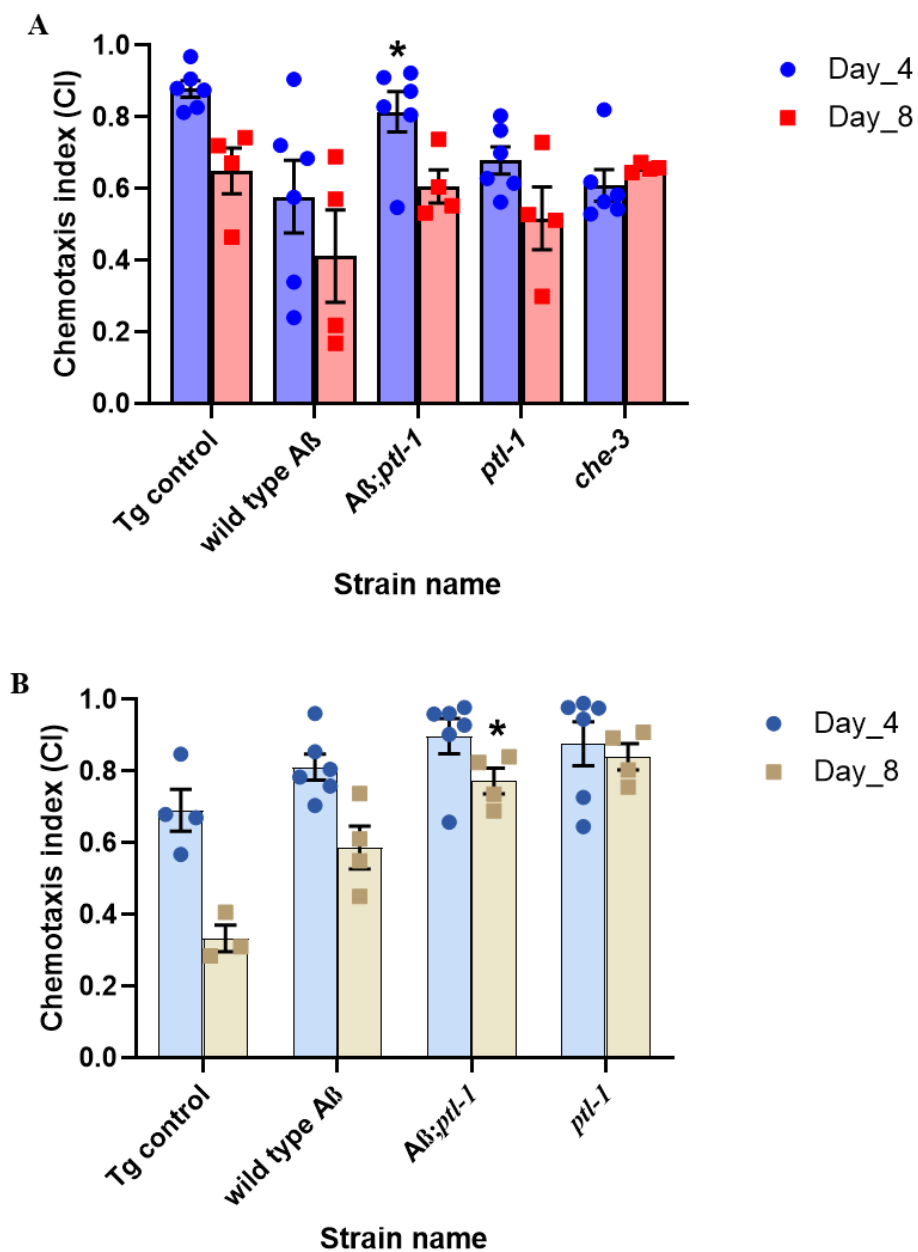


Figure 5.5: Transgenic *C. elegans* strain expressing A β peptide in a *ptl-1* genetic background causes increase in chemotactic responses towards volatile odorants.

Bar graph showing the chemotaxis index of *C. elegans* strains towards Diacetyl (A) and Benzaldehyde (B) on Day 4 and Day 8. (n=4-6, 100-200 worms/ replicate). An unpaired t test was used to compare the chemotaxis index of wild type A β and A β ;*ptl-1* strain. *p<0.05.

showed significant decrease in the body bends in comparison to the transgenic control strain on day 8 ($p < 0.0001$), but difference diminishes on day 12 ($p = 0.12$). When comparing the mean speeds between these strains, the $A\beta;ptl-1$ showed drastic reduction in mean speed in comparison to transgenic control strain on day 8 ($p < 0.0001$) and day 12 ($p = 0.0002$) (Figure 5.6B). On the other hand, there is a significant decrease in body bends of $A\beta;ptl-1$ strain in comparison to the *ptl-1* null strain only on day 4 ($p = 0.0023$), but not on day 8 ($p = 0.99$) or day 12 ($p = 0.93$). Similarly, there was a drastic reduction in the mean speed between the $A\beta;ptl-1$ strain and the *ptl-1* null strain on day 4 ($p = 0.0012$) but diminished on day 8 ($p = 0.99$) and day 12 ($p = 0.63$). However, the difference in the body bends and mean speed between the $A\beta;ptl-1$ strain and the wild type $A\beta$ strain was not statistically significant at all time points. Furthermore, the maximum speed, considered to be an important indicator of health span, was also compared in these strains (Hahm et al., 2015). As can be seen in Figure 5.6C, there was a significant reduction in maximum speed of the $A\beta;ptl-1$ strain on day 4 ($p = 0.014$) and day 12 ($p = 0.0009$) compared to the *ptl-1* null strain. On the other hand, the maximum speed of the $A\beta;ptl-1$ strain in comparison to the transgenic control strain and wild type $A\beta$ strain was not significantly different across all age groups. Furthermore, there was no significant difference the mean amplitude of the $A\beta;ptl-1$ strain compared to the *ptl-1* null strain and the transgenic control strain. However, there was a significant increase in the mean amplitude of the $A\beta;ptl-1$ strain compared to the wild type $A\beta$ strain on day 12 ($p = 0.0046$) (Supplementary Figure 5.4A). In contrast, there were no significant differences in the mean wavelength and the frequency of head bends between any of the strains (Supplementary Figure 5.4B,C). Thus, there were significant differences in the body bends, mean speed and maximum speed between the *ptl-1* strain and the $A\beta;ptl-1$ strains starting at Day 4. On the contrary, the $A\beta;ptl-1$ and the wild type $A\beta$ strain did not show significant differences in the motility parameters on solid media.

Secondly, motility was assessed in liquid media on day 4 (young worms), day 8 (middle-aged) and day 12 (old worms). The number of thrashes (body bends/30s) was similar in all the strains on day 4 (Figure 5.7A). However, there was a drastic age-associated decline in the number of thrashes of the $A\beta;ptl-1$ expressing strain in comparison to the transgenic control strain and *ptl-1* null strain on day 8 ($p < 0.0001$) and day 12 ($p < 0.0001$). In fact, both the $A\beta$ -expressing strains showed a similar decline in the body bends with age and therefore the difference in the number of thrashes between the two

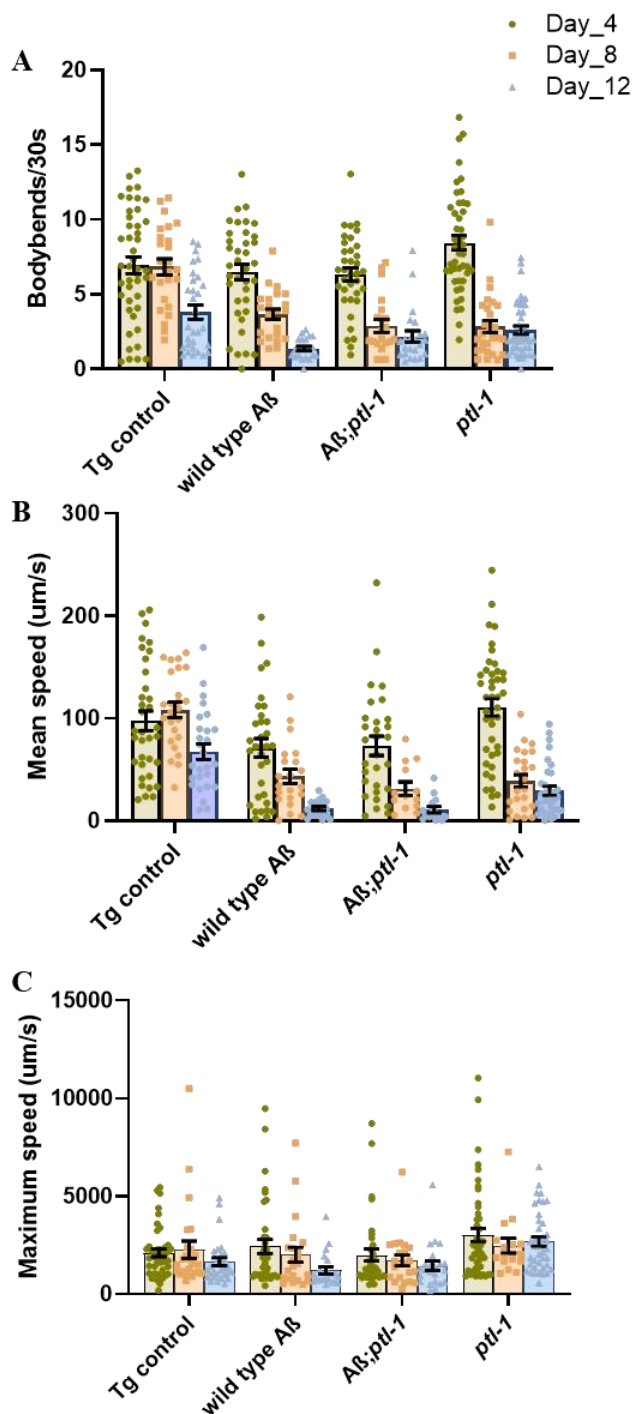


Figure 5.6: Transgenic *C. elegans* strain expressing A β in a *ptl-1* genetic background showed age-related locomotory defects on solid media.

A) Bodybends/30s. B) Mean speed ($\mu\text{m/s}$). C) Maximum speed ($\mu\text{m/s}$). All data were analysed using two-way ANOVA followed by post hoc Tukey multiple comparisons test. Significance values represent pairwise comparisons between A β ;ptl-1 and ptl-1 strain (n=3, 5-15 worms/replicate).

strains was insignificant on day 8 ($p = 0.86$) and day 12 ($p > 0.99$). Mean swimming speed is closely related to the number of thrashes and therefore showed similar results. The A β -expressing strains showed similar age-related decline in mean speed and the difference between the two being statistically insignificant on day 4 ($p = 0.47$), day 8 ($p = 0.89$) and day 12 ($p = 0.99$). In contrast, the mean swimming speed showed a similar significant decline in A β ;*ptl-1* strain on day 8 ($p < 0.0001$) and day 12 ($p < 0.0001$) compared to the *ptl-1* null strain and the transgenic control strain (Figure 5.7B). The number of waves initiated either from the head or tail of the worms per unit time known as the wave initiation rate was also estimated from the motility data (Figure 5.7C). The wave initiation rate of the A β ;*ptl-1* strain was significantly lower starting at day 4 in comparison to the transgenic control strain ($p < 0.0001$), the wild type A β strain ($p = 0.0011$) and the *ptl-1* null strain ($p = 0.0055$). Furthermore, the difference in the wave initiation rates between the A β -expressing strains diminishes on day 8 ($p > 0.99$) and day 12 ($p = 0.97$). However, the wave initiation rate of the A β ;*ptl-1* strain was significantly lower than the transgenic control strain on day 8 ($p < 0.0001$) and day 12 ($p < 0.0001$). Similarly, the difference in the wave initiation rate between the A β ;*ptl-1* strain and the *ptl-1* null strain was significantly lower on day 8 ($p < 0.0001$) and day 12 ($p = 0.0011$). The activity of the worms was also measured to get an idea of how vigorously the worm bends while swimming over time. As can be seen in Figure 5.7D, there was a significant reduction in the activity of the A β ;*ptl-1* strain in comparison to the transgenic control strain in all age groups ($p < 0.0001$). Similarly, the activity of the A β ;*ptl-1* strain was significantly lower than the *ptl-1* null strain at day 4 ($p = 0.0002$), day 8 ($p < 0.0001$) and day 12 ($p < 0.0001$). In contrast, the activity of the A β ;*ptl-1* strain and the wild type A β strain was not significantly different in all age groups. The parameter brush stroke gives an indication of the depth of the movement that the worm has accomplished in a given stroke (body bend). The A β ;*ptl-1* strain shows significant reduction in brush stroke in comparison to the transgenic control strain ($p = 0.048$) and the *ptl-1* null strain ($p = 0.0003$) on day 12 (Supplementary Figure 5.5A). However, the A β -expressing strains do not show a significant difference in the brush stroke in all age groups. The dynamic amplitude or the curvature range measuring how much “stretching” occurs in a single stroke was compared between the strains (Supplementary Figure 5.5B). There was no significant difference in the dynamic amplitude of the A β ;*ptl-1* strain in comparison to the transgenic control strain and the *ptl-1* null strain in all age groups. However, the dynamic amplitude of the wild type A β strain was significantly higher than the A β ;*ptl-1* strain on

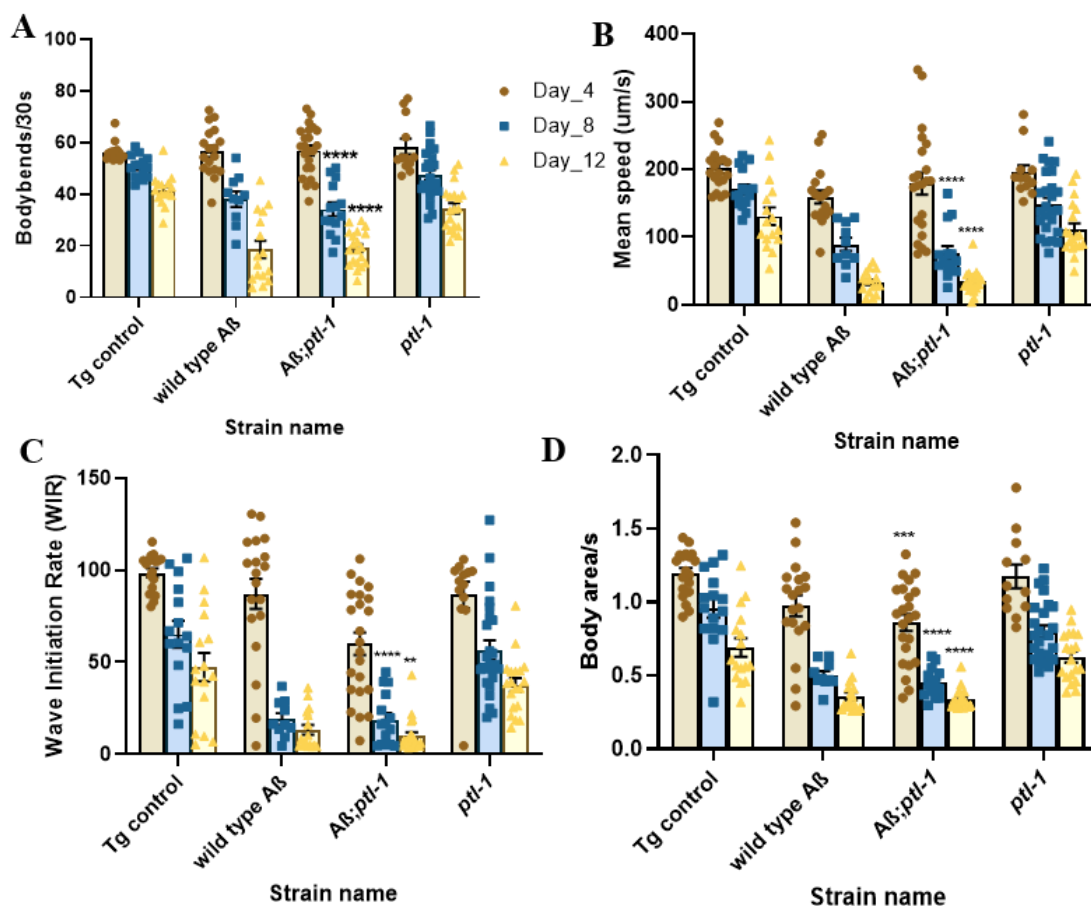


Figure 5.7: Transgenic *C. elegans* strain expressing A β in a *ptl-1* genetic background enhances the severity of the motility defects on liquid media.

A) number of thrashes in liquid (body bends/30s). B) Mean swimming speed ($\mu\text{m/s}$). C) Wave initiation rate. D) Activity in liquid (body area/s) ($\mu\text{m/s}$). All data were analysed using two-way ANOVA followed by post hoc Tukey multiple comparisons test. Significance values represent pairwise comparisons between A β ;ptl-1 and ptl-1 strain (n=2, 5-15 worms/replicate). ns not significant, *p < 0.05, **p < 0.01, ***p < 0.001.

day 12 ($p = 0.010$). However, the mean number of waves did not vary across all age groups for all the strains. Moreover, the relative percentage of time the worm spends curled up was also measured and it was found that the $A\beta;ptl-1$ strain showed significant high curling distance as compared to the transgenic control strain ($p = 0.0096$) and the $ptl-1$ null strain ($p = 0.026$) on day 8, which diminishes on day 12. The extent of curling in the $A\beta$ -expressing strains was not significantly different across all age groups (Supplementary Figure 5.5D). Therefore, both the wild type $A\beta$ and the $A\beta;ptl-1$ strain showed similar age-related decline in motility. When comparing the $A\beta;ptl-1$ strain with the $ptl-1$ strain and the transgenic control strain, there were significant reduction in the number of thrashes, mean swimming speed, wave initiation rate, activity index, brush stroke, and dynamic amplitude in the $A\beta;ptl-1$ strain, particularly on Day 8 and Day 12. Therefore, expression of $A\beta$ in a $ptl-1$ genetic background increases the severity of the motility defect when compared to the $ptl-1$ null strain.

5.3.7 Transgenic *C. elegans* strain expressing $A\beta$ in a $ptl-1$ null background shows deficits in dopaminergic signalling

To assess deficits in learning dependent behaviours, experience-based motility assays were performed. The basal slowing response in the worms mediated by dopaminergic signalling refers to the slowing down of well-fed worms in the presence of food and therefore diminished basal slowing response indicates deficits in dopaminergic signalling (Sawin et al., 2000). As can be seen in Figure 5.8A, all the worms strains show basal slowing response in the presence of food on day 4, except the positive control strain CB1112 [*cat-2 (e1112) II*], which is known to be deficient in dopaminergic signalling. However, the basal slowing response was diminished by day 8 (Figure 5.8B) and day 12 (Figure 5.8C) in all the worms strains except the transgenic control strain. In addition, there was no difference in the severity of the basal slowing response in wild type $A\beta$ strain, $ptl-1$ null strain and the new $A\beta;ptl-1$ strain. Thus, both the $A\beta$ expressing strains and $ptl-1$ strain show basal slowing response, particularly in middle-aged and old animals.

The enhanced slowing response mediated by serotonergic signalling was assessed by measuring the slowing response of starved worms in the presence of food. As shown in Supplementary Figure 5.6A, there was a significant difference in the movement of the young adult worms of all strains in the presence and absence of bacteria measured in

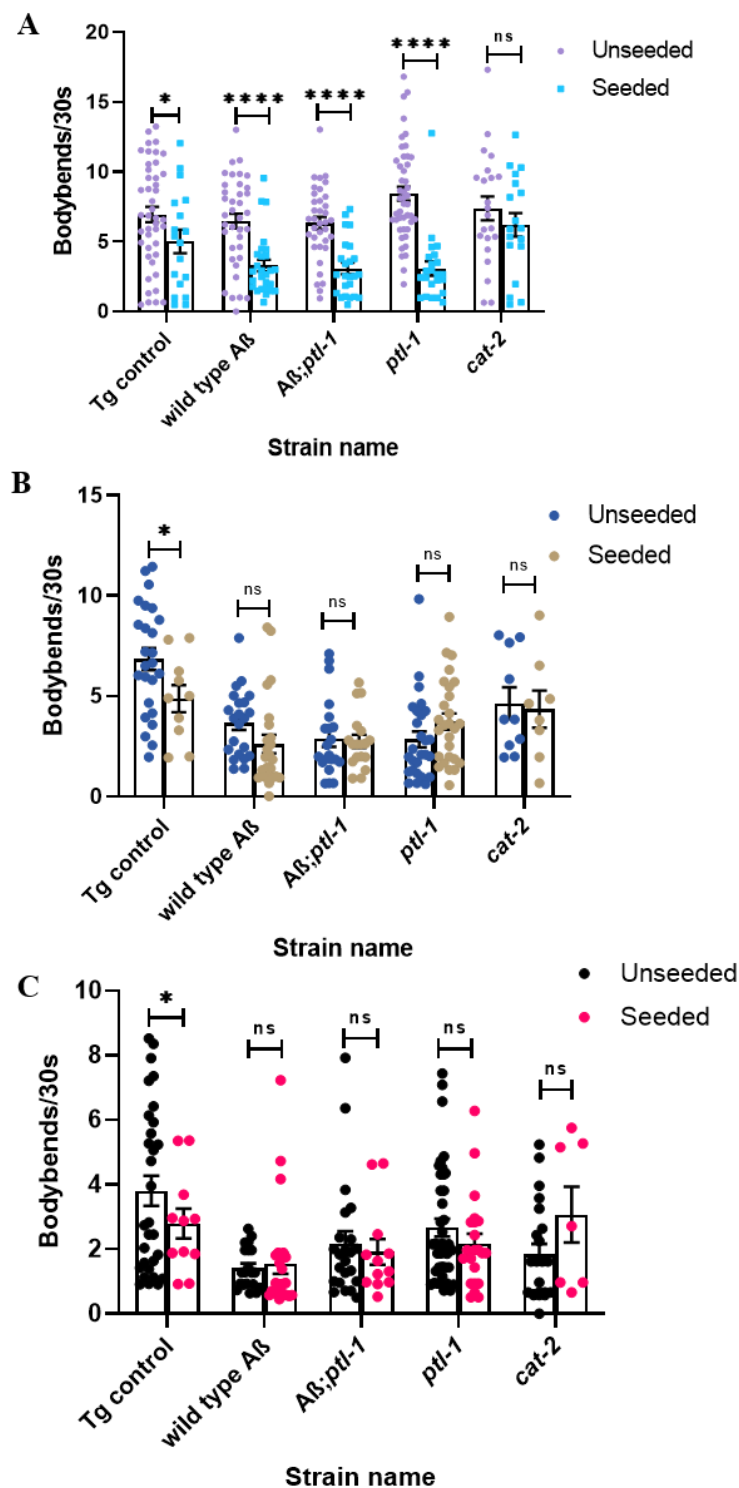


Figure 5.8: Transgenic *C. elegans* strain expressing A β peptide in a *ptl-1* genetic background show deficits in dopaminergic signalling.

A) Day 4. B) Day 8. C) Day 12. An unpaired t test was used to test for differences in the slowing responses on seeded and unseeded plates. ns not significant, **** $p < 0.0001$.

terms of body bends on day 4. The control strain MT7988 [*bas-1 (ad446)* III] and CB1141 [*cat-4 (e1141)*V] did not show any slowing response, as expected, because they are deficient in dopamine and serotonin (Sawin et al., 2000). Similarly, all the strains including the transgenic control WG731 show diminished slowing response on day 8 and day 12 (Supplementary Figure 5.6B,C). Hence, the enhanced slowing response assays are not very sensitive for older worms and it is difficult to know which strains are deficient in serotonergic signalling as all the starved and older worms slow down significantly in the presence of food irrespective of the genotype.

5.4 Discussion

In this chapter, a new *C. elegans* AD model was generated to study the effects of A β peptide expression associated with tau loss of function by expressing the A β peptide in a *ptl-1* null genetic background. When compared to the transgenic control strain, the new A β ;*ptl-1* strain displayed a shortened lifespan, egg-laying and locomotion defects, enhanced chemotaxis towards diacetyl and benzaldehyde, and deficits in dopaminergic signalling. In comparison to the *ptl-1* null strain, the new A β ;*ptl-1* strain showed reduced lifespan, increased rate of aging, reduced brood size, impaired motility on solid and liquid media, and a significant reduction in maximum speed. Finally, when compared to the strain that expresses A β in the wild type background, the A β ;*ptl-1* strain showed differences such as severe egg-laying deficits and improved chemotaxis towards volatile odorants.

Since tau is an important microtubule binding protein, it performs several functions *in vivo* (Baas et al., 1991; Chen et al., 1992; Cleveland et al., 1977; Ittner et al., 2010; Lee et al., 1998; Liao et al., 1998; Morris et al., 2011; Reynolds et al., 2008; Weingarten et al., 1975). There are two possible ways in which tau results in neurodegeneration and thereby disease: (1) it could assume a toxic gain of function as its levels increase, eventually resulting in tau accumulation and aggregation (Avila et al., 2004; Clavaguera et al., 2009; Gomez-Ramos et al., 2006; Ittner et al., 2008) or (2) a loss of physiological function that results in disease (Gomez-Isla et al., 1997; Santacruz et al., 2005). It is difficult to discern the functions of tau in mammalian models as there exists a complex functional redundancy between MAP2, MAP4 and tau (Dehmelt and Halpain, 2005; Sontag et al., 2012). Tau knockout mice generated do not show any defects in neuronal development or function (Dawson et al., 2001; Harada et al., 1994; Ke et al., 2012; Tucker et al., 2001), which may be due to the compensatory functions of the other MAPs (Harada et al., 1994). In contrast, there was a report of a mouse AD model wherein loss of tau appeared to aggravate the effects of mutated APP (Dawson et al., 2010). Interestingly, a study showed that elimination of tau in a mouse model of AD expressing human precursor protein with familial AD mutation is beneficial against A β induced deficits (Roberson et al., 2007). Roberson et al. study supports previous cell-based studies which showed that cultured hippocampal neurons from the tau knockout mice when treated with fibrillar A β were protected against A β induced toxicity (Rapoport et al., 2002). However, targeting

endogenous tau may have complications as tau knockout mice show behavioural impairment and structural abnormalities with advancing age (Ikegami et al., 2000).

Many animal studies have focussed on tau toxic gain of function, with some studies employing gene-targeted approaches to study endogenous tau (Gotz et al., 2010; Gotz and Ittner, 2008). The effects of toxic gain of tau function have been studied by overexpressing human tau in the *C. elegans* neurons (Kraemer et al., 2003). Wang et al. generated a *C. elegans* AD model by expressing both human tau and A β peptide in the neurons and showed that the strain recapitulates AD-like pathology such as synaptic fatigue, cognitive aging, and shorter longevity (Ballard et al., 2011; Larson et al., 2004; Schroeder and Koo, 2005; Wang et al., 2018; Zhao et al., 2010). PTL-1 in *C. elegans* is the only homolog of tau/MAP2 in the worm, suggesting that there is shared physiological function between tau/MAP2 family members (Gordon et al., 2008; McDermott et al., 1996). Hence, it should also be possible to study the *in vivo* toxicity of the A β peptide associated with tau loss of function in *C. elegans* in the absence of other compensatory MAPs.

5.4.1 A β expression in tau null background results in behavioural changes in specific neuronal subsets

Quantitative measures of A β expression indicates that in the tau null background, expression was moderately reduced relative to the wild type background (Figure 5.1). This contrasts with the studies in a mouse model of AD in which there was no changes in expression of the human precursor protein or behavioural phenotype when levels of tau were reduced (Roberson et al., 2007). However, the reduction in A β expression observed in A β ;*ptl-1* strain is not likely to be driven by the absence of tau, as there are other aspects of genetic background that can influence A β expression. The differences in gene expression is relatively minor and thus may not be biologically significant.

There is an increase in the chemotactic ability of worms expressing A β in the *ptl-1* null background which indicates that expression of A β is unable to cause a behavioural deficit in the absence of PTL-1 and that the absence of PTL-1 may be protective against A β -induced toxicity specifically in the chemosensory neurons (Figure 5.5). There have been reports that suggest the possibility that tau reduction could protect against AD and other neurological conditions associated with excitotoxicity (Roberson et al., 2007).

When compared to the strain that expressed A β in the wild type background, the transgenic control strain, and the *ptl-1* null strain, while there was no overall difference in the growth of this new worm strain (Figure 5.2), there was both a reduction in overall lifespan and an increase in the rate of aging (Figure 5.3). The null *ptl-1* strain has previously been shown reduction in longevity relative to wild type *C. elegans* (Chew et al., 2013). Expression of A β in this *ptl-1* null genetic background further reduces the lifespan of the animals and increases the severity of the phenotypes.

The new strain showed a significantly impaired egg-laying in comparison to the transgenic control strain, the *ptl-1* null strain and the wild type A β strain. The rate of egg-production in this A β ;*ptl-1* strain was reduced, which contributes to the lower number of eggs retained *in utero* and the drastic reduction in brood size (Figure 5.4). This decline in reproductive health is in part driven by the mutation *ptl-1* in *C. elegans*, which has caused deterioration of neuronal health and predisposing the neurons to neurodegeneration (Chew et al., 2013; Dawson et al., 2010). Thus, the expression of A β in this already stressed nervous system may hasten the appearance of behavioural deficits.

5.4.2 Some behavioural deficits are a result of neuronal A β expression irrespective of the genetic background

Motility parameters measured on solid and liquid media did not show differences between strains expressing A β in different genetic backgrounds (Figure 5.6 and Figure 5.7). In addition, all the A β -expressing strains and the *ptl-1* mutant strain APD004 showed deficits in dopaminergic signalling with advancing age measured using an experienced-based motility assay (Figure 5.8). The dopaminergic signalling undergoes several changes during the process of aging, and decreasing dopamine could increase hypo-activity causing gait disturbances and contribute to the decline of functions (Robert et al., 2010). However, the role of the dopaminergic system in AD is still under debate (Attems et al., 2007; Portet et al., 2009) in part because several neurotransmitters and modulators including acetylcholine, serotonin and dopamine are differentially altered in the brains of individual with AD (Kar et al., 2004). Unfortunately, the assay used to quantify severity of dysfunction in the dopaminergic system in this study was not sensitive enough to detect differences between strains, and thus using a more sensitive assay might be informative about the impacts of A β and tau on dopaminergic signalling.

The enhanced slowing response assay was used to measure deficits in serotonergic signalling (Sawin et al., 2000). There were no differences in slowing response between the strains with advancing age (Supplementary Figure 5.6). As there is an overall reduction in the movement with age, differences in slowing responses between the worms with advancing age become correspondingly difficult to detect. Therefore, more sensitive measures may be required to assess deficits in serotonergic neurotransmitter signalling in aging worms.

As previously mentioned *ptl-1* is expressed in the neurons and a null mutation in this gene results in shorter lifespan and loss of neuronal integrity. In addition, studies have suggested that PTL-1 regulates structural integrity of the neurons in a cell autonomous way (Chew et al., 2014). Some neuronal subsets may be more susceptible to damage via A β -induced neurotoxicity than other cell types and this results in an increase in the severity of the behavioural deficit. Furthermore, previous studies have suggested that loss of tau may predispose the neurons to axonal pathology and neurodegeneration in the stressed central nervous system (Dawson et al., 2010).

Mechanisms that link A β and tau pathology have been proposed, but not fully established and this remains a challenge in AD research (Blurton-Jones and Laferla, 2006; Oddo et al., 2006). Since tau can lead to neurodegeneration independently in the absence of other pathological events, it could be a key mediator of neurodegeneration acting downstream of other pathological insults including expression of A β (Goedert and Jakes, 2005; Rapoport et al., 2002; von Bergen et al., 2001). Various other pathological events such as A β mediated toxicity, oxidative stress and inflammation may trigger or contribute to the detachment of tau from the microtubules (Andersen, 2004; King et al., 2006; Liu et al., 2005; Moreira et al., 2005; Rapoport et al., 2002). Previous studies have shown that A β can interfere with tau inducing conformational changes and neurodegeneration (Spires-Jones and Hyman, 2014; Stancu et al., 2014). Collectively, loss of tau function studies have suggested that the disease pathology observed in tauopathies, including AD, may be the result of loss of physiological function of tau upon aging (Hannan et al., 2016).

5.5 Conclusion

A new strain was generated and characterised expressing the A β peptide in a *ptl-1* null genetic background. The strain showed behavioural deficits such as impaired locomotory

behaviour and deficits in dopaminergic signalling with advancing age, as well as those that were aggravated by the expression of A β in the absence of the tau orthologue *ptl-1* (i.e. the *ptl-1* null allele *ok621*) such as reduced lifespan and an egg-laying deficit. In contrast, the strain showed improvement in chemotactic response towards volatile odorants. Although *C. elegans* strains expressing the A β and tau have been beneficial in studying the role of toxic tau gain of function, this new strain will help in understanding the role of the loss of physiological tau in AD, a crucial addition to the already existing strains. A complete understanding of the role of aberrant tau function in the presence of A β -induced neurotoxicity or other pathological stressors to the neurons may drive future mechanistic studies and therapeutic interventions.

Chapter Six

General discussion

Alzheimer's disease is a prevalent neurodegenerative disease with no cure. New animal models are thus needed to both understand disease progression and develop new treatment strategies. AD, like the majority of age-related neurodegenerative diseases have been associated with the accumulation of specific proteins in the central nervous system, resulting in toxic insult to the neurons, neuronal dysfunction and cell death (Teschendorf and Link, 2009). One of the central hypothesis in the field of AD research is the amyloid cascade hypothesis which postulates that the aggregation and accumulation of A β plays a major role in initiating the cascade of events that ultimately lead to a disease state (Hardy and Higgins, 1992; Tanzi and Bertram, 2005; Haass and Selkoe, 2007; Shankar et al., 2008; Teplow, 2013). However, despite more than 20 years of intensive research, the precise mechanism by which these soluble or insoluble A β species exert their toxic effects *in vivo* remains unclear. No clinical trial that aimed to target A β has progressed further than phase III, possibly due to reasons including the treatment targeting the insoluble plaques instead of soluble oligomers, treatment being administered at a later stage of the disease, and poor brain penetration (Tolar et al., 2020). Animal models, particularly mouse models, have historically been used in screens for identifying drug candidates to go into human clinical trials. Those treatments that showed promise in animal models have failed in clinical trials, which suggests that those animal models are not predictive of treatment success in human disease. Moreover, these drugs are therapeutic and are designed to target people who already have the disease: the aim of the drug treatment is to either arrest progression or restore the impairment. Therefore, it is critical to have a simple *in vivo* model that can recapitulate disease initiation and progression to better define targets in the context of developing drugs for therapy. The new model should not only show disease-relevant phenotypes upon expression of the A β peptide, but also express different concentrations of A β correlated with severity of phenotype. Additionally, a well-designed model would also shed light on the different effects of soluble vs insoluble A β and other mechanistic questions related to A β toxicity. Hence, the aim of this thesis was to develop new tools to study A β toxicity *in vivo*.

I used the invertebrate experimental system *C. elegans* to model AD as it offers several advantages to study the molecular and cellular mechanisms of neurodegenerative diseases. *C. elegans* displays a remarkable degree of behavioural complexity despite having a nervous system consisting of 302 neurons. Its entire nervous system has been extensively mapped using electron micrographs of serial sections and found to consist of 5000 chemical synapses, 2000 neuromuscular junctions, and 600 gap junctions (Nuttley et al., 2002; White et al., 1986). This allows gene expression to be interpreted in the context of a very precise anatomical wiring diagram. Cellular ablation studies have correlated loss of specific sets of neurons with specific behavioural responses that are remarkably reproducible, thereby permitting the study of certain aspects of the disease at single cell resolution in the worms (Bargmann and Avery, 1995; Hart and Chao, 2010). In addition, due to its short lifespan, the temporal sequence of events relating to AD pathogenesis can be quantified. One of the biggest advantages of using *C. elegans* as an *in vivo* model to study behavioural deficits associated with A β peptide expression is that the worm does not have its own endogenous A β . This is beneficial in developing an AD model, as any significant behavioural deficit seen in the transgenic A β -expressing *C. elegans* strain would be due to the A β transgene only, thereby enabling us to study the causal relationship of this peptide: a direct test of the amyloid cascade hypothesis.

6.1 Neuronal A β 1-42 expression results in age-associated behavioural deficits

The first main finding of the thesis was that expression of A β 1-42 in *C. elegans* neurons results in age-associated AD relevant behavioural deficits. As reported in Chapter 2, a new *C. elegans* strain was genetically engineered to express the A β transgene in the nervous system using the pan-neuronal promoter *snb-1*. Earlier work demonstrated that expression of A β in the *C. elegans* body wall muscles resulted in a severe, fully penetrant, age-dependent paralysis phenotype as a readout of A β -induced toxicity. In addition, this strain also showed *in vivo* accumulation of A β by immunohistochemistry and the presence of soluble A β oligomers by size exclusion chromatography (McColl et al., 2012). *C. elegans* have 95 body wall muscle cells arranged in four longitudinal bands forming a single layer of cells running along the length of the worm (Gieseler et al., 2017). High levels of A β -expression in this model may be due to higher intrinsic activity

of the muscle-specific promoter *unc-54*. Since AD is a neurodegenerative disorder, this muscle-expression A β *C. elegans* strain is not directly relevant to the A β pathology in AD, which is neuronal. Instead, this strain may closely model Inclusion Body Myositis (IBM), a progressive muscle disease associated with intramuscular A β deposition (Askanas and Engel, 2001). On the other hand, the pan-neuronal A β -expressing transgenic *C. elegans* strain described here showed several behavioural phenotypes such as reduced lifespan, impaired locomotion, deficits in healthspan indicators such as fecundity and maximum speed, along with relatively mild defects in behaviours correlated with neuronal dysfunction such as chemotaxis, neurotransmitter signalling, and short-term associative memory. These findings are corroborated by previous reports on *C. elegans* neuronal AD models that showed reduced longevity, impaired locomotion, egg-laying defects, and reduced chemotaxis responses (Dosanjh et al., 2010; Fong et al., 2016).

The differences in the behavioural phenotypes between the muscle and neuronal strains may be due to either (i) quantitative differences in the level of A β expression in the muscle and neurons, or (ii) differences in the response of the muscle and neuronal cells to A β expression (Teschendorf and Link, 2009). Although 1/3rd of worm cells are neurons, the biomass is less than 1/3 because the neurons are smaller, whereas muscle have higher biomass which causes quantitative differences in the levels of A β expression. Therefore, *C. elegans* strains expressing A β in the body wall muscle prove beneficial to study the biochemistry of the A β peptide because of high levels of expression of the transgene. By contrast, neuronal expression of the transgene results in disease relevant behavioural phenotypes and therefore may be well suited to study the cell biology aspect of the disease. This in turn may provide insights into the biology of the organism upon A β transgene expression.

As shown in Figure 6.1, several *C. elegans* phenotypes such as locomotion, egg-laying, chemotaxis, pharyngeal pumping, and lifespan are predictors of neuronal health. Remarkably, each of these behaviours is modulated by distinct and intricate neural networks consisting of specific subset of neurons, which gives rise to a simple behavioural output which can be readily assayed. Behaviours such as motility and pharyngeal pumping have been correlated with the lifespan. Some behaviours may be indicators of physiological health such as maximum speed and fecundity, which may or may not necessarily be indicative of neuronal health. In addition, there are behaviours that

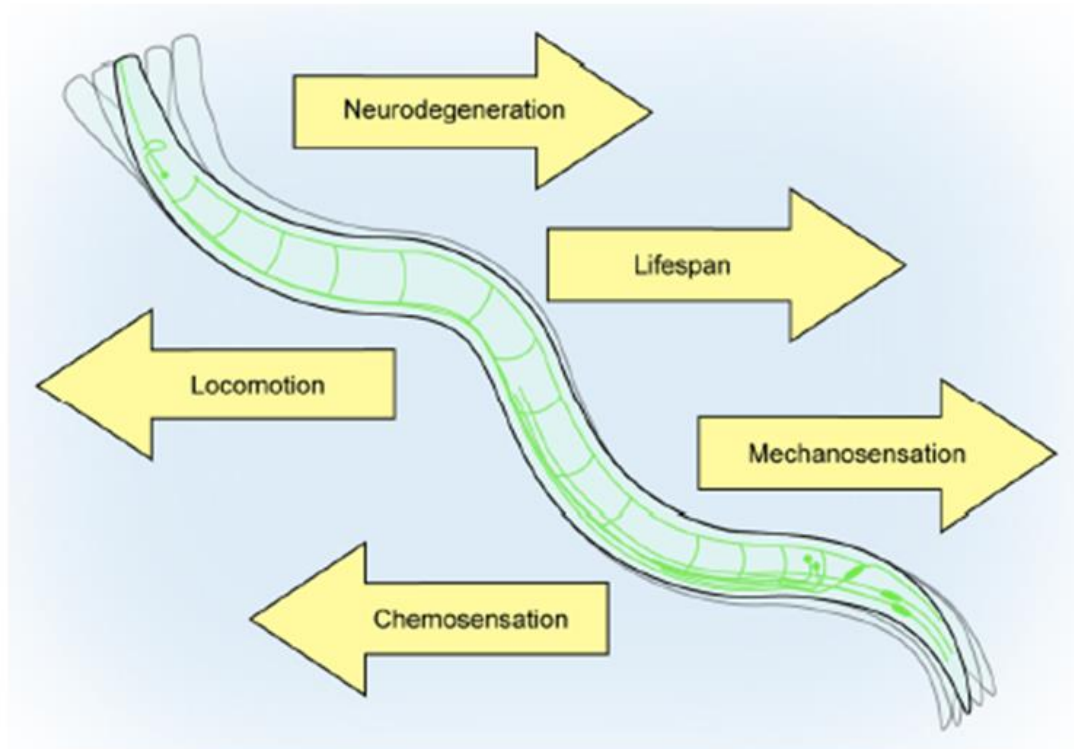


Figure 6.1: Measurable outputs of neuronal health.

As the entire nervous system has been mapped and the cellular lineage of *C. elegans* defined, *C. elegans* behaviour is a predictable output of neuronal function. Locomotion, chemosensation, and mechanosensation are elicited by distinct neuronal networks; thus, distinct changes in behaviour can be designated to alterations in the function of individual neurons and subtypes. Using tissue-specific expression of fluorescent proteins, changes in neuronal function can be assayed as aberrations in neuronal structure or integrity. As molecular mechanisms of protein stability and neuronal structure are modulated by aging pathways, changes in lifespan primarily reflect macro effects on the animal (Adapted from Griffin, Caldwell, & Caldwell, 2017).

are modulated by specific subsets of neurons such as chemotaxis. Locomotion is an important behavioural output in *C. elegans* regulated by a neural circuit generating sinusoidal bends in response to diverse sensory cues. The sensory cues are integrated by the sensory neurons, which then transmit this information to the interneurons that mediate the flow of this information to the motor neurons and finally to the muscle (Figure 6.2) (de Bono and Maricq, 2005). Given this context, behaviour is initiated at the neurons upstream of the pathway and executed in the muscle, and therefore locomotory deficits may arise either because of defects in muscle or neurons. For instance, the ‘uncoordinated’ phenotype is an abnormal locomotion phenotype such as twitching, halting, odd jerky motions, curling or kinky motion, and partial or rigid paralysis, and may arise as a result of mutations in genes expressed in either muscle, neurons or even in other tissues. There are 111 *Unc* genes in *C. elegans*, but 71 of those primarily affect the nervous system and not the muscle (Gieseler et al., 2017). The locomotory deficits observed in my strain are neuronal deficits resulting from A β expression in the neurons upstream of this pathway (Figure 6.2). To test this more explicitly, A β expression may be targeted to specific neuronal subsets to assess the effects on the severity of the different phenotype.

Neuronal deficits can be explained by either neuronal dysfunction or neuronal death. Behavioural deficits such as chemotactic defects and deficits in basal slowing responses arising due to neuronal dysfunction are early indicators of disease pathogenesis. This A β 1-42 expressing strain WG643 showing early behavioural deficits will prove beneficial in the study of neuronal dysfunction as it is possible to intervene in this pathway at an early stage presumably while the worms are alive. These results demonstrate that the *C. elegans* model presented here provides a useful new tool to understand early-stage progression of the disease and A β toxicity.

6.2 Behavioural deficit dependent on A β concentration

Low levels of A β are protective; however, high levels of A β resulting from an imbalance between production and clearance lead to accumulation of A β and an increase in A β aggregation, which triggers a pathogenic cascade ultimately leading to disease (Sadigh-Eteghad et al., 2015). Therefore, there may be a correlation between A β concentration and the initiation and progression of the disease, rather than the end point of the disease. To

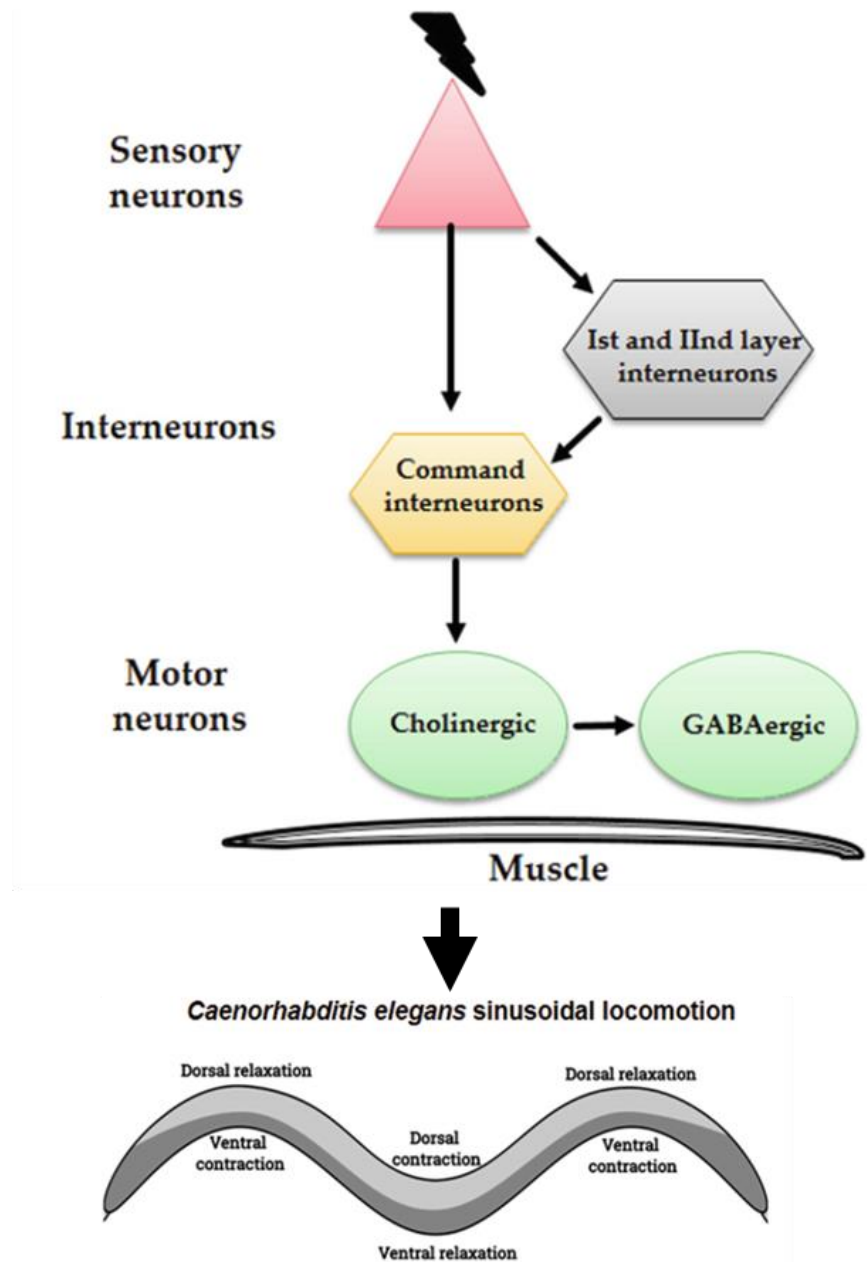


Figure 6.2: Schematic representing the *C. elegans* locomotory circuit

Diverse environmental cues sensed by the sensory neurons are processed and integrated at the interneurons. The processed information reaches the command interneurons, the premotor neurons, that decide the direction of locomotion and manifest the outcome at the neuromuscular junction by coordinated action of cholinergic and GABAergic motor neurons synapsing onto the body wall muscles. The alternating waves of contraction and relaxation along the body of the animal drives locomotion in *C. elegans* (Adapted from Thapliyal & Babu, 2018)

explore this idea, *C. elegans* strains expressing varying levels of A β were generated using two different pan-neuronal promoters, *rgef-1* and *snb-1* (Chapter 3). The variation in the A β expression in these strains may be due to the combination of the intrinsic promoter activity driving the A β expression and variation in the copy number of the A β transgene integrated by conventional transgenesis. In addition, a neuronal A β -expressing strain published during the course of this thesis was also included. This strain was previously shown to have a reduced lifespan, deficits in egg-laying and locomotory behaviours. The early onset of middle-aged behaviours in these animals correlated with metabolic decline and electron transport failure that preceded A β toxicity (Fong et al., 2016). The A β transgene copy number analysis in these strains demonstrates that transgene copy number incorporated into the transgene array is random when using transgenesis by microinjection and highlights the importance of evaluating the copy number of transgene in each independently derived transgenic strain. Furthermore, the analysis of transcript abundance by qRT-PCR shows that, the level of transgene in these strains is correlated with copy number. Therefore, the second main finding of this thesis was that increase in the concentration of A β results in an increase in the severity of the behavioural deficits such as lifespan, motility in liquid, and fecundity.

Table 6.1 shows the ranking of the A β -expressing strains according to the severity of the disease phenotype. There were notably statistically significant differences between these strains for some but not all phenotypes. Nevertheless, the A β -expressing strains have been ranked on the basis of phenotype severity, wherein 1 indicates a mild phenotype and 3 indicates a severe phenotype. This may be correlated with the levels of A β transcript abundance ranging from high to low. In addition to increased severity, the high A β -expressing strain also showed earlier onset of the chemotactic defect. However, it remains to be established if A β acts in a continuous dose-dependent manner or whether there is a threshold of A β concentration beyond which severe behavioural deficits are induced irrespective of the concentration i.e. stepwise rather than continuous dose response.

Future work could include generating several transgenic *C. elegans* strains expressing varying levels of the A β transgene to better correlate expression with the severity of the behavioural deficit. This could be achieved by using CRISPR to integrate specific number of A β transgene copies at a specific location in the *C. elegans* genome. It was also observed that there are some phenotypes, such as deficits in dopaminergic signalling, that are more sensitive to the presence of A β . Synaptic dysfunction is an early indicator of AD

and oligomeric A β may trigger this dysfunction (Selkoe and Podlisny, 2002). My results therefore provide insight into the relationship between A β toxicity and severity of the behavioural deficit.

Table 6.1: Correlation between expression levels and severity of disease phenotype

	<i>Psnb-1::</i> <i>Aβ1-42</i>	<i>Prgef-1::</i> <i>Aβ1-42</i>	<i>Punc-119::</i> <i>Aβ1-42</i>
Expression level	High	Medium	Low
Lifespan	3	2	1
Brood size	3	2	1
Egg retention	3	2	1
Chemotaxis (diacetyl)	3	2	1
Motility on solid media	3	3	1
Motility on liquid media	3	2	1
Basal slowing response	3	3	3

6.3 Different variants of A β result in specific behavioural deficits.

Studies have shown that A β peptides in the human AD brain have ragged amino- and carboxy- termini in addition the full length A β 1-42 peptide (Masters et al., 1985; Portelius et al., 2010). However, the relative importance of these A β variants in the pathogenesis of AD is relatively unexplored. Approximately, 64% of the A β peptides in the human AD brain were shown to be truncated at residue 4 (Masters et al., 1985). In an attempt to explore the nature of the A β species, the fourth chapter of the thesis focussed on 3 different species of A β . The first A β species was the truncated A β 4-42, and worms expressing this peptide showed several behavioural deficits similar to those seen in the worms expressing the A β 1-42 transgene (with a few exceptions). There was a drastic reduction in brood size, which may be indicator of decline in overall health. In contrast, the A β 4-42-expressing strain performed better in terms of motility and in its ability to sense diacetyl. The differences in the physiochemical properties of the two A β peptides could possibly lead to specific differences in behavioural deficits. A key double transgenic strain expressing both the A β 1-42 and A β 4-42 would be beneficial to see if there was synergy between the two peptides.

The second A β species studied was the mouse A β . Mice do not accumulate amyloid, which suggests that mouse A β is not as intrinsically pathogenic as the human A β peptide. Moreover, transgenic mouse models, such as such as Tg2576 (9) and APP^{swe}/PS1^{dE9} (APP/PS1), accumulate A β variants distinct from those found in the human AD brain (Kalback et al., 2002). There were clearly defined behavioural differences in the mouse A β - and human A β -expressing strain. The mouse A β -expressing strain did not show any behavioural differences relative to the control, which may be attributed to either the low *in vivo* toxicity of the peptide or to the low copy number of the transgene in this strain.

Another A β species that has been described contains a G37L substitution in the full length A β 1-42 peptide. The “glycine zipper” motifs at the C-terminal of A β (amino acid residues 24-39) are known to play an important role in oligomerization and toxicity in *C. elegans*; hence, amino acid substitutions such as G37L ameliorate A β toxicity when expressed in cell culture or *C. elegans* body wall muscles (Fonte et al., 2011). Transgenic *C. elegans* strains were generated co-expressing the full length A β 1-42 and the A β 1-42G37L in the neurons and were expected to show reduction in the severity of the behavioural phenotype in comparison to the strain expressing only A β 1-42. Although these new strains did not show reduction in A β toxicity *in vivo*, there were differences in behavioural phenotypes observed when the A β 1-42 transgene expression was driven by pan-neuronal promoters, indicating differences in the timing and level of transgene expression. Moreover, the copy number of the A β 1-42G37L was extremely high and variable in these strains. The ‘variation’ in copy number may either reflect real heterogeneity in copy number or that the copy number assay has reached its limit of linearity in the correlation between PCR signal and copy number. As mentioned above, the variation in number of copies of the transgene randomly integrated into the *C. elegans* genome is a limitation of conventional transgenesis. One possible way to circumvent this problem of high copy number variation would be to decrease the concentration of the plasmid used for microinjections. Different concentrations of the plasmid and different promoters could be used to obtain an allelic series of transgene expression which would allow more sophisticated study of the biology. Alternatively, arrays containing specific number of A β copies could be engineered and CRISPR technology employed to knock these arrays into a specific location in the *C. elegans* genome. Although it was observed that the A β expression levels were much less variable in these strains, it would be beneficial to determine the relative expression of the two A β transgenes in these strains by RT-qPCR.

In the human AD brain, there is a spectrum of A β peptides expressed in different concentrations and ratios, which make study of the *in vivo* toxicity of these peptides complex. The preliminary evidence from these transgenic strains suggests that *C. elegans* can be utilized to reconstruct the complexity in a much more controlled fashion, by not only exploring the biological properties of a single peptide in isolation but also building the complexity of the system one component at a time to determine the effects of interactions between different peptides.

6.4 Phenotypic impact of A β expression in different genetic background.

Although *C. elegans* has most of the components of the APP processing pathway, it lacks the β -secretase, the A β domain, and therefore endogenous A β . Using genetic tools in *C. elegans*, it is possible to study different aspects of the disease-causing APP pathway by expressing A β and mutating different genes to observe their effects on the *in vivo* toxicity of A β . The ability to examine these effects in the absence of endogenous factors is a key benefit of using *C. elegans*. For example, in addition to A β and tau that are implicated as major drivers in the pathogenesis of the disease, there are other relatively minor players and modifiers in humans such as the apolipoprotein E gene. Because of the homology between humans and *C. elegans*, it is possible to manipulate other components of the genetic background. For this study (Chapter 5), the *C. elegans* tau ortholog, *ptl-1*, was chosen because this would presumably be an important gene known to interact with A β . It is possible that tau facilitates the pathogenic effects of A β in AD. Although the *ptl-1* null strain shows neuronal deficits such as reduced sensitivity to sensory stimuli, the development of abnormal structures called neuronal blebbing with age, *ptl-1* is not essential for the worms (Chew et al., 2013; Gordon et al., 2008). Tau can contribute to the pathogenesis of the disease either by gain- or loss- of function effects. To study *in vivo* effects of tau associated with gain of function, *C. elegans* strains described previously express both tau and A β in the nervous system (Fang et al., 2019). The *C. elegans* strain described here is the first strain showing the *in vivo* effects of A β associated with tau loss of function. Expressing the A β in a *ptl-1* null mutant background showed reduction in longevity, drastically reduced brood size, and impaired motility in solid and liquid media. Future work can involve expressing the human tau at a range of levels in a *ptl-1* null background along with A β also being expressed at a range of levels, to determine which

is the 'upstream driver' and which is the 'downstream potentiator'. In addition, there is a possibility of creating worm/human chimeras of the tau gene given that there are two distinct domains in PTL-1: one that is conserved (MT binding) but also one that is divergent. This work also highlights that differences in genetic background can play an important role in the development of AD.

6.5 Conclusions and future prospects

The body of work presented in this thesis demonstrates the feasibility of *C. elegans* as an *in vivo* model to investigate different facets of AD. A β expression in the *C. elegans* nervous system gives rise to a complex pleiotropy of effects on *C. elegans* biology, including reproduction, motility, sensory processes, and all these processes have been affected to a lesser or greater extent. Neuronal health is an aspect of overall physiological health and thus it is not surprising that neurodegenerative conditions will have pleiotropic phenotypes that are not mediated directly by neurons. The challenge is to uncover the biology that links them. For instance, neuronal dysfunction affects fecundity or lifespan, which are two of the most fundamental fitness parameters. There undoubtedly is a link, and the data shown here support the existence of that link, but do not shed light on the nature of the link. Therefore, the next step would be to determine the event that is triggered by neuronal A β expression that ultimately leads to those pleiotropic phenotypes, and how that shared trigger or initiation event is an A β -related function and to determine the phenotype specific downstream events that lead to specific behavioural deficits. The statistical testing has clearly shown that there is an earlier onset of age-related decline in phenotypes in the A β expressing strains. However, it is difficult to analyse rate of disease progression in these strains as the data acquired do not allow distinction between the rates of age-related decline. Overall, all the strains show age-related decline regardless of genotype, particularly between Day 8 and Day 12. Therefore, the utility of these models is to investigate the mechanism of disease onset by determining how A β initiates neuronal decline. This will also aid in understanding disease progression, identifying the determinants that may be common between initiation and progression of the disease, which may ultimately allow the identification of a phenotype that is predictive of a therapeutic outcome in humans.

The *C. elegans* model described here has a fair chance of making relevant progress in AD research. In support of this idea, the critical next steps are outlined below.

1. A β expression has been validated at transcript level in these strains. Hence the next step would be to perform proteomic analysis to determine if the A β peptide being expressed is processed correctly.
2. Measure the extent of neurodegeneration in these transgenic strains. *C. elegans* is optically transparent and crossing the A β -expressing strains with GFP and other reporter strains would reveal where neurodegeneration occurs. Previous studies have shown age-associated neurodegeneration in a *C. elegans* AD model by co-expressing A β and GFP in the glutamatergic neurons. Of those, five distinct neurons present in the tail were shown to degenerate with age in response to the expression of A β (Serrano-Saiz et al., 2013). This will make it possible to look at early events in the disease — such as initiation and progression — rather than directly looking the end point, neuronal death. In addition, optogenetic methods such as calcium imaging of neurons can be used to test if the neurons function normally. Functional reporter studies are more likely to identify early events that lead to dysfunction prior to cell death.
3. Another sign of age-related decline is mitochondrial dysfunction. Therefore, the next step would be to assess the mitochondrial function in these strains by measuring mitochondrial respiration using Seahorse respirometers. Earlier work suggests that A β contributes to mitochondrial dysfunction by causing impairment of the electron transport chain complexes and elevation of reactive oxygen species (Moreira et al., 2010; Ng et al., 2014).
4. Initiate genetic screens to identify novel interactors that suppress the A β -associated phenotype. Cohen et. al used the muscle expressing A β model to investigate the roles of two important modulators of *C. elegans* lifespan, the insulin growth factor 1 like signalling (ILLS) pathway and heat shock factor (HSF) in A β toxicity. When *daf-2* was mutated in the A β -expressing strain, it not only caused an increase in the lifespan but also attenuated the paralysis phenotype suggesting molecular links between aging and A β toxicity (Cohen et al., 2006).
5. Employ these strains in high-throughput drug screens. Other *C. elegans* neurodegeneration models have been used to test drug efficacy. For instance, the effects of the *Ginkgo biloba* extract on A β toxicity was tested in a neuronal A β

model (Wu et al., 2006). When treated with PBT-2, a drug assumed to act on A β via modulating its metal ion binding interactions, the muscle A β -expressing strain showed significant and robust reduction in the A β -induced paralysis phenotype (McColl et al., 2012).

In summary, this new *C. elegans* toolkit developed here will aid in identifying the cellular and molecular mechanisms of disease pathogenesis and drive future pharmaceutical interventions.

Supplementary Information

Supplementary tables

Supplementary Table 1: List of common reagents used in the study

Name	Composition
LB media	Add 10 g Bacto-tryptone, 5 g yeast extract and 5 g NaCl in 1 litre of distilled water. Sterilize by autoclaving.
LB agar	Add 10 g Bacto-tryptone, 5 g yeast extract and 5 g NaCl, 15 g agar and 1 ml 1M NaOH in 1 litre of distilled water. Sterilize by autoclaving.
LB glycerol	LB media + 30% Glycerol. Sterilize by autoclaving.
Ligation reaction (Promega)	2X Rapid ligation buffer, 1 μ l T4 DNA ligase, add the vector and insert to make up the volume of the reaction mix to 10 μ l. (Insert: Vector ratio was adjusted to 3:1). Ligation mix was incubated at 25 °C for 30 min. Transformation of <i>E.coli</i> competent cells Top10 was carried out with 1-2 μ l of the ligation mix using standard protocols.
Nematode growth medium (NGM)	Add 3 g NaCl, 2.5 g peptone and 17g agar in 975 ml water. Sterilize by autoclaving. Allow the media to cool to 55 °C, then sterilely add 1 ml cholesterol (5 mg/ml), 1 ml 1M MgSO ₄ , 1 ml 1M CaCl ₂ and 25 ml 1M Potassium phosphate buffer pH 6.0. Pour media into plates.
M9 buffer	22 mM KH ₂ PO ₄ , 42 mM Na ₂ HPO ₄ , 86 mM NaCl and 1 mM MgSO ₄ . Sterilize by autoclaving.
S buffer	6.5 mM K ₂ HPO ₄ , 43.5 mM KH ₂ PO ₄ , 100 mM NaCl . Sterilize by autoclaving
S basal	5.85 g NaCl, 1 g K ₂ HPO ₄ , 6 g KH ₂ PO ₄ , 1 ml cholesterol (5 mg/ml in ethanol), H ₂ O to 1 litre. Sterilize by autoclaving.
Worm Freezing media	S buffer + 30% glycerol. Sterilize by autoclaving.
Single worm lysis buffer	985 μ l direct PCR lysis reagent (mouse tail) from Viagen Biotech and 15 μ l Proteinase K (20 mg/ml) from Roche

Supplementary Table 2: List of Primers used in the study

Gene name	Forward Primer (5'-3')	Reverse Primer (5'-3')	Amplicon size (bp)
<i>rgef-1</i> promoter	GAATCTGCAGC GAGTCAACTGA AATCCG	TAATCCCGGGCG TCGTCGTCGTCG ATGC	2670
<i>rgef-1</i> promoter internal primers	GGAGAGAAAGA GGACACAAATA AG	GGTCTCGAGTGT ATATGATCTT	1010
<i>snb-1</i> promoter	GGCGTCTAGAA AATATTAATTTA GTGATGTCAA	ATTTCCCGGGGA TGTCGTCAAGAT GGTCTTA	2023
<i>Y45F10D.4</i>	CGAGAACCCGC GAAATGTCGGA	CGGTTGCCAGGG AAGATGAGGC	191
<i>cdc-42</i>	CTGCTGGACAG GAAGATTACG	CTCGGACATTCT CGAATGAAG	111
Amyloid β 42	AGAATTCCGAC ATGACTCAGG	CACCATGAGTCC AATGATTGC	108
M13 Reverse Primer	N/A	GCGGATAACAAT TTCACACAGG	N/A
<i>unc-54</i> 3'UTR_seq	N/A	TAGAAGTCAGAG GCACGG	Sequencing primer
PTL-1_mutant (Gordon et al., 2008)	TTTTCCGGAGGT TGCAGTAGAAC	GGCAAATTGTGA TCCAGTGATGG	464
PTL-1_WT (Gordon et al., 2008)	TTTTCCGGAGGT TGCAGTAGAAC	GCGTTGAGACGA GGGAGTAG	735

Supplementary Table 3: Details of expression plasmids used in this study

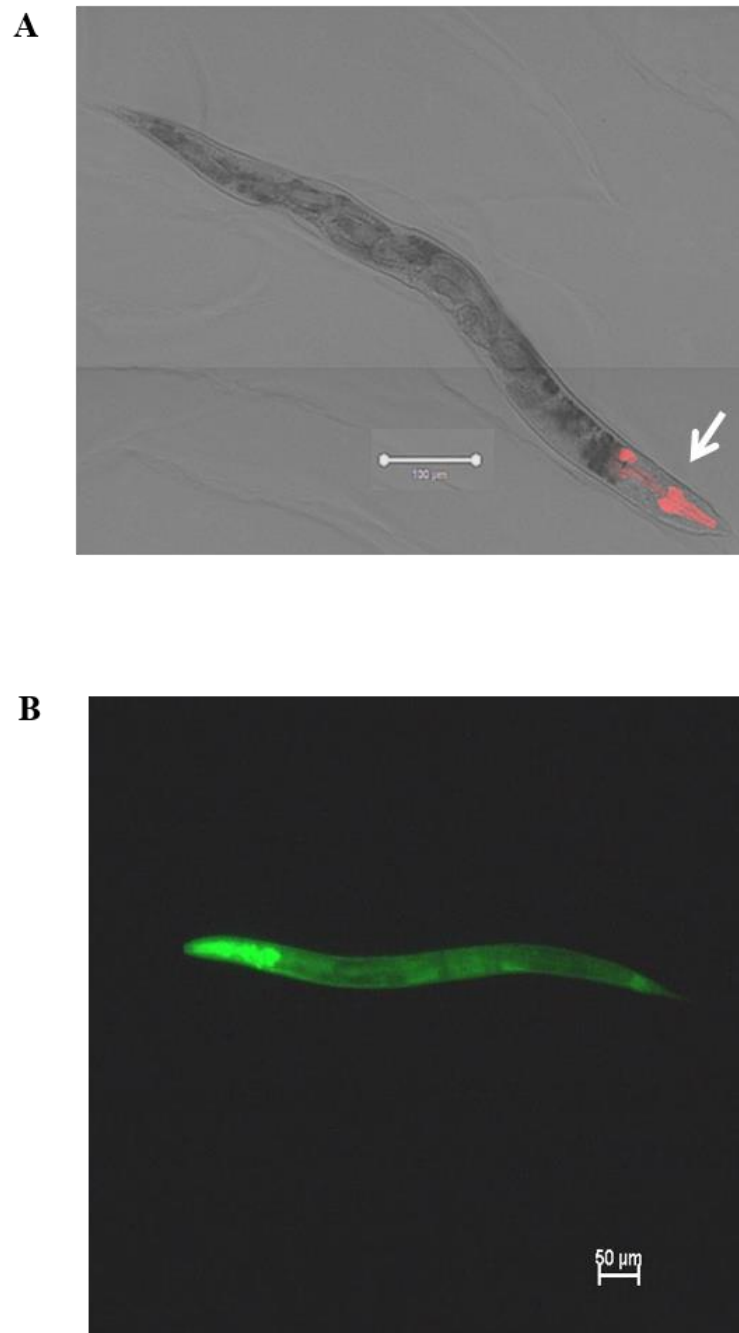
Expression plasmid	Vector backbone	Promoter	Insert	Clones confirmed by
pAB42	pPD49.26	Promoter less	A β 1-42	✓ Restriction digestion ✓ PCR ✓ Sequencing
pEXAB42	pAB42	<i>rgef-1</i> (pan-neuronal)	A β 1-42	✓ Restriction digestion ✓ PCR ✓ Sequencing
pEXGFP	pPD95.77	<i>rgef-1</i> (pan-neuronal)	GFP	✓ Restriction digestion ✓ PCR ✓ Sequencing
pEXAB442	pPD49.26	<i>rgef-1</i> (pan-neuronal)	A β 4-42	✓ Restriction digestion ✓ PCR ✓ Sequencing
pSNB1	pPD49.26	<i>snb-1</i> (pan-neuronal)	NA	✓ Restriction digestion ✓ PCR ✓ Sequencing
pSNB1GFP	pPD95.77	<i>snb-1</i> (pan-neuronal)	GFP	✓ Restriction digestion ✓ PCR ✓ Sequencing
pSNB1AB42	pAB42	<i>snb-1</i> (pan-neuronal)	A β 1-42	✓ Restriction digestion ✓ PCR ✓ Sequencing
pSNB1AB442	pSNB1	<i>snb-1</i> (pan-neuronal)	A β 4-42	✓ Restriction digestion ✓ PCR ✓ Sequencing
pMouseAB	pSNB1	<i>snb-1</i> (pan-neuronal)	R5G,Y10F ,H13R A β 1-42	✓ Restriction digestion ✓ PCR ✓ Sequencing
pA β 42G37L	pSNB1	<i>snb-1</i> (pan-neuronal)	G37L A β 1-42	✓ Restriction digestion ✓ PCR ✓ Sequencing
pGMC104	NA	NA	A β 4-42	From Gawain
pGMC107	NA	NA	G37L A β 1-42	From Gawain
pGMC110	NA	NA	R5G,Y10F ,H13R A β 1-42	From Gawain
pCL354	pPD49.26	<i>unc-54</i> (body wall muscle)	A β 1-42	N/A
pAV1944	pPD49.26	<i>myo2</i> (pharyngeal muscles)	<i>mCherry</i>	N/A

Supplementary Table 4: Details of transgenic *C. elegans* strains generated in this study

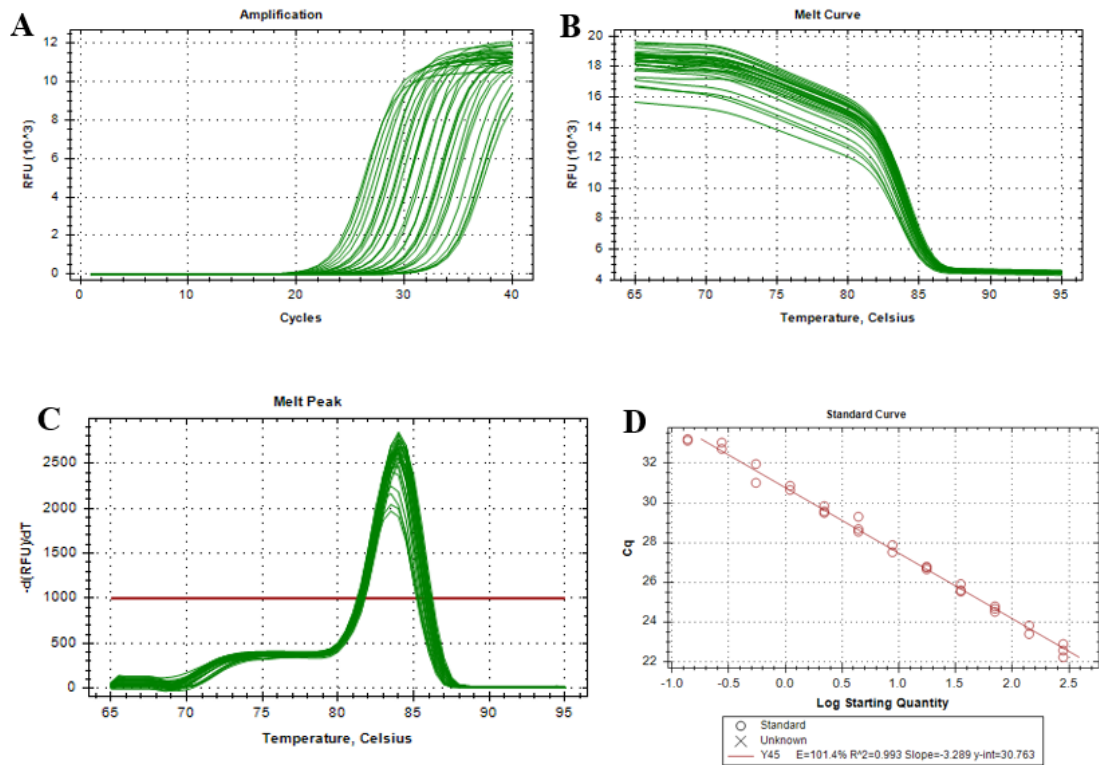
Strain name	Conc. of expression plasmid (ng/ μ l)	Conc. of pAV1944/pAV119 (ng/ μ l)	Conc. of genomic DNA (ng/ μ l)
GMC205	NA	2.5	50
WG643	pSNB1AB42 - 25	2.5	50
WG663	pEXAB42 - 25	2.5	50
WG709	pEXAB442 - 10	2.5	100
WG724	pMouseAB42 -25	2.5	50
WG657	pA β 42G37L - 25	2.5	50
WG731	NA	2.5	50
WG625	pEXGFP - 50	NA	50
WG700	pSNB1GFP - 50	NA	50

Supplementary Table 5: List of transgenic *C. elegans* strains used in the study

Strain name	Genotype
GMC205	<i>Pmyo-2::mCherry</i>
WG731	<i>Pmyo-2::mCherry</i>
WG643	<i>Psnb-1::huAβ1-42 + Pmyo-2::mCherry</i>
WG663	<i>Prgef-1::huAβ1-42 + Pmyo-2::mCherry</i>
WG709	<i>Prgef-1::huAβ4-42 + Pmyo-2::mCherry</i>
WG724	<i>Psnb-1::mouseAβ1-42 + Pmyo-2::mCherry</i>
WG657	<i>Psnb-1::huAβ1-42G37L+ Pmyo-2:GFP</i>
WG664	[<i>Prgef-1::huAβ1-42 + Pmyo-2::mCherry</i>] + [<i>Psnb-1::huAβ1-42G37L + Pmyo-2:GFP</i>]
WG666	[<i>Psnb-1::huAβ1-42 + Pmyo-2::mCherry</i>] + [<i>Psnb-1::huAβ1-42G37L + Pmyo-2:GFP</i>]
WG673	<i>Psnb-1::huAβ1-42 + Pmyo-2::mCherry; ptl-1</i>
GMC296	<i>Punc-54::huAβ1-42 + Pmyo-2::mCherry</i>
GRU101	<i>gnals1 (Pmyo-2::YFP)</i>
GRU102	<i>gnals2 (Pmyo-2::YFP + Punc-119::huAβ1-42)</i>

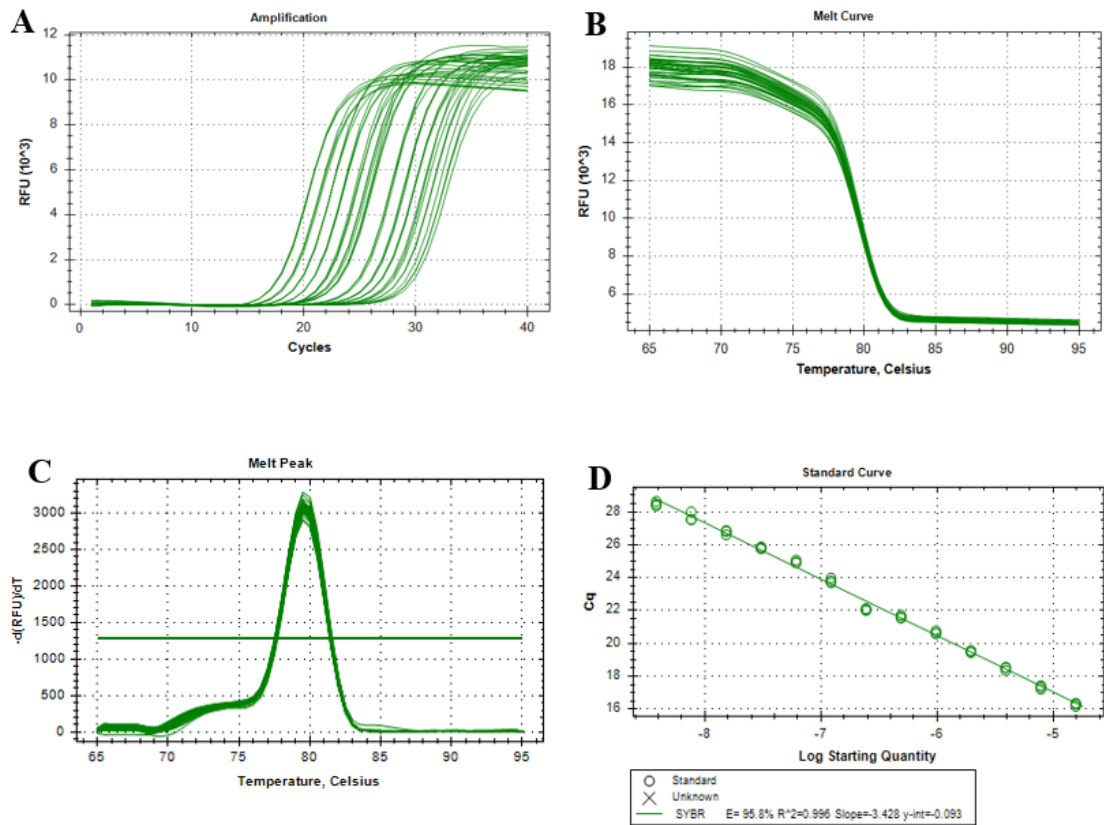
Supplementary information for Chapter 2**Supplementary Figure 2.1: Fluorescence images of the GFP expressing transgenic *C. elegans* strain generated in this study.**

A) A β -expressing transgenic strain expressing mCherry in the pharyngeal muscles (as indicated by the arrow). Scale bar = 100 μ m. B) Transgenic strain WG700 expressing GFP driven by pan-neuronal *snb-1* promoter. GFP expression is evident in head and tail neuron regions. The GFP expression on the body of the worm indicates network of the nerves running along the length of the nervous system. Scale bar = 50 μ m.



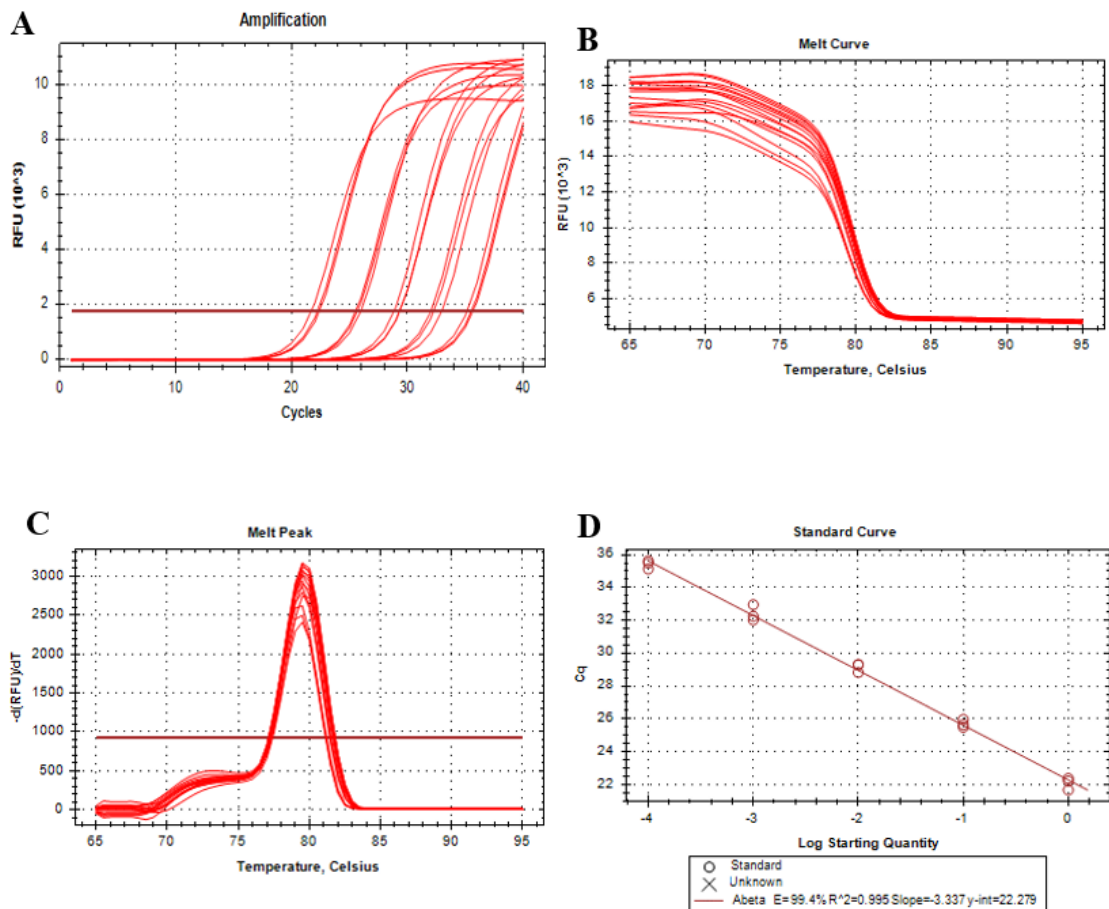
Supplementary Figure 2.2: Quantitative PCR to generate a standard curve for reference gene *Y45F10D.4* using *C. elegans* genomic DNA as template.

A) Amplification curves obtained using 2-fold serial dilutions of the template DNA. B) Melt curve analysis. C) Melt peak profile showing a single peak for all the reactions indicating absence of non-specific amplification. D). Standard curve generated showing reaction efficiency E of 101.4%.



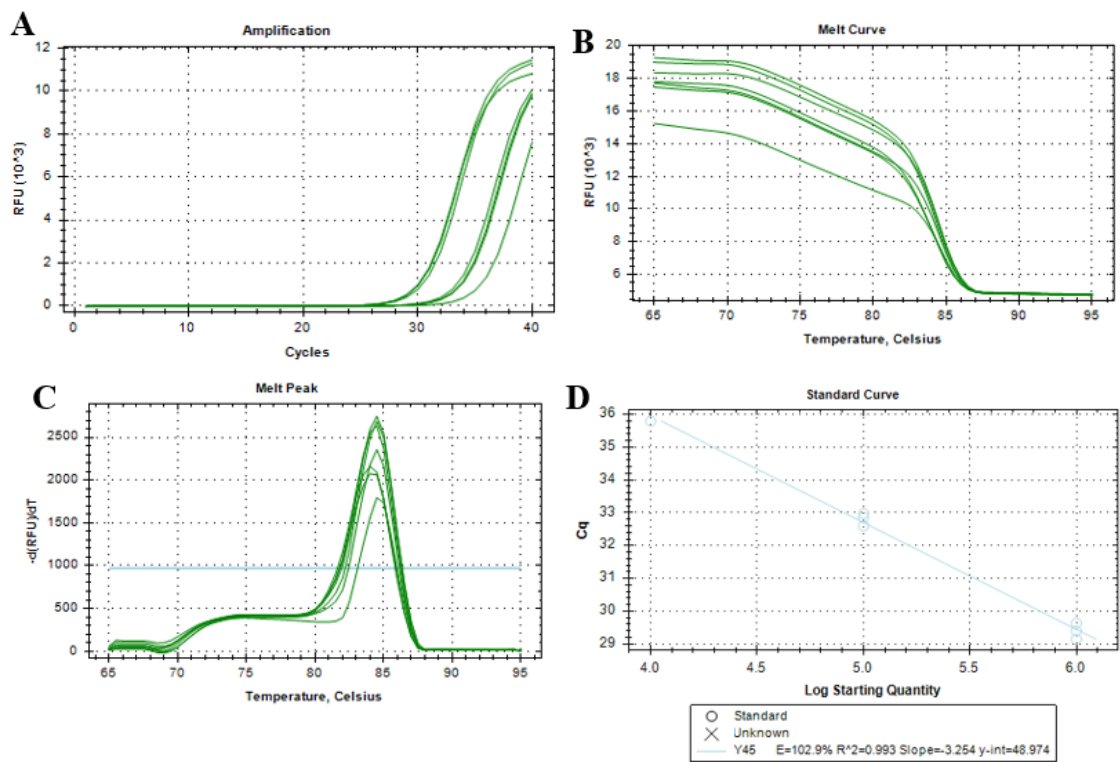
Supplementary Figure 2.3: Quantitative PCR to generate a standard curve for Amyloid β 1-42 using plasmid DNA as template.

A) Amplification curves obtained using 2-fold serial dilutions of the template DNA. B) Melt curve analysis. C) Melt peak profile shows a single peak for all reactions indicating absence of non-specific amplification. D) Standard curve generated showing the reaction efficiency E of 95.8%.



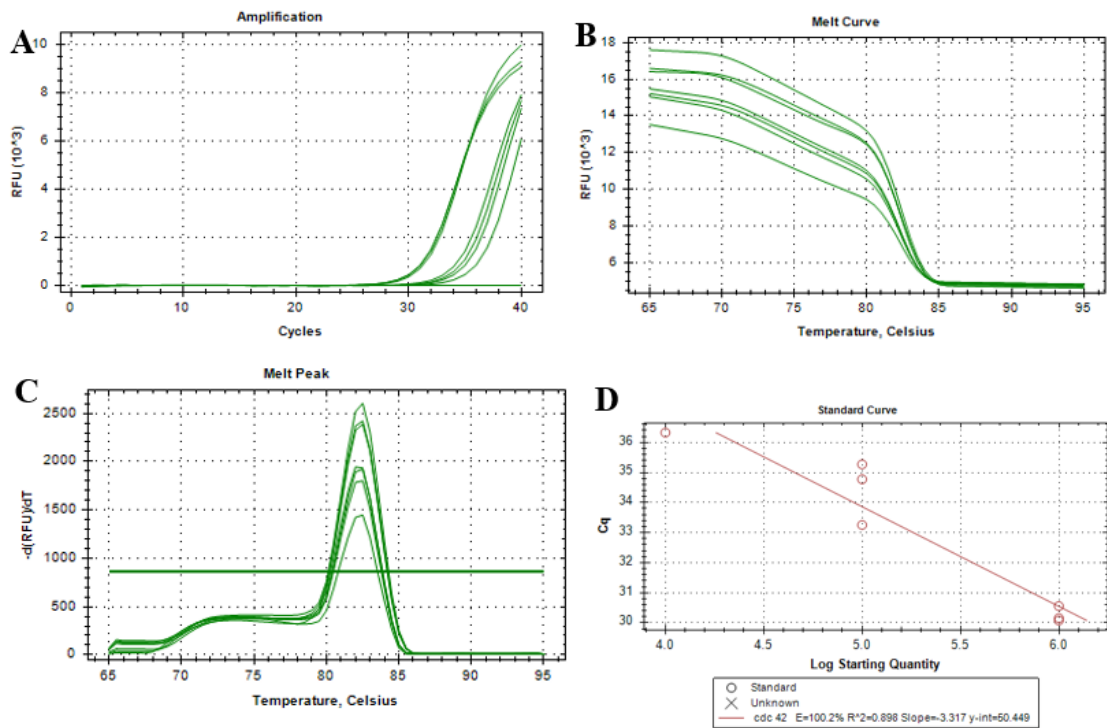
Supplementary Figure 2.4: RT-qPCR to generate a standard curve for Amyloid β 1-42 using GMC296 cDNA as template.

A) Amplification curves obtained using 10-fold serial dilutions of the template DNA. B) Melt curve analysis. C) Melt peak profile shows one single peak for all the reactions indicating absence of non-specific amplification. D). Standard curve generated showing the reaction efficiency E of 81.2%.



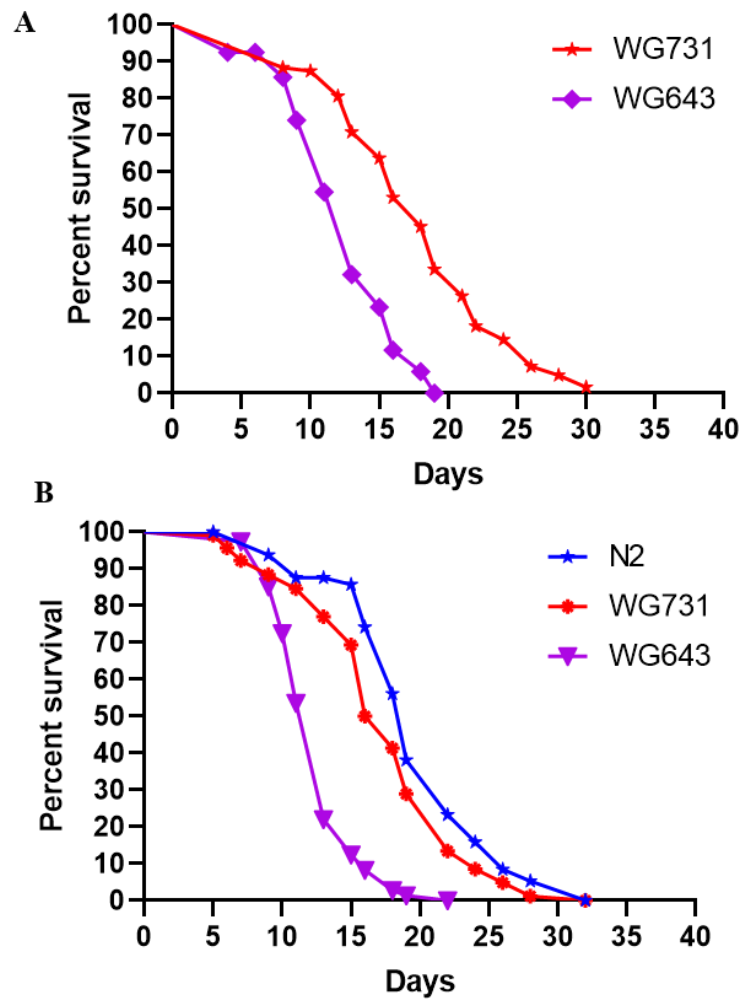
Supplementary Figure 2.5: RT-qPCR to generate a standard curve for *Y45F10D.4* using GMC296 cDNA as template.

A). Amplification curves obtained using 10-fold serial dilutions of the template DNA. B) Melt curve analysis. C) Melt peak profile shows one single peak for all the reactions indicating absence of non-specific amplification. D). Standard curve generated showing the reaction efficiency E of 102.9%.



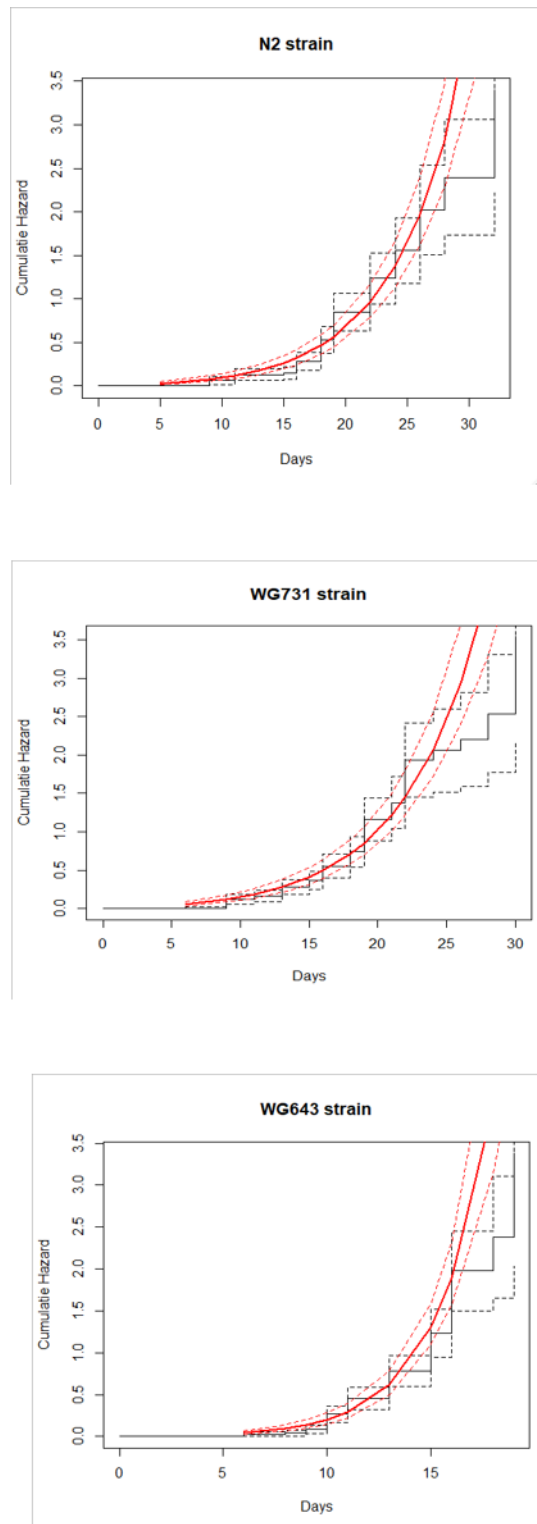
Supplementary Figure 2.6: RT-qPCR to generate a standard curve for *cdc-42* using GMC296 cDNA as template.

A). Amplification curves obtained using 10-fold serial dilutions of the template DNA. B) Melt curve analysis. C) Melt peak profile shows one single peak for all the reactions indicating absence of non-specific amplification. D). Standard curve generated showing the reaction efficiency E of 100.2%.



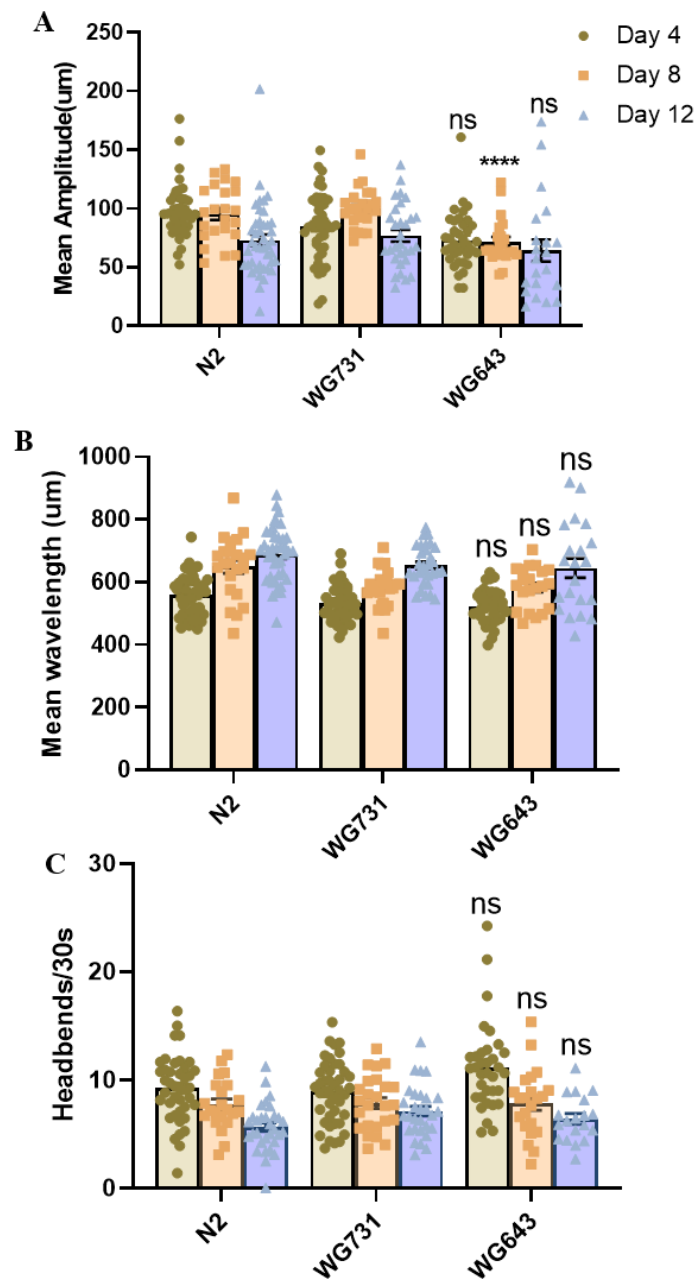
Supplementary Figure 2.7: Survival curves for the remained biological replicates.

A) Survival curve for Lifespan assay for second biological replicate (n=120 worms/replicate). B) Survival curve for Lifespan assay for third biological replicate (n=120 worms/replicate). **N2**, wild type Bristol strain; **WG731** [*Pmyo-2::mCherry*]; **WG643** [*Pmyo-2::mCherry + Psnb-1::huAβ1-42*].



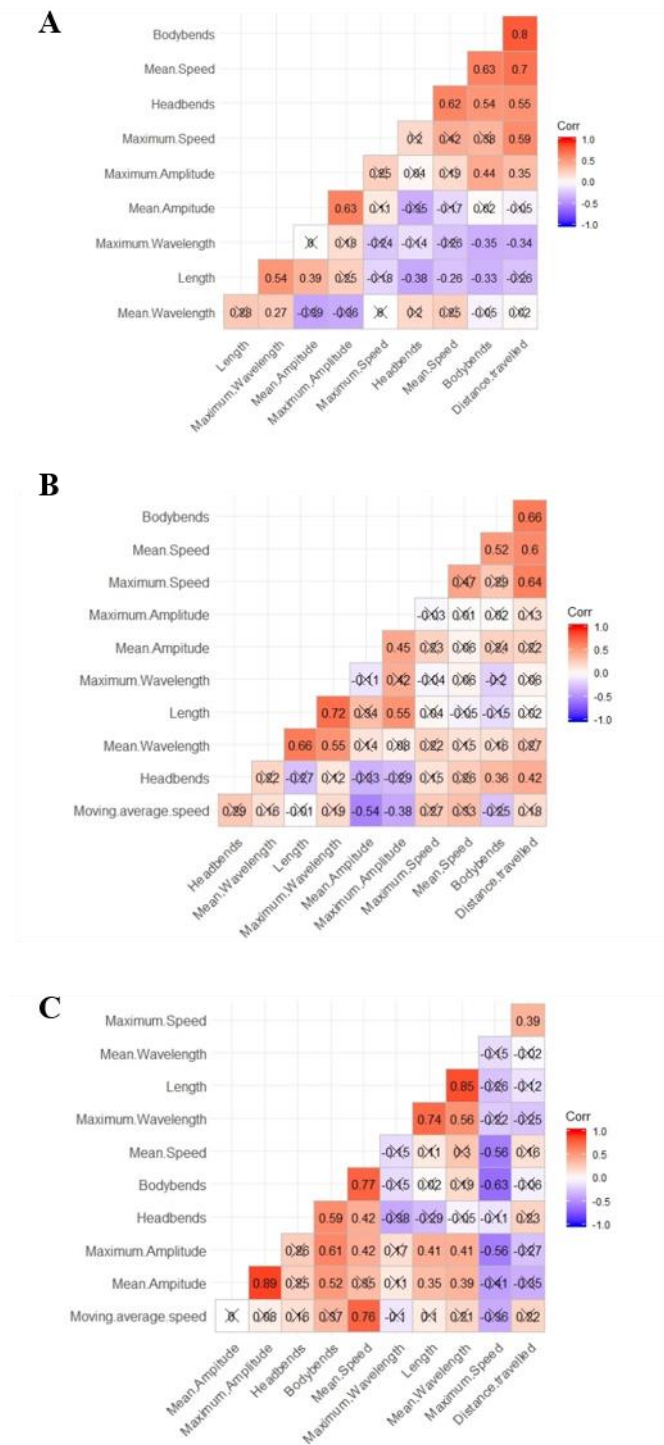
Supplementary Figure 2.8: Cumulative hazard plot derived using maximum likelihood estimate.

The Gompertz rate coefficient (G) and initial mortality rate (A) were estimated from the shape and rate of the curve respectively. The mortality rate doubling time (MRDT) was calculated using the G values.



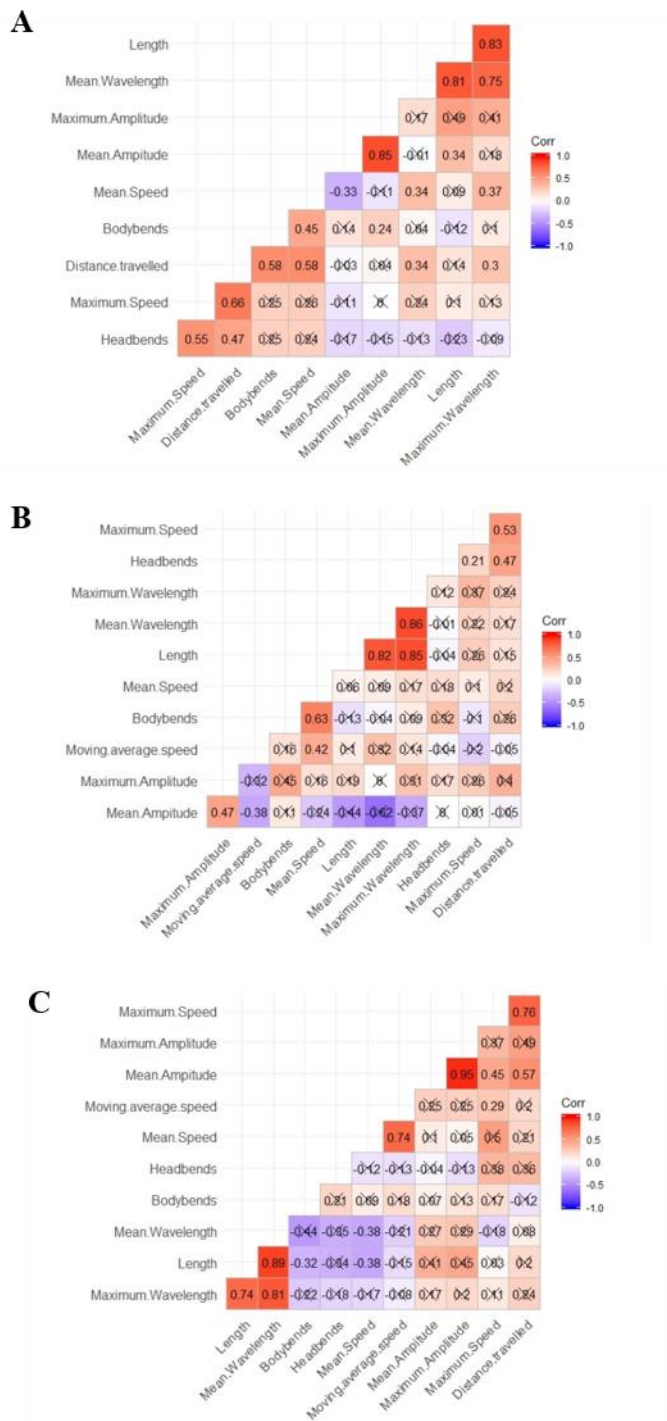
Supplementary Figure 2.9: Measurement of motility parameters of transgenic *C. elegans* strains on solid media.

A) Mean wavelength.) B) Mean amplitude. C) Head bends/30s. All data analysed by two-way ANOVA followed by post hoc Tukey multiple comparisons test. Significance values represent pairwise comparison between transgenic control WG731 and A β -expressing strain WG643 (n=3, 5-15 worms/replicate). ns not significant, *p < 0.05, **p < 0.01, ***p < 0.001. **N2**, wild type Bristol strain; **WG731** [*Pmyo-2::mCherry*]; **WG643** [*Pmyo-2::mCherry* + *Psnb-1::huA β 1-42*].



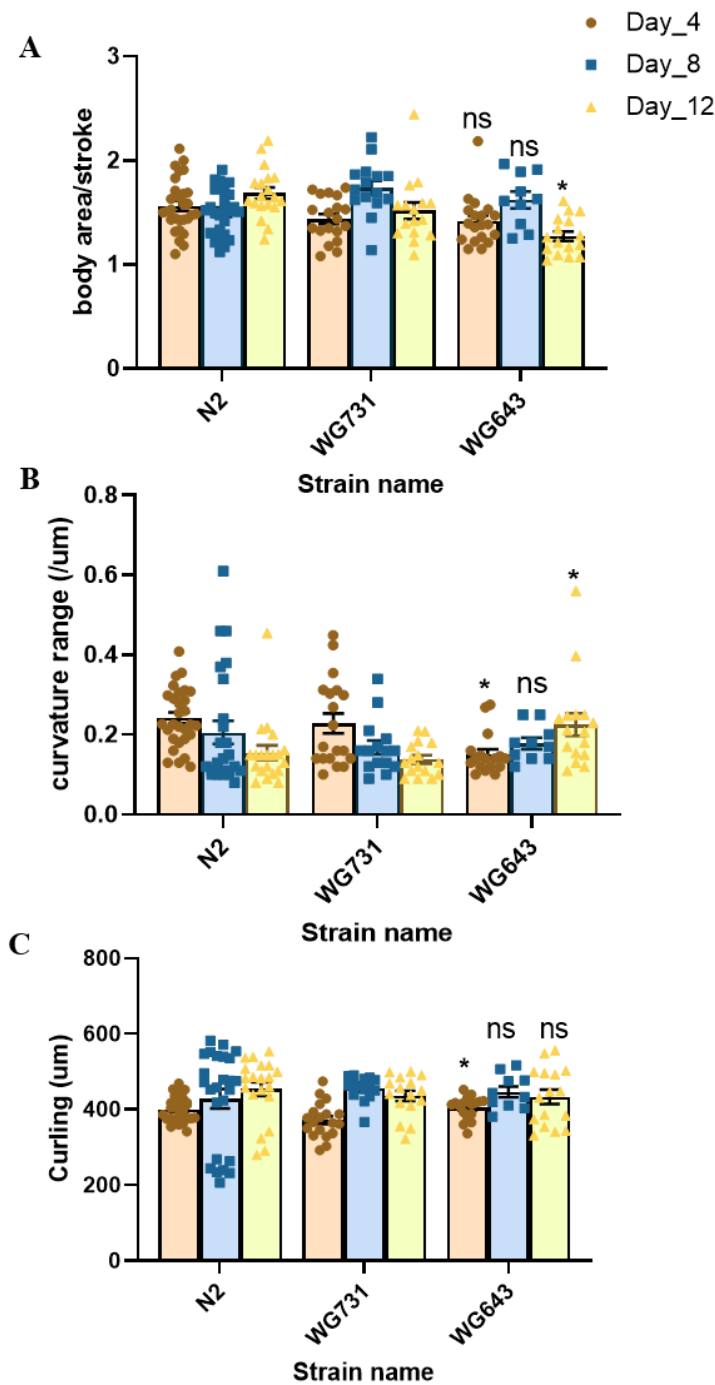
Supplementary Figure 2.10: Correlation heat map of WG731 motility parameters on solid media.

A) Day 4. B) Day 8. C) Day 12. Anything that is crossed out indicates non-significant correlations. WG731 [*Pmyo2::mCherry*].



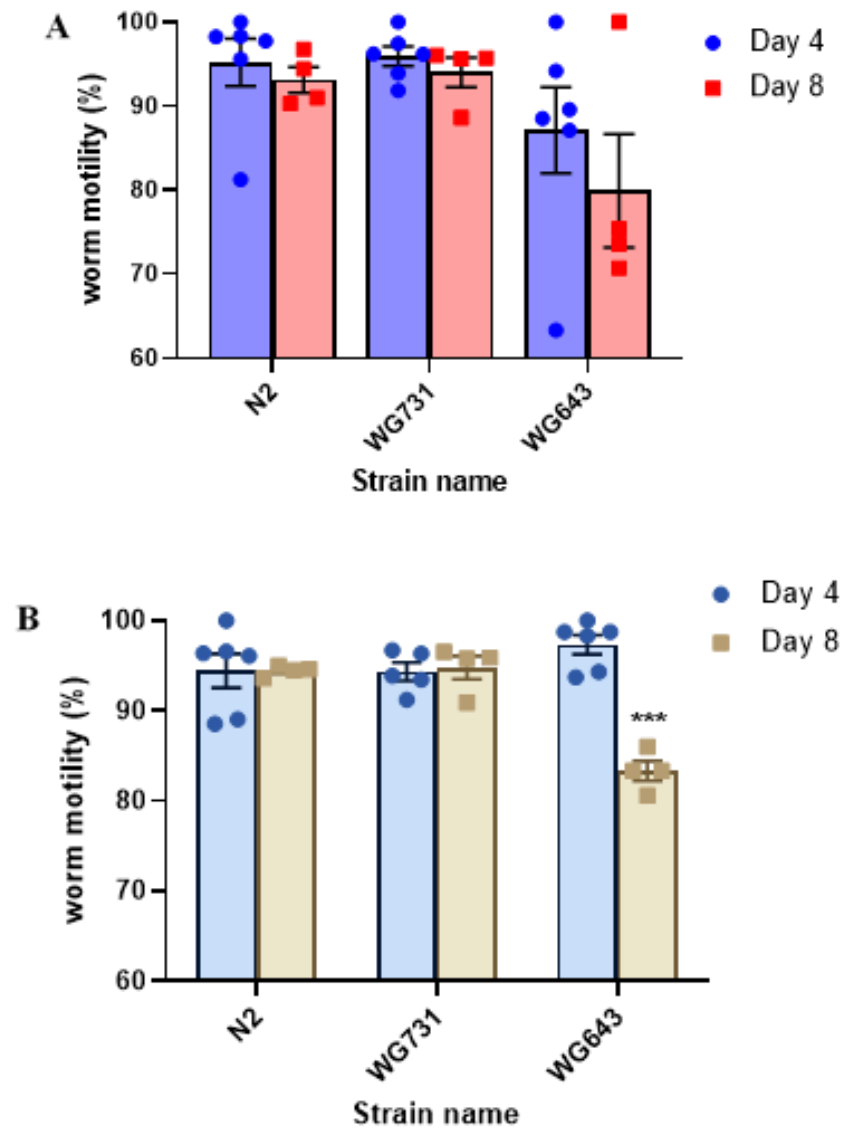
Supplementary Figure 2.11: Correlation heat map of WG643 motility parameters on solid media.

A) Day 4. B) Day 8. C) Day 12. Anything that is crossed out indicates non-significant correlations. WG643 [*Pmyo-2::mCherry* + *Psnb-1::huAβ1-42*]

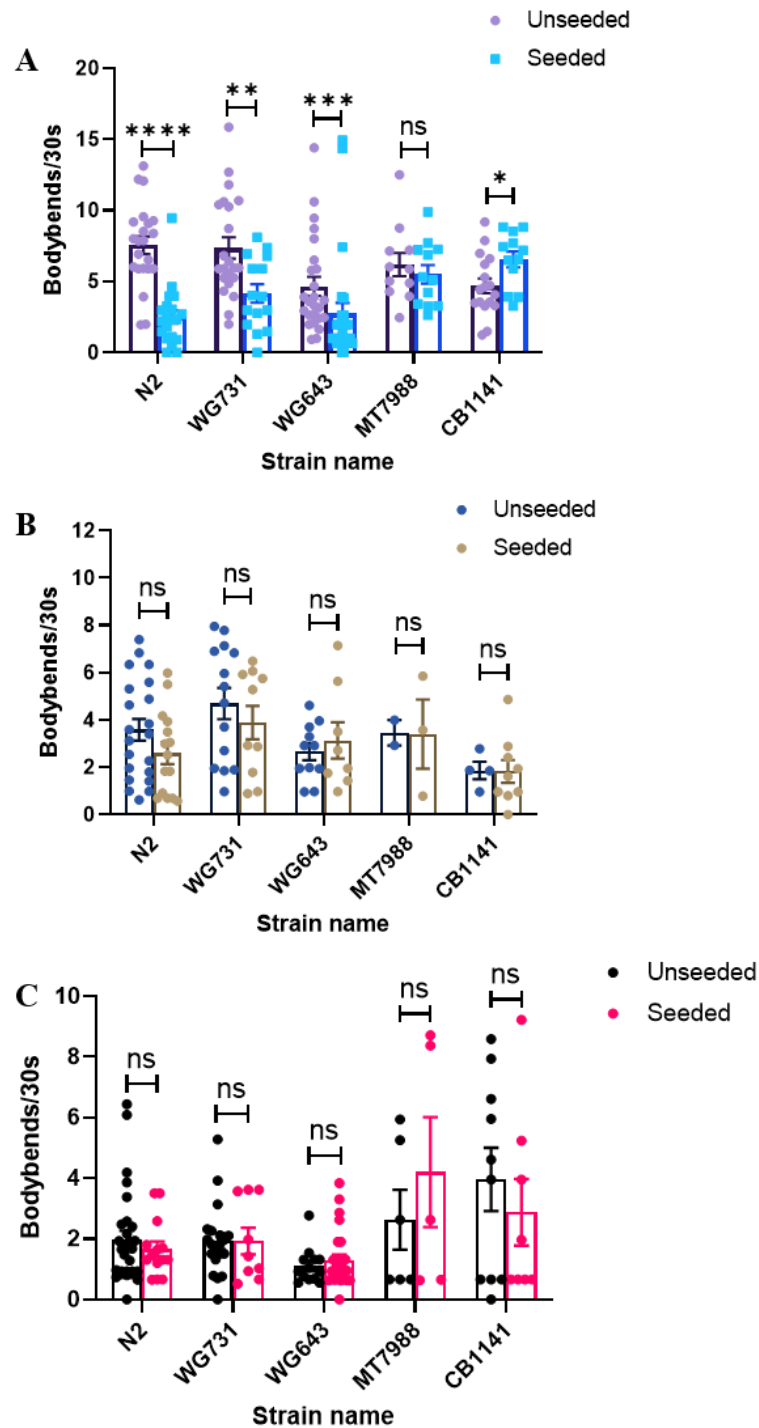


Supplementary Figure 2.12: Age-related changes in motility of transgenic *C. elegans* strains in liquid media.

A) Brush stroke (Body area/s). B) Dynamic amplitude (curvature range / μm). C) Mean waves D) Curling (μm), (n=2, 5-15 worms/replicate). All data analysed by two-way ANOVA followed by post hoc Tukey multiple comparisons test. Significance values represent pairwise comparison between transgenic control WG731 and A β -expressing strain WG643 at each timepoint. ns not significant, *p < 0.05, **p < 0.01, ***p < 0.001, N2, wild type Bristol strain ; WG731 [*Pmyo-2::mCherry*]; WG643 [*Pmyo-2::mCherry* + *Psnb-1::huA β 1-42*].



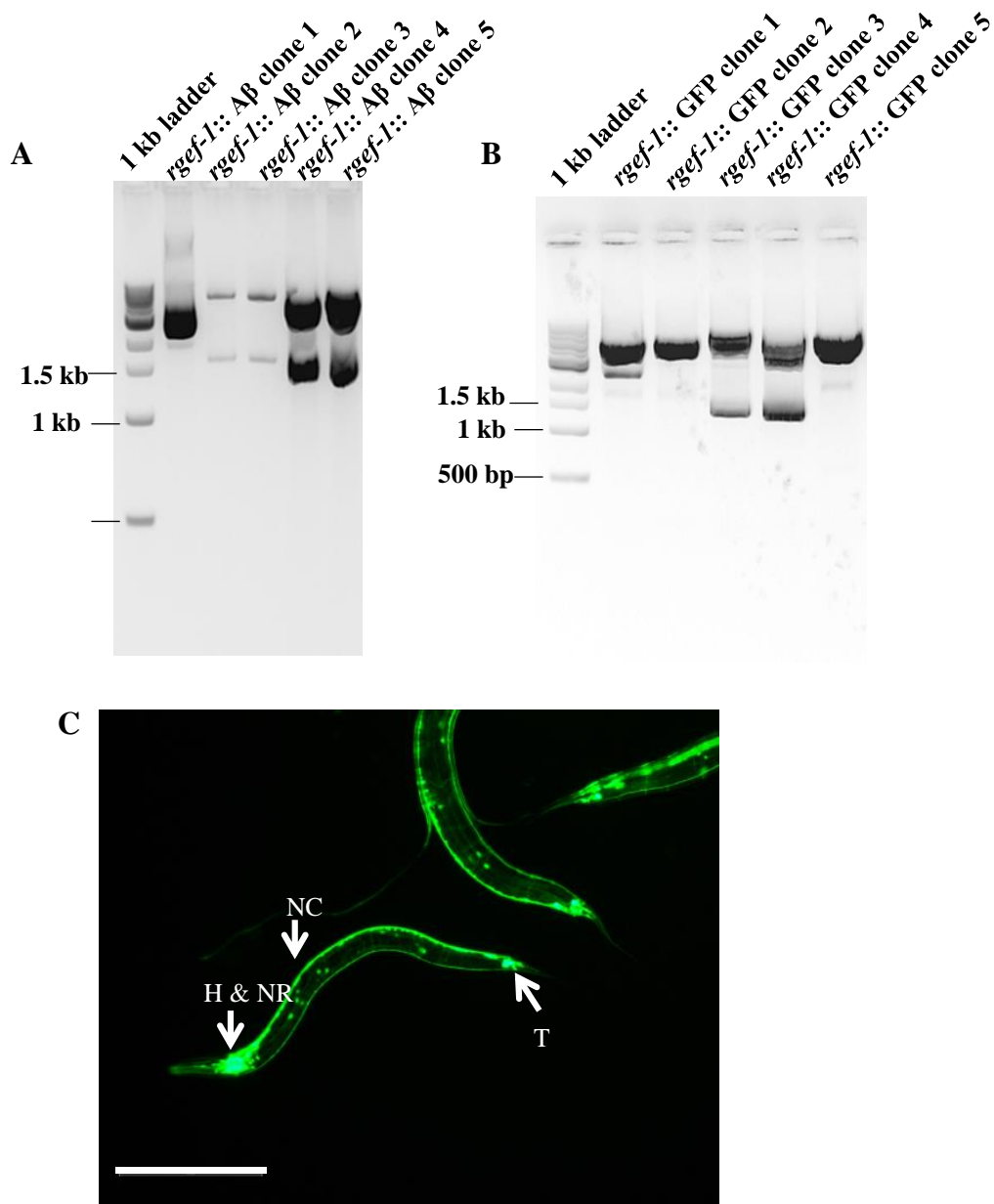
Supplementary Figure 2.13: Percentage motility of the worms on chemotaxis plates calculated as %worms moved from the origin after 1 hour of the chemotaxis assay. A) Diacetyl. B) Benzaldehyde. An unpaired t test was used to determine significance in movement between transgenic control strain WG731 and A β expressing strain WG643, ***P<0.001. N2, wild type Bristol strain, WG731 [*Pmyo-2::mCherry*]; WG643 [*Pmyo-2::mCherry* + *Psnb-1::huA β 1-42*].



Supplementary Figure 2.14: Age-related enhanced slowing response of A β expressing strain.

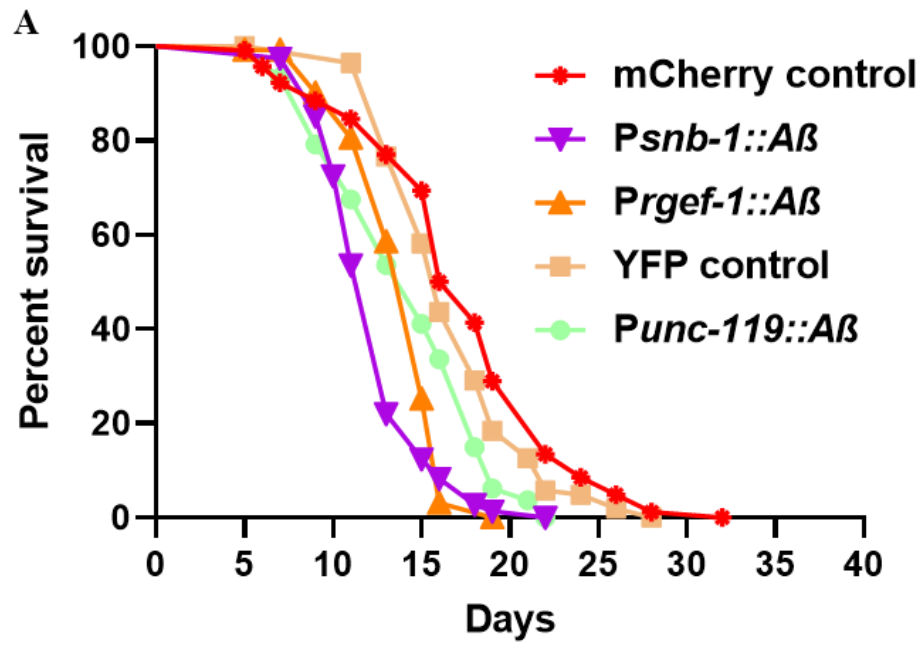
A) Day 4. B) Day 8. C) Day 12. (n = 2, 5-15 worms/replicate). An unpaired t test was performed to test for significance in slowing response, ns not significant, *p < 0.05, **p < 0.01, ***p < 0.001, ****p < 0.0001. **N2**, wild type Bristol strain; **WG731** [*Pmyo-2::mCherry*]; **WG643** [*Pmyo-2::mCherry + Psnb-1::huA β 1-42*], **MT7988** [*bas-1 (ad446)* III] (Loer & Kenyon, 1993), **CB1141** [*cat-4 (e1141)* V] (Sulston, Dew, & Brenner, 1975).

Supplementary information for Chapter 3

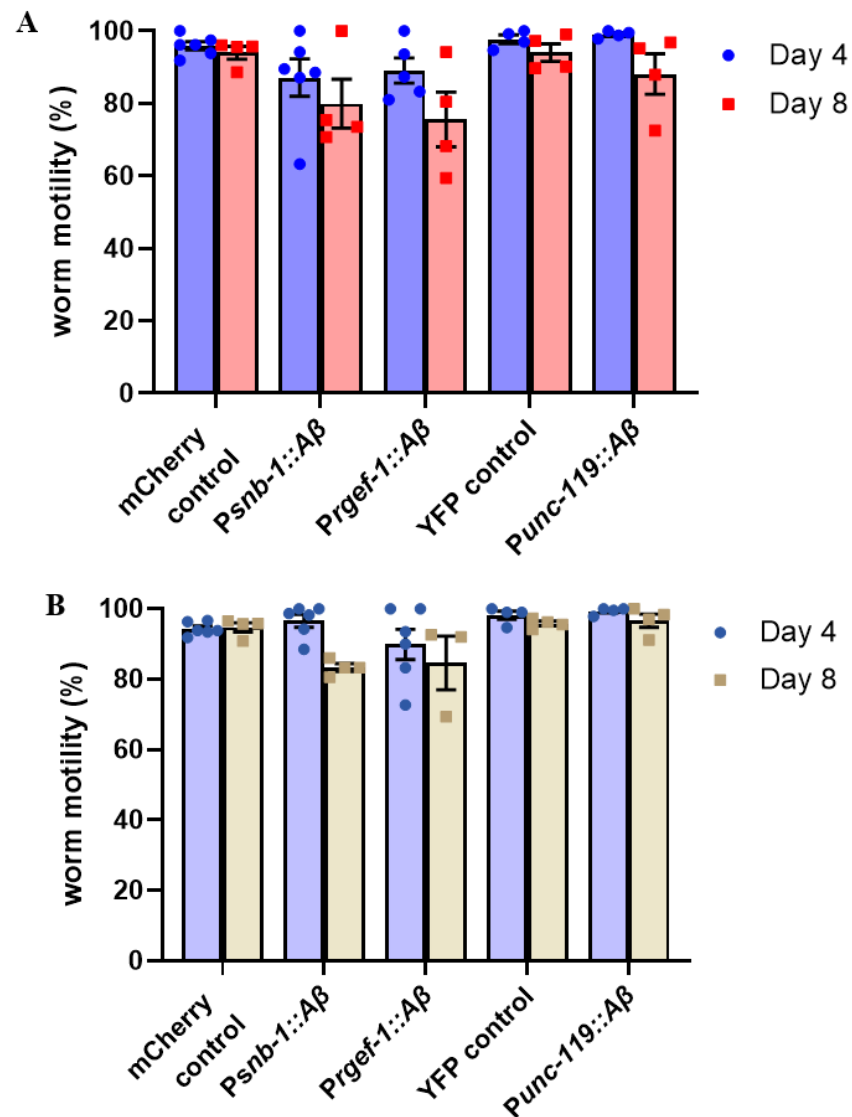


Supplementary Figure 3.1: Confirmation of transgene expression clones and fluorescence images of the pan-neuronal GFP expressing transgenic *C. elegans* strains

(A, B) Restriction enzyme digestion of pAB42*rgef-1* and pPD95.77*rgef-1* clones using Pst I and Xho I shows release of partial *rgef-1* fragment at expected size of 1560 bp. Xho I has an internal site in the *rgef-1* promoter fragment and therefore cuts within the fragment. C) Transgenic strain WG625 expressing GFP throughout the nervous system driven by *rgef-1* promoter. GFP expression is evident in head and nerve ring (H & NR), Dorsal and Ventral nerve cord (NC) and Tail neurons (T). The GFP expressing spots on the body of the worm indicate cell bodies. Scale bar = 100 μ m.

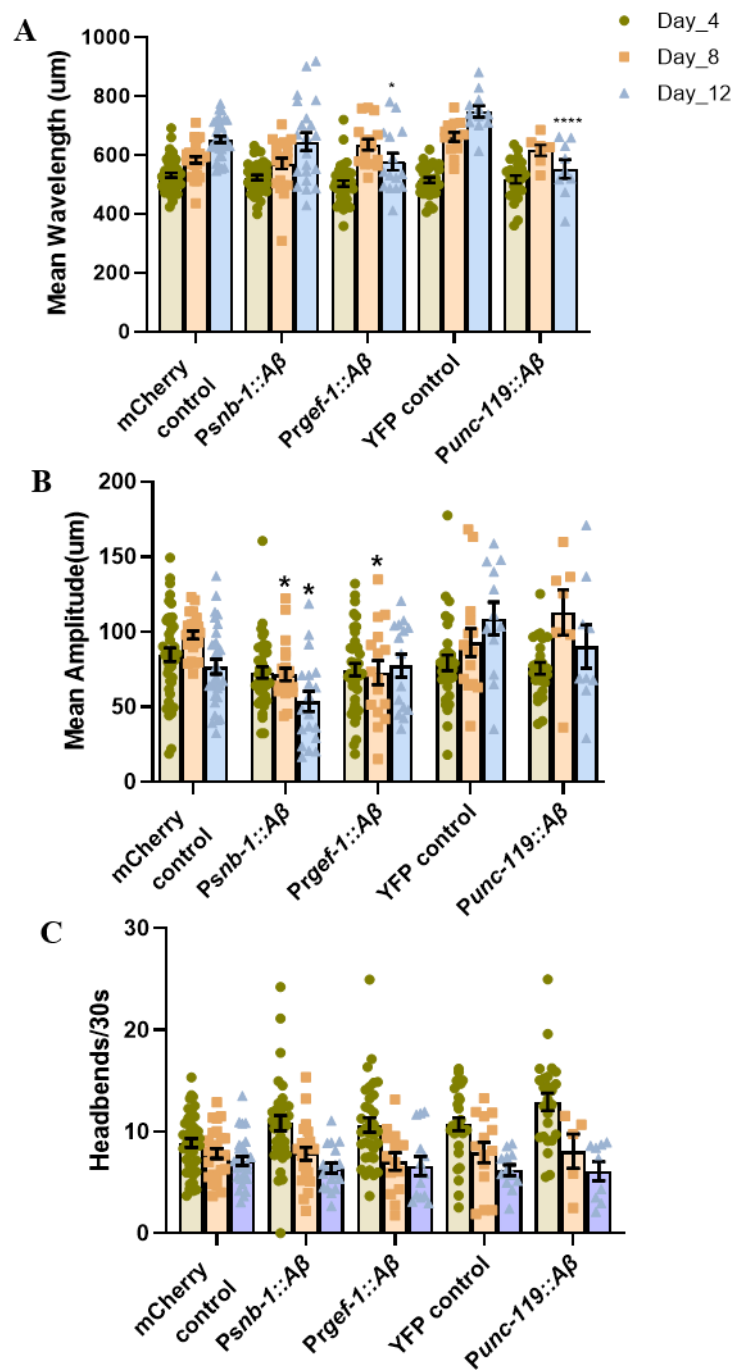


Supplementary Figure 3.2: Survival curves for the remaining biological replicates.



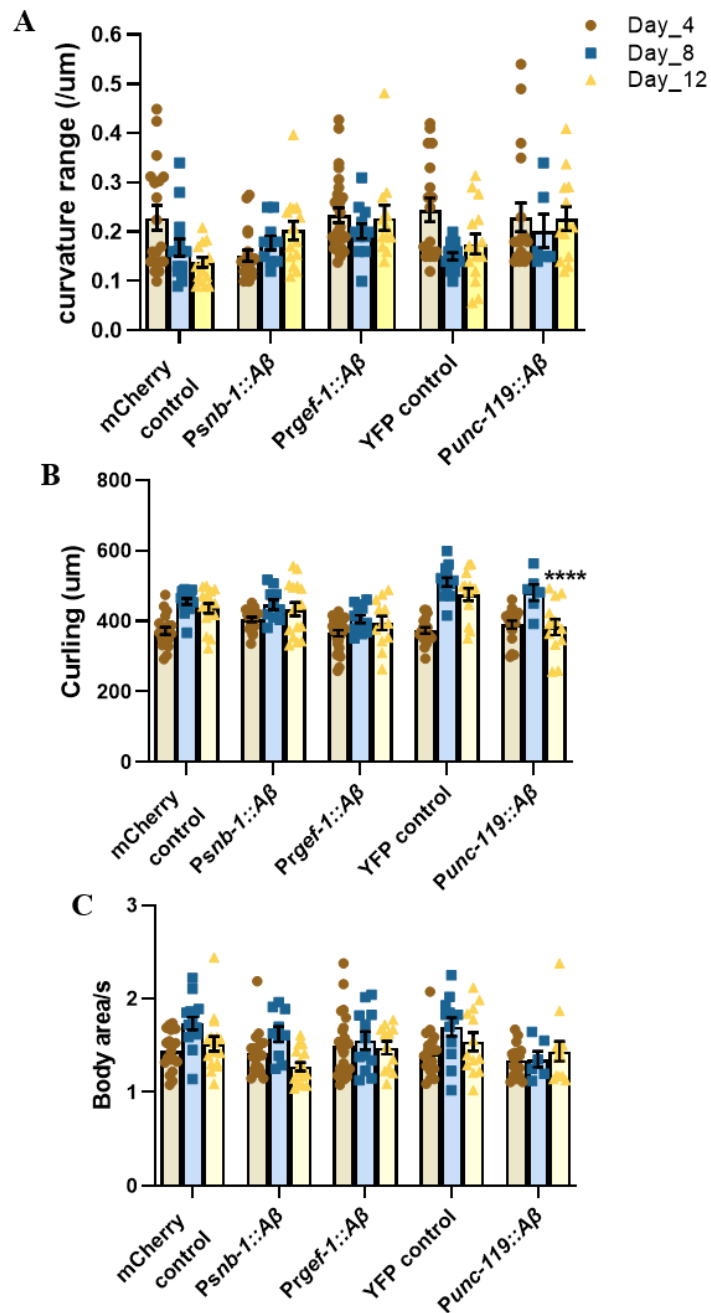
Supplementary Figure 3.3: Percentage mobility of the *C. elegans* strains on chemotaxis plates.

Mobility of the all the worm strains on standard chemotaxis plates measured by calculating the % of worms moved away from the origin after 1 hour. A) % mobility on Diacetyl chemotaxis plates of young (day 4) and middle-aged (day 8) worms. B) % mobility on Benzaldehyde chemotaxis plates of young (day 4) and middle-aged (day 8) worms.



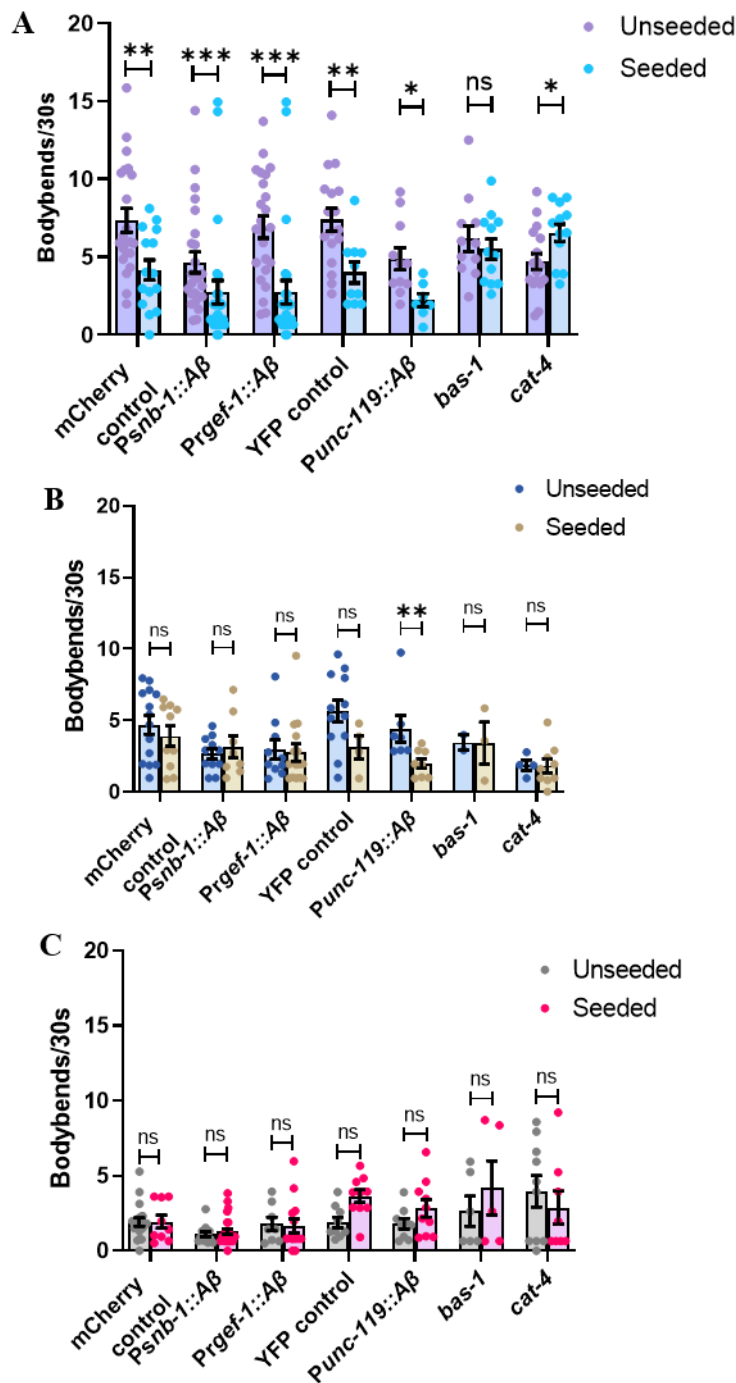
Supplementary Figure 3.4: Measurement of motility parameters of the transgenic *C. elegans* strains on solid media.

A) Mean wavelength. B) Mean amplitude. C) Head bends/30s. All data analysed using two way ANOVA followed by post hoc Tukey multiple comparisons test (n = 3, 5-15 worms/replicate) *p < 0.05, ****p < 0.0001,



Supplementary Figure 3.5: Measurement of motility parameters of the transgenic *C. elegans* strains in liquid media

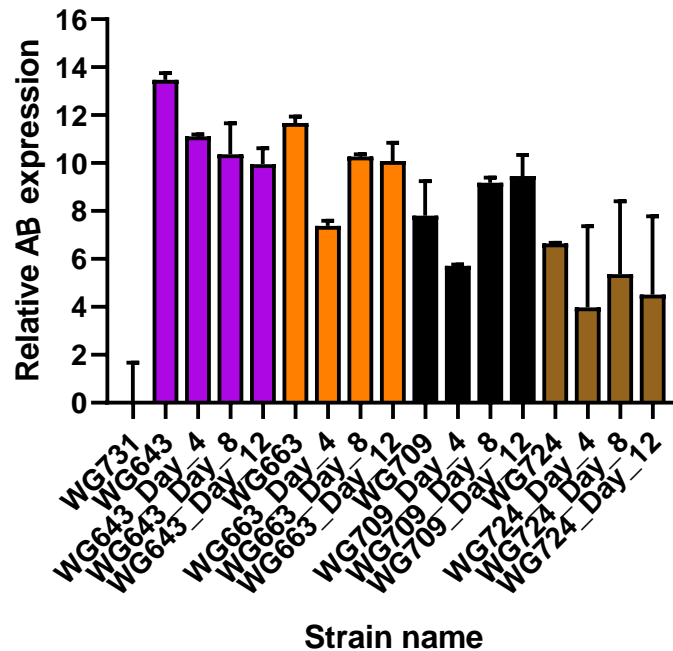
A) Dynamic amplitude (curvature range(μm)) B) Curling (μm), C) Brush stroke (body area/s) All data analysed using two way ANOVA followed by post hoc Tukey multiple comparisons test (n = 2, 5-15 worms/replicate)****p < 0.0001



Supplementary Figure 3.6: Enhanced slowing responses of pan-neuronal Aβ expressing strains.

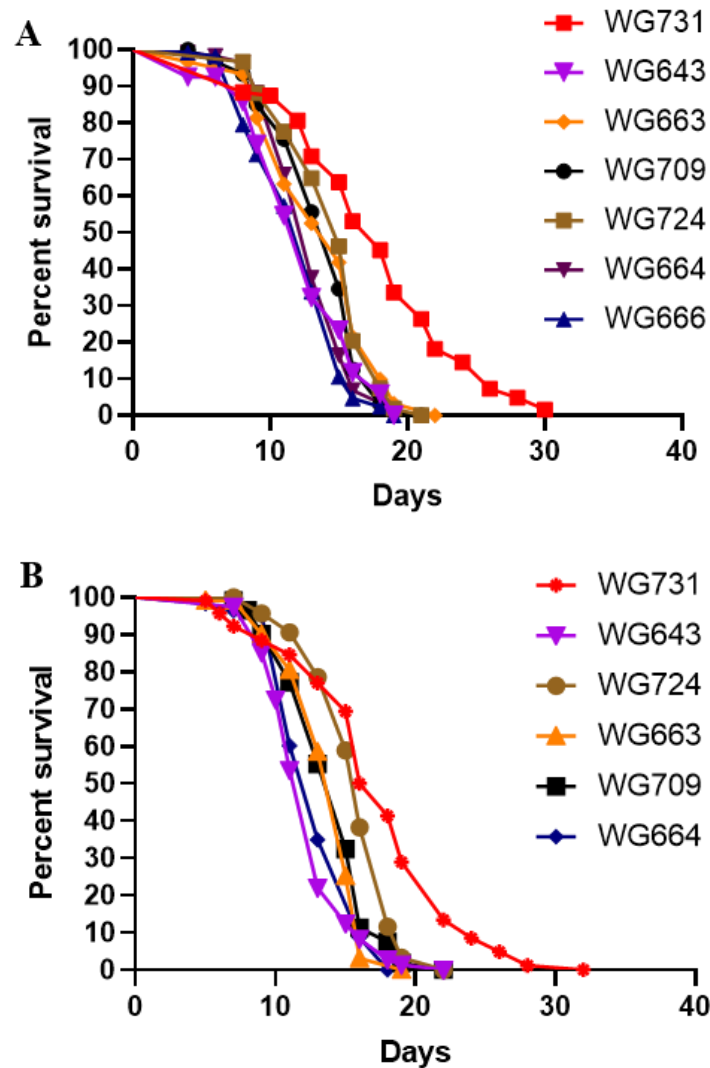
A) Day 4. B) Day 8. C) Day 12. An unpaired t test was performed to test for significance in slowing response (n=2,5-15 worms/replicate), ns 'not significant' *p < 0.05 **p < 0.01, ***p < 0.001.

Supplementary information for Chapter 4



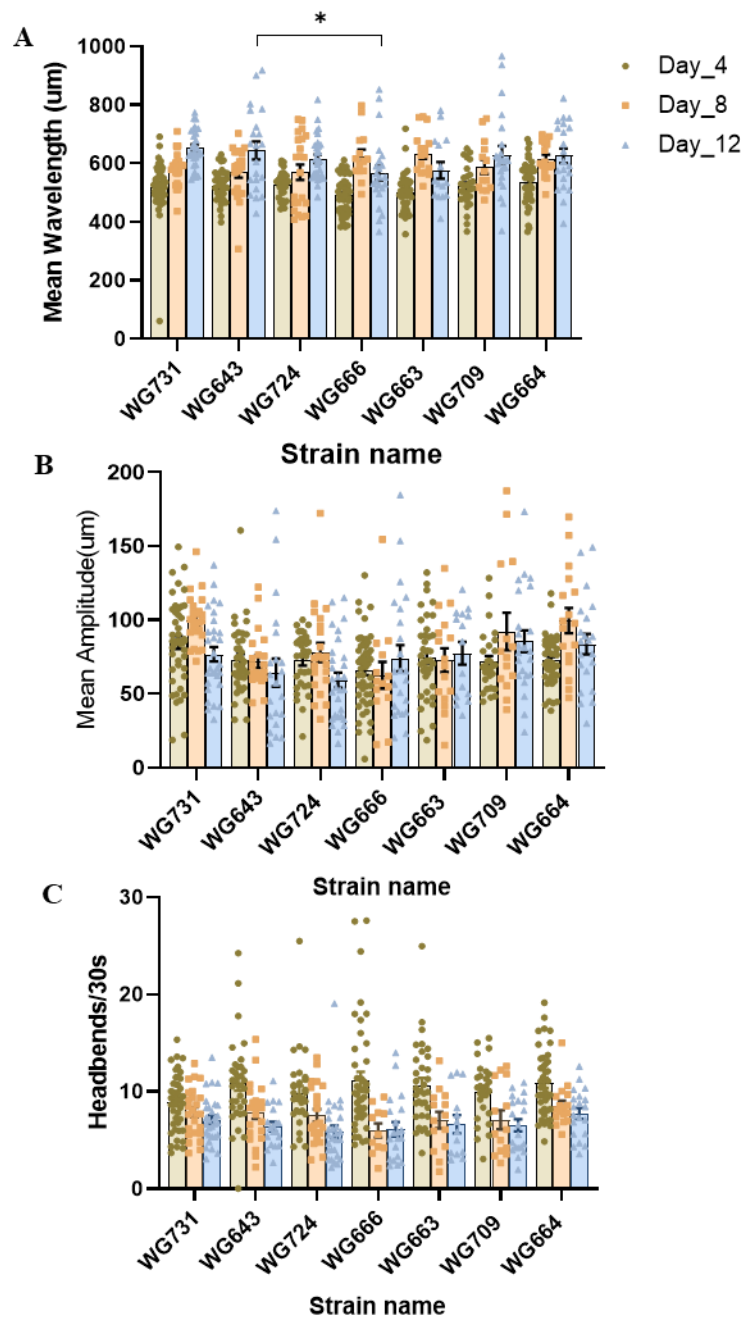
Supplementary Figure 4.1: Comparison of A β expression levels in the pan-neuronal A β strains.

RT-qPCR showing the relative expression of the A β transgene normalized to reference genes *cdc-42* and *Y45F10D.4*, **WG731** [*Pmyo-2::mCherry*], **WG643** [*Pmyo-2::mCherry + Psnb-1::huA β 1-42*], **WG663** [*Pmyo2:mCherry + Prgef-1::huA β 1-42*], **WG709** [*Pmyo-2::mCherry + Prgef-1::huA β 4-42*]; **WG724** [*Pmyo-2::mCherry + Psnb-1:mouseA β 1-42*].



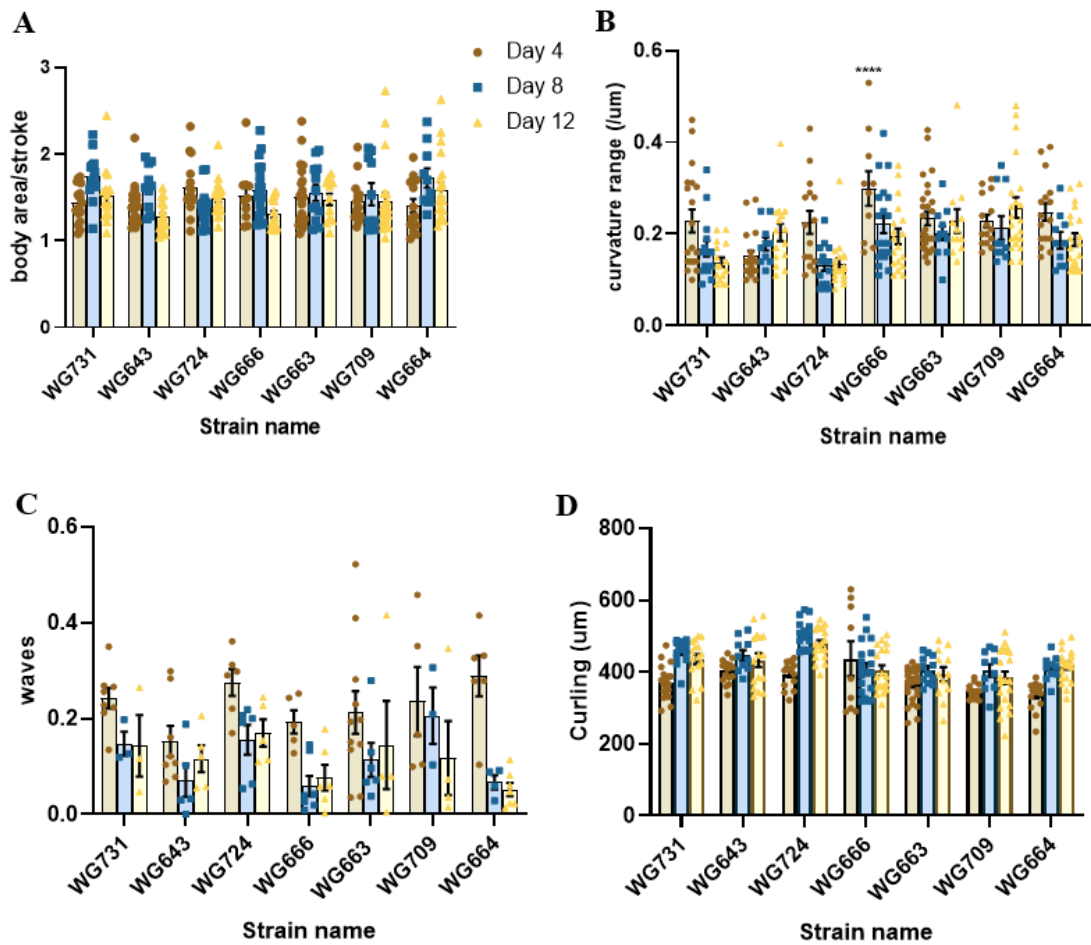
Supplementary Figure 4.2: Survival curves for the remaining biological replicates.

WG731 [*Pmyo-2::mCherry*], **WG643** [*Pmyo-2::mCherry* + *Psnb-1::huAβ1-42*], **WG663** [*Pmyo2::mCherry* + *Prgef-1::huAβ1-42*], **WG709** [*Pmyo-2::mCherry* + *Prgef-1::huAβ4-42*]; **WG724** [*Pmyo-2::mCherry* + *Psnb-1::mouseAβ1-42*], **WG657** [*Pmyo2::GFP* + *Psnb-1::huAβ1-42G37L*], **WG664** [*Pmyo2::mCherry* + *Prgef-1::huAβ1-42*; *Pmyo2::GFP* + *Psnb-1::huAβ1-42G37L*], **WG666** [*Pmyo2::mCherry* + *Psnb-1::huAβ1-42*; *Pmyo2::GFP* + *Psnb-1::huAβ1-42G37L*].



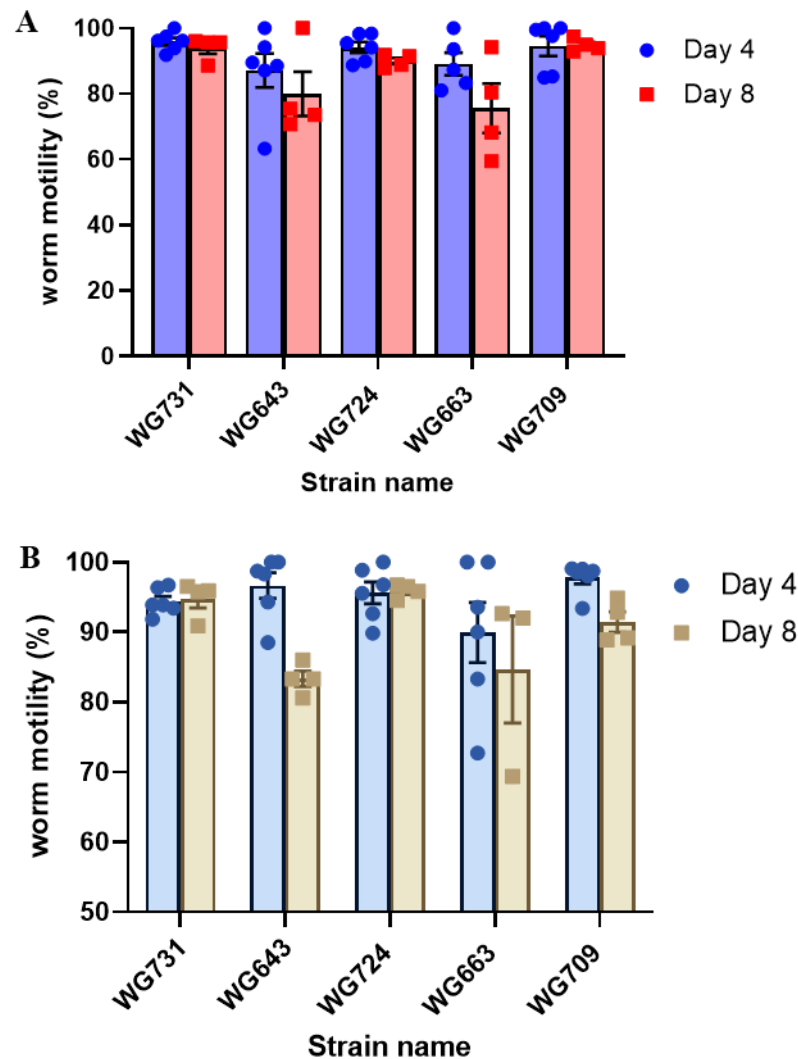
Supplementary Figure 4.3: Measurement of motility parameters of transgenic *C. elegans* strains on solid media.

A) Mean wavelength.) B) Mean amplitude. C) Head bends/30s. All data were analysed using two way ANOVA followed by post hoc Tukey multiple comparisons test, (n=3, 5-15 worms/replicate). The strains WG666 and WG724 were compared to the WG643 strain whereas the strains WG709 and WG664 were compared to the WG663 strain *p < 0.05, **WG731** [*Pmyo-2::mCherry*], **WG643** [*Pmyo-2::mCherry + Psnb-1::huAβ1-42*], **WG663** [*Pmyo2:mCherry + Prgef-1::huAβ1-42*], **WG709** [*Pmyo-2::mCherry + Prgef-1:huAβ4-42*]; **WG724** [*Pmyo-2::mCherry + Psnb-1:mouseAβ1-42*], **WG657** [*Pmyo2:GFP + Psnb-1::huAβ1-42G37L*], **WG664** [*Pmyo2:mCherry + Prgef-1::huAβ1-42; Pmyo2:GFP + Psnb-1::huAβ1-42G37L*], **WG666** [*Pmyo2:mCherry + Psnb-1::huAβ1-42; Pmyo2:GFP + Psnb-1::huAβ1-42G37L*],



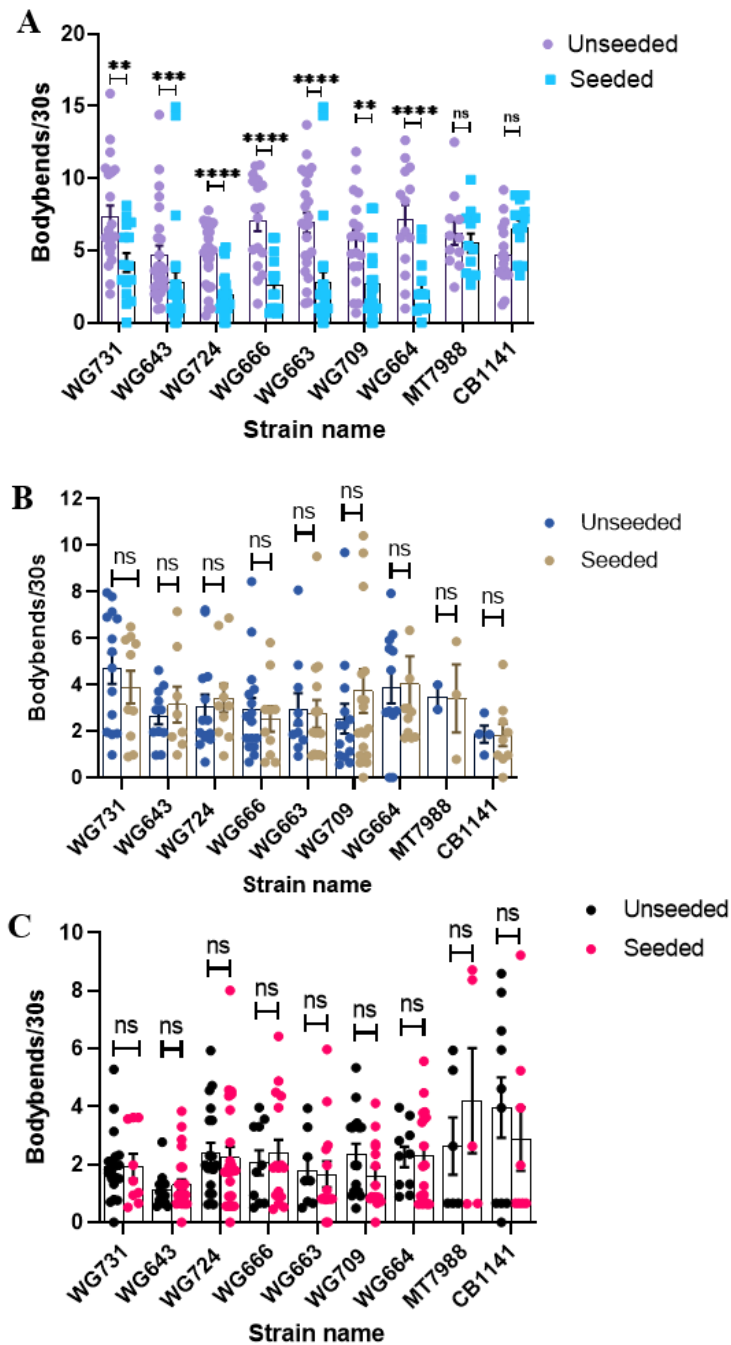
Supplementary Figure 4.4: Age-related changes in motility of transgenic *C. elegans* strains in liquid media.

A) Brush stroke (Body area/s). B) Dynamic amplitude (curvature range / μm). C) Mean waves. D) Curling (μm). All data were analysed using two-way ANOVA followed by post hoc Tukey multiple comparisons test, ($n=2,5-15$ worms/replicate). The strains WG666 and WG724 were compared to the WG643 strain whereas the strains WG709 and WG664 were compared to the WG663 strain *** $p < 0.0001$, **WG731** [*Pmyo-2::mCherry*], **WG643** [*Pmyo-2::mCherry* + *Psnb-1::huA β 1-42*], **WG663** [*Pmyo2::mCherry* + *Prgef-1::huA β 1-42*], **WG709** [*Pmyo-2::mCherry* + *Prgef-1::huA β 4-42*]; **WG724** [*Pmyo-2::mCherry* + *Psnb-1::mouseA β 1-42*], **WG657** [*Pmyo2::GFP* + *Psnb-1::huA β 1-42G37L*], **WG664** [*Pmyo2::mCherry* + *Prgef-1::huA β 1-42*; *Pmyo2::GFP* + *Psnb-1::huA β 1-42G37L*], **WG666** [*Pmyo2::mCherry* + *Psnb-1::huA β 1-42*; *Pmyo2::GFP* + *Psnb-1::huA β 1-42G37L*]



Supplementary Figure 4.5: Percentage mobility of transgenic *C. elegans* strains on chemotaxis plates

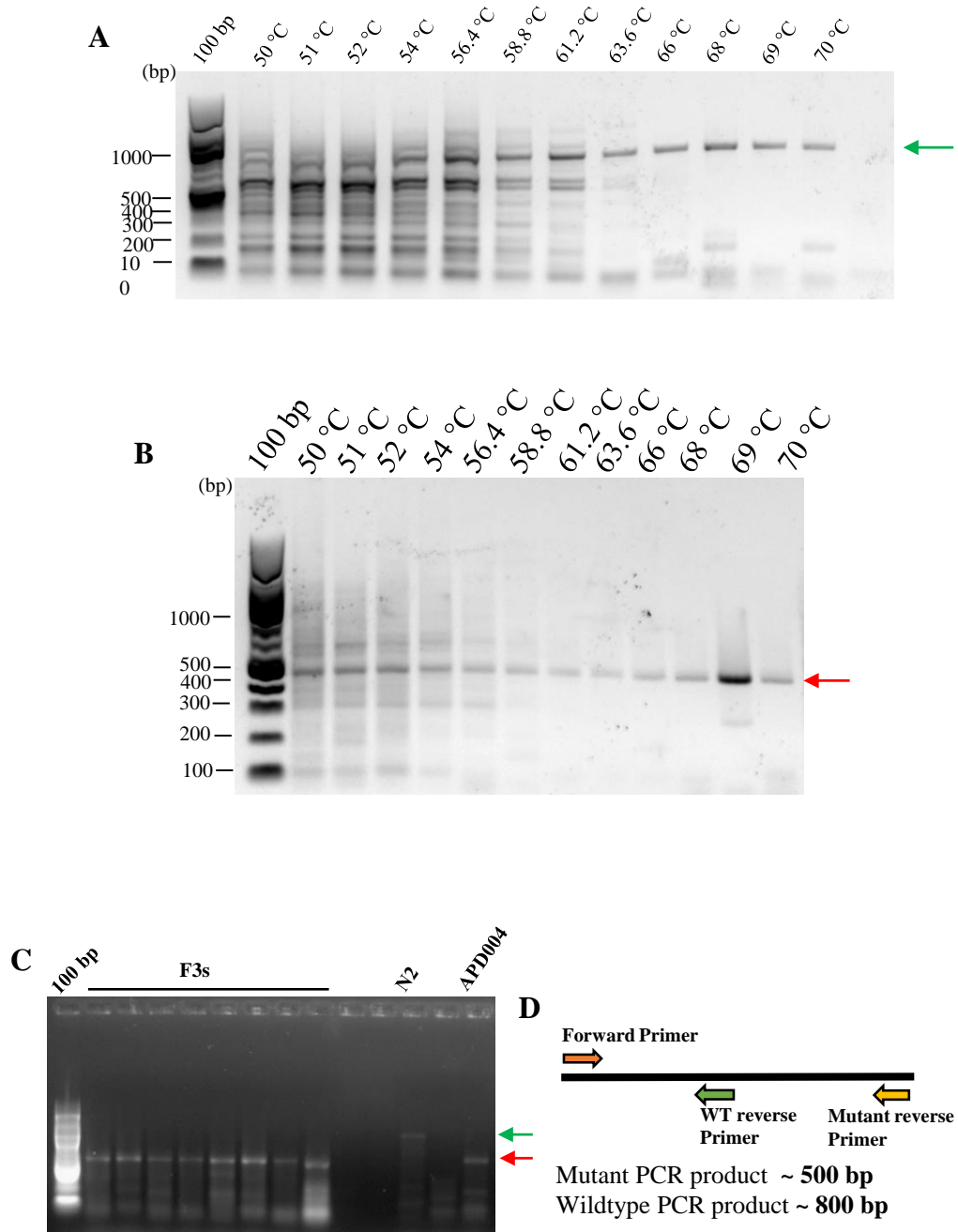
Mobility of all the worm strains on standard chemotaxis plates measured by calculating the % of worms that moved away from the origin after 1 h A) % mobility on diacetyl chemotaxis plates of young (day 4) and middle-aged (day 8). B) % mobility on benzaldehyde chemotaxis plates of young (day 4) and middle-aged (day 8) worms. The strain WG724 was compared to the WG643 strain whereas the strain WG709 was compared to the WG663 strain. An unpaired t test was used to test for significance in motility between strain at each timepoint, ns not significant, * $p < 0.05$, ** $p < 0.01$, *** $p < 0.001$. **WG731** [*Pmyo-2::mCherry*], **WG643** [*Pmyo-2::mCherry + Psnb-1::huAβ1-42*], **WG663** [*Pmyo-2::mCherry + Prgef-1::huAβ1-42*], **WG709** [*Pmyo-2::mCherry + Prgef-1::huAβ4-42*]; **WG724** [*Pmyo-2::mCherry + Psnb-1::mouseAβ1-42*], **WG657** [*Pmyo-2::GFP + Psnb-1::huAβ1-42G37L*].



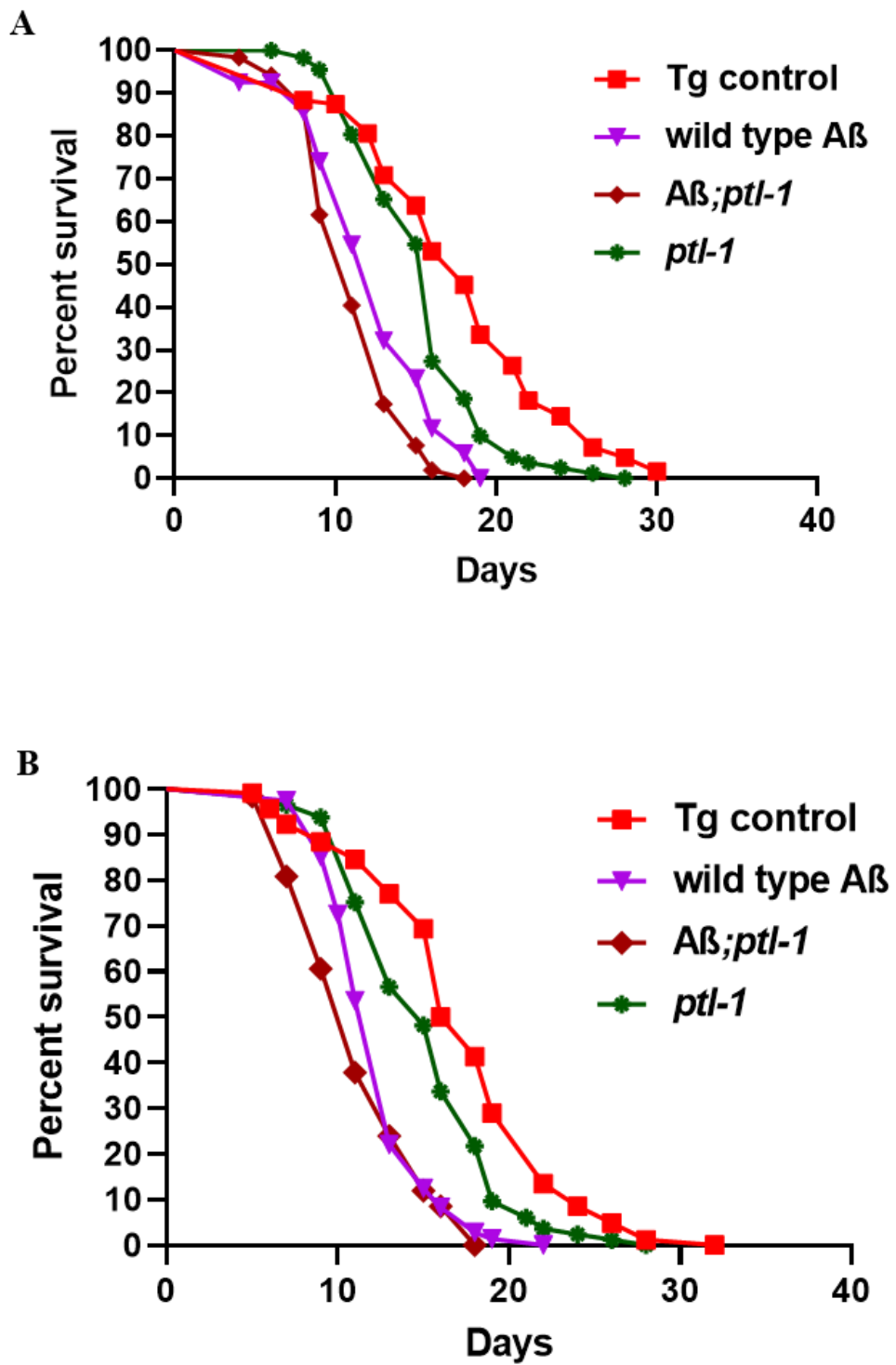
Supplementary Figure 4.6: Pan-neuronal A β expressing strains show diminished enhanced slowing response..

A) Day 4. B) Day 8. C) Day 12. An unpaired t test was performed to test for significance in slowing response (n=2,5-15 worms/replicate), ns not significant, **p < 0.01, ***p < 0.001, **WG731** [*Pmyo-2::mCherry*], **WG643** [*Pmyo-2::mCherry + Psnb-1::huA β 1-42*], **WG663** [*Pmyo-2::mCherry + Prgef-1::huA β 1-42*], **WG709** [*Pmyo-2::mCherry + Prgef-1::huA β 4-42*]; **WG724** [*Pmyo-2::mCherry + Psnb-1::mouseA β 1-42*], **WG657** [*Pmyo-2::GFP + Psnb-1::huA β 1-42G37L*], **WG664** [*Pmyo-2::mCherry + Prgef-1::huA β 1-42; Pmyo-2::GFP + Psnb-1::huA β 1-42G37L*], **WG666** [*Pmyo-2::mCherry + Psnb-1::huA β 1-42; Pmyo-2::GFP + Psnb-1::huA β 1-42G37L*], **MT7988** [*bas-1 (ad446) III*] (Loer and Kenyon, 1993), **CB1141** [*cat-4 (e1141) V*] (Sulston et al., 1975), **MT8943** [*bas-1(ad446) III; cat-4 (e1141) V*].

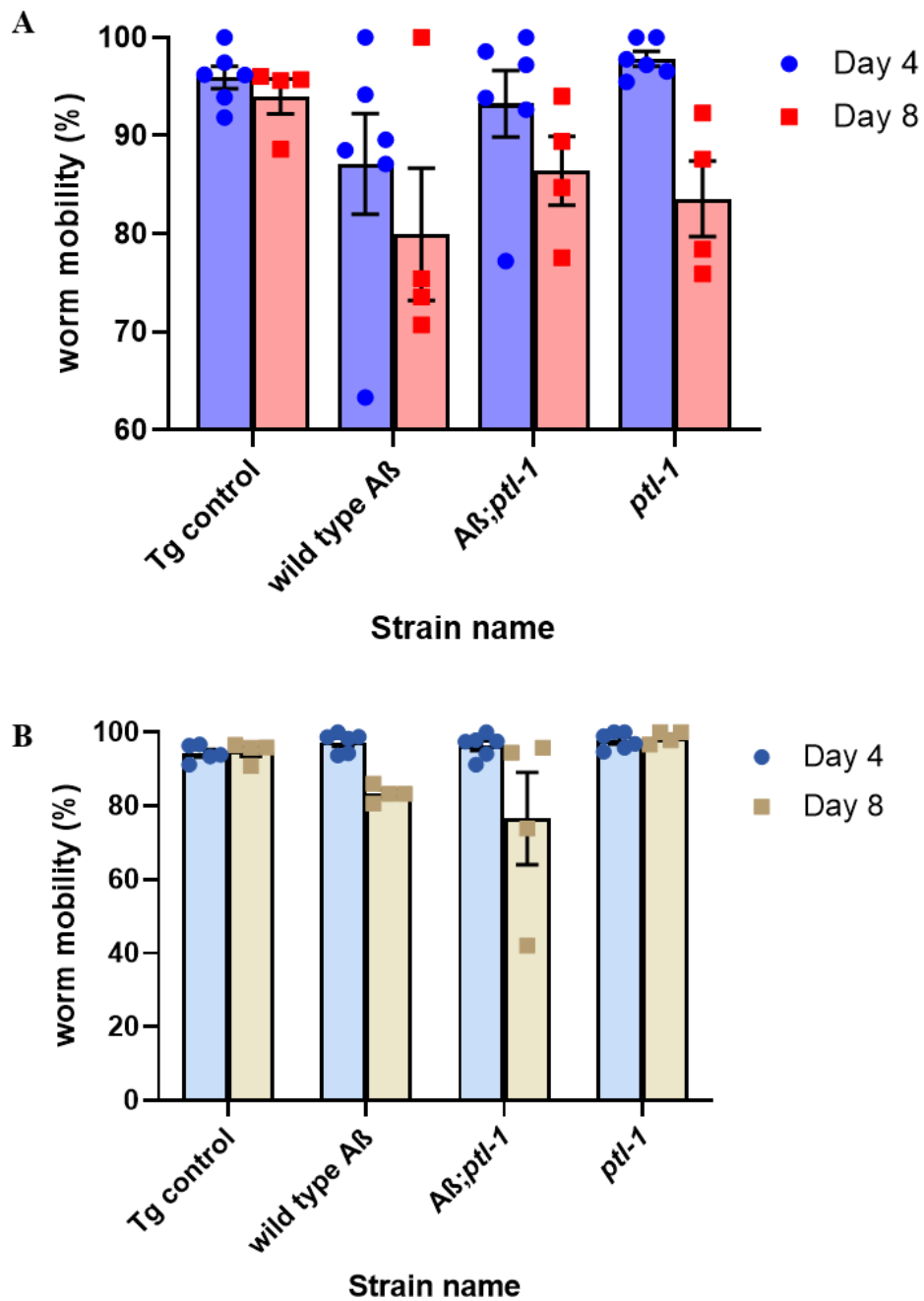
Supplementary information for Chapter 5

**Supplementary Figure 5.1: Competitive PCR strategy for screening *ptl-1* mutants**

A) Gradient PCR using wild type DNA as template. B) Gradient PCR using *ptl-1* mutant APD004 DNA as template. C) PCR screening for homozygous *ptl-1* mutant F3s. D) Schematic illustration of competitive PCR strategy. Red arrow indicates mutant PCR product and green arrow indicates wild type PCR product.

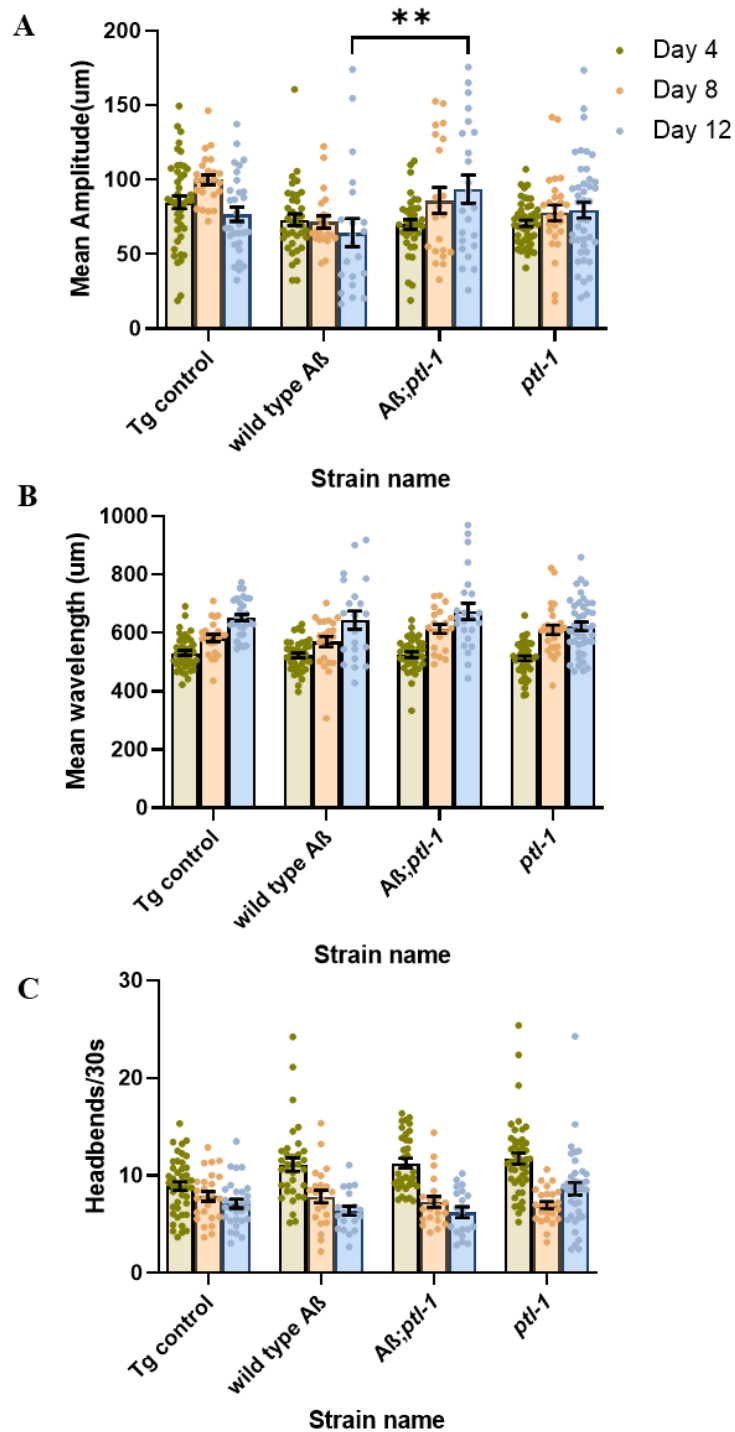


Supplementary Figure 5.2: Survival curves for the remaining biological replicates



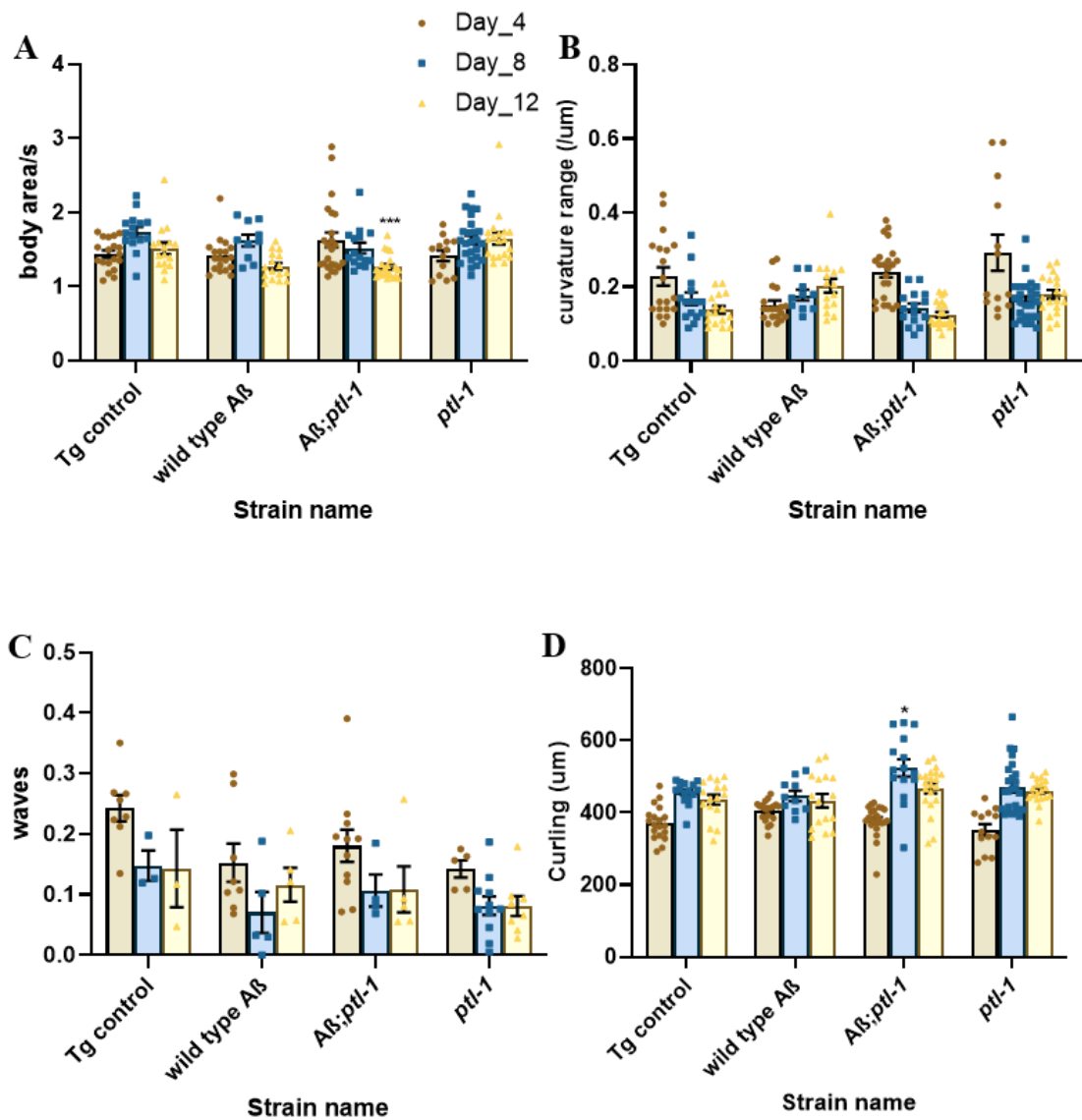
Supplementary Figure 5.3: Percentage mobility of the *C. elegans* strains on chemotaxis plates

Mobility of the all the worm strains on standard chemotaxis plates measured by calculating the % of worms moved away from the origin after 1 hour. A) % mobility on Diacetyl chemotaxis plates of young (day 4) and middle-aged (day 8) worms. B) worms. % mobility on Benzaldehyde chemotaxis plates of young (day 4) and middle-aged (day 8) worms.



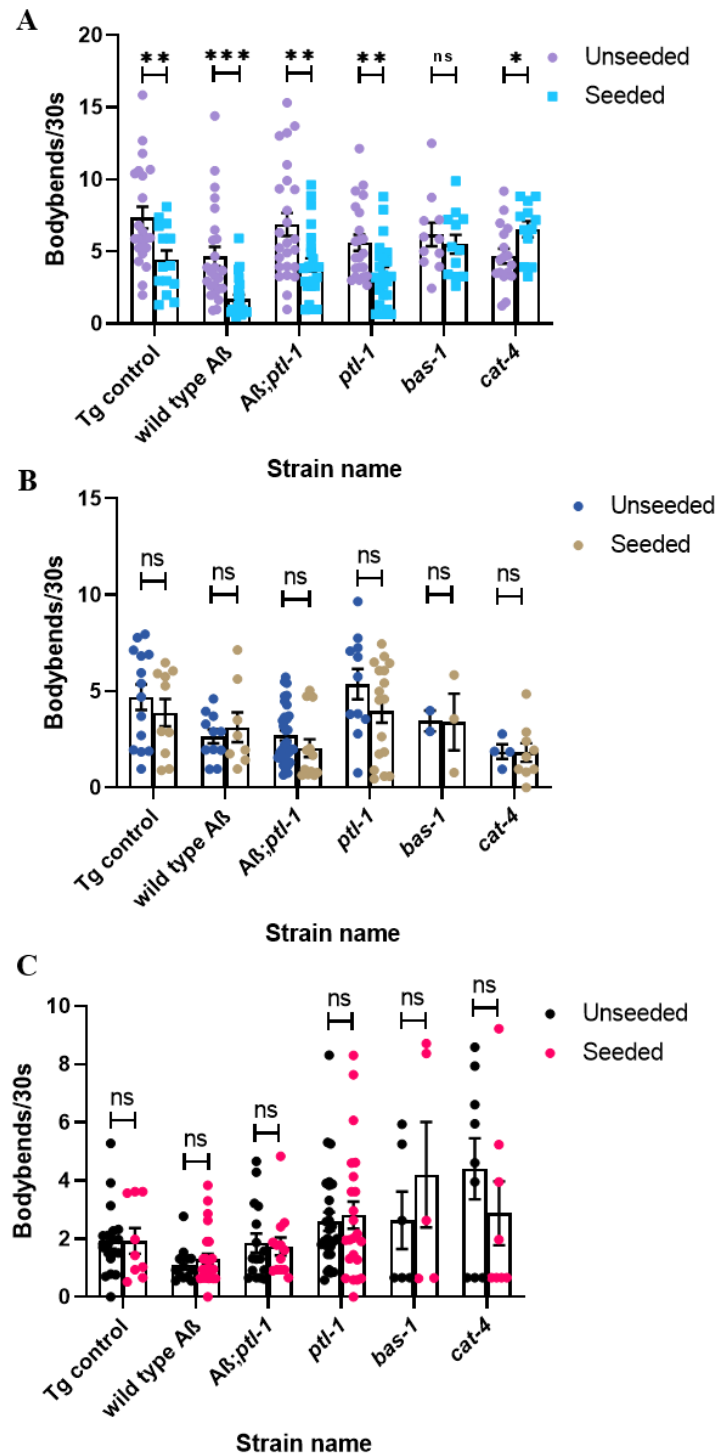
Supplementary Figure 5.4: Measurement of motility parameters of the *C. elegans* strains on solid media

A) Mean wavelength B) Mean amplitude C) Head bends/30s. All data were analysed using two way ANOVA followed by Tukey multiple comparisons test, (n=3,5-15 worms/replicate, **p < 0.01



Supplementary Figure 5.5: Measurement of motility parameters of the *C. elegans* strains in liquid media

A) Brush stroke (Body area/s) B) Dynamic amplitude (curvature range (μ m)) C) Mean waves D) Curling (μ m). All data was analysed using two way ANOVA followed by post hoc Tukey multiple comparisons test (n=2, 5-15 worms/replicate) *p < 0.05, ***p < 0.001,



Supplementary Figure 5.6: Enhanced slowing response assays.

A) Day 4 B) Day 8 C) Day 12. An unpaired t test was used to determine significant differences in slowing responses (n=2, 5-15 worms/replicate), ns not significant, * $p < 0.05$, ** $p < 0.01$, *** $p < 0.001$

Bibliography

Adlard, P.A., Cherny, R.A., Finkelstein, D.I., Gautier, E., Robb, E., Cortes, M., Volitakis, I., Liu, X., Smith, J.P., Perez, K., *et al.* (2008). Rapid restoration of cognition in Alzheimer's transgenic mice with 8-hydroxy quinoline analogs is associated with decreased interstitial Abeta. *Neuron* 59, 43-55.

Alexander, A.G., Marfil, V., and Li, C. (2014). Use of *Caenorhabditis elegans* as a model to study Alzheimer's disease and other neurodegenerative diseases. *Front Genet* 5, 279.

Ali, S.J., and Rajini, P.S. (2012). Elicitation of dopaminergic features of Parkinson's disease in *C. elegans* by monocrotophos, an organophosphorous insecticide. *CNS Neurol Disord Drug Targets* 11, 993-1000.

Altun-Gultekin, Z., Andachi, Y., Tsalik, E.L., Pilgrim, D., Kohara, Y., and Hobert, O. (2001). A regulatory cascade of three homeobox genes, *ceh-10*, *ttx-3* and *ceh-23*, controls cell fate specification of a defined interneuron class in *C. elegans*. *Development* 128, 1951-1969.

Ameen-Ali, K.E., Wharton, S.B., Simpson, J.E., Heath, P.R., Sharp, P., and Berwick, J. (2017). Review: Neuropathology and behavioural features of transgenic murine models of Alzheimer's disease. *Neuropathol Appl Neurobiol* 43, 553-570.

Amrit, F.R., Ratnappan, R., Keith, S.A., and Ghazi, A. (2014). The *C. elegans* lifespan assay toolkit. *Methods* 68, 465-475.

Andersen, J.K. (2004). Oxidative stress in neurodegeneration: cause or consequence? *Nat Med* 10 Suppl, S18-25.

Andux, S., and Ellis, R.E. (2008). Apoptosis maintains oocyte quality in aging *Caenorhabditis elegans* females. *PLoS Genet* 4, e1000295.

Arriagada, P.V., Growdon, J.H., Hedley-Whyte, E.T., and Hyman, B.T. (1992a). Neurofibrillary tangles but not senile plaques parallel duration and severity of Alzheimer's disease. *Neurology* 42, 631-639.

Arriagada, P.V., Marzloff, K., and Hyman, B.T. (1992b). Distribution of Alzheimer-type pathologic changes in nondemented elderly individuals matches the pattern in Alzheimer's disease. *Neurology* 42, 1681-1688.

Asami-Odaka, A., Ishibashi, Y., Kikuchi, T., Kitada, C., and Suzuki, N. (1995). Long amyloid beta-protein secreted from wild-type human neuroblastoma IMR-32 cells. *Biochemistry* 34, 10272-10278.

Ashe, K.H. (2001). Learning and memory in transgenic mice modeling Alzheimer's disease. *Learn Mem* 8, 301-308.

Askanas, V., and Engel, W.K. (2001). Inclusion-body myositis: newest concepts of pathogenesis and relation to aging and Alzheimer disease. *J Neuropathol Exp Neurol* 60, 1-14.

Attems, J., Quass, M., and Jellinger, K.A. (2007). Tau and alpha-synuclein brainstem pathology in Alzheimer disease: relation with extrapyramidal signs. *Acta Neuropathol* 113, 53-62.

Atwood, C.S., Obrenovich, M.E., Liu, T., Chan, H., Perry, G., Smith, M.A., and Martins, R.N. (2003). Amyloid-beta: a chameleon walking in two worlds: a review of the trophic and toxic properties of amyloid-beta. *Brain Res Brain Res Rev* 43, 1-16.

Avila, J., Lucas, J.J., Perez, M., and Hernandez, F. (2004). Role of tau protein in both physiological and pathological conditions. *Physiol Rev* 84, 361-384.

Baas, P.W., Pienkowski, T.P., and Kosik, K.S. (1991). Processes induced by tau expression in Sf9 cells have an axon-like microtubule organization. *The Journal of cell biology* 115, 1333-1344.

Ballard, C., Gauthier, S., Corbett, A., Brayne, C., Aarsland, D., and Jones, E. (2011). Alzheimer's disease. *Lancet* 377, 1019-1031.

Ballatore, C., Lee, V.M., and Trojanowski, J.Q. (2007). Tau-mediated neurodegeneration in Alzheimer's disease and related disorders. *Nat Rev Neurosci* 8, 663-672.

Bansal, A., Zhu, L.J., Yen, K., and Tissenbaum, H.A. (2015). Uncoupling lifespan and healthspan in *Caenorhabditis elegans* longevity mutants. *Proc Natl Acad Sci U S A* 112, E277-286.

Bao, H., Daniels, R.W., MacLeod, G.T., Charlton, M.P., Atwood, H.L., and Zhang, B. (2005). AP180 maintains the distribution of synaptic and vesicle proteins in the nerve terminal and indirectly regulates the efficacy of Ca²⁺-triggered exocytosis. *J Neurophysiol* 94, 1888-1903.

Barage, S.H., and Sonawane, K.D. (2015). Amyloid cascade hypothesis: Pathogenesis and therapeutic strategies in Alzheimer's disease. *Neuropeptides* 52, 1-18.

Barclay, J.W., Morgan, A., and Burgoyne, R.D. (2012). Neurotransmitter release mechanisms studied in *Caenorhabditis elegans*. *Cell Calcium* 52, 289-295.

Bard, F., Cannon, C., Barbour, R., Burke, R.L., Games, D., Grajeda, H., Guido, T., Hu, K., Huang, J., Johnson-Wood, K., *et al.* (2000). Peripherally administered antibodies against amyloid beta-peptide enter the central nervous system and reduce pathology in a mouse model of Alzheimer disease. *Nat Med* 6, 916-919.

Bargmann, C.I. (2006). Chemosensation in *C. elegans*. *WormBook*, 1-29.

Bargmann, C.I., and Avery, L. (1995). Laser killing of cells in *Caenorhabditis elegans*. *Methods Cell Biol* 48, 225-250.

Bargmann, C.I., Hartweg, E., and Horvitz, H.R. (1993). Odorant-selective genes and neurons mediate olfaction in *C. elegans*. *Cell* 74, 515-527.

Bargmann, C.I., and Horvitz, H.R. (1991). Chemosensory neurons with overlapping functions direct chemotaxis to multiple chemicals in *C. elegans*. *Neuron* 7, 729-742.

Bayer, T.A., Cappai, R., Masters, C.L., Beyreuther, K., and Multhaup, G. (1999). It all sticks together--the APP-related family of proteins and Alzheimer's disease. *Mol Psychiatry* 4, 524-528.

Bellingham, S.A., Ciccotosto, G.D., Needham, B.E., Fodero, L.R., White, A.R., Masters, C.L., Cappai, R., and Camakaris, J. (2004). Gene knockout of amyloid precursor protein and amyloid precursor-like protein-2 increases cellular copper levels in primary mouse cortical neurons and embryonic fibroblasts. *J Neurochem* 91, 423-428.

Bernhard, N., and van der Kooy, D. (2000). A behavioral and genetic dissection of two forms of olfactory plasticity in *Caenorhabditis elegans*: adaptation and habituation. *Learn Mem* 7, 199-212.

Bertram, L., Lill, C.M., and Tanzi, R.E. (2010). The genetics of Alzheimer disease: back to the future. *Neuron* 68, 270-281.

Binder, L.I., Frankfurter, A., and Rebhun, L.I. (1985). The distribution of tau in the mammalian central nervous system. *The Journal of cell biology* 101, 1371-1378.

- Bitan, G., Kirkitadze, M.D., Lomakin, A., Vollers, S.S., Benedek, G.B., and Teplow, D.B. (2003). Amyloid beta -protein (Abeta) assembly: Abeta 40 and Abeta 42 oligomerize through distinct pathways. *Proc Natl Acad Sci U S A* *100*, 330-335.
- Blurton-Jones, M., and Laferla, F.M. (2006). Pathways by which Abeta facilitates tau pathology. *Curr Alzheimer Res* *3*, 437-448.
- Bouter, Y., Dietrich, K., Wittnam, J.L., Rezaei-Ghaleh, N., Pillot, T., Papot-Couturier, S., Lefebvre, T., Sprenger, F., Wirths, O., Zweckstetter, M., *et al.* (2013). N-truncated amyloid beta (Abeta) 4-42 forms stable aggregates and induces acute and long-lasting behavioral deficits. *Acta Neuropathol* *126*, 189-205.
- Brand, A.H., and Perrimon, N. (1993). Targeted gene expression as a means of altering cell fates and generating dominant phenotypes. *Development* *118*, 401-415.
- Brandt, R., Gergou, A., Wacker, I., Fath, T., and Hutter, H. (2009). A *Caenorhabditis elegans* model of tau hyperphosphorylation: induction of developmental defects by transgenic overexpression of Alzheimer's disease-like modified tau. *Neurobiol Aging* *30*, 22-33.
- Brandt, R., Leger, J., and Lee, G. (1995). Interaction of tau with the neural plasma membrane mediated by tau's amino-terminal projection domain. *The Journal of cell biology* *131*, 1327-1340.
- Brenner, S. (1974). The genetics of *Caenorhabditis elegans*. *Genetics* *77*, 71-94.
- Brothers, H.M., Gosztyla, M.L., and Robinson, S.R. (2018). The Physiological Roles of Amyloid-beta Peptide Hint at New Ways to Treat Alzheimer's Disease. *Front Aging Neurosci* *10*, 118.
- Brouwers, N., Slegers, K., Engelborghs, S., Bogaerts, V., Serneels, S., Kamali, K., Corsmit, E., De Leenheir, E., Martin, J.J., De Deyn, P.P., *et al.* (2006). Genetic risk and transcriptional variability of amyloid precursor protein in Alzheimer's disease. *Brain* *129*, 2984-2991.
- Bryan, K.J., Lee, H., Perry, G., Smith, M.A., and Casadesus, G. (2009). Transgenic Mouse Models of Alzheimer's Disease: Behavioral Testing and Considerations. In *Methods of Behavior Analysis in Neuroscience*, nd, and J.J. Buccafusco, eds. (Boca Raton (FL)).

- Bucciantini, M., Giannoni, E., Chiti, F., Baroni, F., Formigli, L., Zurdo, J., Taddei, N., Ramponi, G., Dobson, C.M., and Stefani, M. (2002). Inherent toxicity of aggregates implies a common mechanism for protein misfolding diseases. *Nature* 416, 507-511.
- Buckingham, S.D., and Sattelle, D.B. (2009). Fast, automated measurement of nematode swimming (thrashing) without morphometry. *BMC Neurosci* 10, 84.
- Buee, L., Bussiere, T., Buee-Scherrer, V., Delacourte, A., and Hof, P.R. (2000). Tau protein isoforms, phosphorylation and role in neurodegenerative disorders. *Brain Res Brain Res Rev* 33, 95-130.
- Bush, A.I., Multhaup, G., Moir, R.D., Williamson, T.G., Small, D.H., Rumble, B., Pollwein, P., Beyreuther, K., and Masters, C.L. (1993). A novel zinc(II) binding site modulates the function of the beta A4 amyloid protein precursor of Alzheimer's disease. *J Biol Chem* 268, 16109-16112.
- Bush, A.I., Pettingell, W.H., Jr., Paradis, M.D., and Tanzi, R.E. (1994). Modulation of A beta adhesiveness and secretase site cleavage by zinc. *J Biol Chem* 269, 12152-12158.
- Bustin, S.A., Benes, V., Garson, J.A., Hellemans, J., Huggett, J., Kubista, M., Mueller, R., Nolan, T., Pfaffl, M.W., Shipley, G.L., *et al.* (2009). The MIQE guidelines: minimum information for publication of quantitative real-time PCR experiments. *Clin Chem* 55, 611-622.
- Byrne, J.H., Walker, D.S., Chew, Y.L., and Schafer, W.R. (2017). *Genetics of Behavior in C. elegans* (Oxford University Press).
- Cabrera, E., Mathews, P., Mezhericher, E., Beach, T.G., Deng, J., Neubert, T.A., Rostagno, A., and Ghiso, J. (2018). A beta truncated species: Implications for brain clearance mechanisms and amyloid plaque deposition. *Biochim Biophys Acta Mol Basis Dis* 1864, 208-225.
- Campion, D., Dumanchin, C., Hannequin, D., Dubois, B., Belliard, S., Puel, M., Thomas-Anterion, C., Michon, A., Martin, C., Charbonnier, F., *et al.* (1999). Early-onset autosomal dominant Alzheimer disease: prevalence, genetic heterogeneity, and mutation spectrum. *Am J Hum Genet* 65, 664-670.
- Chalfie, M., Sulston, J.E., White, J.G., Southgate, E., Thomson, J.N., and Brenner, S. (1985). The neural circuit for touch sensitivity in *Caenorhabditis elegans*. *J Neurosci* 5, 956-964.

- Chartier-Harlin, M.C., Crawford, F., Houlden, H., Warren, A., Hughes, D., Fidani, L., Goate, A., Rossor, M., Roques, P., Hardy, J., *et al.* (1991). Early-onset Alzheimer's disease caused by mutations at codon 717 of the beta-amyloid precursor protein gene. *Nature* 353, 844-846.
- Chen, F., David, D., Ferrari, A., and Gotz, J. (2004). Posttranslational modifications of tau--role in human tauopathies and modeling in transgenic animals. *Curr Drug Targets* 5, 503-515.
- Chen, J., Kanai, Y., Cowan, N.J., and Hirokawa, N. (1992). Projection domains of MAP2 and tau determine spacings between microtubules in dendrites and axons. *Nature* 360, 674-677.
- Chen, L., Fu, Y., Ren, M., Xiao, B., and Rubin, C.S. (2011). A RasGRP, C. elegans RGEF-1b, couples external stimuli to behavior by activating LET-60 (Ras) in sensory neurons. *Neuron* 70, 51-65.
- Chen, N., Harris, T.W., Antoshechkin, I., Bastiani, C., Bieri, T., Blasiar, D., Bradnam, K., Canaran, P., Chan, J., Chen, C.K., *et al.* (2005). WormBase: a comprehensive data resource for Caenorhabditis biology and genomics. *Nucleic Acids Res* 33, D383-389.
- Chen, P., Martinez-Finley, E.J., Bornhorst, J., Chakraborty, S., and Aschner, M. (2013). Metal-induced neurodegeneration in C. elegans. *Front Aging Neurosci* 5, 18.
- Chen, X., Barclay, J.W., Burgoyne, R.D., and Morgan, A. (2015). Using C. elegans to discover therapeutic compounds for ageing-associated neurodegenerative diseases. *Chem Cent J* 9, 65.
- Chew, Y.L., Fan, X., Gotz, J., and Nicholas, H.R. (2013). PTL-1 regulates neuronal integrity and lifespan in C. elegans. *J Cell Sci* 126, 2079-2091.
- Chew, Y.L., Fan, X., Gotz, J., and Nicholas, H.R. (2014). Regulation of age-related structural integrity in neurons by protein with tau-like repeats (PTL-1) is cell autonomous. *Sci Rep* 4, 5185.
- Chiba, T., Yamada, M., Sasabe, J., Terashita, K., Shimoda, M., Matsuoka, M., and Aiso, S. (2009). Amyloid-beta causes memory impairment by disturbing the JAK2/STAT3 axis in hippocampal neurons. *Mol Psychiatry* 14, 206-222.
- Churcher, I. (2006). Tau therapeutic strategies for the treatment of Alzheimer's disease. *Curr Top Med Chem* 6, 579-595.

- Cinar, H.N., Sweet, K.L., Hosemann, K.E., Earley, K., and Newman, A.P. (2001). The SEL-12 presenilin mediates induction of the *Caenorhabditis elegans* uterine pi cell fate. *Dev Biol* 237, 173-182.
- Clavaguera, F., Bolmont, T., Crowther, R.A., Abramowski, D., Frank, S., Probst, A., Fraser, G., Stalder, A.K., Beibel, M., Staufenbiel, M., *et al.* (2009). Transmission and spreading of tauopathy in transgenic mouse brain. *Nat Cell Biol* 11, 909-913.
- Cleveland, D.W., Hwo, S.Y., and Kirschner, M.W. (1977). Physical and chemical properties of purified tau factor and the role of tau in microtubule assembly. *J Mol Biol* 116, 227-247.
- Cohen, E., Bieschke, J., Perciavalle, R.M., Kelly, J.W., and Dillin, A. (2006). Opposing activities protect against age-onset proteotoxicity. *Science* 313, 1604-1610.
- Cooper, J.F., Dues, D.J., Spielbauer, K.K., Machiela, E., Senchuk, M.M., and Van Raamsdonk, J.M. (2015). Delaying aging is neuroprotective in Parkinson's disease: a genetic analysis in *C. elegans* models. *NPJ Parkinsons Dis* 1, 15022.
- Croll, N.A. (1975). Behavioural analysis of nematode movement. *Adv Parasitol* 13, 71-122.
- Cummings, J.L., Cohen, S., van Dyck, C.H., Brody, M., Curtis, C., Cho, W., Ward, M., Friesenhahn, M., Rabe, C., Brunstein, F., *et al.* (2018). ABBY: A phase 2 randomized trial of crenezumab in mild to moderate Alzheimer disease. *Neurology* 90, e1889-e1897.
- Dahlgren, K.N., Manelli, A.M., Stine, W.B., Jr., Baker, L.K., Krafft, G.A., and LaDu, M.J. (2002). Oligomeric and fibrillar species of amyloid-beta peptides differentially affect neuronal viability. *J Biol Chem* 277, 32046-32053.
- Daigle, I., and Li, C. (1993). *apl-1*, a *Caenorhabditis elegans* gene encoding a protein related to the human beta-amyloid protein precursor. *Proc Natl Acad Sci U S A* 90, 12045-12049.
- Dalbey, R.E., and Von Heijne, G. (1992). Signal peptidases in prokaryotes and eukaryotes--a new protease family. *Trends Biochem Sci* 17, 474-478.
- Davis, D.G., Schmitt, F.A., Wekstein, D.R., and Markesbery, W.R. (1999). Alzheimer neuropathologic alterations in aged cognitively normal subjects. *J Neuropathol Exp Neurol* 58, 376-388.

- Dawson, H.N., Cantillana, V., Jansen, M., Wang, H., Vitek, M.P., Wilcock, D.M., Lynch, J.R., and Laskowitz, D.T. (2010). Loss of tau elicits axonal degeneration in a mouse model of Alzheimer's disease. *Neuroscience* 169, 516-531.
- Dawson, H.N., Ferreira, A., Eyster, M.V., Ghoshal, N., Binder, L.I., and Vitek, M.P. (2001). Inhibition of neuronal maturation in primary hippocampal neurons from tau deficient mice. *J Cell Sci* 114, 1179-1187.
- de Bono, M., and Maricq, A.V. (2005). Neuronal substrates of complex behaviors in *C. elegans*. *Annu Rev Neurosci* 28, 451-501.
- De Felice, F.G., Vieira, M.N., Saraiva, L.M., Figueroa-Villar, J.D., Garcia-Abreu, J., Liu, R., Chang, L., Klein, W.L., and Ferreira, S.T. (2004). Targeting the neurotoxic species in Alzheimer's disease: inhibitors of Abeta oligomerization. *FASEB J* 18, 1366-1372.
- De Strooper, B. (2003). Aph-1, Pen-2, and Nicastrin with Presenilin generate an active gamma-Secretase complex. *Neuron* 38, 9-12.
- Dehmelt, L., and Halpain, S. (2005). The MAP2/Tau family of microtubule-associated proteins. *Genome Biol* 6, 204.
- Delacourte, A., Sergeant, N., Champain, D., Wattez, A., Muraige, C.A., Lebert, F., Pasquier, F., and David, J.P. (2002). Nonoverlapping but synergetic tau and APP pathologies in sporadic Alzheimer's disease. *Neurology* 59, 398-407.
- Desai, C., and Horvitz, H.R. (1989). *Caenorhabditis elegans* mutants defective in the functioning of the motor neurons responsible for egg laying. *Genetics* 121, 703-721.
- Di Carlo, M. (2012). Simple model systems: a challenge for Alzheimer's disease. *Immun Ageing* 9, 3.
- Dickinson, D.J., Ward, J.D., Reiner, D.J., and Goldstein, B. (2013). Engineering the *Caenorhabditis elegans* genome using Cas9-triggered homologous recombination. *Nat Methods* 10, 1028-1034.
- Dickman, D.K., Lu, Z., Meinertzhagen, I.A., and Schwarz, T.L. (2006). Altered synaptic development and active zone spacing in endocytosis mutants. *Curr Biol* 16, 591-598.
- Dickson, D.W., Crystal, H.A., Bevona, C., Honer, W., Vincent, I., and Davies, P. (1995). Correlations of synaptic and pathological markers with cognition of the elderly. *Neurobiol Aging* 16, 285-298; discussion 298-304.

- Dickson, D.W., Crystal, H.A., Mattiace, L.A., Masur, D.M., Blau, A.D., Davies, P., Yen, S.H., and Aronson, M.K. (1992). Identification of normal and pathological aging in prospectively studied nondemented elderly humans. *Neurobiol Aging* *13*, 179-189.
- Dietrich, K., Bouter, Y., Muller, M., and Bayer, T.A. (2018). Synaptic Alterations in Mouse Models for Alzheimer Disease-A Special Focus on N-Truncated Abeta 4-42. *Molecules* *23*.
- Dietzl, G., Chen, D., Schnorrer, F., Su, K.C., Barinova, Y., Fellner, M., Gasser, B., Kinsey, K., Oppel, S., Scheiblaue, S., *et al.* (2007). A genome-wide transgenic RNAi library for conditional gene inactivation in *Drosophila*. *Nature* *448*, 151-156.
- Dimitriadi, M., and Hart, A.C. (2010). Neurodegenerative disorders: insights from the nematode *Caenorhabditis elegans*. *Neurobiol Dis* *40*, 4-11.
- Donnelly, J.L., Clark, C.M., Leifer, A.M., Pirri, J.K., Haburcak, M., Francis, M.M., Samuel, A.D., and Alkema, M.J. (2013). Monoaminergic orchestration of motor programs in a complex *C. elegans* behavior. *PLoS Biol* *11*, e1001529.
- Doody, R.S., Thomas, R.G., Farlow, M., Iwatsubo, T., Vellas, B., Joffe, S., Kieburtz, K., Raman, R., Sun, X., Aisen, P.S., *et al.* (2014). Phase 3 trials of solanezumab for mild-to-moderate Alzheimer's disease. *N Engl J Med* *370*, 311-321.
- Dosanjh, L.E., Brown, M.K., Rao, G., Link, C.D., and Luo, Y. (2010). Behavioral phenotyping of a transgenic *Caenorhabditis elegans* expressing neuronal amyloid-beta. *J Alzheimers Dis* *19*, 681-690.
- Drake, J., Link, C.D., and Butterfield, D.A. (2003). Oxidative stress precedes fibrillar deposition of Alzheimer's disease amyloid beta-peptide (1-42) in a transgenic *Caenorhabditis elegans* model. *Neurobiol Aging* *24*, 415-420.
- Duff, K., Eckman, C., Zehr, C., Yu, X., Prada, C.M., Perez-tur, J., Hutton, M., Buee, L., Harigaya, Y., Yager, D., *et al.* (1996). Increased amyloid-beta₄₂(43) in brains of mice expressing mutant presenilin 1. *Nature* *383*, 710-713.
- Echeverria, V., and Cuervo, A.C. (2002). Intracellular A-beta amyloid, a sign for worse things to come? *Mol Neurobiol* *26*, 299-316.
- Edison, P., Archer, H.A., Hinz, R., Hammers, A., Pavese, N., Tai, Y.F., Hotton, G., Cutler, D., Fox, N., Kennedy, A., *et al.* (2007). Amyloid, hypometabolism, and cognition in Alzheimer disease: an [¹¹C]PIB and [¹⁸F]FDG PET study. *Neurology* *68*, 501-508.

Eriksen, J.L., and Janus, C.G. (2007). Plaques, tangles, and memory loss in mouse models of neurodegeneration. *Behav Genet* 37, 79-100.

Esch, F.S., Keim, P.S., Beattie, E.C., Blacher, R.W., Culwell, A.R., Oltersdorf, T., McClure, D., and Ward, P.J. (1990). Cleavage of amyloid beta peptide during constitutive processing of its precursor. *Science* 248, 1122-1124.

Ewald, C.Y., and Li, C. (2010). Understanding the molecular basis of Alzheimer's disease using a *Caenorhabditis elegans* model system. *Brain Struct Funct* 214, 263-283.

Fagan, A.M., Mintun, M.A., Shah, A.R., Aldea, P., Roe, C.M., Mach, R.H., Marcus, D., Morris, J.C., and Holtzman, D.M. (2009). Cerebrospinal fluid tau and ptau(181) increase with cortical amyloid deposition in cognitively normal individuals: implications for future clinical trials of Alzheimer's disease. *EMBO Mol Med* 1, 371-380.

Fang-Yen, C., Wyart, M., Xie, J., Kawai, R., Kodger, T., Chen, S., Wen, Q., and Samuel, A.D. (2010). Biomechanical analysis of gait adaptation in the nematode *Caenorhabditis elegans*. *Proc Natl Acad Sci U S A* 107, 20323-20328.

Fang, E.F., Hou, Y., Palikaras, K., Adriaanse, B.A., Kerr, J.S., Yang, B., Lautrup, S., Hasan-Olive, M.M., Caponio, D., Dan, X., *et al.* (2019). Mitophagy inhibits amyloid-beta and tau pathology and reverses cognitive deficits in models of Alzheimer's disease. *Nat Neurosci* 22, 401-412.

Fatouros, C., Pir, G.J., Biernat, J., Koushika, S.P., Mandelkow, E., Mandelkow, E.M., Schmidt, E., and Baumeister, R. (2012). Inhibition of tau aggregation in a novel *Caenorhabditis elegans* model of tauopathy mitigates proteotoxicity. *Hum Mol Genet* 21, 3587-3603.

Fay, D.S., Fluet, A., Johnson, C.J., and Link, C.D. (1998). In vivo aggregation of beta-amyloid peptide variants. *J Neurochem* 71, 1616-1625.

Findeis, M.A. (2007). The role of amyloid beta peptide 42 in Alzheimer's disease. *Pharmacol Ther* 116, 266-286.

Fire, A., Harrison, S.W., and Dixon, D. (1990). A modular set of lacZ fusion vectors for studying gene expression in *Caenorhabditis elegans*. *Gene* 93, 189-198.

Flaherty, D.B., Soria, J.P., Tomasiewicz, H.G., and Wood, J.G. (2000). Phosphorylation of human tau protein by microtubule-associated kinases: GSK3beta and cdk5 are key participants. *J Neurosci Res* 62, 463-472.

- Florez-McClure, M.L., Hohsfield, L.A., Fonte, G., Bealor, M.T., and Link, C.D. (2007). Decreased insulin-receptor signaling promotes the autophagic degradation of beta-amyloid peptide in *C. elegans*. *Autophagy* 3, 569-580.
- Fong, S., Teo, E., Ng, L.F., Chen, C.B., Lakshmanan, L.N., Tsoi, S.Y., Moore, P.K., Inoue, T., Halliwell, B., and Gruber, J. (2016). Energy crisis precedes global metabolic failure in a novel *Caenorhabditis elegans* Alzheimer Disease model. *Sci Rep* 6, 33781.
- Fonte, V., Dostal, V., Roberts, C.M., Gonzales, P., Lacor, P.N., Velasco, P.T., Magrane, J., Dingwell, N., Fan, E.Y., Silverman, M.A., *et al.* (2011). A glycine zipper motif mediates the formation of toxic beta-amyloid oligomers in vitro and in vivo. *Mol Neurodegener* 6, 61.
- Francis, R., McGrath, G., Zhang, J., Ruddy, D.A., Sym, M., Apfeld, J., Nicoll, M., Maxwell, M., Hai, B., Ellis, M.C., *et al.* (2002). *aph-1* and *pen-2* are required for Notch pathway signaling, gamma-secretase cleavage of betaAPP, and presenilin protein accumulation. *Dev Cell* 3, 85-97.
- Fraser, P.E., Nguyen, J.T., Inouye, H., Surewicz, W.K., Selkoe, D.J., Podlisny, M.B., and Kirschner, D.A. (1992). Fibril formation by primate, rodent, and Dutch-hemorrhagic analogues of Alzheimer amyloid beta-protein. *Biochemistry* 31, 10716-10723.
- Frokjaer-Jensen, C., Davis, M.W., Hopkins, C.E., Newman, B.J., Thummel, J.M., Olesen, S.P., Grunnet, M., and Jorgensen, E.M. (2008). Single-copy insertion of transgenes in *Caenorhabditis elegans*. *Nat Genet* 40, 1375-1383.
- Fuellen, G., Jansen, L., Cohen, A.A., Luyten, W., Gogol, M., Simm, A., Saul, N., Cirulli, F., Berry, A., Antal, P., *et al.* (2019). Health and Aging: Unifying Concepts, Scores, Biomarkers and Pathways. *Aging Dis* 10, 883-900.
- Fukumoto, H., Takahashi, H., Tarui, N., Matsui, J., Tomita, T., Hirode, M., Sagayama, M., Maeda, R., Kawamoto, M., Hirai, K., *et al.* (2010). A noncompetitive BACE1 inhibitor TAK-070 ameliorates Abeta pathology and behavioral deficits in a mouse model of Alzheimer's disease. *J Neurosci* 30, 11157-11166.
- Fulga, T.A., Elson-Schwab, I., Khurana, V., Steinhilb, M.L., Spires, T.L., Hyman, B.T., and Feany, M.B. (2007). Abnormal bundling and accumulation of F-actin mediates tau-induced neuronal degeneration in vivo. *Nat Cell Biol* 9, 139-148.
- Gama Sosa, M.A., De Gasperi, R., and Elder, G.A. (2012). Modeling human neurodegenerative diseases in transgenic systems. *Hum Genet* 131, 535-563.

- Gandy, S., and Petanceska, S. (2001). Regulation of alzheimer beta-amyloid precursor trafficking and metabolism. *Adv Exp Med Biol* 487, 85-100.
- Gao, G., Wan, W., Zhang, S., Redden, D.T., and Allison, D.B. (2008). Testing for differences in distribution tails to test for differences in 'maximum' lifespan. *BMC Med Res Methodol* 8, 49.
- Gardner, M., Rosell, M., and Myers, E.M. (2013). Measuring the effects of bacteria on *C. elegans* behavior using an egg retention assay. *J Vis Exp*, e51203.
- Ghidoni, R., Paterlini, A., Albertini, V., Stoppani, E., Binetti, G., Fuxe, K., Benussi, L., and Agnati, L.F. (2011). A window into the heterogeneity of human cerebrospinal fluid Abeta peptides. *J Biomed Biotechnol* 2011, 697036.
- Ghosh, R., and Emmons, S.W. (2008). Episodic swimming behavior in the nematode *C. elegans*. *J Exp Biol* 211, 3703-3711.
- Giacobini, E., and Gold, G. (2013). Alzheimer disease therapy--moving from amyloid-beta to tau. *Nat Rev Neurol* 9, 677-686.
- Gidalevitz, T., Ben-Zvi, A., Ho, K.H., Brignull, H.R., and Morimoto, R.I. (2006). Progressive disruption of cellular protein folding in models of polyglutamine diseases. *Science* 311, 1471-1474.
- Gidalevitz, T., Krupinski, T., Garcia, S., and Morimoto, R.I. (2009). Destabilizing protein polymorphisms in the genetic background direct phenotypic expression of mutant SOD1 toxicity. *PLoS Genet* 5, e1000399.
- Gieseler, K., Qadota, H., and Benian, G.M. (2017). Development, structure, and maintenance of *C. elegans* body wall muscle. *WormBook* 2017, 1-59.
- Glenn, C.F., Chow, D.K., David, L., Cooke, C.A., Gami, M.S., Iser, W.B., Hanselman, K.B., Goldberg, I.G., and Wolkow, C.A. (2004). Behavioral deficits during early stages of aging in *Caenorhabditis elegans* result from locomotory deficits possibly linked to muscle frailty. *J Gerontol A Biol Sci Med Sci* 59, 1251-1260.
- Glenner, G.G., and Wong, C.W. (1984). Alzheimer's disease: initial report of the purification and characterization of a novel cerebrovascular amyloid protein. *Biochem Biophys Res Commun* 120, 885-890.

Goedert, M., Baur, C.P., Ahringer, J., Jakes, R., Hasegawa, M., Spillantini, M.G., Smith, M.J., and Hill, F. (1996). PTL-1, a microtubule-associated protein with tau-like repeats from the nematode *Caenorhabditis elegans*. *J Cell Sci* 109 (Pt 11), 2661-2672.

Goedert, M., and Jakes, R. (2005). Mutations causing neurodegenerative tauopathies. *Biochim Biophys Acta* 1739, 240-250.

Gomez-Isla, T., Hollister, R., West, H., Mui, S., Growdon, J.H., Petersen, R.C., Parisi, J.E., and Hyman, B.T. (1997). Neuronal loss correlates with but exceeds neurofibrillary tangles in Alzheimer's disease. *Ann Neurol* 41, 17-24.

Gomez-Ramos, A., Diaz-Hernandez, M., Cuadros, R., Hernandez, F., and Avila, J. (2006). Extracellular tau is toxic to neuronal cells. *FEBS Lett* 580, 4842-4850.

Gordon, P., Hingula, L., Krasny, M.L., Swienckowski, J.L., Pokrywka, N.J., and Raley-Susman, K.M. (2008). The invertebrate microtubule-associated protein PTL-1 functions in mechanosensation and development in *Caenorhabditis elegans*. *Dev Genes Evol* 218, 541-551.

Gotz, J., Gladbach, A., Pennanen, L., van Eersel, J., Schild, A., David, D., and Ittner, L.M. (2010). Animal models reveal role for tau phosphorylation in human disease. *Biochim Biophys Acta* 1802, 860-871.

Gotz, J., and Ittner, L.M. (2008). Animal models of Alzheimer's disease and frontotemporal dementia. *Nat Rev Neurosci* 9, 532-544.

Gotz, J., Streffer, J.R., David, D., Schild, A., Hoernkli, F., Pennanen, L., Kurosinski, P., and Chen, F. (2004). Transgenic animal models of Alzheimer's disease and related disorders: histopathology, behavior and therapy. *Mol Psychiatry* 9, 664-683.

Gotz, J., Xia, D., Leinenga, G., Chew, Y.L., and Nicholas, H. (2013). What Renders TAU Toxic. *Front Neurol* 4, 72.

Gouras, G.K., Tsai, J., Naslund, J., Vincent, B., Edgar, M., Checler, F., Greenfield, J.P., Haroutunian, V., Buxbaum, J.D., Xu, H., *et al.* (2000). Intraneuronal A β 42 accumulation in human brain. *Am J Pathol* 156, 15-20.

Goutte, C., Hepler, W., Mickey, K.M., and Priess, J.R. (2000). *aph-2* encodes a novel extracellular protein required for GLP-1-mediated signaling. *Development* 127, 2481-2492.

- Goutte, C., Tsunozaki, M., Hale, V.A., and Priess, J.R. (2002). APH-1 is a multipass membrane protein essential for the Notch signaling pathway in *Caenorhabditis elegans* embryos. *Proc Natl Acad Sci U S A* 99, 775-779.
- Greenstein, D. (2005). Control of oocyte meiotic maturation and fertilization. *WormBook*, 1-12.
- Greenwald, I. (2005). LIN-12/Notch signaling in *C. elegans*. *WormBook*, 1-16.
- Griffin, E.F., Caldwell, K.A., and Caldwell, G.A. (2017). Genetic and Pharmacological Discovery for Alzheimer's Disease Using *Caenorhabditis elegans*. *ACS Chem Neurosci* 8, 2596-2606.
- Grun, D., Kirchner, M., Thierfelder, N., Stoeckius, M., Selbach, M., and Rajewsky, N. (2014). Conservation of mRNA and protein expression during development of *C. elegans*. *Cell Rep* 6, 565-577.
- Guthrie, C.R., Schellenberg, G.D., and Kraemer, B.C. (2009). SUT-2 potentiates tau-induced neurotoxicity in *Caenorhabditis elegans*. *Hum Mol Genet* 18, 1825-1838.
- Haass, C., and Selkoe, D.J. (1993). Cellular processing of beta-amyloid precursor protein and the genesis of amyloid beta-peptide. *Cell* 75, 1039-1042.
- Haass, C., and Selkoe, D.J. (2007). Soluble protein oligomers in neurodegeneration: lessons from the Alzheimer's amyloid beta-peptide. *Nat Rev Mol Cell Biol* 8, 101-112.
- Hahm, J.H., Kim, S., DiLoreto, R., Shi, C., Lee, S.J., Murphy, C.T., and Nam, H.G. (2015). *C. elegans* maximum velocity correlates with healthspan and is maintained in worms with an insulin receptor mutation. *Nat Commun* 6, 8919.
- Han, S.K., Lee, D., Lee, H., Kim, D., Son, H.G., Yang, J.S., Lee, S.V., and Kim, S. (2016). OASIS 2: online application for survival analysis 2 with features for the analysis of maximal lifespan and healthspan in aging research. *Oncotarget* 7, 56147-56152.
- Hannan, S.B., Drager, N.M., Rasse, T.M., Voigt, A., and Jahn, T.R. (2016). Cellular and molecular modifier pathways in tauopathies: the big picture from screening invertebrate models. *J Neurochem* 137, 12-25.
- Harada, A., Oguchi, K., Okabe, S., Kuno, J., Terada, S., Ohshima, T., Sato-Yoshitake, R., Takei, Y., Noda, T., and Hirokawa, N. (1994). Altered microtubule organization in small-calibre axons of mice lacking tau protein. *Nature* 369, 488-491.

Hardaway, J.A., Hardie, S.L., Whitaker, S.M., Baas, S.R., Zhang, B., Bermingham, D.P., Lichtenstein, A.J., and Blakely, R.D. (2012). Forward genetic analysis to identify determinants of dopamine signaling in *Caenorhabditis elegans* using swimming-induced paralysis. *G3 (Bethesda)* 2, 961-975.

Hardy, J.A., and Higgins, G.A. (1992). Alzheimer's disease: the amyloid cascade hypothesis. *Science* 256, 184-185.

Hariharan, I.K., and Haber, D.A. (2003). Yeast, flies, worms, and fish in the study of human disease. *N Engl J Med* 348, 2457-2463.

Harkany, T., Abraham, I., Timmerman, W., Laskay, G., Toth, B., Sasvari, M., Konya, C., Sebens, J.B., Korf, J., Nyakas, C., *et al.* (2000). beta-amyloid neurotoxicity is mediated by a glutamate-triggered excitotoxic cascade in rat nucleus basalis. *Eur J Neurosci* 12, 2735-2745.

Harmeier, A., Wozny, C., Rost, B.R., Munter, L.M., Hua, H., Georgiev, O., Beyermann, M., Hildebrand, P.W., Weise, C., Schaffner, W., *et al.* (2009). Role of amyloid-beta glycine 33 in oligomerization, toxicity, and neuronal plasticity. *J Neurosci* 29, 7582-7590.

Harper, J.D., and Lansbury, P.T., Jr. (1997). Models of amyloid seeding in Alzheimer's disease and scrapie: mechanistic truths and physiological consequences of the time-dependent solubility of amyloid proteins. *Annu Rev Biochem* 66, 385-407.

Harper, J.D., Wong, S.S., Lieber, C.M., and Lansbury, P.T. (1997). Observation of metastable Abeta amyloid protofibrils by atomic force microscopy. *Chem Biol* 4, 119-125.

Harris, T.W., Chen, N., Cunningham, F., Tello-Ruiz, M., Antoshechkin, I., Bastiani, C., Bieri, T., Blasiar, D., Bradnam, K., Chan, J., *et al.* (2004). WormBase: a multi-species resource for nematode biology and genomics. *Nucleic Acids Res* 32, D411-417.

Hart, A.C., and Chao, M.Y. (2010). From Odors to Behaviors in *Caenorhabditis elegans*. In *The Neurobiology of Olfaction*, A. Menini, ed. (Boca Raton (FL)).

Hedgecock, E.M., and Russell, R.L. (1975). Normal and mutant thermotaxis in the nematode *Caenorhabditis elegans*. *Proc Natl Acad Sci U S A* 72, 4061-4065.

Heidary, G., and Fortini, M.E. (2001). Identification and characterization of the *Drosophila tau* homolog. *Mech Dev* 108, 171-178.

- Hellemans, J., Mortier, G., De Paepe, A., Speleman, F., and Vandesompele, J. (2007). qBase relative quantification framework and software for management and automated analysis of real-time quantitative PCR data. *Genome Biol* 8, R19.
- Hepler, R.W., Grimm, K.M., Nahas, D.D., Breese, R., Dodson, E.C., Acton, P., Keller, P.M., Yeager, M., Wang, H., Shughrue, P., *et al.* (2006). Solution state characterization of amyloid beta-derived diffusible ligands. *Biochemistry* 45, 15157-15167.
- Herard, A.S., Besret, L., Dubois, A., Dauguet, J., Delzescaux, T., Hantraye, P., Bonvento, G., and Moya, K.L. (2006). siRNA targeted against amyloid precursor protein impairs synaptic activity in vivo. *Neurobiol Aging* 27, 1740-1750.
- Herndon, L.A., Schmeissner, P.J., Dudaronek, J.M., Brown, P.A., Listner, K.M., Sakano, Y., Paupard, M.C., Hall, D.H., and Driscoll, M. (2002). Stochastic and genetic factors influence tissue-specific decline in ageing *C. elegans*. *Nature* 419, 808-814.
- Hobert, O. (2003). Behavioral plasticity in *C. elegans*: paradigms, circuits, genes. *J Neurobiol* 54, 203-223.
- Hoe, H.S., Lee, K.J., Carney, R.S., Lee, J., Markova, A., Lee, J.Y., Howell, B.W., Hyman, B.T., Pak, D.T., Bu, G., *et al.* (2009). Interaction of reelin with amyloid precursor protein promotes neurite outgrowth. *J Neurosci* 29, 7459-7473.
- Honig, L.S., Vellas, B., Woodward, M., Boada, M., Bullock, R., Borrie, M., Hager, K., Andreasen, N., Scarpini, E., Liu-Seifert, H., *et al.* (2018). Trial of Solanezumab for Mild Dementia Due to Alzheimer's Disease. *N Engl J Med* 378, 321-330.
- Hoogewijs, D., Houthoofd, K., Matthijssens, F., Vandesompele, J., and Vanfleteren, J.R. (2008). Selection and validation of a set of reliable reference genes for quantitative sod gene expression analysis in *C. elegans*. *BMC Mol Biol* 9, 9.
- Hornsten, A., Lieberthal, J., Fadia, S., Malins, R., Ha, L., Xu, X., Daigle, I., Markowitz, M., O'Connor, G., Plasterk, R., *et al.* (2007). APL-1, a *Caenorhabditis elegans* protein related to the human beta-amyloid precursor protein, is essential for viability. *Proc Natl Acad Sci U S A* 104, 1971-1976.
- Horvitz, H.R., Chalfie, M., Trent, C., Sulston, J.E., and Evans, P.D. (1982). Serotonin and octopamine in the nematode *Caenorhabditis elegans*. *Science* 216, 1012.

- Hsiao, K., Chapman, P., Nilsen, S., Eckman, C., Harigaya, Y., Younkin, S., Yang, F., and Cole, G. (1996). Correlative memory deficits, Abeta elevation, and amyloid plaques in transgenic mice. *Science* 274, 99-102.
- Huang, C., Xiong, C., and Kornfeld, K. (2004). Measurements of age-related changes of physiological processes that predict lifespan of *Caenorhabditis elegans*. *Proc Natl Acad Sci U S A* 101, 8084-8089.
- Huang, X., Atwood, C.S., Hartshorn, M.A., Multhaup, G., Goldstein, L.E., Scarpa, R.C., Cuajungco, M.P., Gray, D.N., Lim, J., Moir, R.D., *et al.* (1999). The A beta peptide of Alzheimer's disease directly produces hydrogen peroxide through metal ion reduction. *Biochemistry* 38, 7609-7616.
- Huang, Y., and Mucke, L. (2012). Alzheimer mechanisms and therapeutic strategies. *Cell* 148, 1204-1222.
- Hughes, S.E., Evason, K., Xiong, C., and Kornfeld, K. (2007). Genetic and pharmacological factors that influence reproductive aging in nematodes. *PLoS Genet* 3, e25.
- Hung, L.W., Ciccotosto, G.D., Giannakis, E., Tew, D.J., Perez, K., Masters, C.L., Cappai, R., Wade, J.D., and Barnham, K.J. (2008). Amyloid-beta peptide (Abeta) neurotoxicity is modulated by the rate of peptide aggregation: Abeta dimers and trimers correlate with neurotoxicity. *J Neurosci* 28, 11950-11958.
- Hunt-Newbury, R., Viveiros, R., Johnsen, R., Mah, A., Anastas, D., Fang, L., Halfnight, E., Lee, D., Lin, J., Lorch, A., *et al.* (2007). High-throughput in vivo analysis of gene expression in *Caenorhabditis elegans*. *PLoS Biol* 5, e237.
- Huttenrauch, M., Brauss, A., Kurdakova, A., Borgers, H., Klinker, F., Liebetanz, D., Salinas-Riester, G., Wiltfang, J., Klafki, H.W., and Wirths, O. (2016). Physical activity delays hippocampal neurodegeneration and rescues memory deficits in an Alzheimer disease mouse model. *Transl Psychiatry* 6, e800.
- Ibanez-Ventoso, C., Herrera, C., Chen, E., Motto, D., and Driscoll, M. (2016). Automated Analysis of *C. elegans* Swim Behavior Using CeleST Software. *J Vis Exp*.
- Ikegami, S., Harada, A., and Hirokawa, N. (2000). Muscle weakness, hyperactivity, and impairment in fear conditioning in tau-deficient mice. *Neurosci Lett* 279, 129-132.
- Ikezu, T. (2008). *Alzheimer's disease* (Springer).

- Iqbal, K., Liu, F., Gong, C.X., and Grundke-Iqbal, I. (2010). Tau in Alzheimer disease and related tauopathies. *Curr Alzheimer Res* 7, 656-664.
- Ittner, L.M., Fath, T., Ke, Y.D., Bi, M., van Eersel, J., Li, K.M., Gunning, P., and Gotz, J. (2008). Parkinsonism and impaired axonal transport in a mouse model of frontotemporal dementia. *Proc Natl Acad Sci U S A* 105, 15997-16002.
- Ittner, L.M., and Gotz, J. (2011). Amyloid-beta and tau--a toxic pas de deux in Alzheimer's disease. *Nat Rev Neurosci* 12, 65-72.
- Ittner, L.M., Ke, Y.D., Delerue, F., Bi, M., Gladbach, A., van Eersel, J., Wolfing, H., Chieng, B.C., Christie, M.J., Napier, I.A., *et al.* (2010). Dendritic function of tau mediates amyloid-beta toxicity in Alzheimer's disease mouse models. *Cell* 142, 387-397.
- Jankowsky, J.L., Slunt, H.H., Ratovitski, T., Jenkins, N.A., Copeland, N.G., and Borchelt, D.R. (2001). Co-expression of multiple transgenes in mouse CNS: a comparison of strategies. *Biomol Eng* 17, 157-165.
- Jarrett, J.T., and Lansbury, P.T., Jr. (1993). Seeding "one-dimensional crystallization" of amyloid: a pathogenic mechanism in Alzheimer's disease and scrapie? *Cell* 73, 1055-1058.
- Jarriault, S., and Greenwald, I. (2005). Evidence for functional redundancy between *C. elegans* ADAM proteins SUP-17/Kuzbanian and ADM-4/TACE. *Dev Biol* 287, 1-10.
- Jawhar, S., Wirths, O., and Bayer, T.A. (2011). Pyroglutamate amyloid-beta (A β): a hatchet man in Alzheimer disease. *J Biol Chem* 286, 38825-38832.
- Jeibmann, A., and Paulus, W. (2009). *Drosophila melanogaster* as a model organism of brain diseases. *Int J Mol Sci* 10, 407-440.
- Jonsson, T., Atwal, J.K., Steinberg, S., Snaedal, J., Jonsson, P.V., Bjornsson, S., Stefansson, H., Sulem, P., Gudbjartsson, D., Maloney, J., *et al.* (2012). A mutation in APP protects against Alzheimer's disease and age-related cognitive decline. *Nature* 488, 96-99.
- Kalback, W., Watson, M.D., Kokjohn, T.A., Kuo, Y.M., Weiss, N., Luehrs, D.C., Lopez, J., Brune, D., Sisodia, S.S., Staufenbiel, M., *et al.* (2002). APP transgenic mice Tg2576 accumulate A β peptides that are distinct from the chemically modified and insoluble peptides deposited in Alzheimer's disease senile plaques. *Biochemistry* 41, 922-928.
- Kaletta, T., and Hengartner, M.O. (2006). Finding function in novel targets: *C. elegans* as a model organism. *Nat Rev Drug Discov* 5, 387-398.

- Kametani, F., and Hasegawa, M. (2018). Reconsideration of Amyloid Hypothesis and Tau Hypothesis in Alzheimer's Disease. *Front Neurosci* 12, 25.
- Kampers, T., Pangalos, M., Geerts, H., Wiech, H., and Mandelkow, E. (1999). Assembly of paired helical filaments from mouse tau: implications for the neurofibrillary pathology in transgenic mouse models for Alzheimer's disease. *FEBS Lett* 451, 39-44.
- Kang, J., Lemaire, H.G., Unterbeck, A., Salbaum, J.M., Masters, C.L., Grzeschik, K.H., Multhaup, G., Beyreuther, K., and Muller-Hill, B. (1987). The precursor of Alzheimer's disease amyloid A4 protein resembles a cell-surface receptor. *Nature* 325, 733-736.
- Kar, S., Slowikowski, S.P., Westaway, D., and Mount, H.T. (2004). Interactions between beta-amyloid and central cholinergic neurons: implications for Alzheimer's disease. *J Psychiatry Neurosci* 29, 427-441.
- Katzman, R. (1986). Alzheimer's disease. *N Engl J Med* 314, 964-973.
- Kauffman, A., Parsons, L., Stein, G., Wills, A., Kaletsky, R., and Murphy, C. (2011). *C. elegans* positive butanone learning, short-term, and long-term associative memory assays. *J Vis Exp*.
- Kauffman, A.L., Ashraf, J.M., Corces-Zimmerman, M.R., Landis, J.N., and Murphy, C.T. (2010). Insulin signaling and dietary restriction differentially influence the decline of learning and memory with age. *PLoS Biol* 8, e1000372.
- Kayed, R., Head, E., Thompson, J.L., McIntire, T.M., Milton, S.C., Cotman, C.W., and Glabe, C.G. (2003). Common structure of soluble amyloid oligomers implies common mechanism of pathogenesis. *Science* 300, 486-489.
- Ke, Y.D., Suchowerska, A.K., van der Hoven, J., De Silva, D.M., Wu, C.W., van Eersel, J., Ittner, A., and Ittner, L.M. (2012). Lessons from tau-deficient mice. *Int J Alzheimers Dis* 2012, 873270.
- Kelly, W.G., Xu, S., Montgomery, M.K., and Fire, A. (1997). Distinct requirements for somatic and germline expression of a generally expressed *Caenorhabditis elegans* gene. *Genetics* 146, 227-238.
- Kidd, M. (1963). Paired helical filaments in electron microscopy of Alzheimer's disease. *Nature* 197, 192-193.

- Kim, J., Chakrabarty, P., Hanna, A., March, A., Dickson, D.W., Borchelt, D.R., Golde, T., and Janus, C. (2013). Normal cognition in transgenic BRI2-Abeta mice. *Mol Neurodegener* 8, 15.
- Kim, J., Onstead, L., Randle, S., Price, R., Smithson, L., Zwizinski, C., Dickson, D.W., Golde, T., and McGowan, E. (2007). Abeta40 inhibits amyloid deposition in vivo. *J Neurosci* 27, 627-633.
- Kim, S., Jeon, T.J., Oberai, A., Yang, D., Schmidt, J.J., and Bowie, J.U. (2005). Transmembrane glycine zippers: physiological and pathological roles in membrane proteins. *Proc Natl Acad Sci U S A* 102, 14278-14283.
- Kimmel, C.B., Ballard, W.W., Kimmel, S.R., Ullmann, B., and Schilling, T.F. (1995). Stages of embryonic development of the zebrafish. *Dev Dyn* 203, 253-310.
- King, M.E., Kan, H.M., Baas, P.W., Erisir, A., Glabe, C.G., and Bloom, G.S. (2006). Tau-dependent microtubule disassembly initiated by prefibrillar beta-amyloid. *The Journal of cell biology* 175, 541-546.
- Kirkitadze, M.D., Bitan, G., and Teplow, D.B. (2002). Paradigm shifts in Alzheimer's disease and other neurodegenerative disorders: the emerging role of oligomeric assemblies. *J Neurosci Res* 69, 567-577.
- Kirkitadze, M.D., and Kowalska, A. (2005). Molecular mechanisms initiating amyloid beta-fibril formation in Alzheimer's disease. *Acta Biochim Pol* 52, 417-423.
- Klein, W.L. (2002). Abeta toxicity in Alzheimer's disease: globular oligomers (ADDLs) as new vaccine and drug targets. *Neurochem Int* 41, 345-352.
- Koh, J.Y., Yang, L.L., and Cotman, C.W. (1990). Beta-amyloid protein increases the vulnerability of cultured cortical neurons to excitotoxic damage. *Brain Res* 533, 315-320.
- Kolata, G. (1985). Down syndrome--Alzheimer's linked. *Science* 230, 1152-1153.
- Korta, J., Clark, D.A., Gabel, C.V., Mahadevan, L., and Samuel, A.D. (2007). Mechanosensation and mechanical load modulate the locomotory gait of swimming *C. elegans*. *J Exp Biol* 210, 2383-2389.
- Kosik, K.S., Joachim, C.L., and Selkoe, D.J. (1986). Microtubule-associated protein tau (tau) is a major antigenic component of paired helical filaments in Alzheimer disease. *Proc Natl Acad Sci U S A* 83, 4044-4048.

Kraemer, B.C., and Schellenberg, G.D. (2007). SUT-1 enables tau-induced neurotoxicity in *C. elegans*. *Hum Mol Genet* *16*, 1959-1971.

Kraemer, B.C., Zhang, B., Leverenz, J.B., Thomas, J.H., Trojanowski, J.Q., and Schellenberg, G.D. (2003). Neurodegeneration and defective neurotransmission in a *Caenorhabditis elegans* model of tauopathy. *Proc Natl Acad Sci U S A* *100*, 9980-9985.

Kuret, J., Congdon, E.E., Li, G., Yin, H., Yu, X., and Zhong, Q. (2005). Evaluating triggers and enhancers of tau fibrillization. *Microsc Res Tech* *67*, 141-155.

Lafaille-Magnan, M.E., Poirier, J., Etienne, P., Tremblay-Mercier, J., Frenette, J., Rosa-Neto, P., Breitner, J.C.S., and Group, P.-A.R. (2017). Odor identification as a biomarker of preclinical AD in older adults at risk. *Neurology* *89*, 327-335.

Lagido, C., McLaggan, D., Flett, A., Pettitt, J., and Glover, L.A. (2009). Rapid sublethal toxicity assessment using bioluminescent *Caenorhabditis elegans*, a novel whole-animal metabolic biosensor. *Toxicol Sci* *109*, 88-95.

Lagido, C., Pettitt, J., Flett, A., and Glover, L.A. (2008). Bridging the phenotypic gap: real-time assessment of mitochondrial function and metabolism of the nematode *Caenorhabditis elegans*. *BMC Physiol* *8*, 7.

Lambert, M.P., Barlow, A.K., Chromy, B.A., Edwards, C., Freed, R., Liosatos, M., Morgan, T.E., Rozovsky, I., Trommer, B., Viola, K.L., *et al.* (1998). Diffusible, nonfibrillar ligands derived from Abeta1-42 are potent central nervous system neurotoxins. *Proc Natl Acad Sci U S A* *95*, 6448-6453.

Laranjeiro, R., Harinath, G., Burke, D., Braeckman, B.P., and Driscoll, M. (2017). Single swim sessions in *C. elegans* induce key features of mammalian exercise. *BMC Biol* *15*, 30.

Larson, E.B., Shadlen, M.F., Wang, L., McCormick, W.C., Bowen, J.D., Teri, L., and Kukull, W.A. (2004). Survival after initial diagnosis of Alzheimer disease. *Ann Intern Med* *140*, 501-509.

Lee, G. (2005). Tau and src family tyrosine kinases. *Biochim Biophys Acta* *1739*, 323-330.

Lee, G., and Leugers, C.J. (2012). Tau and tauopathies. *Prog Mol Biol Transl Sci* *107*, 263-293.

- Lee, G., Newman, S.T., Gard, D.L., Band, H., and Panchamoorthy, G. (1998). Tau interacts with src-family non-receptor tyrosine kinases. *J Cell Sci* 111 (Pt 21), 3167-3177.
- Lemere, C.A., Spooner, E.T., Leverone, J.F., Mori, C., and Clements, J.D. (2002). Intranasal immunotherapy for the treatment of Alzheimer's disease: *Escherichia coli* LT and LT(R192G) as mucosal adjuvants. *Neurobiol Aging* 23, 991-1000.
- Levine, H., 3rd (1995). Soluble multimeric Alzheimer beta(1-40) pre-amyloid complexes in dilute solution. *Neurobiol Aging* 16, 755-764.
- Levitan, D., Doyle, T.G., Brousseau, D., Lee, M.K., Thinakaran, G., Slunt, H.H., Sisodia, S.S., and Greenwald, I. (1996). Assessment of normal and mutant human presenilin function in *Caenorhabditis elegans*. *Proc Natl Acad Sci U S A* 93, 14940-14944.
- Levitan, D., and Greenwald, I. (1995). Facilitation of lin-12-mediated signalling by sel-12, a *Caenorhabditis elegans* S182 Alzheimer's disease gene. *Nature* 377, 351-354.
- Levitan, D., Lee, J., Song, L., Manning, R., Wong, G., Parker, E., and Zhang, L. (2001). PS1 N- and C-terminal fragments form a complex that functions in APP processing and Notch signaling. *Proc Natl Acad Sci U S A* 98, 12186-12190.
- Lewczuk, P., Esselmann, H., Bibl, M., Paul, S., Svitek, J., Miertschischk, J., Meyrer, R., Smirnov, A., Maler, J.M., Klein, C., *et al.* (2004). Electrophoretic separation of amyloid beta peptides in plasma. *Electrophoresis* 25, 3336-3343.
- Lewis, H., Beher, D., Cookson, N., Oakley, A., Piggott, M., Morris, C.M., Jaros, E., Perry, R., Ince, P., Kenny, R.A., *et al.* (2006). Quantification of Alzheimer pathology in ageing and dementia: age-related accumulation of amyloid-beta(42) peptide in vascular dementia. *Neuropathol Appl Neurobiol* 32, 103-118.
- Li, C., Ebrahimi, A., and Schluesener, H. (2013). Drug pipeline in neurodegeneration based on transgenic mice models of Alzheimer's disease. *Ageing Res Rev* 12, 116-140.
- Li, J., Kanekiyo, T., Shinohara, M., Zhang, Y., LaDu, M.J., Xu, H., and Bu, G. (2012). Differential regulation of amyloid-beta endocytic trafficking and lysosomal degradation by apolipoprotein E isoforms. *J Biol Chem* 287, 44593-44601.
- Li, X., and Greenwald, I. (1997). HOP-1, a *Caenorhabditis elegans* presenilin, appears to be functionally redundant with SEL-12 presenilin and to facilitate LIN-12 and GLP-1 signaling. *Proc Natl Acad Sci U S A* 94, 12204-12209.

- Li, Y., Rinne, J.O., Mosconi, L., Pirraglia, E., Rusinek, H., DeSanti, S., Kemppainen, N., Nagren, K., Kim, B.C., Tsui, W., *et al.* (2008). Regional analysis of FDG and PIB-PET images in normal aging, mild cognitive impairment, and Alzheimer's disease. *Eur J Nucl Med Mol Imaging* 35, 2169-2181.
- Liao, H., Li, Y., Brautigan, D.L., and Gundersen, G.G. (1998). Protein phosphatase 1 is targeted to microtubules by the microtubule-associated protein Tau. *J Biol Chem* 273, 21901-21908.
- Lichtenthaler, S.F., Multhaup, G., Masters, C.L., and Beyreuther, K. (1999). A novel substrate for analyzing Alzheimer's disease gamma-secretase. *FEBS Lett* 453, 288-292.
- Link, C.D. (1995). Expression of human beta-amyloid peptide in transgenic *Caenorhabditis elegans*. *Proc Natl Acad Sci U S A* 92, 9368-9372.
- Link, C.D. (2001). Transgenic invertebrate models of age-associated neurodegenerative diseases. *Mech Ageing Dev* 122, 1639-1649.
- Link, C.D. (2005). Invertebrate models of Alzheimer's disease. *Genes Brain Behav* 4, 147-156.
- Link, C.D. (2006). *C. elegans* models of age-associated neurodegenerative diseases: lessons from transgenic worm models of Alzheimer's disease. *Experimental gerontology* 41, 1007-1013.
- Link, C.D., Taft, A., Kapulkin, V., Duke, K., Kim, S., Fei, Q., Wood, D.E., and Sahagan, B.G. (2003). Gene expression analysis in a transgenic *Caenorhabditis elegans* Alzheimer's disease model. *Neurobiol Aging* 24, 397-413.
- Liu, K., Solano, I., Mann, D., Lemere, C., Mercken, M., Trojanowski, J.Q., and Lee, V.M. (2006). Characterization of Abeta11-40/42 peptide deposition in Alzheimer's disease and young Down's syndrome brains: implication of N-terminally truncated Abeta species in the pathogenesis of Alzheimer's disease. *Acta Neuropathol* 112, 163-174.
- Liu, K.S., and Sternberg, P.W. (1995). Sensory regulation of male mating behavior in *Caenorhabditis elegans*. *Neuron* 14, 79-89.
- Liu, Q., Lee, H.G., Honda, K., Siedlak, S.L., Harris, P.L., Cash, A.D., Zhu, X., Avila, J., Nunomura, A., Takeda, A., *et al.* (2005). Tau modifiers as therapeutic targets for Alzheimer's disease. *Biochim Biophys Acta* 1739, 211-215.

- Loer, C.M., and Kenyon, C.J. (1993). Serotonin-deficient mutants and male mating behavior in the nematode *Caenorhabditis elegans*. *J Neurosci* *13*, 5407-5417.
- Logovinsky, V., Satlin, A., Lai, R., Swanson, C., Kaplow, J., Osswald, G., Basun, H., and Lannfelt, L. (2016). Safety and tolerability of BAN2401--a clinical study in Alzheimer's disease with a protofibril selective Abeta antibody. *Alzheimers Res Ther* *8*, 14.
- Lue, L.F., Kuo, Y.M., Roher, A.E., Brachova, L., Shen, Y., Sue, L., Beach, T., Kurth, J.H., Rydel, R.E., and Rogers, J. (1999). Soluble amyloid beta peptide concentration as a predictor of synaptic change in Alzheimer's disease. *Am J Pathol* *155*, 853-862.
- Luo, Y., Wu, Y., Brown, M., and Link, C.D. (2009). *Caenorhabditis elegans* Model for Initial Screening and Mechanistic Evaluation of Potential New Drugs for Aging and Alzheimer's Disease. In *Methods of Behavior Analysis in Neuroscience*, nd, and J.J. Buccafusco, eds. (Boca Raton (FL)).
- Luyten, W., Antal, P., Braeckman, B.P., Bundy, J., Cirulli, F., Fang-Yen, C., Fuellen, G., Leroi, A., Liu, Q., Martorell, P., *et al.* (2016). Ageing with elegans: a research proposal to map healthspan pathways. *Biogerontology* *17*, 771-782.
- Maas, T., Eidenmuller, J., and Brandt, R. (2000). Interaction of tau with the neural membrane cortex is regulated by phosphorylation at sites that are modified in paired helical filaments. *J Biol Chem* *275*, 15733-15740.
- Mariol, M.C., Walter, L., Bellemin, S., and Gieseler, K. (2013). A rapid protocol for integrating extrachromosomal arrays with high transmission rate into the *C. elegans* genome. *J Vis Exp*, e50773.
- Markaki, M., and Tavernarakis, N. (2010). Modeling human diseases in *Caenorhabditis elegans*. *Biotechnol J* *5*, 1261-1276.
- Masters, C.L., Simms, G., Weinman, N.A., Multhaup, G., McDonald, B.L., and Beyreuther, K. (1985). Amyloid plaque core protein in Alzheimer disease and Down syndrome. *Proc Natl Acad Sci U S A* *82*, 4245-4249.
- Materi, W., and Pilgrim, D. (2005). Novel *Caenorhabditis elegans* unc-119 axon outgrowth defects correlate with behavioral phenotypes that are partially rescued by nonneural unc-119. *Genesis* *42*, 104-116.
- Mathew, D., Popescu, A., and Budnik, V. (2003). *Drosophila* amphiphysin functions during synaptic Fasciclin II membrane cycling. *J Neurosci* *23*, 10710-10716.

- Matthews, K.A., Kaufman, T.C., and Gelbart, W.M. (2005). Research resources for *Drosophila*: the expanding universe. *Nat Rev Genet* 6, 179-193.
- Mattson, M.P. (2004). Pathways towards and away from Alzheimer's disease. *Nature* 430, 631-639.
- Maulik, M., Mitra, S., Bult-Ito, A., Taylor, B.E., and Vayndorf, E.M. (2017). Behavioral Phenotyping and Pathological Indicators of Parkinson's Disease in *C. elegans* Models. *Front Genet* 8, 77.
- Mawuenyega, K.G., Sigurdson, W., Ovod, V., Munsell, L., Kasten, T., Morris, J.C., Yarasheski, K.E., and Bateman, R.J. (2010). Decreased clearance of CNS beta-amyloid in Alzheimer's disease. *Science* 330, 1774.
- Mazanetz, M.P., and Fischer, P.M. (2007). Untangling tau hyperphosphorylation in drug design for neurodegenerative diseases. *Nat Rev Drug Discov* 6, 464-479.
- McColl, G., Roberts, B.R., Gunn, A.P., Perez, K.A., Tew, D.J., Masters, C.L., Barnham, K.J., Cherny, R.A., and Bush, A.I. (2009). The *Caenorhabditis elegans* A beta 1-42 model of Alzheimer disease predominantly expresses A beta 3-42. *J Biol Chem* 284, 22697-22702.
- McColl, G., Roberts, B.R., Pukala, T.L., Kenche, V.B., Roberts, C.M., Link, C.D., Ryan, T.M., Masters, C.L., Barnham, K.J., Bush, A.I., *et al.* (2012). Utility of an improved model of amyloid-beta (A β (1-42)) toxicity in *Caenorhabditis elegans* for drug screening for Alzheimer's disease. *Mol Neurodegener* 7, 57.
- McDermott, J.B., Aamodt, S., and Aamodt, E. (1996). *ptl-1*, a *Caenorhabditis elegans* gene whose products are homologous to the tau microtubule-associated proteins. *Biochemistry* 35, 9415-9423.
- McKay, S.J., Johnsen, R., Khattri, J., Asano, J., Baillie, D.L., Chan, S., Dube, N., Fang, L., Goszczynski, B., Ha, E., *et al.* (2003). Gene expression profiling of cells, tissues, and developmental stages of the nematode *C. elegans*. *Cold Spring Harb Symp Quant Biol* 68, 159-169.
- McLaggan, D., Amezaga, M.R., Petra, E., Frost, A., Duff, E.I., Rhind, S.M., Fowler, P.A., Glover, L.A., and Lagido, C. (2012). Impact of sublethal levels of environmental pollutants found in sewage sludge on a novel *Caenorhabditis elegans* model biosensor. *PLoS One* 7, e46503.

- McLean, C.A., Cherny, R.A., Fraser, F.W., Fuller, S.J., Smith, M.J., Beyreuther, K., Bush, A.I., and Masters, C.L. (1999). Soluble pool of Abeta amyloid as a determinant of severity of neurodegeneration in Alzheimer's disease. *Ann Neurol* 46, 860-866.
- Mello, C., and Fire, A. (1995). DNA transformation. *Methods Cell Biol* 48, 451-482.
- Mello, C.C., Kramer, J.M., Stinchcomb, D., and Ambros, V. (1991). Efficient gene transfer in *C.elegans*: extrachromosomal maintenance and integration of transforming sequences. *EMBO J* 10, 3959-3970.
- Mendenhall, A.R., Wu, D., Park, S.K., Cypser, J.R., Tedesco, P.M., Link, C.D., Phillips, P.C., and Johnson, T.E. (2011). Genetic dissection of late-life fertility in *Caenorhabditis elegans*. *J Gerontol A Biol Sci Med Sci* 66, 842-854.
- Mesce, K.A., and Pierce-Shimomura, J.T. (2010). Shared Strategies for Behavioral Switching: Understanding How Locomotor Patterns are Turned on and Off. *Front Behav Neurosci* 4.
- Meyer, M.R., Tschanz, J.T., Norton, M.C., Welsh-Bohmer, K.A., Steffens, D.C., Wyse, B.W., and Breitner, J.C. (1998). APOE genotype predicts when--not whether--one is predisposed to develop Alzheimer disease. *Nat Genet* 19, 321-322.
- Mhatre, S.D., Paddock, B.E., Saunders, A.J., and Marena, D.R. (2013). Invertebrate models of Alzheimer's disease. *J Alzheimers Dis* 33, 3-16.
- Miedel, M.T., Graf, N.J., Stephen, K.E., Long, O.S., Pak, S.C., Perlmutter, D.H., Silverman, G.A., and Luke, C.J. (2012). A pro-cathepsin L mutant is a luminal substrate for endoplasmic-reticulum-associated degradation in *C. elegans*. *PLoS One* 7, e40145.
- Miklossy, J., Taddei, K., Suva, D., Verdile, G., Fonte, J., Fisher, C., Gnjec, A., Ghika, J., Suard, F., Mehta, P.D., *et al.* (2003). Two novel presenilin-1 mutations (Y256S and Q222H) are associated with early-onset Alzheimer's disease. *Neurobiol Aging* 24, 655-662.
- Millan Sanchez, M., Heyn, S.N., Das, D., Moghadam, S., Martin, K.J., and Salehi, A. (2012). Neurobiological elements of cognitive dysfunction in down syndrome: exploring the role of APP. *Biol Psychiatry* 71, 403-409.
- Miyasaka, T., Ding, Z., Gengyo-Ando, K., Oue, M., Yamaguchi, H., Mitani, S., and Ihara, Y. (2005). Progressive neurodegeneration in *C. elegans* model of tauopathy. *Neurobiol Dis* 20, 372-383.

- Moreira, P.I., Carvalho, C., Zhu, X., Smith, M.A., and Perry, G. (2010). Mitochondrial dysfunction is a trigger of Alzheimer's disease pathophysiology. *Biochim Biophys Acta* 1802, 2-10.
- Moreira, P.I., Smith, M.A., Zhu, X., Nunomura, A., Castellani, R.J., and Perry, G. (2005). Oxidative stress and neurodegeneration. *Ann N Y Acad Sci* 1043, 545-552.
- Mori, I. (1999). Genetics of chemotaxis and thermotaxis in the nematode *Caenorhabditis elegans*. *Annu Rev Genet* 33, 399-422.
- Morley, J.E., Farr, S.A., Nguyen, A.D., and Xu, F. (2019). What is the Physiological Function of Amyloid-Beta Protein? *The journal of nutrition, health & aging* 23, 225-226.
- Morley, J.F., Brignull, H.R., Weyers, J.J., and Morimoto, R.I. (2002). The threshold for polyglutamine-expansion protein aggregation and cellular toxicity is dynamic and influenced by aging in *Caenorhabditis elegans*. *Proc Natl Acad Sci U S A* 99, 10417-10422.
- Morris, M., Maeda, S., Vossel, K., and Mucke, L. (2011). The many faces of tau. *Neuron* 70, 410-426.
- Morrison, J.H., and Hof, P.R. (1997). Life and death of neurons in the aging brain. *Science* 278, 412-419.
- Mucke, L. (2009). Neuroscience: Alzheimer's disease. *Nature* 461, 895-897.
- Mullard, A. (2017). BACE inhibitor bust in Alzheimer trial. *Nat Rev Drug Discov* 16, 155.
- Munter, L.M., Botev, A., Richter, L., Hildebrand, P.W., Althoff, V., Weise, C., Kaden, D., and Multhaup, G. (2010). Aberrant amyloid precursor protein (APP) processing in hereditary forms of Alzheimer disease caused by APP familial Alzheimer disease mutations can be rescued by mutations in the APP GxxxG motif. *J Biol Chem* 285, 21636-21643.
- Munter, L.M., Voigt, P., Harmeier, A., Kaden, D., Gottschalk, K.E., Weise, C., Pipkorn, R., Schaefer, M., Langosch, D., and Multhaup, G. (2007). GxxxG motifs within the amyloid precursor protein transmembrane sequence are critical for the etiology of Aβ₄₂. *EMBO J* 26, 1702-1712.

- Murakami, H., Bessinger, K., Hellmann, J., and Murakami, S. (2008). Manipulation of serotonin signal suppresses early phase of behavioral aging in *Caenorhabditis elegans*. *Neurobiol Aging* 29, 1093-1100.
- Murphy, M.P., and LeVine, H., 3rd (2010). Alzheimer's disease and the amyloid-beta peptide. *J Alzheimers Dis* 19, 311-323.
- Murrell, J., Farlow, M., Ghetti, B., and Benson, M.D. (1991). A mutation in the amyloid precursor protein associated with hereditary Alzheimer's disease. *Science* 254, 97-99.
- Nance, J., and Frokjaer-Jensen, C. (2019). The *Caenorhabditis elegans* Transgenic Toolbox. *Genetics* 212, 959-990.
- Napolitano, F., D'Angelo, F., Bimonte, M., Perrina, V., D'Ambrosio, C., Scaloni, A., Russo, T., and Zambrano, N. (2008). A differential proteomic approach reveals an evolutionary conserved regulation of Nme proteins by Fe65 in *C. elegans* and mouse. *Neurochem Res* 33, 2547-2555.
- Naslund, J., Schierhorn, A., Hellman, U., Lannfelt, L., Roses, A.D., Tjernberg, L.O., Silberring, J., Gandy, S.E., Winblad, B., Greengard, P., *et al.* (1994). Relative abundance of Alzheimer A beta amyloid peptide variants in Alzheimer disease and normal aging. *Proc Natl Acad Sci U S A* 91, 8378-8382.
- Newman, M., Ebrahimie, E., and Lardelli, M. (2014). Using the zebrafish model for Alzheimer's disease research. *Front Genet* 5, 189.
- Ng, L.F., Gruber, J., Cheah, I.K., Goo, C.K., Cheong, W.F., Shui, G., Sit, K.P., Wenk, M.R., and Halliwell, B. (2014). The mitochondria-targeted antioxidant MitoQ extends lifespan and improves healthspan of a transgenic *Caenorhabditis elegans* model of Alzheimer disease. *Free Radic Biol Med* 71, 390-401.
- Nilsberth, C., Westlind-Danielsson, A., Eckman, C.B., Condron, M.M., Axelman, K., Forsell, C., Sten, C., Luthman, J., Teplow, D.B., Younkin, S.G., *et al.* (2001). The 'Arctic' APP mutation (E693G) causes Alzheimer's disease by enhanced A beta protofibril formation. *Nat Neurosci* 4, 887-893.
- Nonet, M.L., Holgado, A.M., Brewer, F., Serpe, C.J., Norbeck, B.A., Holleran, J., Wei, L., Hartwig, E., Jorgensen, E.M., and Alfonso, A. (1999). UNC-11, a *Caenorhabditis elegans* AP180 homologue, regulates the size and protein composition of synaptic vesicles. *Mol Biol Cell* 10, 2343-2360.

- Nonet, M.L., Saifee, O., Zhao, H., Rand, J.B., and Wei, L. (1998). Synaptic transmission deficits in *Caenorhabditis elegans* synaptobrevin mutants. *J Neurosci* 18, 70-80.
- Nunomura, A., Castellani, R.J., Lee, H.-g., Moreira, P.I., Zhu, X., Perry, G., and Smith, M.A. (2006). Neuropathology in Alzheimer's Disease: Awakening from a Hundred-Year-Old Dream. *Sci Aging Knowl Environ* 2006, pe10-.
- Nuttley, W.M., Atkinson-Leadbetter, K.P., and Van Der Kooy, D. (2002). Serotonin mediates food-odor associative learning in the nematode *Caenorhabditis elegans*. *Proc Natl Acad Sci U S A* 99, 12449-12454.
- Nuttley, W.M., Harbinder, S., and van der Kooy, D. (2001). Regulation of distinct attractive and aversive mechanisms mediating benzaldehyde chemotaxis in *Caenorhabditis elegans*. *Learn Mem* 8, 170-181.
- O'Brien, R.J., and Wong, P.C. (2011). Amyloid precursor protein processing and Alzheimer's disease. *Annu Rev Neurosci* 34, 185-204.
- Oddo, S., Caccamo, A., Tran, L., Lambert, M.P., Glabe, C.G., Klein, W.L., and LaFerla, F.M. (2006). Temporal profile of amyloid-beta (A β) oligomerization in an in vivo model of Alzheimer disease. A link between A β and tau pathology. *J Biol Chem* 281, 1599-1604.
- Omura, D.T., Clark, D.A., Samuel, A.D., and Horvitz, H.R. (2012). Dopamine signaling is essential for precise rates of locomotion by *C. elegans*. *PLoS One* 7, e38649.
- Ostrowitzki, S., Deptula, D., Thurfjell, L., Barkhof, F., Bohrmann, B., Brooks, D.J., Klunk, W.E., Ashford, E., Yoo, K., Xu, Z.X., *et al.* (2012). Mechanism of amyloid removal in patients with Alzheimer disease treated with gantenerumab. *Arch Neurol* 69, 198-207.
- Ostrowitzki, S., Lasser, R.A., Dorflinger, E., Scheltens, P., Barkhof, F., Nikolcheva, T., Ashford, E., Retout, S., Hofmann, C., Delmar, P., *et al.* (2017). A phase III randomized trial of gantenerumab in prodromal Alzheimer's disease. *Alzheimers Res Ther* 9, 95.
- Panula, P., Sallinen, V., Sundvik, M., Kolehmainen, J., Torkko, V., Tiittula, A., Moshnyakov, M., and Podlasz, P. (2006). Modulatory neurotransmitter systems and behavior: towards zebrafish models of neurodegenerative diseases. *Zebrafish* 3, 235-247.
- Park, S., Ahuja, M., Kim, M.S., Brailoiu, G.C., Jha, A., Zeng, M., Baydyuk, M., Wu, L.G., Wassif, C.A., Porter, F.D., *et al.* (2016). Fusion of lysosomes with secretory

organelles leads to uncontrolled exocytosis in the lysosomal storage disease mucopolipidosis type IV. *EMBO Rep* 17, 266-278.

Piccini, A., Russo, C., Gliozzi, A., Relini, A., Vitali, A., Borghi, R., Giliberto, L., Armirotti, A., D'Arrigo, C., Bachi, A., *et al.* (2005). beta-amyloid is different in normal aging and in Alzheimer disease. *J Biol Chem* 280, 34186-34192.

Pickett, C.L., and Kornfeld, K. (2013). Age-related degeneration of the egg-laying system promotes matricidal hatching in *Caenorhabditis elegans*. *Aging Cell* 12, 544-553.

Pierce-Shimomura, J.T., Chen, B.L., Mun, J.J., Ho, R., Sarkis, R., and McIntire, S.L. (2008). Genetic analysis of crawling and swimming locomotory patterns in *C. elegans*. *Proc Natl Acad Sci U S A* 105, 20982-20987.

Pike, C.J., Overman, M.J., and Cotman, C.W. (1995). Amino-terminal deletions enhance aggregation of beta-amyloid peptides in vitro. *J Biol Chem* 270, 23895-23898.

Podlisny, M.B., Walsh, D.M., Amarante, P., Ostaszewski, B.L., Stimson, E.R., Maggio, J.E., Teplow, D.B., and Selkoe, D.J. (1998). Oligomerization of endogenous and synthetic amyloid beta-protein at nanomolar levels in cell culture and stabilization of monomer by Congo red. *Biochemistry* 37, 3602-3611.

Portelius, E., Bogdanovic, N., Gustavsson, M.K., Volkman, I., Brinkmalm, G., Zetterberg, H., Winblad, B., and Blennow, K. (2010). Mass spectrometric characterization of brain amyloid beta isoform signatures in familial and sporadic Alzheimer's disease. *Acta Neuropathol* 120, 185-193.

Portet, F., Scarmeas, N., Cosentino, S., Helzner, E.P., and Stern, Y. (2009). Extrapyrmidal signs before and after diagnosis of incident Alzheimer disease in a prospective population study. *Arch Neurol* 66, 1120-1126.

Praitis, V., and Maduro, M.F. (2011). Transgenesis in *C. elegans*. *Methods Cell Biol* 106, 161-185.

Prasher, V.P., Farrer, M.J., Kessling, A.M., Fisher, E.M., West, R.J., Barber, P.C., and Butler, A.C. (1998). Molecular mapping of Alzheimer-type dementia in Down's syndrome. *Ann Neurol* 43, 380-383.

Price, D.L., and Sisodia, S.S. (1998). Mutant genes in familial Alzheimer's disease and transgenic models. *Annu Rev Neurosci* 21, 479-505.

- Price, D.L., Sisodia, S.S., and Borchelt, D.R. (1998a). Genetic neurodegenerative diseases: the human illness and transgenic models. *Science* 282, 1079-1083.
- Price, D.L., Tanzi, R.E., Borchelt, D.R., and Sisodia, S.S. (1998b). Alzheimer's disease: genetic studies and transgenic models. *Annu Rev Genet* 32, 461-493.
- Price, J.L., McKeel, D.W., Jr., Buckles, V.D., Roe, C.M., Xiong, C., Grundman, M., Hansen, L.A., Petersen, R.C., Parisi, J.E., Dickson, D.W., *et al.* (2009). Neuropathology of nondemented aging: presumptive evidence for preclinical Alzheimer disease. *Neurobiol Aging* 30, 1026-1036.
- Priller, C., Bauer, T., Mitteregger, G., Krebs, B., Kretzschmar, H.A., and Herms, J. (2006). Synapse formation and function is modulated by the amyloid precursor protein. *J Neurosci* 26, 7212-7221.
- Puzzo, D., Lee, L., Palmeri, A., Calabrese, G., and Arancio, O. (2014). Behavioral assays with mouse models of Alzheimer's disease: practical considerations and guidelines. *Biochem Pharmacol* 88, 450-467.
- Qiu, C., Kivipelto, M., and von Strauss, E. (2009). Epidemiology of Alzheimer's disease: occurrence, determinants, and strategies toward intervention. *Dialogues Clin Neurosci* 11, 111-128.
- Rahayel, S., Frasnelli, J., and Joubert, S. (2012). The effect of Alzheimer's disease and Parkinson's disease on olfaction: a meta-analysis. *Behav Brain Res* 231, 60-74.
- Ranganathan, R., Sawin, E.R., Trent, C., and Horvitz, H.R. (2001). Mutations in the *Caenorhabditis elegans* serotonin reuptake transporter MOD-5 reveal serotonin-dependent and -independent activities of fluoxetine. *J Neurosci* 21, 5871-5884.
- Rankin, C.H. (2004). Invertebrate learning: what can't a worm learn? *Curr Biol* 14, R617-618.
- Rankin, C.H., Beck, C.D., and Chiba, C.M. (1990). *Caenorhabditis elegans*: a new model system for the study of learning and memory. *Behav Brain Res* 37, 89-92.
- Rao, X., Huang, X., Zhou, Z., and Lin, X. (2013). An improvement of the $2^{-(\Delta\Delta CT)}$ method for quantitative real-time polymerase chain reaction data analysis. *Biostat Bioinforma Biomath* 3, 71-85.

- Rapoport, M., Dawson, H.N., Binder, L.I., Vitek, M.P., and Ferreira, A. (2002). Tau is essential to beta -amyloid-induced neurotoxicity. *Proc Natl Acad Sci U S A* 99, 6364-6369.
- Reitz, C. (2012). Alzheimer's disease and the amyloid cascade hypothesis: a critical review. *Int J Alzheimers Dis* 2012, 369808.
- Resende, R., Ferreiro, E., Pereira, C., and Resende de Oliveira, C. (2008). Neurotoxic effect of oligomeric and fibrillar species of amyloid-beta peptide 1-42: involvement of endoplasmic reticulum calcium release in oligomer-induced cell death. *Neuroscience* 155, 725-737.
- Restif, C., Ibanez-Ventoso, C., Vora, M.M., Guo, S., Metaxas, D., and Driscoll, M. (2014). CeleST: computer vision software for quantitative analysis of *C. elegans* swim behavior reveals novel features of locomotion. *PLoS Comput Biol* 10, e1003702.
- Reynolds, C.H., Garwood, C.J., Wray, S., Price, C., Kellie, S., Perera, T., Zvelebil, M., Yang, A., Sheppard, P.W., Varndell, I.M., *et al.* (2008). Phosphorylation regulates tau interactions with Src homology 3 domains of phosphatidylinositol 3-kinase, phospholipase Cgamma1, Grb2, and Src family kinases. *J Biol Chem* 283, 18177-18186.
- Ricciarelli, R., and Fedele, E. (2017). The Amyloid Cascade Hypothesis in Alzheimer's Disease: It's Time to Change Our Mind. *Curr Neuropharmacol* 15, 926-935.
- Ridge, P.G., Ebbert, M.T., and Kauwe, J.S. (2013). Genetics of Alzheimer's disease. *Biomed Res Int* 2013, 254954.
- Rinne, J.O., Brooks, D.J., Rossor, M.N., Fox, N.C., Bullock, R., Klunk, W.E., Mathis, C.A., Blennow, K., Barakos, J., Okello, A.A., *et al.* (2010). ¹¹C-PiB PET assessment of change in fibrillar amyloid- β ; load in patients with Alzheimer's disease treated with bapineuzumab: a phase 2, double-blind, placebo-controlled, ascending-dose study. *The Lancet Neurology* 9, 363-372.
- Rissman, R.A., Poon, W.W., Blurton-Jones, M., Oddo, S., Torp, R., Vitek, M.P., LaFerla, F.M., Rohn, T.T., and Cotman, C.W. (2004). Caspase-cleavage of tau is an early event in Alzheimer disease tangle pathology. *J Clin Invest* 114, 121-130.
- Rivard, L., Srinivasan, J., Stone, A., Ochoa, S., Sternberg, P.W., and Loer, C.M. (2010). A comparison of experience-dependent locomotory behaviors and biogenic amine neurons in nematode relatives of *Caenorhabditis elegans*. *BMC Neurosci* 11, 22.

- Roberson, E.D., Scarce-Levie, K., Palop, J.J., Yan, F., Cheng, I.H., Wu, T., Gerstein, H., Yu, G.Q., and Mucke, L. (2007). Reducing endogenous tau ameliorates amyloid beta-induced deficits in an Alzheimer's disease mouse model. *Science* 316, 750-754.
- Robert, P.H., Mulin, E., Mallea, P., and David, R. (2010). REVIEW: Apathy diagnosis, assessment, and treatment in Alzheimer's disease. *CNS Neurosci Ther* 16, 263-271.
- Roberts, B.R., Lind, M., Wagen, A.Z., Rembach, A., Frugier, T., Li, Q.X., Ryan, T.M., McLean, C.A., Doecke, J.D., Rowe, C.C., *et al.* (2017). Biochemically-defined pools of amyloid-beta in sporadic Alzheimer's disease: correlation with amyloid PET. *Brain* 140, 1486-1498.
- Roberts, B.R., Ryan, T.M., Bush, A.I., Masters, C.L., and Duce, J.A. (2012). The role of metallobiology and amyloid-beta peptides in Alzheimer's disease. *J Neurochem* 120 Suppl 1, 149-166.
- Rollins, J.A., Howard, A.C., Dobbins, S.K., Washburn, E.H., and Rogers, A.N. (2017). Assessing Health Span in *Caenorhabditis elegans*: Lessons From Short-Lived Mutants. *J Gerontol A Biol Sci Med Sci* 72, 473-480.
- Rolls, M.M., Satoh, D., Clyne, P.J., Henner, A.L., Uemura, T., and Doe, C.Q. (2007). Polarity and intracellular compartmentalization of *Drosophila* neurons. *Neural Dev* 2, 7.
- Rose, J.K., and Rankin, C.H. (2001). Analyses of habituation in *Caenorhabditis elegans*. *Learn Mem* 8, 63-69.
- Rovelet-Lecrux, A., Hannequin, D., Raux, G., Le Meur, N., Laquerriere, A., Vital, A., Dumanchin, C., Feuillet, S., Brice, A., Vercelletto, M., *et al.* (2006). APP locus duplication causes autosomal dominant early-onset Alzheimer disease with cerebral amyloid angiopathy. *Nat Genet* 38, 24-26.
- Roy, S., Zhang, B., Lee, V.M., and Trojanowski, J.Q. (2005). Axonal transport defects: a common theme in neurodegenerative diseases. *Acta Neuropathol* 109, 5-13.
- Rubinstein, A.L. (2006). Zebrafish assays for drug toxicity screening. *Expert Opin Drug Metab Toxicol* 2, 231-240.
- Russo, C., Salis, S., Dolcini, V., Venezia, V., Song, X.H., Teller, J.K., and Schettini, G. (2001). Amino-terminal modification and tyrosine phosphorylation of [corrected] carboxy-terminal fragments of the amyloid precursor protein in Alzheimer's disease and Down's syndrome brain. *Neurobiol Dis* 8, 173-180.

- Russo, C., Violani, E., Salis, S., Venezia, V., Dolcini, V., Damonte, G., Benatti, U., D'Arrigo, C., Patrone, E., Carlo, P., *et al.* (2002). Pyroglutamate-modified amyloid beta-peptides--AbetaN3(pE)--strongly affect cultured neuron and astrocyte survival. *J Neurochem* 82, 1480-1489.
- Sadigh-Eteghad, S., Sabermarouf, B., Majidi, A., Talebi, M., Farhoudi, M., and Mahmoudi, J. (2015). Amyloid-beta: a crucial factor in Alzheimer's disease. *Med Princ Pract* 24, 1-10.
- Sadigh-Eteghad, S., Talebi, M., and Farhoudi, M. (2012). Association of apolipoprotein E epsilon 4 allele with sporadic late onset Alzheimer's disease. A meta-analysis. *Neurosciences (Riyadh)* 17, 321-326.
- Sadigh-Eteghad, S., Talebi, M., Farhoudi, M., Golzari, S.E.J., Sabermarouf, B., and Mahmoudi, J. (2014). Beta-amyloid exhibits antagonistic effects on alpha 7 nicotinic acetylcholine receptors in orchestrated manner. *J Med Hypotheses Ide* 8, 49-52.
- Saleem, S., and Kannan, R.R. (2018). Zebrafish: an emerging real-time model system to study Alzheimer's disease and neurospecific drug discovery. *Cell Death Discov* 4, 45.
- Salloway, S., Sperling, R., Fox, N.C., Blennow, K., Klunk, W., Raskind, M., Sabbagh, M., Honig, L.S., Porsteinsson, A.P., Ferris, S., *et al.* (2014). Two phase 3 trials of bapineuzumab in mild-to-moderate Alzheimer's disease. *N Engl J Med* 370, 322-333.
- Santacruz, K., Lewis, J., Spire, T., Paulson, J., Kotilinek, L., Ingelsson, M., Guimaraes, A., DeTure, M., Ramsden, M., McGowan, E., *et al.* (2005). Tau suppression in a neurodegenerative mouse model improves memory function. *Science* 309, 476-481.
- Saraceno, C., Musardo, S., Marcello, E., Pelucchi, S., and Di Luca, M. (2013). Modeling Alzheimer's disease: from past to future. *Front Pharmacol* 4, 77.
- Sasakura, H., Tsukada, Y., Takagi, S., and Mori, I. (2013). Japanese studies on neural circuits and behavior of *Caenorhabditis elegans*. *Front Neural Circuits* 7, 187.
- Sawin, E.R., Ranganathan, R., and Horvitz, H.R. (2000). *C. elegans* locomotory rate is modulated by the environment through a dopaminergic pathway and by experience through a serotonergic pathway. *Neuron* 26, 619-631.
- Schafer, W.F. (2006). Genetics of egg-laying in worms. *Annu Rev Genet* 40, 487-509.
- Schafer, W.R. (2005). Egg-laying. *WormBook*, 1-7.

Schieb, H., Kratzin, H., Jahn, O., Mobius, W., Rabe, S., Staufenbiel, M., Wiltfang, J., and Klafki, H.W. (2011). Beta-amyloid peptide variants in brains and cerebrospinal fluid from amyloid precursor protein (APP) transgenic mice: comparison with human Alzheimer amyloid. *J Biol Chem* 286, 33747-33758.

Scholl, M., Wall, A., Thordardottir, S., Ferreira, D., Bogdanovic, N., Langstrom, B., Almkvist, O., Graff, C., and Nordberg, A. (2012). Low PiB PET retention in presence of pathologic CSF biomarkers in Arctic APP mutation carriers. *Neurology* 79, 229-236.

Schon, E.A., and Area-Gomez, E. (2010). Is Alzheimer's disease a disorder of mitochondria-associated membranes? *J Alzheimers Dis* 20 Suppl 2, S281-292.

Schreiber, M.A., Pierce-Shimomura, J.T., Chan, S., Parry, D., and McIntire, S.L. (2010). Manipulation of behavioral decline in *Caenorhabditis elegans* with the Rag GTPase regulator. *PLoS Genet* 6, e1000972.

Schroeder, B.E., and Koo, E.H. (2005). To think or not to think: synaptic activity and A β release. *Neuron* 48, 873-875.

Schroeter, S., Khan, K., Barbour, R., Doan, M., Chen, M., Guido, T., Gill, D., Basi, G., Schenk, D., Seubert, P., *et al.* (2008). Immunotherapy reduces vascular amyloid-beta in PDAPP mice. *J Neurosci* 28, 6787-6793.

Selkoe, D.J. (2001). Alzheimer's disease: genes, proteins, and therapy. *Physiol Rev* 81, 741-766.

Selkoe, D.J. (2013). SnapShot: pathobiology of Alzheimer's disease. *Cell* 154, 468-468 e461.

Selkoe, D.J., and Podlisny, M.B. (2002). Deciphering the genetic basis of Alzheimer's disease. *Annu Rev Genomics Hum Genet* 3, 67-99.

Sergeant, N., Bombois, S., Ghestem, A., Drobecq, H., Kostanjevecki, V., Missiaen, C., Watez, A., David, J.P., Vanmechelen, E., Sergheraert, C., *et al.* (2003). Truncated beta-amyloid peptide species in pre-clinical Alzheimer's disease as new targets for the vaccination approach. *J Neurochem* 85, 1581-1591.

Serrano-Saiz, E., Poole, R.J., Felton, T., Zhang, F., De La Cruz, E.D., and Hobert, O. (2013). Modular control of glutamatergic neuronal identity in *C. elegans* by distinct homeodomain proteins. *Cell* 155, 659-673.

Sevigny, J., Chiao, P., Bussiere, T., Weinreb, P.H., Williams, L., Maier, M., Dunstan, R., Salloway, S., Chen, T., Ling, Y., *et al.* (2016). The antibody aducanumab reduces Abeta plaques in Alzheimer's disease. *Nature* 537, 50-56.

Shankar, G.M., Li, S., Mehta, T.H., Garcia-Munoz, A., Shepardson, N.E., Smith, I., Brett, F.M., Farrell, M.A., Rowan, M.J., Lemere, C.A., *et al.* (2008). Amyloid-beta protein dimers isolated directly from Alzheimer's brains impair synaptic plasticity and memory. *Nat Med* 14, 837-842.

Shankar, G.M., and Walsh, D.M. (2009). Alzheimer's disease: synaptic dysfunction and Abeta. *Mol Neurodegener* 4, 48.

Ship, J.A., Pearson, J.D., Cruise, L.J., Brant, L.J., and Metter, E.J. (1996). Longitudinal changes in smell identification. *J Gerontol A Biol Sci Med Sci* 51, M86-91.

Sinnige, T., Ciryam, P., Casford, S., Dobson, C.M., de Bono, M., and Vendruscolo, M. (2019). Expression of the amyloid-beta peptide in a single pair of *C. elegans* sensory neurons modulates the associated behavioural response. *PLoS One* 14, e0217746.

Slunt, H.H., Thinakaran, G., Von Koch, C., Lo, A.C., Tanzi, R.E., and Sisodia, S.S. (1994). Expression of a ubiquitous, cross-reactive homologue of the mouse beta-amyloid precursor protein (APP). *J Biol Chem* 269, 2637-2644.

Son, H.G., Altintas, O., Kim, E.J.E., Kwon, S., and Lee, S.V. (2019). Age-dependent changes and biomarkers of aging in *Caenorhabditis elegans*. *Aging Cell* 18, e12853.

Sontag, J.M., Nunbhakdi-Craig, V., White, C.L., 3rd, Halpain, S., and Sontag, E. (2012). The protein phosphatase PP2A/Balpha binds to the microtubule-associated proteins Tau and MAP2 at a motif also recognized by the kinase Fyn: implications for tauopathies. *J Biol Chem* 287, 14984-14993.

Spires-Jones, T.L., and Hyman, B.T. (2014). The intersection of amyloid beta and tau at synapses in Alzheimer's disease. *Neuron* 82, 756-771.

Sprecher, C.A., Grant, F.J., Grimm, G., O'Hara, P.J., Norris, F., Norris, K., and Foster, D.C. (1993). Molecular cloning of the cDNA for a human amyloid precursor protein homolog: evidence for a multigene family. *Biochemistry* 32, 4481-4486.

Stancu, I.C., Vasconcelos, B., Terwel, D., and Dewachter, I. (2014). Models of beta-amyloid induced Tau-pathology: the long and "folded" road to understand the mechanism. *Mol Neurodegener* 9, 51.

Standaert, D.G., and Yacoubian, T.A. (2010). Target validation: the Parkinson disease perspective. *Dis Model Mech* 3, 259-262.

Stelzma, R.A., Schnitzlein, H.N., and Murlagh, F.R. (1995). An English Translation of Alzheimer's 1907. Paper, "ijber eine eigenartige Erlranliung der Hirnrinde" *Clin Anat* 8, 429-431.

Stiernagle, T. (2006). Maintenance of *C. elegans*. *WormBook*, 1-11.

Stinchcomb, D.T., Shaw, J.E., Carr, S.H., and Hirsh, D. (1985). Extrachromosomal DNA transformation of *Caenorhabditis elegans*. *Mol Cell Biol* 5, 3484-3496.

Sulston, J., Dew, M., and Brenner, S. (1975). Dopaminergic neurons in the nematode *Caenorhabditis elegans*. *J Comp Neurol* 163, 215-226.

Sun, G.H., Raji, C.A., Maceachern, M.P., and Burke, J.F. (2012). Olfactory identification testing as a predictor of the development of Alzheimer's dementia: a systematic review. *Laryngoscope* 122, 1455-1462.

Takahashi, R.H., Milner, T.A., Li, F., Nam, E.E., Edgar, M.A., Yamaguchi, H., Beal, M.F., Xu, H., Greengard, P., and Gouras, G.K. (2002a). Intraneuronal Alzheimer abeta42 accumulates in multivesicular bodies and is associated with synaptic pathology. *Am J Pathol* 161, 1869-1879.

Takahashi, R.H., Nam, E.E., Edgar, M., and Gouras, G.K. (2002b). Alzheimer beta-amyloid peptides: normal and abnormal localization. *Histol Histopathol* 17, 239-246.

Tanis, J.E., Moresco, J.J., Lindquist, R.A., and Koelle, M.R. (2008). Regulation of serotonin biosynthesis by the G proteins Galphao and Galphaq controls serotonin signaling in *Caenorhabditis elegans*. *Genetics* 178, 157-169.

Tanzi, R.E., and Bertram, L. (2005). Twenty years of the Alzheimer's disease amyloid hypothesis: a genetic perspective. *Cell* 120, 545-555.

Tax, F.E., Thomas, J.H., Ferguson, E.L., and Horvitz, H.R. (1997). Identification and characterization of genes that interact with lin-12 in *Caenorhabditis elegans*. *Genetics* 147, 1675-1695.

Teplow, D.B. (2013). On the subject of rigor in the study of amyloid beta-protein assembly. *Alzheimers Res Ther* 5, 39.

Terry, R.D., Masliah, E., Salmon, D.P., Butters, N., DeTeresa, R., Hill, R., Hansen, L.A., and Katzman, R. (1991). Physical basis of cognitive alterations in Alzheimer's disease: synapse loss is the major correlate of cognitive impairment. *Ann Neurol* 30, 572-580.

Teschendorf, D., and Link, C.D. (2009). What have worm models told us about the mechanisms of neuronal dysfunction in human neurodegenerative diseases? *Mol Neurodegener* 4, 38.

Teshiba, E., Miyahara, K., and Takeya, H. (2016). Glucose-induced abnormal egg-laying rate in *Caenorhabditis elegans*. *Biosci Biotechnol Biochem* 80, 1436-1439.

Tew, D.J., Bottomley, S.P., Smith, D.P., Ciccotosto, G.D., Babon, J., Hinds, M.G., Masters, C.L., Cappai, R., and Barnham, K.J. (2008). Stabilization of neurotoxic soluble beta-sheet-rich conformations of the Alzheimer's disease amyloid-beta peptide. *Biophys J* 94, 2752-2766.

Tissenbaum, H.A. (2012). Genetics, Life Span, Health Span, and the Aging Process in *Caenorhabditis elegans*. *The Journals of Gerontology: Series A* 67A, 503-510.

Tissenbaum, H.A. (2015). Using *C. elegans* for aging research. *Invertebr Reprod Dev* 59, 59-63.

Tolar, M., Abushakra, S., and Sabbagh, M. (2020). The path forward in Alzheimer's disease therapeutics: Reevaluating the amyloid cascade hypothesis. *Alzheimer's & dementia : the journal of the Alzheimer's Association*.

Tomiyama, T., Nagata, T., Shimada, H., Teraoka, R., Fukushima, A., Kanemitsu, H., Takuma, H., Kuwano, R., Imagawa, M., Ataka, S., *et al.* (2008). A new amyloid beta variant favoring oligomerization in Alzheimer's-type dementia. *Ann Neurol* 63, 377-387.

Torayama, I., Ishihara, T., and Katsura, I. (2007). *Caenorhabditis elegans* integrates the signals of butanone and food to enhance chemotaxis to butanone. *J Neurosci* 27, 741-750.

Trent, C., Tsuing, N., and Horvitz, H.R. (1983). Egg-laying defective mutants of the nematode *Caenorhabditis elegans*. *Genetics* 104, 619-647.

Treusch, S., Hamamichi, S., Goodman, J.L., Matlack, K.E., Chung, C.Y., Baru, V., Shulman, J.M., Parrado, A., Bevis, B.J., Valastyan, J.S., *et al.* (2011). Functional links between Abeta toxicity, endocytic trafficking, and Alzheimer's disease risk factors in yeast. *Science* 334, 1241-1245.

- Tucker, K.L., Meyer, M., and Barde, Y.A. (2001). Neurotrophins are required for nerve growth during development. *Nat Neurosci* 4, 29-37.
- Van Dam, D., and De Deyn, P.P. (2011). Animal models in the drug discovery pipeline for Alzheimer's disease. *Br J Pharmacol* 164, 1285-1300.
- Vandesompele, J., De Preter, K., Pattyn, F., Poppe, B., Van Roy, N., De Paepe, A., and Speleman, F. (2002). Accurate normalization of real-time quantitative RT-PCR data by geometric averaging of multiple internal control genes. *Genome Biol* 3, RESEARCH0034.
- Velayudhan, L., Pritchard, M., Powell, J.F., Proitsi, P., and Lovestone, S. (2013). Smell identification function as a severity and progression marker in Alzheimer's disease. *Int Psychogeriatr* 25, 1157-1166.
- Venken, K.J., and Bellen, H.J. (2005). Emerging technologies for gene manipulation in *Drosophila melanogaster*. *Nat Rev Genet* 6, 167-178.
- Verdile, G., Fuller, S., Atwood, C.S., Laws, S.M., Gandy, S.E., and Martins, R.N. (2004). The role of beta amyloid in Alzheimer's disease: still a cause of everything or the only one who got caught? *Pharmacol Res* 50, 397-409.
- Verdile G., M.R.N. (2009). *Molecular Genetics of Alzheimer's Disease*, Vol 23 (Berlin, Heidelberg: Springer).
- Vidal-Gadea, A., Topper, S., Young, L., Crisp, A., Kressin, L., Elbel, E., Maples, T., Brauner, M., Erbguth, K., Axelrod, A., *et al.* (2011). *Caenorhabditis elegans* selects distinct crawling and swimming gaits via dopamine and serotonin. *Proc Natl Acad Sci U S A* 108, 17504-17509.
- von Bergen, M., Barghorn, S., Li, L., Marx, A., Biernat, J., Mandelkow, E.M., and Mandelkow, E. (2001). Mutations of tau protein in frontotemporal dementia promote aggregation of paired helical filaments by enhancing local beta-structure. *J Biol Chem* 276, 48165-48174.
- von Heijne, G. (1983). Patterns of amino acids near signal-sequence cleavage sites. *Eur J Biochem* 133, 17-21.
- Wade-Martins, R. (2012). Genetics: The MAPT locus-a genetic paradigm in disease susceptibility. *Nat Rev Neurol* 8, 477-478.

Waggoner, L.E., Zhou, G.T., Schafer, R.W., and Schafer, W.R. (1998). Control of alternative behavioral states by serotonin in *Caenorhabditis elegans*. *Neuron* 21, 203-214.

Walsh, D.M., Klyubin, I., Fadeeva, J.V., Cullen, W.K., Anwyl, R., Wolfe, M.S., Rowan, M.J., and Selkoe, D.J. (2002). Naturally secreted oligomers of amyloid beta protein potently inhibit hippocampal long-term potentiation in vivo. *Nature* 416, 535-539.

Walsh, D.M., Lomakin, A., Benedek, G.B., Condron, M.M., and Teplow, D.B. (1997). Amyloid beta-protein fibrillogenesis. Detection of a protofibrillar intermediate. *J Biol Chem* 272, 22364-22372.

Walsh, D.M., and Selkoe, D.J. (2007). A beta oligomers - a decade of discovery. *J Neurochem* 101, 1172-1184.

Wang, C., Li, Q., Redden, D.T., Weindruch, R., and Allison, D.B. (2004). Statistical methods for testing effects on "maximum lifespan". *Mech Ageing Dev* 125, 629-632.

Wang, C., Saar, V., Leung, K.L., Chen, L., and Wong, G. (2018). Human amyloid beta peptide and tau co-expression impairs behavior and causes specific gene expression changes in *Caenorhabditis elegans*. *Neurobiol Dis* 109, 88-101.

Wang, J., Dickson, D.W., Trojanowski, J.Q., and Lee, V.M. (1999). The levels of soluble versus insoluble brain A β distinguish Alzheimer's disease from normal and pathologic aging. *Exp Neurol* 158, 328-337.

Wang, X., Sliwoski, G.R., and Buttner, E.A. (2011). The relevance of *Caenorhabditis elegans* genetics for understanding human psychiatric disease. *Harv Rev Psychiatry* 19, 210-218.

Ward, S. (1973). Chemotaxis by the nematode *Caenorhabditis elegans*: identification of attractants and analysis of the response by use of mutants. *Proc Natl Acad Sci U S A* 70, 817-821.

Wasco, W., Bupp, K., Magendantz, M., Gusella, J.F., Tanzi, R.E., and Solomon, F. (1992). Identification of a mouse brain cDNA that encodes a protein related to the Alzheimer disease-associated amyloid beta protein precursor. *Proc Natl Acad Sci U S A* 89, 10758-10762.

Wasco, W., Gurubhagavatula, S., Paradis, M.D., Romano, D.M., Sisodia, S.S., Hyman, B.T., Neve, R.L., and Tanzi, R.E. (1993a). Isolation and characterization of APLP2

encoding a homologue of the Alzheimer's associated amyloid beta protein precursor. *Nat Genet* 5, 95-100.

Wasco, W., Peppercorn, J., and Tanzi, R.E. (1993b). Search for the genes responsible for familial Alzheimer's disease. *Ann N Y Acad Sci* 695, 203-208.

Wehling, E.I., Lundervold, A.J., Nordin, S., and Wollschlaeger, D. (2016). Longitudinal Changes in Familiarity, Free and Cued Odor Identification, and Edibility Judgments for Odors in Aging Individuals. *Chem Senses* 41, 155-161.

Weingarten, M.D., Lockwood, A.H., Hwo, S.Y., and Kirschner, M.W. (1975). A protein factor essential for microtubule assembly. *Proc Natl Acad Sci U S A* 72, 1858-1862.

Weinshenker, D., Garriga, G., and Thomas, J.H. (1995). Genetic and pharmacological analysis of neurotransmitters controlling egg-laying in *C. elegans*. *J Neurosci* 15, 6975-6985.

Wen, J.Y., Kumar, N., Morrison, G., Rambaldini, G., Runciman, S., Rousseau, J., and van der Kooy, D. (1997). Mutations that prevent associative learning in *C. elegans*. *Behav Neurosci* 111, 354-368.

White, J.G., Southgate, E., Thomson, J.N., and Brenner, S. (1986). The structure of the nervous system of the nematode *Caenorhabditis elegans*. *Philos Trans R Soc Lond B Biol Sci* 314, 1-340.

Wilcox, K.C., Lacor, P.N., Pitt, J., and Klein, W.L. (2011). Abeta oligomer-induced synapse degeneration in Alzheimer's disease. *Cell Mol Neurobiol* 31, 939-948.

Wildsmith, K.R., Holley, M., Savage, J.C., Skerrett, R., and Landreth, G.E. (2013). Evidence for impaired amyloid beta clearance in Alzheimer's disease. *Alzheimers Res Ther* 5, 33.

Wilson, C.A., Doms, R.W., and Lee, V.M. (1999). Intracellular APP processing and A beta production in Alzheimer disease. *J Neuropathol Exp Neurol* 58, 787-794.

Wiltfang, J., Esselmann, H., Bibl, M., Smirnov, A., Otto, M., Paul, S., Schmidt, B., Klafki, H.W., Maler, M., Dyrks, T., *et al.* (2002). Highly conserved and disease-specific patterns of carboxyterminally truncated Abeta peptides 1-37/38/39 in addition to 1-40/42 in Alzheimer's disease and in patients with chronic neuroinflammation. *J Neurochem* 81, 481-496.

- Withee, J., Galligan, B., Hawkins, N., and Garriga, G. (2004). *Caenorhabditis elegans* WASP and Ena/VASP proteins play compensatory roles in morphogenesis and neuronal cell migration. *Genetics* 167, 1165-1176.
- Wittenburg, N., Eimer, S., Lakowski, B., Rohrig, S., Rudolph, C., and Baumeister, R. (2000). Presenilin is required for proper morphology and function of neurons in *C. elegans*. *Nature* 406, 306-309.
- Wu, Y., Wu, Z., Butko, P., Christen, Y., Lambert, M.P., Klein, W.L., Link, C.D., and Luo, Y. (2006). Amyloid-beta-induced pathological behaviors are suppressed by Ginkgo biloba extract EGb 761 and ginkgolides in transgenic *Caenorhabditis elegans*. *J Neurosci* 26, 13102-13113.
- Xi, Y., Noble, S., and Ekker, M. (2011). Modeling neurodegeneration in zebrafish. *Curr Neurol Neurosci Rep* 11, 274-282.
- Yamada, T., Sasaki, H., Furuya, H., Miyata, T., Goto, I., and Sakaki, Y. (1987). Complementary DNA for the mouse homolog of the human amyloid beta protein precursor. *Biochem Biophys Res Commun* 149, 665-671.
- Yao, S.C., Hart, A.D., and Terzella, M.J. (2013). An evidence-based osteopathic approach to Parkinson disease. *Osteopathic Family Physician* 5, 96-101.
- Yatin, S.M., Varadarajan, S., Link, C.D., and Butterfield, D.A. (1999). In vitro and in vivo oxidative stress associated with Alzheimer's amyloid beta-peptide (1-42). *Neurobiol Aging* 20, 325-330; discussion 339-342.
- Yen, K., Steinsaltz, D., and Mobbs, C.V. (2008). Validated analysis of mortality rates demonstrates distinct genetic mechanisms that influence lifespan. *Experimental gerontology* 43, 1044-1051.
- Yong, W., Lomakin, A., Kirkitadze, M.D., Teplow, D.B., Chen, S.H., and Benedek, G.B. (2002). Structure determination of micelle-like intermediates in amyloid beta -protein fibril assembly by using small angle neutron scattering. *Proc Natl Acad Sci U S A* 99, 150-154.
- Yu, L., Petyuk, V.A., Tasaki, S., Boyle, P.A., Gaiteri, C., Schneider, J.A., De Jager, P.L., and Bennett, D.A. (2019). Association of Cortical beta-Amyloid Protein in the Absence of Insoluble Deposits With Alzheimer Disease. *JAMA Neurol* 76, 818-826.

Zambrano, N., Bimonte, M., Arbucci, S., Gianni, D., Russo, T., and Bazzicalupo, P. (2002). *feh-1* and *apl-1*, the *Caenorhabditis elegans* orthologues of mammalian Fe65 and beta-amyloid precursor protein genes, are involved in the same pathway that controls nematode pharyngeal pumping. *J Cell Sci* *115*, 1411-1422.

Zhang, Y., Chen, D., Smith, M.A., Zhang, B., and Pan, X. (2012). Selection of reliable reference genes in *Caenorhabditis elegans* for analysis of nanotoxicity. *PLoS One* *7*, e31849.

Zhao, L.N., Lu, L., Chew, L.Y., and Mu, Y. (2014). Alzheimer's disease--a panorama glimpse. *Int J Mol Sci* *15*, 12631-12650.

Zhao, X.L., Wang, W.A., Tan, J.X., Huang, J.K., Zhang, X., Zhang, B.Z., Wang, Y.H., YangCheng, H.Y., Zhu, H.L., Sun, X.J., *et al.* (2010). Expression of beta-amyloid induced age-dependent presynaptic and axonal changes in *Drosophila*. *J Neurosci* *30*, 1512-1522.